



**INSTITUTO POTOSINO DE INVESTIGACIÓN  
CIENTÍFICA Y TECNOLÓGICA, A.C.**

**POSGRADO EN CIENCIAS AMBIENTALES**

**Microbial Processes Driven by the Redox Capacity of  
Natural Organic Matter Suppress the Emission of  
Greenhouse Gases in Wetland Sediments**

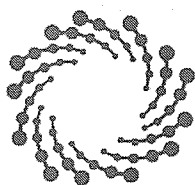
Tesis que presenta

**Edgardo Iván Valenzuela Reyes**

Para obtener el grado de

**Doctor en Ciencias Ambientales**

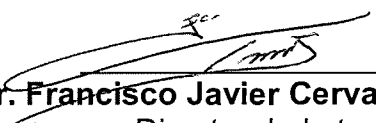
San Luis Potosí, S.L.P., diciembre, 2019



**IPICYT**

## Constancia de aprobación de la tesis

La tesis “*Microbial Processes Driven by the Redox Capacity of Natural Organic Matter Suppress the Emission of Greenhouse Gases in Wetland Sediments*” presentada para obtener el Grado de Doctor en Ciencias Ambientales fue elaborada por **Edgardo Iván Valenzuela Reyes** y aprobada el trece de diciembre del dos mil diecinueve por los suscritos, designados por el Colegio de Profesores de la División de Ciencias Ambientales del Instituto Potosino de Investigación Científica y Tecnológica, A.C.

  
**Dr. Francisco Javier Cervantes Carrillo**  
Director de la tesis

  
**Dra. Sonia Lorena Arriaga García**  
Miembro del Comité Tutorial

  
**Dr. Frédéric Thalasso Siret**  
Miembro del Comité Tutorial

  
**Dr. Cesar Nieto Delgado**  
Miembro del Comité Tutorial

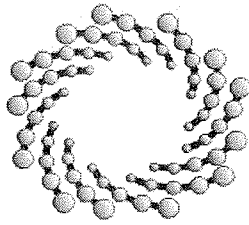


## Créditos Institucionales

Esta tesis fue elaborada en los Laboratorios de la División de Ciencias Ambientales, del Instituto Potosino de Investigación Científica y Tecnológica, A.C., bajo la dirección del Dr. Francisco Javier Cervantes Carrillo.

Durante la realización del trabajo el autor recibió una beca académica del Consejo Nacional de Ciencia y Tecnología (No. 299501).

El trabajo descrito en el Capítulo V de esta tesis fue llevado a cabo en los laboratorios del Grupo de Geomicrobiología del Instituto de Geociencias de la Universidad Eberhard Karls de Tuebingen, en Tuebingen, Alemania. Esta parte de la tesis fue co-asesorada por el Prof. Andreas Kappler durante una estancia corta de investigación financiada por el Servicio Alemán de Intercambio Académico (*Deutscher Akademischer Austauschdienst, DAAD*) dentro del marco del programa Short Term Research Grants, 2018 (beca #: 57378443).



**IPICYT**

# Instituto Potosino de Investigación Científica y Tecnológica, A.C.

## Acta de Examen de Grado

El Secretario Académico del Instituto Potosino de Investigación Científica y Tecnológica, A.C., certifica que en el Acta 020 del Libro Primero de Actas de Exámenes de Grado del Programa de Doctorado en Ciencias Ambientales está asentado lo siguiente:

En la ciudad de San Luis Potosí a los 13 días del mes de diciembre del año 2019, se reunió a las 12:00 horas en las instalaciones del Instituto Potosino de Investigación Científica y Tecnológica, A.C., el Jurado integrado por:

|  |                        |                  |
|--|------------------------|------------------|
| <b>Dra. Sonia Lorena Arriaga García</b>        | <b>Presidenta</b>      | <b>IPICYT</b>    |
| <b>Dr. Frédéric Thalasso Siret</b>             | <b>Secretario</b>      | <b>CINVESTAV</b> |
| <b>Dr. Cesar Nieto Delgado</b>                 | <b>Sinodal</b>         | <b>IPICYT</b>    |
| <b>Dr. Francisco Javier Cervantes Carrillo</b> | <b>Sinodal externo</b> | <b>UNAM</b>      |

a fin de efectuar el examen, que para obtener el Grado de:

**DOCTOR EN CIENCIAS AMBIENTALES**

sustentó el C.

**Edgardo Iván Valenzuela Reyes**

sobre la Tesis intitulada:

*Microbial Processes Driven by the Redox Capacity of Natural Organic Matter Suppress the Emission of Greenhouse Gases in Wetland Sediments*

que se desarrolló bajo la dirección de

**Dr. Francisco Javier Cervantes Carrillo**

El Jurado, después de deliberar, determinó

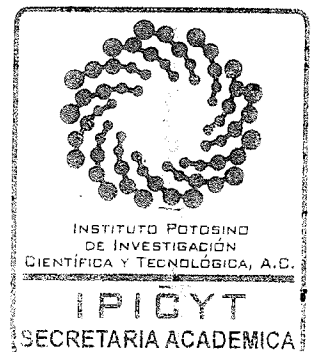
**APROBARLO**

Dándose por terminado el acto a las 13:36 horas, procediendo a la firma del Acta los integrantes del Jurado. Dando fe el Secretario Académico del Instituto.

A petición del interesado y para los fines que al mismo convengan, se extiende el presente documento en la ciudad de San Luis Potosí, S.L.P., México, a los 13 días del mes de diciembre de 2019.

  
**Mtra. Ivonne Lizette Cuevas Vélez**  
Jefa del Departamento del Posgrado

  
**Dr. Marcial Bonilla Marín**  
Secretario Académico



## Content of the Thesis

|                                      |       |
|--------------------------------------|-------|
| Constancia de aprobación de la tesis | ii    |
| Créditos institucionales             | iii   |
| Acta de examen                       | iv    |
| Contenido de la Tesis                | v     |
| Lista de Tablas                      | xiii  |
| Lista de Figuras                     | xiv   |
| Lista de Abreviaciones               | xviii |
| Agradecimientos                      | xx    |
| Summary                              | xxii  |
| Resumen                              | xxv   |

### **CHAPTER I (Introduction): Contribution of Humic Substances to Suppress the Emission of Greenhouse Gases**

|   |           |
|---|-----------|
| <b>Abstract</b>   | <b>2</b>  |
| <b>1.1 What are humic substances?</b>   | <b>3</b>  |
| <b>1.1.1</b> The redox properties of humic substances.  | <b>5</b>  |
| <b>1.1.2</b> Humus reducing and oxidizing microorganisms.   | <b>8</b>  |
| <b>1.2 Mechanisms for greenhouse gases emission suppression by humus reducing/oxidizing microorganisms.</b> | <b>10</b> |
| <b>1.2.1</b> Methanogenesis suppression by Humic Substances.  | <b>10</b> |
| <b>1.2.2</b> Humic substances as terminal electron acceptor for the anaerobic oxidation of methane.         | <b>12</b> |
| <b>1.2.3</b> Humic Substances as electron shuttles for AOM with metallic oxides as                          | <b>16</b> |

|  |           |
|--|-----------|
| Terminal Electron Acceptor.  |           |
| <b>1.2.4</b> Inter-species electron transfer mediated by Humic Substances promotes Greenhouse Gases consumption. | <b>18</b> |
| <b>1.2.5</b> Sulfur cryptic cycling elicited by Humic Substances and its effect on AOM.                          | <b>20</b> |
| <b>1.3</b> <b>Scope of the Doctoral Dissertation</b>   | <b>21</b> |
| <b>1.4</b> <b>Hypotheses and Objectives</b>  | <b>21</b> |
| <b>1.5</b> <b>References</b>   | <b>22</b> |

## **CHAPTER II: Anaerobic methane oxidation linked to microbial reduction of natural organic matter**

|  |           |
|--|-----------|
| <b>Abstract</b>  | <b>31</b> |
| <b>2.1</b> <b>Introduction</b>   | <b>32</b> |
| <b>2.2</b> <b>Materials and Methods</b>  | <b>34</b> |
| <b>2.2.1</b> Sediment sampling and characterization  | <b>34</b> |
| <b>2.2.2</b> Sediment incubations  | <b>36</b> |
| <b>2.2.3</b> Enrichment incubations with AQDS  | <b>36</b> |
| <b>2.2.4</b> Analytical techniques   | <b>38</b> |
| <b>2.2.4.1</b> Isotopic carbon dioxide and methane measurements  | <b>38</b> |
| <b>2.2.4.2</b> Methane quantification in AQDS enrichment   | <b>39</b> |
| <b>2.2.4.3</b> Determination of electron accepting functional groups in solid phase by XPS                     | <b>40</b> |
| <b>2.2.4.4</b> Determination of electron accepting functional groups in solid phase by Micro-ATR-FT-IR imaging | <b>40</b> |

|                 |  |           |
|-----------------|--|-----------|
| <b>2.2.4.5</b>  | Determination of electron accepting functional groups in liquid phase by high resolution UV-Vis-NIR spectroscopy | <b>41</b> |
| <b>2.2.4.6</b>  | Nitrite and nitrate determinations   | <b>41</b> |
| <b>2.2.4.7</b>  | Sulfate and sulfide determinations   | <b>42</b> |
| <b>2.2.4.8</b>  | Humic substances reduction and ferrous iron measurements   | <b>42</b> |
| <b>2.2.4.9</b>  | Total carbon (TC), total organic carbon (TOC) and total inorganic carbon (TIC) measurements                      | <b>43</b> |
| <b>2.2.4.10</b> | Total, volatile and fixed solids   | <b>43</b> |
| <b>2.2.4.11</b> | Elemental composition  | <b>44</b> |
| <b>2.2.4.12</b> | DNA extraction, PCR amplification and Sequencing   | <b>44</b> |
| <b>2.2.4.13</b> | Bioinformatic Analysis   | <b>45</b> |
| <b>2.2.4.14</b> | Accession numbers  | <b>46</b> |
| <b>2.3</b>      | <b>Results</b>   | <b>47</b> |
| <b>2.3.1</b>    | Kinetics of <sup>13</sup> C-methane oxidation and electron balances  | <b>47</b> |
| <b>2.3.2</b>    | Spectroscopic evidence on presence and reduction of functional groups in NOM                                     | <b>52</b> |
| <b>2.3.3</b>    | Microbial communities performing AOM   | <b>56</b> |
| <b>2.3.4</b>    | AOM linked to AQDS reduction   | <b>59</b> |
| <b>2.4</b>      | <b>Discussion</b>  | <b>62</b> |
| <b>2.4.1</b>    | NOM as terminal acceptor fueling AOM in wetland sediments  | <b>62</b> |
| <b>2.4.2</b>    | Microbial communities in wetland sediments performing AOM  | <b>63</b> |
| <b>2.5</b>      | <b>Ecological significance</b>   | <b>64</b> |
| <b>2.6</b>      | <b>References</b>  | <b>68</b> |

## **CHAPTER III: Electron Shuttling Mediated by Humic Substances Fuels Anaerobic Methane Oxidation and Carbon Burial**

|   |           |
|---|-----------|
| <b>Abstract</b>   | <b>74</b> |
| <b>3.1 Introduction</b>   | <b>75</b> |
| <b>3.2 Materials and Methods</b>  | <b>77</b> |
| <b>3.2.1</b> Wetland description and sediment sampling  | <b>77</b> |
| <b>3.2.2</b> Microcosms set-up  | <b>78</b> |
| <b>3.2.2.1</b> Long-term incubations  | <b>78</b> |
| <b>3.2.2.1.1</b> Inoculation and first incubation cycle   | <b>78</b> |
| <b>3.2.2.1.2</b> Second incubation cycle  | <b>79</b> |
| <b>3.2.2.2</b> Incubations with <sup>13</sup> C-methane   | <b>79</b> |
| <b>3.2.2.3</b> Destructive sampling incubations   | <b>80</b> |
| <b>3.2.3</b> Chemical determinations  | <b>81</b> |
| <b>3.2.4</b> Mineral characterization of the sediment   | <b>82</b> |
| <b>3.3 Calculations</b>   | <b>83</b> |
| <b>3.3.1</b> Fractional enrichment of <sup>13</sup> CO <sub>2</sub>   | <b>83</b> |
| <b>3.3.2</b> Electron balances  | <b>83</b> |
| <b>3.3.3</b> AOM assessment via carbonate precipitation   | <b>84</b> |
| <b>3.4 Results</b>  | <b>86</b> |
| <b>3.4.1</b> Net CH <sub>4</sub> oxidation linked to goethite reduction mediated by HS                              | <b>86</b> |
| <b>3.4.2</b> Incubations with <sup>13</sup> CH <sub>4</sub> to asses AOM linked to HS and ferrihydrite<br>reduction | <b>88</b> |
| <b>3.4.2.1</b> Reduction of electron acceptors  | <b>91</b> |
| <b>3.4.2.1.1</b> Reduction of intrinsic NOM and added PPHS  | <b>91</b> |



|           |   |     |
|-----------|---|-----|
| 3.4.2.1.2 | Ferrihydrite reduction  | 94  |
| 3.4.2.1.3 | Sulfate reduction   | 98  |
| 3.4.3     | AOM assessment under artificial conditions and destructive sampling | 100 |
| 3.4.4     | Mineral characterization of wetland sediment performing AOM         | 102 |
| 3.4       | <b>Discussion</b>   | 105 |
| 3.5       | <b>Conclusions</b>  | 108 |
| 3.6       | <b>References</b>   | 109 |

## **CHAPTER IV: Humic Substances Mediate Anaerobic Methane Oxidation Linked to Nitrous Oxide Reduction**

|         |   |     |
|---------|---|-----|
|         | <b>Abstract</b>   | 115 |
| 4.1     | <b>Introduction</b>   | 116 |
| 4.2     | <b>Materials and Methods</b>  | 118 |
| 4.2.1   | Wetland and sediment sampling description   | 118 |
| 4.2.2   | Microcosms set-up   | 118 |
| 4.2.2.1 | Kinetics of N <sub>2</sub> O reduction  | 118 |
| 4.2.2.2 | Kinetics of simultaneous N <sub>2</sub> O and <sup>13</sup> CH <sub>4</sub> consumption | 120 |
| 4.2.3   | Analytical techniques   | 121 |
| 4.2.3.1 | Sulfate, sulfide, nitrate and nitrite measurements                                      | 121 |
| 4.2.3.2 | Isotopic carbon dioxide and nitrous oxide determinations                                | 121 |
| 4.2.3.3 | Determination of electron-donating capacity in microcosms' slurry samples               | 122 |
| 4.2.4   | Molecular analysis  | 122 |
| 4.2.4.1 | DNA extraction and pooling  | 122 |
| 4.2.4.2 | <i>nosZ</i> cloning   | 123 |

|           |  |     |
|-----------|--|-----|
| 4.2.4.3   | Genomic libraries construction and Sequencing  | 123 |
| 4.2.4.4   | <i>nosZ</i> bioinformatic analysis   | 124 |
| 4.2.4.5   | 16s bioinformatic analysis   | 124 |
| 4.2.5     | Accession numbers  | 125 |
| 4.2.6     | Electron balances calculations   | 125 |
| 4.3       | <b>Results</b>   | 127 |
| 4.3.1     | Kinetics of N <sub>2</sub> O reduction with reduced PPHS as electron donor                   | 127 |
| 4.3.2     | AOM linked to N <sub>2</sub> O reduction mediated by HS                                      | 129 |
| 4.3.2.1   | N <sub>2</sub> O reduction rates   | 129 |
| 4.3.2.2   | AOM and its coupling with N <sub>2</sub> O reduction   | 132 |
| 4.3.2.3   | PPHS redox pattern during AOM linked to N <sub>2</sub> O reduction                           | 134 |
| 4.3.2.4   | Microbial communities potentially involved in AOM linked to N <sub>2</sub> O reduction       | 136 |
| 4.3.2.4.1 | Bacterial taxa   | 136 |
| 4.3.2.4.2 | Archaeal taxa  | 139 |
| 4.4       | <b>Discussion</b>  | 141 |
| 4.4.1     | Redox active moieties in humus suppress the emission of GHGs from organotrophic environments | 141 |
| 4.4.2     | Microbial communities potentially involved   | 143 |
| 4.5       | <b>Conclusions</b>   | 145 |
| 4.6       | <b>References</b>  | 146 |

## **CHAPTER V: Assessing the Effect of Sulfur/Organic Matter Interactions in the Methane Dynamics of a Coastal Wetland Sediment**

|     |                     |     |
|-----|---------------------|-----|
|     | <b>Abstract</b>     | 155 |
| 5.1 | <b>Introduction</b> | 157 |

|                  |   |            |
|------------------|---|------------|
| <b>5.2</b>       | <b>Materials and Methods</b>  | <b>157</b> |
| <b>5.2.1</b>     | Chemical assay  | <b>157</b> |
| <b>5.2.1.1</b>   | Microcosms set-up   | <b>158</b> |
| <b>5.2.1.2</b>   | Microcosms sampling   | <b>158</b> |
| <b>5.2.1.2.1</b> | Sulfide   | <b>158</b> |
| <b>5.2.1.2.2</b> | Sulfate and Thiosulfate   | <b>158</b> |
| <b>5.2.1.2.3</b> | Zero-valent (elemental) Sulfur  | <b>159</b> |
| <b>5.2.1.2.4</b> | Electron Shuttling Capacity of PPHS   | <b>159</b> |
| <b>5.2.1.3</b>   | Assessing of Anaerobic Oxidation of Methane   | <b>159</b> |
| <b>5.2.2</b>     | Analytical techniques   | <b>161</b> |
| <b>5.2.2.1</b>   | Sulfur species determinations   | <b>161</b> |
| <b>5.2.2.2</b>   | Methane determinations  | <b>161</b> |
| <b>5.2.2.3</b>   | Reduction of the functional moieties of PPHS  | <b>162</b> |
| <b>5.2.2.4</b>   | Analysis of sediment post-incubation  | <b>162</b> |
| <b>5.3</b>       | <b>Results</b>  | <b>163</b> |
| <b>5.3.1</b>     | Sulfide oxidation by Pahokee Peat Humic Substances  | <b>163</b> |
| <b>5.3.2</b>     | Methane dynamics as affected by PPHS and/or Sulfate   | <b>167</b> |
| <b>5.3.3</b>     | Electron acceptors driving AOM  | <b>174</b> |
| <b>5.4</b>       | Discussion  | <b>176</b> |
| <b>5.4.1</b>     | Oxidation of dissolved sulfide with Pahokee Peat Humic substances as<br>electron acceptor                                 | <b>176</b> |
| <b>5.4.2</b>     | Methanotrophic and methanogenic activities affected by sulfate and<br>Pahokee Peat Humic substances as electron acceptors | <b>177</b> |
| <b>5.5</b>       | <b>Conclusions</b>  | <b>178</b> |
| <b>5.6</b>       | <b>References</b>   | <b>179</b> |

## CHAPTER VI: General Discussion, Perspectives and Concluding

### Remarks

|                |   |            |
|----------------|---|------------|
| <b>6.1</b>     | <b>Introduction</b>   | <b>184</b> |
| <b>6.2</b>     | <b>Relevance of Humic Substances fueling Greenhouse Gas Consuming Processes</b>   | <b>185</b> |
| <b>6.3</b>     | <b>Future Challenges</b>  | <b>189</b> |
| <b>6.3.1</b>   | Identifying microbes responsible for HS mediated AOM in natural organotrophic settings  | <b>190</b> |
| <b>6.3.1.1</b> | Involvement of ANME in HS mediated AOM  | <b>190</b> |
| <b>6.3.1.2</b> | Involvement of non-ANME Euryarchaeota in HS mediated AOM  | <b>192</b> |
| <b>6.3.1.3</b> | Involvement of archaea outside the Euryarchaeota phylum in HS mediated AOM  | <b>193</b> |
| <b>6.3.2</b>   | Elucidation of environmental factors affecting HS dependent AOM   | <b>194</b> |
| <b>6.3.2.1</b> | Humic substances dependent AOM in recurrently anoxic environments   | <b>196</b> |
| <b>6.4</b>     | <b>Biotechnological potential of HS reducing CH<sub>4</sub> oxidizing microbes</b>  | <b>198</b> |
| <b>6.4.1</b>   | CH <sub>4</sub> oxidizing/humus reducing microbes and their potential role in electricity production  | <b>198</b> |
| <b>6.4.2</b>   | CH <sub>4</sub> oxidizing/quinone reducing microbes for engineered CH <sub>4</sub> emission suppression in natural environments by using quinone-containing materials | <b>200</b> |
| <b>6.4.3</b>   | CH <sub>4</sub> oxidizing/humus reducing microbes in wastewater treatment processes   | <b>201</b> |
| <b>6.4</b>     | <b>Concluding Remarks</b>   | <b>202</b> |
| <b>6.5</b>     | <b>References</b>   | <b>204</b> |

## List of Tables

### Tables presented in CHAPTER I

|                  |  |          |
|------------------|--|----------|
| <b>Table 1.1</b> | Examples of the variability of the electron accepting capacity of several types of humic materials extracted from natural settings as well as from commonly used sources of humic and fulvic acids commercially available. | <b>6</b> |
|------------------|--|----------|

### Tables presented in CHAPTER II

|                  |   |           |
|------------------|---|-----------|
| <b>Table 2.1</b> | Sediment and water chemical characterization.   | <b>35</b> |
| <b>Table 2.2</b> | Contribution of different electron acceptors on anaerobic oxidation of methane in wetland sediment incubations at the end of exponential phase (20 days of incubation). | <b>52</b> |

### Tables presented in CHAPTER III

|                  |  |           |
|------------------|--|-----------|
| <b>Table 3.1</b> | Number of milli-electron equivalents (meq L <sup>-1</sup> ) derived from methane oxidation, linked to leonardite and goethite reduction. | <b>87</b> |
| <b>Table 3.2</b> | Reduction of intrinsic and added electron acceptors at the end of the 21-days incubation cycle under quasi natural conditions.           | <b>92</b> |

### Tables presented in CHAPTER V

|                  |   |            |
|------------------|---|------------|
| <b>Table 5.1</b> | Comparison of reports regarding dissolved sulfide (HS <sup>-</sup> ) oxidation by humic substances or model quinones. | <b>169</b> |
|------------------|---|------------|

### Tables presented in CHAPTER VI

|                  |  |            |
|------------------|--|------------|
| <b>Table 6.1</b> | Known anaerobic methanotrophic archaea (ANME) and the terminal electron acceptors they can employ to carry out anaerobic oxidation of methane (AOM). | <b>184</b> |
|------------------|--|------------|

## List of Figures

### Figures presented in CHAPTER I

|                   |   |           |
|-------------------|---|-----------|
| <b>Figure 1.1</b> | Schematic representation of the formation, structure and redox properties of humic substances.  | <b>4</b>  |
| <b>Figure 1.2</b> | SCOPUS based search on the scientific interest in Humic Substances.   | <b>9</b>  |
| <b>Figure 1.3</b> | Mechanisms for methanogenesis suppression by Humic Substances.  | <b>11</b> |
| <b>Figure 1.4</b> | Mechanisms for Anaerobic Methane Oxidation driven by Humic Substances.  | <b>14</b> |
| <b>Figure 1.5</b> | RAOMs fueling AOM by shuttling electrons towards iron oxides.   | <b>15</b> |
| <b>Figure 1.6</b> | Simultaneous CH <sub>4</sub> and N <sub>2</sub> O consumption through an extracellular electron transfer process mediated by the redox-active moieties in Humic Substances. | <b>18</b> |
| <b>Figure 1.7</b> | Sulfur cycling by Humic Substances (HS) and the its effect on anaerobic methane oxidation (AOM).  | <b>20</b> |

### Figures presented in CHAPTER II

|                   |  |           |
|-------------------|--|-----------|
| <b>Figure 2.1</b> | Geographic localization of the sediment and water sampling point within Yucatan Peninsula.   | <b>34</b> |
| <b>Figure 2.2</b> | Schematic representation of sequential incubation cycles for AQDS dependent methanotrophic activity.   | <b>38</b> |
| <b>Figure 2.3</b> | Anaerobic methane oxidation measured as <sup>13</sup> CO <sub>2</sub> production in microcosms' headspace and <sup>13</sup> C enrichment calculated as <sup>13</sup> FCO <sub>2</sub> ( <sup>13</sup> CO <sub>2</sub> / <sup>13</sup> CO <sub>2</sub> + <sup>12</sup> CO <sub>2</sub> ). | <b>47</b> |
| <b>Figure 2.4</b> | Production of <sup>13</sup> CO <sub>2</sub> and reduction of intrinsic or added electron acceptors at the end of the exponential phase (20 days of incubation).  | <b>48</b> |
| <b>Figure 2.5</b> | Produced <sup>12</sup> CH <sub>4</sub> in wetland sediment microcosms.   | <b>50</b> |

|                    |  |           |
|--------------------|--|-----------|
| <b>Figure 2.6</b>  | Spectroscopic evidence of the presence of quinone moieties and their reduction in wetland sediment samples.  | <b>53</b> |
| <b>Figure 2.7</b>  | High performance Ultraviolet-Visible-Near Infrared spectra obtained from liquid samples before and after incubation with $^{13}\text{CH}_4$ .  | <b>55</b> |
| <b>Figure 2.8</b>  | Archaeal composition in wetland sediment samples performing AOM.   | <b>58</b> |
| <b>Figure 2.9</b>  | Bacterial community composition, and associated respiring capabilities, in wetland sediment samples performing AOM based on 16s rRNA gene libraries obtained by MiSeq ILLUMINA technology. | <b>59</b> |
| <b>Figure 2.10</b> | AOM with AQDS as electron acceptor by an enrichment derived from wetland sediment.   | <b>60</b> |
| <b>Figure 2.11</b> | Schematic representation of methane generation and consumption by wetland sediment biota.  | <b>65</b> |

### Figures presented in CHAPTER III

|                    |  |            |
|--------------------|--|------------|
| <b>Figure 3.1</b>  | Net anaerobic methane oxidation linked to leonardite mediated reduction of goethite.   | <b>86</b>  |
| <b>Figure 3.2</b>  | Net $^{13}\text{CH}_4$ consumption and $^{13}\text{C}$ -carbon dioxide enrichment.   | <b>89</b>  |
| <b>Figure 3.3</b>  | $^{13}\text{FCO}_2$ values for the endogenous controls (lacking added $^{13}\text{CH}_4$ ) incubated under the quasi-natural conditions).                            | <b>90</b>  |
| <b>Figure 3.4</b>  | Microbial reduction of intrinsic NOM and the mixture of intrinsic NOM/ <i>Pahokee Peat</i> humic substances.   | <b>93</b>  |
| <b>Figure 3.5</b>  | Acid extractable ferrous iron measured by the ferrozine technique over time.   | <b>94</b>  |
| <b>Figure 3.6</b>  | Solubility diagram for siderite.   | <b>96</b>  |
| <b>Figure 3.7</b>  | Effect of ferrihydrite reduction, mediated by <i>Pahokee Peat</i> humic substances on anaerobic methane oxidation assessed as ferrous iron carbonates precipitation. | <b>97</b>  |
| <b>Figure 3.8</b>  | Sulfate consumption over incubation time.  | <b>99</b>  |
| <b>Figure 3.9</b>  | Evidence of AOM mediated by <i>Pahokee Peat</i> humic substances with ferrihydrite as terminal electron acceptor.  | <b>100</b> |
| <b>Figure 3.10</b> | XRD diffractograms displaying the mineral phases found after   | <b>103</b> |

incubation under the experimental conditions tested.

**Figure 3.11** ESEM-EDS exploration of wetland sediment after incubation. **104**

**Figure 3.12** Schematic representation of methane consumption by wetland sediment biota with humic substances as electron shuttle and Fe(III) as TEA. **107**

#### **Figures presented in CHAPTER IV**

**Figure 4.1** Nitrous oxide reduction linked to re-oxidation of reduced functional groups in *Pahokee Peat* Humic Substances (PPHS<sub>red</sub>). **128**

**Figure 4.2** Nitrous oxide reduction promoted by *Pahokee Peat* Humic Substances (PPHS) acting as electron shuttle and <sup>13</sup>CH<sub>4</sub> as the electron donor. **130**

**Figure 4.3** Nitrous oxide reduction promoted by *Pahokee Peat* Humic Substances (PPHS) acting as electron shuttle and <sup>13</sup>CH<sub>4</sub> as the electron donor. **131**

**Figure 4.4** Anaerobic <sup>13</sup>CH<sub>4</sub> oxidation measured as <sup>13</sup>CO<sub>2</sub> production and its relationship with N<sub>2</sub>O reduction in presence of *Pahokee Peat* Humic Substances (PPHS). **133**

**Figure 4.5** Reduction of *Pahokee Peat* Humic Substances (PPHS) under the different experimental conditions during incubation time. **134**

**Figure 4.6** Schematic representation of anaerobic CH<sub>4</sub> oxidation linked to N<sub>2</sub>O reduction mediated by the electron shuttling capacity of humic substances (HS). **135**

**Figure 4.7** Composition of the bacterial communities found in selected experimental treatments at the end of the incubation period. **137**

**Figure 4.8** *nosZ* gene diversity found by cloning at the end of the incubation period. **138**

**Figure 4.9** Composition of the archaeal communities found in selected experimental treatments at the end of the incubation period. **140**

#### **Figures presented in CHAPTER V**

**Figure 5.1** Transformation of dissolved sulfide (HS<sup>-</sup>) upon reaction with *Pahokee Peat* Humic substances and formation of oxidized **163**



|                   |  |            |
|-------------------|--|------------|
|                   | products.  |            |
| <b>Figure 5.2</b> | Analysis of products coming from dissolved sulfide (HS <sup>-</sup> ) transformation by PPHS.  | <b>165</b> |
| <b>Figure 5.3</b> | Fourier-transformed infrared (FTIR) spectra of PPHS after reaction with sulfide.   | <b>166</b> |
| <b>Figure 5.4</b> | Anaerobic methane oxidation performed by wetland sediment microbiota as affected by sulfate (SO <sub>4</sub> <sup>2-</sup> ), <i>Pahokee Peat</i> Humic Substances (PPHS), both, and none.               | <b>170</b> |
| <b>Figure 5.5</b> | Effect of the different electron acceptors employed on methanogenesis.   | <b>172</b> |
| <b>Figure 5.6</b> | Sulfate (SO <sub>4</sub> <sup>2-</sup> ) reduction and dissolved sulfide (HS <sup>-</sup> ) production.  | <b>174</b> |
| <b>Figure 5.7</b> | Electron donating capacity of <i>Pahokee Peat</i> Humic Substances (PPHS) at the end of each incubation cycle.   | <b>175</b> |
| <b>Figure 5.8</b> | Schematic representation of sulfide chemical reaction and CH <sub>4</sub> oxidizing/HS reducing microbial communities competing for the reduction of the functional moieties in Humic Substances (PPHS). | <b>178</b> |

#### **Figures presented in CHAPTER VI**

|                   |  |            |
|-------------------|--|------------|
| <b>Figure 6.1</b> | SCOPUS based search on the scientific interest in the Anaerobic Oxidation of Methane process.  | <b>187</b> |
| <b>Figure 6.2</b> | Compendium of thermodynamic feasibility and stoichiometry of environmentally relevant reactions driven by humic substances (HS) with a potential impact on the emission of greenhouse gases: CH <sub>4</sub> and N <sub>2</sub> O.           | <b>195</b> |
| <b>Figure 6.3</b> | Schematic representation of theoretical cycles of Humics Substances (HS) oxidation by oxygen (O <sub>2</sub> ) perpetuating the anaerobic oxidation of methane (AOM) during several cycles in a hypothetical recurrently anoxic environment. | <b>197</b> |
| <b>Figure 6.4</b> | Potential bio and bio-electrochemical technologies based on the capabilities of quinone/HS reducing, CH <sub>4</sub> oxidizing microorganisms.   | <b>199</b> |
| <b>Figure 6.5</b> | Placement of the scientific contributions made in this thesis within the 20 years of research on the role of redox-active organic compounds (RAOMs) in ecologically relevant reactions   | <b>203</b> |

## List of Abbreviations

|   |   |
|---|---|
| <b>AH<sub>2</sub>QDS:</b> anthrahydroquinone-2,6-disulfonate                                  | <b>ESEM:</b> Environmental scanning electron microscopy       |
| <b>AQDS:</b> anthraquinone-2,6-disulfonate  | <b>FA:</b> fulvic acid  |
| <b>AQS:</b> anthraquinone-2-sulfonic acid or 9,10-anthraquinone-2-sulfonic acid               | <b>FTIR:</b> Fourier-transform infrared spectroscopy          |
| <b>AOM:</b> anaerobic oxidation of methane  | <b>GC:</b> gas chromatograph                                  |
| <b>ANAMMOX:</b> anaerobic oxidation of ammonium   | <b>GHG:</b> Greenhouse gases                                  |
| <b>ANME:</b> anaerobic methanotrophic archaea   | <b>GW:</b> Global warming                                     |
| <b>DAMO:</b> denitrifying anaerobic oxidation of methane                                      | <b>HA:</b> Humic acids  |
| <b>DIET:</b> direct inter-species electron transfer   | <b>HOM:</b> humus oxidizing microorganism                     |
| <b>DHVEG:</b> Deep Sea Hydrothermal Vent Group  | <b>HRM:</b> humus reducing microorganism                      |
| <b>DNA:</b> deoxyribonucleic acid   | <b>HS:</b> Humic substances                                   |
| <b>DOM:</b> dissolved organic matter  | <b>ICDD:</b> International Center of Diffraction Data         |
| $\Delta G^\circ$ : Standard Gibbs free energy (units = kJ mol <sup>-1</sup> )                 | <b>ICP:</b> inductively coupled plasma                        |
| $E^\circ$ : Standard redox potential (units = mV, V)  | <b>IET:</b> inter-species electron transfer                   |
| <b>EAC:</b> electron accepting capacity   | <b>IHSS:</b> International Humic Substances Society           |
| <b>ED:</b> electron donor   | <b>MBGD:</b> Marine Benthic Group D                           |
| <b>EDC:</b> electron donating capacity  | <b><i>mcrA</i>:</b> methyl-coenzyme A reductase encoding gene |
| <b>EDS:</b> Energy dispersive spectroscopy  | <b>MCG:</b> Miscellaneous Crenarchaeotic Group                |
| <b>EET:</b> extracellular electron transfer   | <b>MGBD:</b> Marine Benthic Group B                           |
| <b>e<sup>-</sup> eq:</b> electron-equivalents (meq, milli electron equivalents... and so on). | <b>MOB:</b> methane oxidizing bacteria (aerobic).             |
|   | <b>MS:</b> mass spectroscopy                                  |

**NAST:** nearest alignment space termination  
**NOM:** natural organic matter  
***nosZ*:** nitrous oxide reductase type II encoding gene  
**OTU:** operational taxonomic unit  
**PCR:** polymerase chain reaction  
**POM:** particulate organic matter  
**PPHS:** *Pahokee Peat* humic substances  
**Q:** quinone  
**Q-HS<sub>ox</sub>:** quinone moiety in oxidized humic substances  
**QH<sub>2</sub>:** hydroquinone  
**QH<sub>2</sub>-HS<sub>red</sub>:** hydroquinone moiety in reduced humic substances

**QUIET:** quinone-mediated extracellular electron transfer  
**RAOM:** Redox-active organic molecules  
**RC-I:** Rice Cluster I  
**SRB:** sulfate-reducing bacteria  
**SR-AOM:** sulfate-reduction dependent AOM  
**TC:** total carbon  
**TOC:** total organic carbon  
**TIC:** total inorganic carbon  
**VSS:** volatile suspended solids  
**XPS:** X-ray photoelectron spectroscopy  
**XRD:** X-ray diffraction

## Agradecimientos

Quiero agradecer a todas aquellas personas que jugaron un rol como mis mentores. Desde 2012 que ingresé a IPICYT como tesista de licenciatura, el personal académico y técnico no solo de la DCA, sino también de la DBM y DMA, han contribuido fundamentalmente a mi formación académica, y por supuesto, a mi formación personal. En especial, quiero agradecer a los docentes del área de Biotecnología e Ingeniería Ambiental, con quienes compartí más tiempo en forma de clases, seminarios y/o tutorías, por tanto, de quienes obtuve una mayor influencia. Quiero mencionar explícita y especialmente mi gratitud hacia mi comité tutorial integrado por el Dr. César Nieto, el Dr. Frederic Thalasso (CINVESTAV), la Dra. Sonia Arriaga (mí también directora de tesis de licenciatura) y el Dr. Francisco Cervantes (mi director de tesis de maestría y doctorado). Gracias por todos los comentarios, consejos, discusiones, tiempo invertido, etc.

Dr. Cervantes, gracias por darme la oportunidad de trabajar en su equipo, de tener la apertura para permitirme expresar mis puntos de vista, ejecutar mis decisiones, y de ir desarrollando un criterio propio. Gracias por permitir que las diferentes piezas mi proyecto de investigación tomaran rumbos propuestos por mí. Sin duda esto ha resultado en una consolidación de la confianza mí mismo, en mis conocimientos, y en mis ideas. Creo que estos aspectos son indispensables para desarrollarme en el futuro como un investigador y, en ese sentido, termino el doctorado sintiéndome capaz. Sepa que he aprendido de usted en un sentido más allá del académico y en todo el espectro del aprendizaje, eso es invaluable.

To Andreas Kappler, my advisor during my short-research stay in beautiful and magical Tübingen, I want to thank the openness to give a Mexican PhD student a space to work in your excellent and brilliant research group. From the experience in your lab and country I took nothing but invaluable experiences which have enriched me as a person and as a scientist. Vielen Dank!

Una parte importante de los resultados plasmados en esta tesis fue posible gracias al trabajo realizado por Karen Avendaño y Claudia Padilla durante la realización de sus trabajos de tesis de licenciatura y maestría respectivamente. Agradezco su esfuerzo, paciencia y muchas valiosas enseñanzas que obtuve mediante estas primeras experiencias como mentor.

Quiero también hacer un agradecimiento especial a las Dra. Esmeralda López Lozano, Katy Juárez, Leticia Vega Alvarado y a los Dres. Sergio Casas Flores, Nicolás Gómez y Alberto Hernández Eligio sin quienes la parte molecular de esta tesis no hubiera sido posible. Gracias por su apertura, aportación y disponibilidad.

La realización de los experimentos descritos en esta tesis no hubiese sido posible sin el apoyo técnico de Ma. Del Carmen Rocha Medina, Ma. Guadalupe Ortega, Dulce Partida, Juan Pablo Rodas, Dra. Angélica Aguilar, Elizabeth Cortés Cedillo, Mario Cardozo, Guillermo Vidriales (DCA), Beatriz Rivera Escoto, Ana Iris Peña Maldonado, Dra. Mariela Bravo (DMA), Ellen Röhm, Lars Grimm, Annette Flicker y Judith Melhorn (Uni Tuebingen), gracias por el apoyo.

Agradezco al personal administrativo y de la oficina de posgrado de IPICYT. Lupita Arriaga asistente de la DCA y una de las personas más trabajadoras que conozco. Ivonne Cuevas, Edith Rodríguez y Tere Casas, quienes nos facilitan tanto las cosas a los estudiantes y sin quienes el posgrado no sería funcional, muchas gracias.

Agradezco también a mis compañeros de posgrado, quienes además de ser muy queridos amigos, aportaron o fueron el detonante de algún pensamiento o idea que influenció de alguna manera algún aspecto de mi trabajo de tesis. En este sentido puedo mencionar a Erika Ríos, Emilia Ríos del Toro y Santiago Cadena, quienes hemos tenido en común el reto de enfrentarnos a la complejidad química y biológica de los sedimentos de distintos ecosistemas. Al ser foráneo en SLP y también durante mi estancia en Tuebingen, los amigos han sido como mi familia durante estos años. En ese sentido me siento extremadamente afortunado de haber tenido como compañeros de generación de maestría, de cubículo(s), de laboratorio y de equipo de trabajo (Cervantes' Team) a todos quienes estuvieron y a quienes no podría nombrar sin que se me escapara algún nombre. De IPICYT me llevo amistades de por vida, tal vez eso sea lo que más agradezco a la institución, haberme hecho coincidir con gente que tanto aprecio, admiro y que forma parte tan importante de mi vida.

Finalmente quiero agradecer y dedicar esta tesis a mi familia. Agradecer por la larga espera, la ausencia, la tolerancia y la paciencia, pero principalmente, por haberme formado como persona y de esa y otras maneras (que implicaron incalculable sacrificio) haberme ayudado a llegar hasta este punto. Los amo y este trabajo, así como todo lo demás (de utilidad) que hago en la vida es por y para ustedes.

**Edgardo I. Valenzuela**

**San Luis Potosí, diciembre 2019**

## Summary

Edgardo I. Valenzuela. 2019. **Microbial Processes Driven by the Redox Capacity of Natural Organic Matter Suppress the Emission of Greenhouse Gases in Wetland Sediments**. Doctoral Thesis, Instituto Potosino de Investigación Científica y Tecnológica A.C, San Luis Potosí, Mexico.

**R**edox-active organic molecules (RAOMs) commonly referred to as *humus* or *humic substances* (HS), represent a fair amount of the carbon stored for hundreds of years through decomposition processes in several ecosystems. Because of the high reactivity that these substances possess, which is given by its high content in electron donating and accepting moieties (redox functional groups), they can mediate several chemical and biological reactions in nature. Within the numerous transformations that these substances may elicit, the linking of global biogeochemical cycles, such as the C, Fe, S and N cycles could result in the suppression of greenhouse gases (GHG) produced via microbial processes. Our hypotheses were based on the fact that HS *reducing*, or *oxidizing* microorganisms, could employ GHG, such as methane (CH<sub>4</sub>) or nitrous oxides (N<sub>2</sub>O) as electron donor or acceptor, respectively, thus providing additional mechanisms of GHG suppression in organotrophic systems, such as wetlands. Despite this potential, little information was available about the role that this RAOMs and related microorganisms could play as GHG sinks. This lack of information inspired the goal of this dissertation, summarized herein, which was to overcome the existing knowledge gaps by **(i)** proving that the microbiota of wetland sediments could employ humic material as terminal electron acceptor for achieving anaerobic methane oxidation, **(ii)** provide evidence on electron shuttling mediated by humic substances supporting CH<sub>4</sub> oxidation with metal oxides as terminal electron

acceptors, **(iii)** elucidating the potential of HS to link GHG consumption ( $\text{CH}_4$  and  $\text{N}_2\text{O}$ ) by promoting inter-species electron transfer and **(iv)** evaluating the effect of a sulfur cryptic cycle promoted by HS on the anaerobic oxidation of methane.

In the first part of my PhD research, it was tested if the microorganisms present in sediments collected from a coastal wetland were able to employ  $\text{CH}_4$  as the electron donor to reduce both a structural analogue of HS (anthraquinone-2,6-disulfonate, AQDS) and the sediment's intrinsic RAOMs. Furthermore, we identified the enrichment of specific bacterial and archaeal phylotypes  $\text{CH}_4$  oxidizing/quinone reducing selective conditions. These results, as well as those anaerobic methane oxidation (AOM) kinetics obtained by inhibition-based tests allowed to propose a mechanism for AOM which involves archaea in a broader spectra than the common ANME lineages, the decoupling of archaea from sulfate-reducing bacterial partners, as well as natural organic matter (NOM) acting not only as an electron sink but also as a substrate for methanogenesis (these results are presented in **Chapter II**).

In the second part of this dissertation (**Chapter III**), it is shown how two sources of HS with distinct chemistry and redox properties could act as electron shuttles for microorganisms to carry out AOM with iron oxides of distinct crystallinity as electron acceptors. Furthermore, it was demonstrated how these RAOMs additionally promoted the sequestration of carbon dioxide ( $\text{CO}_2$ ) coming from  $\text{CH}_4$  mineralization by eliciting the precipitation of iron carbonates due to the parallel enhanced iron reduction. These findings show how a relevant mechanism of AOM in wetland sediments, which links the C and Fe cycles, can be hindered by geochemical phenomena triggered by the geochemical conditions prevailing.

In the third part of my PhD research, the capability of microorganisms presents in wetland sediments to consume not only  $\text{CH}_4$  but also  $\text{N}_2\text{O}$  in a coupled manner was evaluated. Evidence is provided demonstrating that HS establish a link between methanotrophic and nitrous oxide reducing microorganisms allowing

AOM to be dependent of N<sub>2</sub>O reduction. These results, presented in **Chapter IV**, are the first demonstration of an inter-species electron transfer mechanism, which uses RAOMs to allow normally non-compatible microbial synergism resulting in diminished CH<sub>4</sub> and N<sub>2</sub>O emissions. Furthermore, N<sub>2</sub>O reducers were identified through cloning methodologies and proposed as potential oxidizers of reduced RAOMs.

For the last part of this research, in **Chapter V**, the objective was to decipher if HS could trigger a cryptic cycling of sulfur, which would result in a positive feedback to sulfate dependent AOM. It was observed that even though HS can oxidize sulfide to oxidized sulfur compounds, *i.e.* thiosulfate, and thus potentially promoting further methane oxidation, AOM was mainly fueled by HS in wetland sediments. Consequently, chemical reduction of the redox moieties in HS would result in a competing process for CH<sub>4</sub> oxidizing/HS reducing microorganisms having a negative impact in the overall rates of CH<sub>4</sub> consumption.

Altogether, the pieces of evidence gathered in this work, which link microbial and chemical processes in the C, Fe, N and S biogeochemical cycles, urge to perform further research to fully decipher the mechanisms by which HS elicit processes mitigating the emission of greenhouse gases to the atmosphere. Knowledge of this nature is critical to assess the autoregulation capacities that microbes possess to lessen GHG emissions and thus assessing their potential impact in current and future scenarios of climate change.



## Resumen

Edgardo I. Valenzuela. 2019. **Rol de los Procesos Microbianos Promovidos por la Capacidad Redox de la Materia Orgánica Natural en la Supresión de la Emisión de Gases de Efecto Invernadero por Sedimentos de Humedales.** Tesis Doctoral, Instituto Potosino de Investigación Científica y Tecnológica A.C, San Luis Potosí, México.

Las moléculas orgánicas con actividad redox (MOAR) históricamente conocidas como *humus* o *sustancias húmicas* (HS), representan una cantidad colosal del carbono almacenado durante cientos de años a través de procesos de descomposición de materia orgánica natural (MON) en diversos ecosistemas. Debido a la reactividad que poseen estas sustancias, que les es conferida por su alto contenido en grupos funcionales donadores y aceptores de electrones (grupos funcionales redox), éstas pueden mediar diferentes reacciones químicas y biológicas en la naturaleza. Dentro de las numerosas transformaciones que estas sustancias en las que estas sustancias pueden participar, la conexión de los ciclos biogeoquímicos, tales como los ciclos del C, Fe, S y N, podría conllevar a la supresión de la emisión de los gases de efecto invernadero (GEI) producidos a través de procesos microbianos de manera natural en los ecosistemas. Las hipótesis planteadas en esta tesis se basaron en el hecho de que los microorganismos reductores y oxidantes de las SH podrían emplear GEI como el metano (CH<sub>4</sub>) o el óxido nitroso (N<sub>2</sub>O) como donador o aceptor de electrones respectivamente, proporcionando así mecanismos adicionales de supresión de GEI en sistemas organotróficos como los humedales. A pesar de este potencial, hasta el momento en el que esta tesis fue concebida, se disponía de información limitada sobre el papel que podrían desempeñar estas sustancias y los microorganismos con capacidad de utilizarlas por sus capacidad redox en el contexto de los sumideros

biológicos de GEI. Esta falta de información inspiró el objetivo de esta investigación de tesis, que en resumen consistía en superar las brechas de conocimiento existentes al **(i)** demostrar que la microbiota de un sedimento de humedal podría emplear material húmico como aceptor terminal de electrones para la oxidación anaerobia de metano, **(ii)** proporcionar evidencia sobre la transferencia de electrones mediada por sustancias húmicas propiciando la oxidación de CH<sub>4</sub> con óxidos metálicos como el sumidero de electrones, **(iii)** dilucidando el potencial de las SH para propiciar el consumo simultáneo de CH<sub>4</sub> y N<sub>2</sub>O al promover procesos de transferencia de electrones inter-especies y **(iv)** evaluar el efecto de los ciclos crípticos de azufre promovidos por SH en la oxidación anaerobia de metano.

En la primera parte de este proyecto doctoral, se evaluó si los microorganismos presentes en los sedimentos de un humedal costero podían emplear CH<sub>4</sub> como donador de electrones para reducir, no solo un análogo estructural (antraquinona-2,6-disulfonato) y una fuente purificada de HS (SH *Pahokee Peat*), sino también las MOAR intrínsecas del sedimento. Además, se detectó el enriquecimiento de filotipos bacterianos y de arquea específicos bajo condiciones de presión selectiva, basados en esto y en resultados obtenidos a partir de pruebas basadas en inhibición de la sulfato-reducción; se propuso un mecanismo para la oxidación anaerobia de metano (OAM) en humedales que involucra arqueas en un espectro más amplio que aquel que sólo considera los linajes de ANME, el desacoplamiento de arqueas del compañero bacteriano sulfato reductor y a la MON tanto como sustrato para metanogénesis (fracción lábil) así como un sumidero de electrones (fracción recalcitrante con propiedades redox). Estos resultados son presentados en el **Capítulo II**.

En la segunda parte de esta disertación (**Capítulo III**), se comprobó cómo dos fuentes de SH con distintas propiedades redox fungieron actuar como transportadores de electrones para que los microorganismos llevaran a cabo la

OAM con óxidos de hierro de distinta cristalinidad como aceptor terminal de electrones. Además, se demostró cómo simultáneamente éstas MOAR promovieron el secuestro de dióxido de carbono ( $\text{CO}_2$ ) proveniente de la mineralización de  $\text{CH}_4$  al inducir la precipitación de carbonatos de hierro debido a las mayores tasas de hierro reducción. Estos hallazgos muestran cómo un mecanismo relevante de OMA en los humedales que une los ciclos C y Fe puede verse obstaculizado por fenómenos geoquímicos provocados por el contexto geoquímico.

En la tercera parte de esta investigación de doctorado, se puso a prueba la capacidad de la biota de humedal para consumir no solo  $\text{CH}_4$  sino también  $\text{N}_2\text{O}$  de manera acoplada. Se proporciona evidencia de que las SH establecen un vínculo entre los microorganismos reductores de óxido nitroso y los microorganismos metanotróficos, el cual que permite que la OAM sea dependiente de la reducción de  $\text{N}_2\text{O}$ . Estos resultados, presentados en el **Capítulo IV**, son la primera demostración de un mecanismo de transferencia de electrones inter-especies que utiliza los grupos funcionales característicos de las MOAR para permitir un sinergismo microbiano normalmente no compatible que resulta en una supresión simultánea de emisiones de  $\text{CH}_4$  y  $\text{N}_2\text{O}$ . Además, los reductores de  $\text{N}_2\text{O}$  se identificaron mediante metodologías de clonación y se propusieron como posibles oxidantes de SH.

Para la última parte de esta investigación, en el **Capítulo V**, el objetivo fue dilucidar si las SH pudieran desencadenar un ciclo críptico de azufre que resultara en una retroalimentación positiva para la OAM dependiente de la reducción de aceptores de electrones azufrados. Descubrimos que a pesar de que las SH pueden oxidar el sulfuro disuelto a compuestos de azufre oxidados, p. ej., tiosulfato, y por lo tanto suscitar mayores tasas de OAM, el consumo biológico de  $\text{CH}_4$  por la microbiota del humedal fue impulsado principalmente por la humus-reducción. En

consecuencia, la reducción química de los grupos funcionales de las SH resultaría en un proceso competitivo para la oxidación de CH<sub>4</sub> dependiente de la reducción de SH que se vería reflejado como un impacto negativo en las tasas de consumo de CH<sub>4</sub>.

En conjunto, la evidencia reunida en este trabajo y que vincula aspectos microbianos y químicos no solo del ciclo biogeoquímico del C, sino también del Fe, N y S, señalan la necesidad de llevar a cabo más investigación de mayor profundidad que dé como resultado un conocimiento profundo sobre los mecanismos mediante el cual las SH puede desencadenar procesos mediante los cuales se define la cantidad neta de GEI que se libera a la atmósfera de la Tierra debido a procesos microbiológicos. El conocimiento de esta naturaleza es fundamental para evaluar las capacidades de autorregulación que poseen las comunidades microbianas para disminuir sus emisiones de GEI y, por lo tanto, evaluar el impacto potencial que estas fuentes naturales pueden tener en los escenarios actuales y futuros del cambio climático.

# CHAPTER I

## INTRODUCTION

# Redox-Active Organic Molecules as Key players in the Suppression of the Emission of Greenhouse Gases

### HIGHLIGHTS

- **Redox-active organic molecules (RAOMs)** *i.e. humic substances (HS)* mediate numerous ecologically important reactions in the environment.
- 20 years of research pinpoint the importance of RAOMs in **suppressing the emission of greenhouse gases (GHG)**.
- Several **phylogenetically diverse archaea and bacteria** are involved in GHG suppressing reactions mediated by RAOMs.
- **New mechanisms** of CH<sub>4</sub> and N<sub>2</sub>O emission **suppression by HS** are proposed in this Thesis.

## Abstract

Redox-active organic molecules (RAOMs) historically known as *humus* or *humic substances* (HS) represent an operationally defined fraction of *natural organic matter* with plentiful outstanding physical and chemical properties. Because of their versatility and functionality, HS have been thoroughly investigated for their use in several technological fields. However, one of the most invaluable assets of these naturally produced RAOMs in nature is their ecological function derived from the several mechanisms in which they can intervene in global biogeochemical cycles. This introduction summarizes the current body of knowledge about how HS, the often overlooked, nonetheless principal, represent a pivotal player in the microbial suppression of emission of greenhouse gases (GHG) from aquatic ecosystems. Due to their exceptional redox properties, beyond suppressing methane emissions coming from microbial decomposition of organic matter (*methanogenesis*), HS can function as the electron sink for globally relevant reactions, such as *anaerobic oxidation of methane* (AOM). Also, by enhancing microbe-metal and/or microbe-microbe interactions, HS can further catalyze metal-dependent AOM or link microbial GHG consuming reactions by enabling inter-species electron transfer. This chapter also underlines the active role of HS in the sulfur cycle, and how the triggered cryptic reactions might affect methane and carbon dioxide dynamics in ecosystems.

## 1.1 What are Humic Substances

*Humic substances* (HS), also known as *humus* or *humic material*, are complex organic compounds which main characteristics are their intricate chemical structure, dark color, richness in redox functional moieties, and resistance to biodegradability<sup>1</sup>. HS are naturally produced and stored in environments in which chemical, enzymatic and microbial processes slowly and incessantly degrade carbonaceous compounds leaving behind this kind of residue. This process has been named *humification* (**Fig. 1**)<sup>1</sup>. Several ecosystems (aquatic and terrestrial) constitute the ideal niche in which humus is formed and preserved during large periods of time, thus HS are believed to be *ubiquitous* in the environment<sup>2</sup>. As an example, it has been estimated that about  $1600 \times 10^{15}$  g of the total biosphere's carbon pool is stored as HS (70% of the soil NOM)<sup>3</sup>. This represents up to 90% of the carbon stored in wetlands and similar freshwater ecosystems and around 0.7-2.4% of *dissolved organic matter* (DOM) in the ocean. Because of the differences on their origin and diagenesis, HS may present variations on their chemical composition, molecular weight, and structure; meaning that there is no general chemical formula for HS<sup>4</sup>. Recently, several reports have challenged general assumptions about the traditional concept and properties of HS. On one hand, Lehman and Kleber<sup>5</sup> have proposed to consider a *continuum of progressively decomposing organic compounds* due to the lack of evidence supporting the formation of HS in soils via the proposed humification model. On the other hand, a couple studies have demonstrated how this *by default* considered recalcitrant molecules can indeed be microbially degraded by fungi or complex organic carbon degrading bacteria<sup>3,6,7</sup>. Furthermore, the utilization of commercial humic acids (HA, a fraction of HS) as electron donor by the biota of a methane producing wetland

sediment did promote methanogenesis and the proliferation of fermenting bacteria suggesting the biodegradation of a fraction of this humic material<sup>8</sup>.

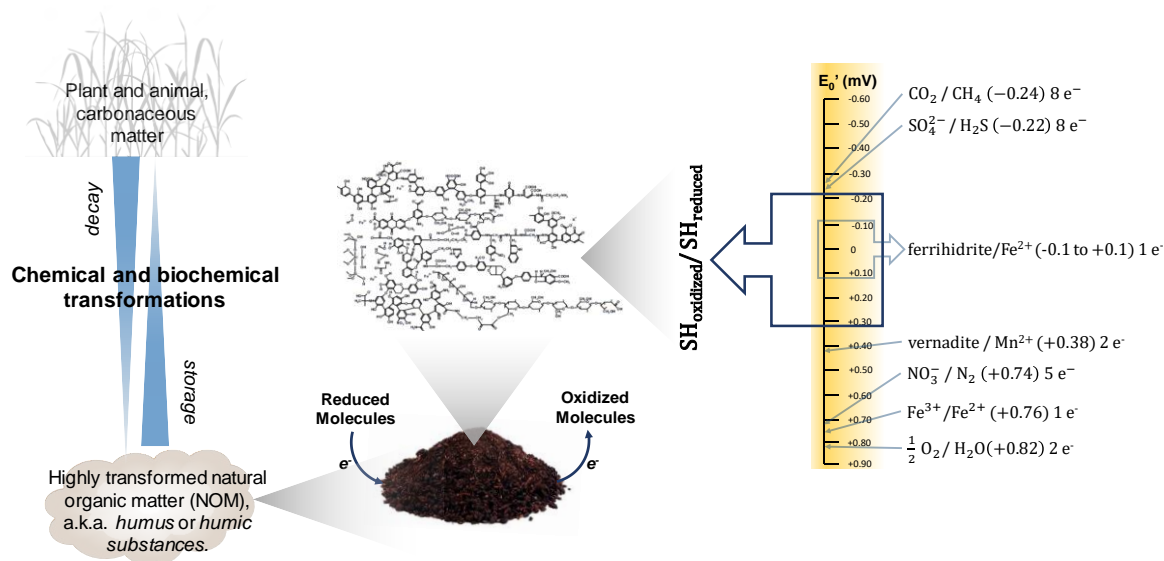


**Fig. 1.1 | Schematic representation of the formation, structure and redox-properties of humic substances, the most important redox-active organic molecules in the environment.** Through chemical and biotic degradation, the highly decomposed organic fraction traditionally known as *humus*, continuously accumulates in organic-rich ecosystems in which it participates in numerous ecologically relevant processes due to the wide range of redox potential given by its functional moieties.

Taking these new approaches into consideration, and considering how some authors have referred to HS *i.e.* as the highly transformed fraction of *natural organic matter* (NOM) with capacity to accept electrons (redox-active)<sup>8</sup>, as organic acids<sup>9</sup>, or as continuously decomposing organic compounds<sup>5</sup>, we will define and often refer to HS as *redox-active organic molecules* (RAOMs) according to the purposes of this dissertation.



### 1.1.1 The Redox Properties of Humic Substances

Because of the many properties that HS display, such as sorption, retention, chelating, and binding properties, they have been subject of research on several fields during almost the whole last century (**Fig. 1.2**). Biological sciences, such as biotechnology and environmental microbiology fields, have thoroughly focused on the development of new technologies to tackle environmental priority issues related to the removal of several kinds of pollutants from wastewater and soils by using HS<sup>10,11</sup>. Most of these developments rely on one of the most exploitable properties of humus, its redox activity<sup>12</sup>.

One of the primordial characteristics of these compounds, is the richness in chemical groups placed at the periphery of their aromatic structural core (**Fig. 1.1**)<sup>13,14</sup>. These moieties can differ in number, chemistry, availability, and redox properties depending on the source of the humic material, thus resulting on a range of redox-potential, reactivity, and *electron accepting capacity* (EAC), which can be very variable amongst the radically different sources of these kinds of RAOMs (**Table 1.1**).

## CHAPTER I

**Table 1.1** | Examples of the variability of the electron accepting capacity of several types of humic materials extracted from natural settings as well as from commonly used sources of humic and fulvic acids commercially available.

| Kind of humic material or Commercial name                              | Source of extraction/Provider                 | EAC*  | Reference  |
|--|---|---|--|
| DOM <sup>†</sup>   | Mer Bleue bog, Ottawa, Canada                 | 0.2 – 6.1 meq** e <sup>-</sup> g <sup>-1</sup> C                      | Heitmann <i>et al.</i> , 2007 <sup>15</sup>                |
| Suwanee River fulvic acid (FA <sup>‡</sup> )                           | Okefenokee Swamp, South Georgia, USA          | ~0.2 µeq*** e <sup>-</sup> g <sup>-1</sup> C                          | Jiang and Kappler, 2007 <sup>16</sup>                      |
| Suwanee River humic acid (HA <sup>§</sup> )                            |   | ~1 µeq e <sup>-</sup> g <sup>-1</sup> C                               |  |
| HA Sodium Salt   | Sigma-Aldrich                                 | ~2 µeq e <sup>-</sup> g <sup>-1</sup> C                               |  |
| Suwanee River II HA (Standard)   | Okefenokee Swamp, South Georgia, USA (IHSS)   | 0.96 meq e <sup>-</sup> g <sup>-1</sup>                               |  |
| Elliott Soil HA (Standard)   | Joliet, Illinois, USA (IHSS)                  | 1.96 meq e <sup>-</sup> g <sup>-1</sup>                               |  |
| Pahokee Peat HA (Standard)   | Florida Everglades, Miami, USA (IHSS)         | 1.68 meq e <sup>-</sup> g <sup>-1</sup>                               |  |
| Leonardite HA (Standard)   | Gascoyne Mine, North Dakota, USA (IHSS)       | 1.71 meq e <sup>-</sup> g <sup>-1</sup>                               | Aeschbacher <i>et al.</i> , 2010 <sup>12</sup>             |
| Nordic Lake HA (Reference)   | Vallsjøen, Skarnes, Norway (IHSS)             | 1.2 meq e <sup>-</sup> g <sup>-1</sup>                                |  |
| Waskish Peat HA (Reference)  | Minnesota, USA (IHSS)                         | 0.98 meq e <sup>-</sup> g <sup>-1</sup>                               |  |
| Pony Lake FA (Reference)   | Antartica (IHSS)                              | 0.49 meq e <sup>-</sup> g <sup>-1</sup>                               |  |
| HA   | Drained thaw lake basin near Barrow Alaska    | 0.2 – 0.5 meq e <sup>-</sup> g <sup>-1</sup>                          | Lipson <i>et al.</i> , 2013 <sup>17</sup>                  |
| HA   | Ancient basin                                 | 0.38±0.13 meq e <sup>-</sup> g <sup>-1</sup>                          |  |
| HA   | Sigma-Aldrich                                 | 0.10 meq e <sup>-</sup> g <sup>-1</sup> dry material                  | Zhang <i>et al.</i> , 2014 <sup>18</sup>                   |
| HA   | Sigma-Aldrich                                 | 2.48 and 1.42±0.02 – 3.35±0.15 µmol e <sup>-</sup> mg C <sup>-1</sup> | Yu <i>et al.</i> , 2015 <sup>19</sup> , 2016 <sup>20</sup> |
| Highly decomposed peat (DOM)   | Neustädter Moor, Germany (cutover bog)        | 9.01±1.74 µmol e <sup>-</sup> (g peat C) <sup>-1</sup>                | Gao <i>et al.</i> , 2018 <sup>21</sup>                     |
| Highly decomposed peat (particulate organic matter, POM <sup>Ω</sup> ) |   | 660.9±8.13 µmol e <sup>-</sup> (g peat C) <sup>-1</sup>               |  |
| Weakly decomposed peat (DOM)   | Mittleres Wietingsmoor, Germany (cutover bog) | 3.64±1.07 µmol e <sup>-</sup> (g peat C) <sup>-1</sup>                | Gao <i>et al.</i> , 2018 <sup>21</sup>                     |
| Weakly decomposed (POM)  |   | 302.9±35.5 µmol e <sup>-</sup> (g peat C) <sup>-1</sup>               |  |
| Long-term oxidized peat material (DOM)                                 | Vechtaer Moor, Germany                        | 10.3±1.52 µmol e <sup>-</sup> (g peat C) <sup>-1</sup>                |  |
| Long-term oxidized peat material (POM)                                 |   | 453.6±16.3 µmol e <sup>-</sup> (g peat C) <sup>-1</sup>               |  |

\*EAC: electron accepting capacity, \*\*meq: mili or \*\*\*µeq: electron micro-equivalents, †DOM: dissolved organic matter, ‡FA: fulvic acids, §HA: humic acids, ΩPOM: particulate organic matter.

## CHAPTER I

The main functional moiety, which confers redox capacity to HS, has been proven to be the *quinone* chemical group<sup>13,14,22</sup>. Depending upon the redox conditions of the environment in which HS can be found, their quinones may be on a fully reduced (*hydroquinone*; QH<sub>2</sub>), fully oxidized (*quinone*; Q), or in an intermediate oxidation state (*semiquinone* radical QH<sup>•</sup>)<sup>23</sup>. Additional non-quinone moieties found in HS are the 1-methyl-2,5-pyrrolidinedione, N-methyl aniline, 3-(methylthio)-propanoic acid, and dimethyl sulfone groups<sup>10,24</sup>. However, due to their predominance in HS, commercially available quinones, such as anthraquinone-2,6-disulfonate (AQDS)<sup>8,25-27</sup>, anthraquinone-2-sulfonic acid (AQS), 5-hydroxy-1,4-naphtoquinone (juglone)<sup>28</sup>, and 2-hydroxy-1,4-naphtoquinone (lawsone)<sup>29</sup> have been traditionally used in experimental settings testing the capability of microorganisms to use HS as electron donor or acceptor.

### 1.1.2 Humus-Reducing and -Oxidizing Microorganisms

Pioneer studies exploring the diversity of microbes capable of using HS and their analogs as electron acceptor<sup>2,30</sup> or donor<sup>31</sup>, revealed that a great diversity of microbes could be able to complete its respiratory chain when oxidizing diverse organic substrates<sup>32</sup>, as well as to reduce oxidized compounds,<sup>33</sup> which includes several important pollutants<sup>10,34</sup>. Specific characteristics of humus-reducing (HRM) and -oxidizing (HOM) microorganisms are: **i)** they can be found in a great diversity of terrestrial and aquatic environments, **ii)** they are phylogenetically diverse (including phylotypes not only from the bacterial, but also from the archaeal domain), and **iii)** they are generally able to reduce or oxidize other electron acceptors or donors, besides HS<sup>35</sup>. Due to these characteristics, these versatile microorganisms can participate in biogeochemical relevant reactions, therefore, linking the C, N, S, Fe, and As cycles (to mention some) by driving or mediating redox reactions and thus thriving in numerous environments. Consequently, HS have been extensively studied with the purpose of taking their potential in environmental and biotechnological applications, comprising areas, such as wastewater treatment and biodegradation of priority pollutants (**Fig. 1.2**). Martínez and colleagues as well as Lipczynska-Kochany (2013, 2018)<sup>10,34</sup>, have extensively reviewed the potential of HRM to be key players in environmentally important fields, such as biodegradation and biotransformation of priority pollutants, including nitro-aromatics, halogenated compounds, and several extensively used dyes. Furthermore, the importance of quinones as promoters for biological energy generation, and nano-catalyst production has also been examined; however, in the last few years the body of knowledge concerning the mechanisms by which HS can intervene in the natural dynamics of microbial GHGs emission has been increasing

considerably (Fig. 1.2). This is of primordial importance due to the current problems of climate change that we as humanity face.

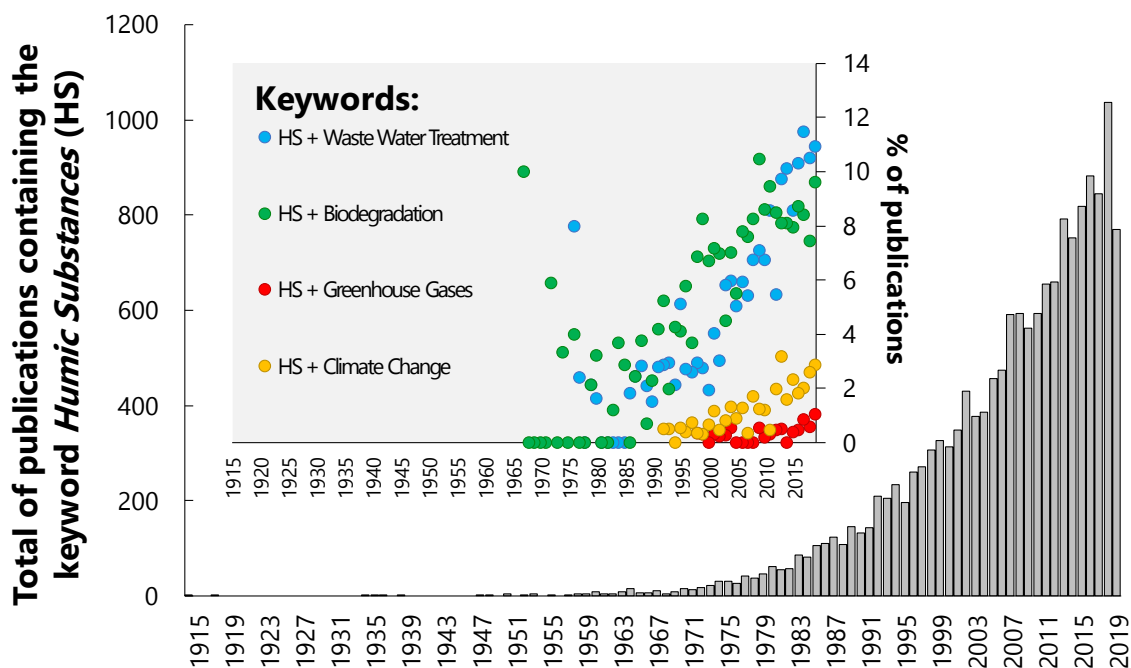


**Fig. 1.2 | SCOPUS based search on the scientific interest in Humic Substances.** The total number of scientific papers published per year in which humic substances is used as a keyword is shown in bars. The insert displays the percentage of papers in which humic substances and other keywords of interest for this dissertation are present within the literature. Calculations were as follows:  $\% = (\# \text{ of papers with the keywords HS and } i. e. \text{ Biodegradation in a year} / \# \text{ of papers with the keywords HS that year}) * 100$ .

## 1.2 Mechanisms for greenhouse gases emission suppression by humus-reducing/oxidizing microorganisms

### 1.2.1 Methanogenesis suppression by Humic Substances

Pioneer studies, which provided the first clues on the role of HS in the suppression of methanogenesis, showed that the anaerobic microbial transformation of halogenated organic pollutants, shifted towards CO<sub>2</sub> production instead of CH<sub>4</sub> generation when an organic rich sediment was supplemented with HS<sup>36</sup>. Later, the inhibition of methanogenesis in sludge and sediment incubations in which volatile fatty acids, hydrogen and phenolic compounds, were used as the substrates, was shown when AQDS was provided since it became the preferred TEA<sup>37,38</sup>. Two mechanisms were proposed as the reason for this effect; on one hand, the oxidation of organic compounds coupled to quinones reduction is thermodynamically more viable than methanogenesis (**Fig. 1.3A and C**); on the other hand, some methanogenic archaea can switch their metabolic pathway towards quinone reduction instead of methanogenesis (**Fig. 1.3B**). This last mechanism was afterwards confirmed by several studies exposing different archaeal phylotypes with this capability (listed in **Table 1.2**) and it was also recently proven in *M. acetivorans* by genetic and transcriptomic analyses<sup>39</sup>.

Several studies aiming to elucidate the dynamics of CH<sub>4</sub> and CO<sub>2</sub> emissions from wetlands, ecosystems that represent the most important natural contributors to the global CH<sub>4</sub> budgets, did observe higher CO<sub>2</sub>:CH<sub>4</sub> ratios than expected from anaerobic decomposition (expected to be 1:1)<sup>40–42</sup>. Keller and colleagues<sup>43</sup> presented the first evidence for suppressed methanogenesis driven by HS in these important environments, by showing that amendment of wetland soils with extracted HS or with commercial source of HS (IHSS, *Pahokee Peat* HS) shifted the

expected CO<sub>2</sub>:CH<sub>4</sub> ratio to much higher values due microbial reduction of HS instead of methanogenesis. Blodau and Deppe (2012)<sup>44</sup> further confirmed these findings in sediments of an ombrotrophic bog.

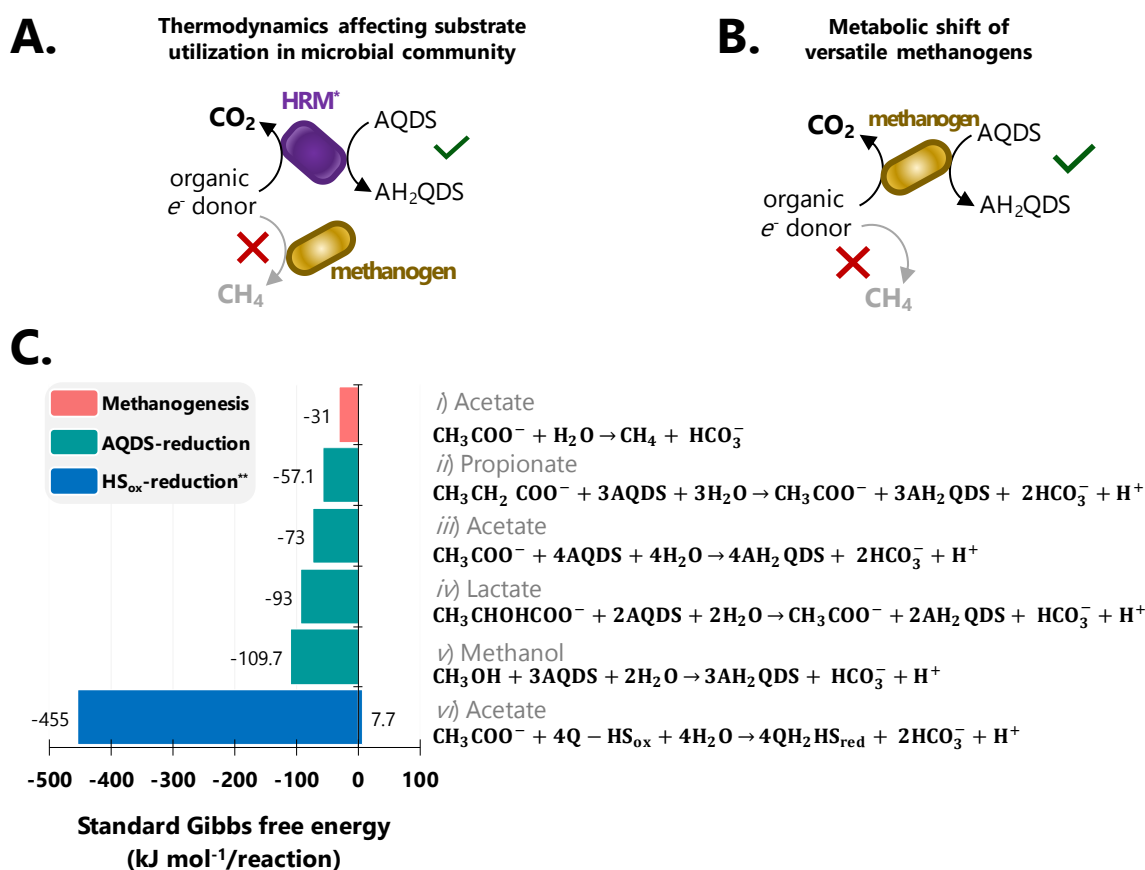


**Fig. 1.3 | Mechanisms for methanogenesis suppression by Humic Substances.**

Superior panels depict the two mechanisms by which HS may suppress methanogenic activity that have been identified so far: AQDS reduction competing for methanogenic substrates due to more favorable thermodynamics **Panel A** (Cervantes *et al*, 2000)<sup>37</sup>, and methanogens switching their metabolic pathway towards quinone reduction, **Panel B** (Cervantes *et al*, 2002)<sup>38</sup>. **Panel C** shows some examples of the higher Gibbs free energy obtained through AQDS and oxidized Humic Substances reduction against the energy obtained through the methanogenic process (modified from Cervantes *et al*

2000<sup>37</sup>). Calculations for acetate oxidation coupled to HS reduction (*Eq. vi*) were done using the Nernst equation, considering 8 electrons transferred towards HS for the complete oxidation of acetate to  $\text{HCO}_3^-$ , and a range of  $E^\circ$  from +300 to -300 mV for HS as proposed by Aeschbacher *et al* (2011)<sup>45</sup> and Straub *et al* (2000)<sup>46</sup>. \*HRM, humus reducing microorganism.

## 1.2.2 Anaerobic methane oxidation driven by microbial reduction of HS

Several indications regarding the documented dynamics of  $\text{CH}_4$  and  $\text{CO}_2$  consuming/producing processes in organotrophic environments, such as wetlands, led to hypothesize that the most abundant electron acceptor in this kind of ecosystem, HS, could fuel anaerobic  $\text{CH}_4$  oxidation (AOM) and thus explaining some inconclusive observations<sup>47</sup>. This hypothesis was supported by: **i**) the high  $\text{CO}_2:\text{CH}_4$  ratios obtained in anoxic sediment incubations<sup>44,48,49</sup>, **ii**) large proportions of AOM activities unexplained by the reduction of traditional inorganic TEA's<sup>50,51</sup> and **iii**) the theoretically physiological capability and energetic feasibility of this process. Regarding the last point, the great diversity and ubiquity of HRM, as well as the wide range of redox-potential of  $\text{HS}^{10}$ , would make the HS-driven AOM process much more feasible than that coupled to sulfate ( $\text{SO}_4^{2-}$ ) reduction, the most common TEA for AOM<sup>52</sup> (**Fig. 1.4D**).

Scheller and colleagues (2016)<sup>53</sup> presented the first evidence demonstrating how an anaerobic methane oxidizing archaeon (ANME), of the 2c clade (from a microbial enrichment coming from a marine sediment) was able to anaerobically oxidize  $\text{CH}_4$  by extracellularly directing electrons towards AQDS and several other artificial TEAs including Sigma-Aldrich HA. Right after, Valenzuela and colleagues (2017, **Chapter II** of this Thesis)<sup>8</sup>, demonstrated how the anaerobic biota of an environmental inoculum taken from a tropical coastal wetland, was able to couple AOM to the reduction of *Pahokee Peat* HS (PPHS) even in the presence of



## CHAPTER I

additional inorganic electron acceptors ( $\text{SO}_4^{2-}$  and  $\text{Fe(III)}$ ) intrinsically present in the sediment. The contribution to mitigating global  $\text{CH}_4$  emissions by this HS-fueled process was estimated to be 1300 Tg of  $\text{CH}_4$  per year considering the global wetland area. Interestingly and contrastingly to that reported by Scheller<sup>53</sup> in analogous AQDS-enriched set-ups, the abundance of ANME, the only archaeal group known to perform AOM activities, was almost undetectable by high-throughput sequencing, thus distinct archaeal groups, such as the Bathyarchaeota, Thaumarchaeota and the Marine Benthic Group D from the Euryarchaeota, were proposed to potentially play a role in the HS-driven AOM process, based on abundances observed via high throughput sequencing (**Fig. 1.4B**). Recently, Bai and colleagues (2019)<sup>54</sup> have demonstrated that another member of the ANME group, the ANME 2-d clade, which was firstly discovered due to its capacity to link AOM to  $\text{NO}_3^-$  reduction<sup>55</sup> and after proven to be capable of reducing Fe and Mn oxides<sup>56</sup>, was also able to couple the methanotrophic process to RAOMs reduction. This discovery reinforces the importance that RAOM may have in the control of the global flux of  $\text{CH}_4$  to the atmosphere and therefore as key players in climate change.

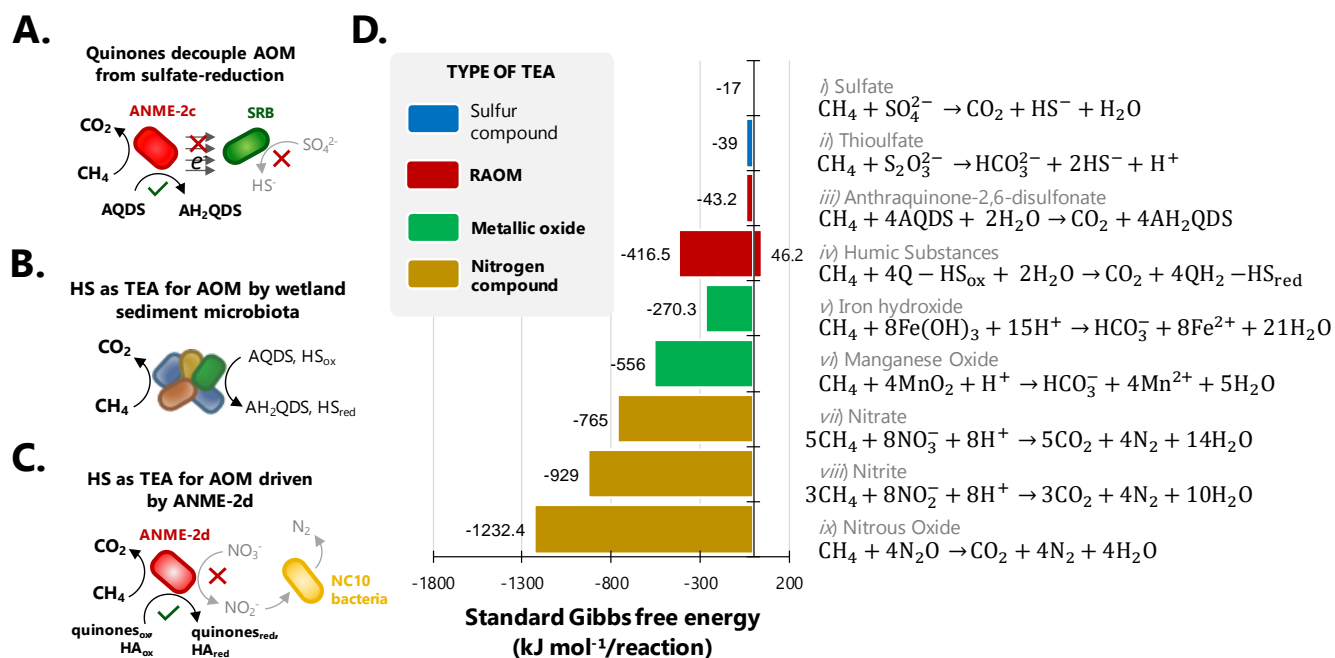


**Fig. 1.4 | Mechanisms for Anaerobic Methane Oxidation driven by Humic Substances.** Panels A to C depict the different scenarios reported in which RAOMs can drive AOM, these include: **Panel A** decoupling from bacterial sulfate-reduction by ANME-2c<sup>53</sup>, **Panel B** NOM and AQDS-driven AOM by the microbial community of a wetland sediment<sup>8</sup> and **Panel C**, displays HA and quinones driven AOM by ANME-2d archaea, which are commonly involved in the nitrogen cycle<sup>54</sup>. Panel D displays a comparison among the thermodynamics of AOM reactions dependent on several electron acceptors. All Gibbs free energy values were taken from previous reports<sup>8,57-59</sup> except for that shown in **Eq. iv** which was calculated using the Nernst equation, considering 8 electrons transferred towards HS for the complete oxidation of CH<sub>4</sub> to CO<sub>2</sub>, and a range of E<sup>o'</sup> from +300 to -300 mV for HS suggested in previous studies<sup>45,46</sup>.

### 1.2.3 Humic substances as electron shuttles for AOM with metallic oxides as TEA

As a follow up to the studies regarding HS-driven AOM, Valenzuela and colleagues (2019, **Chapter III** of this Thesis)<sup>60</sup> provided the first evidence showing that HS could further promote CH<sub>4</sub> oxidation by acting as an electron shuttle and consequently catalyzing the dissimilatory reduction of iron minerals. Goethite and ferrihydrite, two forms of iron oxides of distinct crystallinity that are commonly found in nature, served as TEA for AOM when two distinct sources of HS (*Leonardite*, a coal mine derived humic material, and PPHS) were provided. Besides prompting AOM, it was observed that HS elicited the formation of inert ferrous iron carbonates, such as siderite, thus sequestering a potent GHG by turning it into inert minerals (**Fig. 1.5A**).

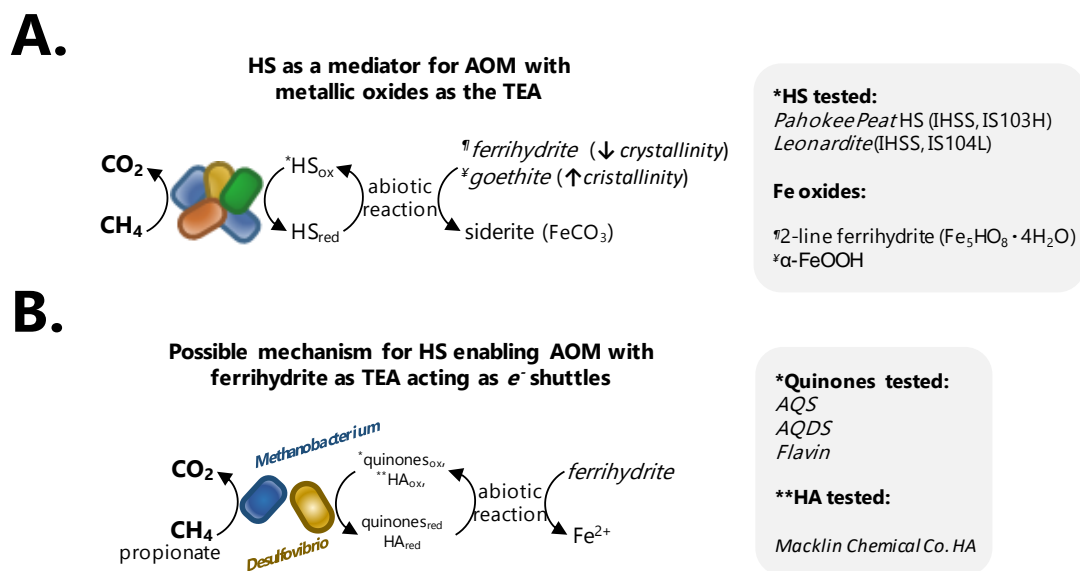


**Fig. 1.5** | RAOMs fueling AOM by shuttling electrons towards iron oxides. Panel A shows the mechanism of carbon burial described by Valenzuela *et al*, 2019<sup>60</sup> in which

## CHAPTER I

different sources of HS served as the electron shuttle for the microbial community of a wetland sediment to perform AOM with iron oxides as the TEA with the concomitant production of inert carbonates. **Panel B** displays the potential archaeal (*Methanobacterium*) and bacterial (*Desulfovibrio*) proposed to carry out this humus-mediated process concomitantly assimilating propionate as C source according to results shown by He *et al*, 2019<sup>61</sup>.

Later, He and colleagues (2019)<sup>61</sup> documented the occurrence of this HS-mediated CH<sub>4</sub> consuming process and observed the predominance of an archaeon from the *Methanobacterium* genera, along with a *Desulfovibrio* bacterium apparently working in syntrophy to carry out this process. It was proposed that *Methanobacterium* could have carried out partially CH<sub>4</sub> oxidation and produced propionate in the process. Therefore, the bacterial partner could have oxidized propionate to CO<sub>2</sub> with the subsequent reduction of ferrihydrite to Fe<sup>2+</sup>. These conclusions were based on the observations of propionate consumption, which exclusively occurred in the presence of 9,10-anthraquinone-2-sulfonic acid (AQS) as an electron carrier concomitantly to CH<sub>4</sub> consumption and ferrihydrite reduction (**Fig. 1.5B**).

Altogether, these studies point out the importance that RAOMs may have by linking the C and Fe cycles through electron shuttling reactions. These discoveries also expand the mechanisms by which Fe, the most abundant metal on Earth may function as a sink for AOM through indirect processes. Previously, microorganisms, such as *Methanoperedens nitroreducens*, have been demonstrated to directly transfer electrons extracellularly towards metallic oxides to accomplish AOM<sup>56</sup>. However, as demonstrated in pioneer studies regarding the electron transferring capacities of HS<sup>23,62</sup>, not all microorganisms are physiologically able to reduce solid extracellular TEAs, such as metallic oxides<sup>63</sup>. Thus, the discovery of methanotrophic

processes that rely on RAOMs as electron shuttles to proceed, expand the possibilities of microbial interactions and niches in which metals, such as Fe and Mn, may help to diminish CH<sub>4</sub> emissions, thus having a huge biogeochemical impact.

#### **1.2.4 Inter-species electron transfer mediated by HS promote GHGs consumption**

Microorganisms employ several mechanisms by which they can overcome individual metabolic restrictions. In order to harvest energy from the degradation of substrates, some microbes are able to extracellularly transfer electrons to microbial partners in a mechanism known as *interspecies electron transfer* (IET)<sup>64</sup>. By this kind of mechanism, different microorganisms, with distinct metabolic capacities, may enable syntrophy *i. e.* sharing the electrons that one microbe harvested from the oxidation of a reduced compound with another organisms, which will use these electrons to reduce a second compound serving as final electron acceptor<sup>65</sup>. However, not every microorganism is able to swap electrons with a partner in a direct manner (*direct interspecies electron transfer*, DIET), some microorganisms require molecules or materials that serve as a bridge for electron transport due to their redox properties.

Quinone-mediated electron transfer (QUIET), is the name given to the process in which two microorganisms share electrons via quinones or quinone-containing materials, such as granular activated carbon, carbon cloths, biochar or HS, which serve as a conductive bridge that enables the electron transporting process<sup>26</sup>. In a similar manner to that in which quinones may catalyze iron reduction through electron shuttling (**Fig. 1.5**), they may link microbial metabolisms *i.e.* ethanol oxidation coupled to fumarate reduction by two species of

*Geobacter* (*G. metallireducens* and *G. sulfurreducens*)<sup>26</sup> or CH<sub>4</sub> production from ethanol consumption by *G. sulfurreducens* and *Methanosaeta*<sup>66</sup>.

Following the same mechanism, Valenzuela *et al*, (*submitted*, **Chapter IV** of this thesis) tested the hypothesis about HS serving as a link between anaerobic methane oxidizers and nitrous oxide reducers via QUIET. Results showed that indeed the microbial community of a coastal wetland sediment could link CH<sub>4</sub> oxidation to N<sub>2</sub>O reduction in a close stoichiometric relationship exclusively when PPHS were present (**Fig. 1.6**).

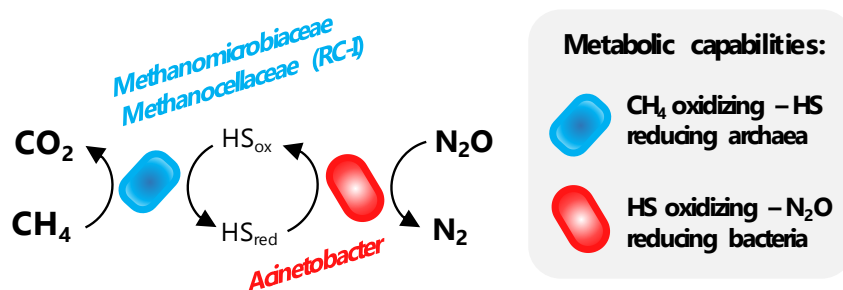


**Fig. 1.6 | Simultaneous CH<sub>4</sub> and N<sub>2</sub>O consumption through an extracellular electron transfer process mediated by the redox-active moieties in Humic Substances.** Methanomicrobiaceae uncultured species and the *Rice Cluster 1* genera (Methanocellaceae family) were the archaeal phylotypes highly enriched and thus proposed to be responsible for the CH<sub>4</sub> oxidation half-reaction. *Acinetobacter* ( $\gamma$ -proteobacteria family) was the most abundant N<sub>2</sub>O reducer seemingly completing the QUIET mediated GHG consuming processes (Valenzuela *et al*, **Chapter IV** of this thesis).

These results are an indication of the potential that HS may have in a global context by suppressing GHG emission via IET processes. Further studies must focus on deciphering additional microbial synergies that could be established through

the QUIET process elicited by humus and the impact that these coupled processes may have in ecosystems, specifically in the cycling of elements.

### 1.2.5 Sulfur cryptic cycling elicited by Humic Substances and its effect on AOM

Previously, some studies gave the first insights on sulfur (S) – NOM interactions with a potential involvement in C cycling and therefore with consequences in CO<sub>2</sub> and CH<sub>4</sub> emissions. Pioneer studies demonstrated that the reaction of dissolved sulfide (HS<sup>-</sup>), the main product from sulfate (SO<sub>4</sub><sup>2-</sup>) reduction, with NOM could result in the incorporation of S into the structure of HS analogs, such as the quinone *Juglone*<sup>28</sup>. Subsequent studies identified that the oxidizing power of the functional moieties of HS could result in the transformation of HS<sup>-</sup> into several sulfurous intermediates, such as elemental sulfur (S<sup>0</sup>)<sup>19</sup> and thiosulfate (S<sub>2</sub>O<sub>3</sub><sup>2-</sup>)<sup>15,67</sup>, as well as incorporation into the organic structure of HS<sup>19,67</sup>.

Heitmann and colleagues (2007)<sup>15</sup>, were the first to discuss the potential effect that S cycling by HS could have in the dynamics of the C cycle, such as organic matter degradation and therefore in CO<sub>2</sub> and CH<sub>4</sub> production. Recently, Valenzuela *et al*, (manuscript in preparation, **Chapter V** of this thesis), demonstrated via chemical assays performed under conditions close to those prevailing in wetland sediment and pore water (pH, temperature, organic matter concentrations and ionic strength), how HS<sup>-</sup> was anoxically oxidized due to the electron accepting moieties of *Pahokee Peat* Humic Substances. The main products of this S cycling process were elemental sulfur (S<sup>0</sup>) and thiosulfate (S<sub>2</sub>O<sub>3</sub><sup>2-</sup>) in that specific order, which agreed with previous studies<sup>15,67</sup> (**Fig. 1.7**).

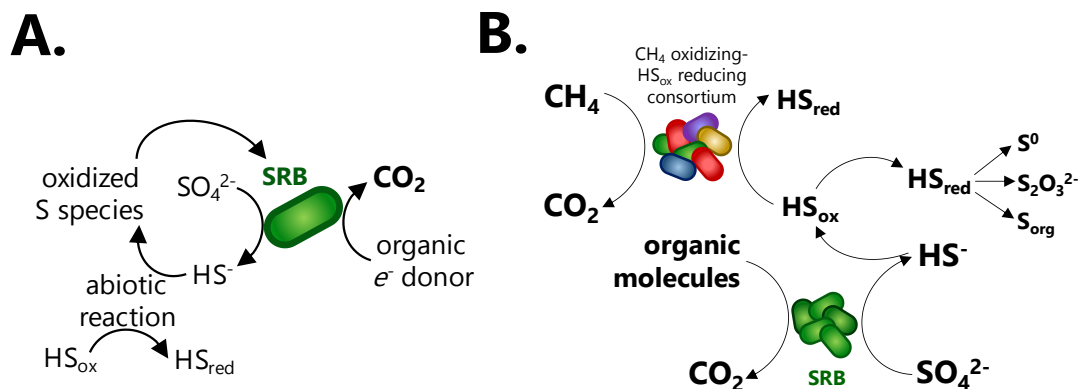


**Fig. 1.7 | Sulfur cycling by Humic Substances (HS) and its effect on anaerobic methane oxidation (AOM).** Panel A displays the model of S cycling by the oxidizing power of HS and the hypothetical positive feedback on sulfate-reducing processes, which would outcompete methanogenesis for electron donors according to Heitmann and colleagues 2006, 2007<sup>15,67</sup>. Panel B shows dissolved sulfide (HS<sup>-</sup>) oxidation and S products formation competing with the HS-dependent AOM process for the oxidized functional moieties of HS as electron acceptors (Valenzuela and colleagues, Chapter V of this thesis).

Additionally, it was verified that sulfur was also incorporated into the organic structure of PPHS by the formation of C-S bonds and thus transforming the chemical and redox properties of the humic material<sup>19,20,68</sup>. Incubation of AOM-performing wetland sediment enriched with SO<sub>4</sub><sup>2-</sup> and/or PPHS as electron acceptors demonstrated that, while methanogenesis suppression occurred due to the extended oxidizing power provided by sulfate, AOM was preferentially driven by humus-reducing microorganisms (**Fig. 1.7**). Furthermore, this humus-dependent methanotrophy was negatively affected by SO<sub>4</sub><sup>2-</sup> reduction due to the chemical reduction of HS and the incorporation of S into the organic humic structure. Although this study fails to prove that indeed a humus-elicited S cryptic cycle could



extend AOM in a microbial culture in which CH<sub>4</sub> oxidation is fueled by S compounds (such as SO<sub>4</sub><sup>2-</sup> or S<sub>2</sub>O<sub>3</sub><sup>2-</sup>), the relevance of this paper resides on the fact that this is the first study evaluating chemical environmental factors, such as the presence of competing electron donors in a process as environmentally relevant as NOM/humus-fueled AOM can be in organotrophic environments.

### 1.3 Scope of the Doctoral Dissertation

Microorganisms are the littlest living entities driving biogeochemical cycles in our planet. Within this context, the *redox active* fraction of natural organic matter, also known as *humic substances*, may play important roles in the suppression of the emission of *greenhouse gases* by eliciting several mechanisms of microbial activity. Since these biological reactions may involve the reduction or oxidation of the redox moieties in this compounds linked to the depletion of potent greenhouse gases such as CH<sub>4</sub> and N<sub>2</sub>O, the main goal of this doctoral dissertation was to describe mechanisms by which humic substances could diminish the emission of CH<sub>4</sub>, N<sub>2</sub>O and CO<sub>2</sub> from wetland sediments.

### 1.4 Hypotheses and Specific Objectives

#### Hypotheses

- By acting as terminal electron acceptor for methanotrophic microorganisms, humic substances could drive the process of anaerobic oxidation of methane. This novel process would represent a missing piece in the understanding of the carbon cycle in environments such as wetlands, the main natural emitters of this potent greenhouse gas.

## CHAPTER I

- The anaerobic oxidation of methane coupled to humic substances reduction, could be further elicited if metallic oxides such as ferric iron minerals act as the terminal electron acceptor by oxidizing the reduced functional groups of humic substances and thus renewing its availability for methanotrophic microbes. This mechanism of humus-prompted *electron shuttling* would link the C and Fe cycles and by consequence expand the extent by which CH<sub>4</sub> emission is suppressed.
- Redox functional groups in humic substances, *i.e.*, quinones, could link the N and C cycles by allowing otherwise non-interacting microbes of *methanotrophic* and *nitrous oxide reducing* metabolisms to establish simultaneous activity via *extracellular electron transfer*.
- Due to its wide range of redox potential, humic substances could intervene in the sulfur cycle by mediating the oxidation of sulfide coming from sulfate-reducing dependent anaerobic methane oxidation. By doing so, additional production of sulfur oxidized compounds could further promote anaerobic methanotrophy fueled by the respiration of sulfur compounds.

### Specific Objectives

- To document the capability of the microbiota of a wetland sediment to link the anaerobic oxidation of methane to the reduction of humic substances and its structural analogues. This includes providing qualitative and quantitative evidence as well as proposing a mechanism considering parallel biological processes (e.g., methanogenesis) and the microbial taxa potentially involved.
- To describe the occurrence of electron shuttling mediated anaerobic oxidation of methane with iron oxides of distinct crystallinity and morphology as the terminal electron acceptors, and proposing the underlying novel mechanism taking into account potential simultaneously occurring chemical processes such as the precipitation of dissolved carbonate and ferrous iron in the form of inert carbonates (e.g., siderite).

## CHAPTER I

- To prove the capability of humic substances to enable the simultaneous consumption of methane and nitrous oxide by mediating the extracellular electron transport between methanotrophic and nitrous oxide reducing microorganisms.
- To test the feasibility of humic substances driving a cryptic cycling of sulfur by provoking the recycling of sulfide coming from sulfate dependent anaerobic oxidation of methane. This includes identifying the organic and inorganic products of sulfide oxidation by humus and evaluating the effect of that this reaction may have on the methanotrophic and methanogenic activities of the microbiota of a wetland sediment.

### 1.5 References

1. **Stevenson, F. J.** Humus Chemistry: Genesis, Composition, Reactions. *Nature* **1983**, *303* (30), 835–836.
2. **Lovley, D. R.**; Coates, J. D.; Blunt-Harris, E. L.; Phillips, E. J. P.; Woodward, J. C. Humic substances as electron acceptors for microbial respiration. *Nature*. 1996, pp 445–448.
3. **Grinhut, T.**; Hadar, Y.; Chen, Y. Degradation and transformation of humic substances by saprotrophic fungi: processes and mechanisms. *Fungal Biol. Rev.* **2007**, *21* (4), 179–189.
4. **MacCarthy, P.** The principles of humic substances: An introduction to the first principle. In *Humic Substances*; 2007.
5. **Lehmann, J.**; Kleber, M. The contentious nature of soil organic matter. *Nature* **2015**, *528* (7580), 60–68.
6. **Ueno, A.**; Shimizu, S.; Tamamura, S.; Okuyama, H.; Naganuma, T.; Kaneko, K. Anaerobic decomposition of humic substances by *Clostridium* from the deep subsurface. *Sci. Rep.* **2016**, *6*, 1–9.
7. **Stern, N.**; Mejia, J.; He, S.; Yang, Y.; Ginder-Vogel, M.; Roden, E. E. Dual Role of Humic Substances As Electron Donor and Shuttle for Dissimilatory Iron Reduction. *Environ. Sci. Technol.* **2018**,

52 (10), 5691–5699.

**8. Valenzuela, E. I.;** Prieto-Davó, A.; López-Lozano, N. E.; Hernández-Eligio, A.; Vega-Alvarado, L.; Juárez, K.; García-González, A. S.; López, M. G.; Cervantes, F. J. Anaerobic Methane Oxidation Driven by Microbial Reduction of Natural Organic Matter in a Tropical Wetland. *Appl. Environ. Microbiol.* **2017**, *83* (11), AEM.00645-17.

**9. Reed, D. C.;** Deemer, B. R.; van Grinsven, S.; Harrison, J. A. Are elusive anaerobic pathways key methane sinks in eutrophic lakes and reservoirs? *Biogeochemistry* **2017**, *134* (1–2), 29–39.

**10. Martinez, C. M.;** Alvarez, L. H.; Celis, L. B.; Cervantes, F. J. Humus-reducing microorganisms and their valuable contribution in environmental processes. *Appl. Microbiol. Biotechnol.* **2013**, *97* (24), 10293–10308.

**11. Field, J. A.** Recalcitrance as a catalyst for new developments. In *Water Science and Technology*; 2001.

**12. Aeschbacher, M.;** Sander, M.; Schwarzenbach, R. P. Novel electrochemical approach to assess the redox properties of humic substances. *Environ. Sci. Technol.* **2010**, *44* (1),

87–93.

**13. Hernández-Montoya, V.;** Alvarez, L. H.; Montes-Morán, M. a.; Cervantes, F. J. Reduction of quinone and non-quinone redox functional groups in different humic acid samples by *Geobacter sulfurreducens*. *Geoderma* **2012**, *183–184*, 25–31.

**14. Scott, D. T.;** Mcknight, D. M.; Blunt-Harris, E. L.; Kolesar, S. E.; Lovley, D. R. Quinone moieties act as electron acceptors in the reduction of humic substances by humics-reducing microorganisms. *Environ. Sci. Technol.* **1998**, *32* (19), 2984–2989.

**15. Heitmann, T.;** Goldhammer, T.; Beer, J.; Blodau, C. Electron transfer of dissolved organic matter and its potential significance for anaerobic respiration in a northern bog. *Glob. Chang. Biol.* **2007**, *13* (8), 1771–1785.

**16. Jiang, J.;** Kappler, A. Kinetics of microbial and chemical reduction of humic substances: Implications for electron shuttling. *Environ. Sci. Technol.* **2008**, *42* (10), 3563–3569.

**17. Lipson, D. A.;** Raab, T. K.; Gorja, D.; Zlamal, J. The contribution of Fe(III) and humic acid reduction to ecosystem respiration in drained thaw lake basins

## CHAPTER I

of the Arctic Coastal Plain. *Global Biogeochem. Cycles* **2013**, *27* (2), 399–409.

**18. Zhang, C.;** Zhang, D.; Li, Z.; Akatsuka, T.; Yang, S.; Suzuki, D.; Katayama, A. Insoluble Fe-humic acid complex as a solid-phase electron mediator for microbial reductive dechlorination. *Environ. Sci. Technol.* **2014**, *48* (11), 6318–6325.

**19. Yu, Z. G.;** Peiffer, S.; Göttlicher, J.; Knorr, K. H. Electron transfer budgets and kinetics of abiotic oxidation and incorporation of aqueous sulfide by dissolved organic matter. *Environ. Sci. Technol.* **2015**, *49* (9), 5441–5449.

**20. Yu, Z. G.;** Orsetti, S.; Haderlein, S. B.; Knorr, K. H. Electron Transfer Between Sulfide and Humic Acid: Electrochemical Evaluation of the Reactivity of Sigma-Aldrich Humic Acid Toward Sulfide. *Aquat. Geochemistry* **2016**, *22* (2), 117–130.

**21. Gao, C.;** Sander, M.; Agethen, S.; Knorr, K.-H. Electron accepting capacity of dissolved and particulate organic matter control CO<sub>2</sub> and CH<sub>4</sub> formation in peat soils. *Geochim. Cosmochim. Acta* **2018**.

**22. Newman, D. K.;** Kolter, R. A role for

excreted quinones in extracellular electron transfer. *Nature* **2000**, *405* (6782), 94–97.

**23. Uchimiya, M.;** Stone, A. T. Reversible redox chemistry of quinones: Impact on biogeochemical cycles. *Chemosphere* **2009**, *77* (4), 451–458.

**24. Fimmen, R. L.;** Cory, R. M.; Chin, Y. P.; Trouts, T. D.; McKnight, D. M. Probing the oxidation-reduction properties of terrestrially and microbially derived dissolved organic matter. *Geochim. Cosmochim. Acta* **2007**, *71* (12), 3003–3015.

**25. Cervantes, F. J.;** Mancilla, A. R.; Ríos-del Toro, E. E.; Alpuche-Solís, A. G.; Montoya-Lorenzana, L. Anaerobic degradation of benzene by enriched consortia with humic acids as terminal electron acceptors. *J. Hazard. Mater.* **2011**, *195*, 201–207.

**26. Smith, J. A.;** Nevin, K. P.; Lovley, D. R. Syntrophic growth via quinone-mediated interspecies electron transfer. *Front. Microbiol.* **2015**, *6* (FEB), 1–8.

**27. Pat-Espadas, A. M.;** Razo-Flores, E.; Rangel-Mendez, J. R.; Cervantes, F. J. Reduction of palladium and production of nano-catalyst by *Geobacter sulfurreducens*. *Appl.*

## CHAPTER I

- Microbiol. Biotechnol.* **2013**, *97* (21), 9553–9560.
- 28. Perlinger, J. A.;** Kalluri, V. M.; Venkatapathy, R.; Angst, W. Addition of hydrogen sulfide to juglone. *Environ. Sci. Technol.* **2002**, *36* (12), 2663–2669.
- 29. Olivo-Alanis, D.;** Garcia-Reyes, R. B.; Alvarez, L. H.; Garcia-Gonzalez, A. Mechanism of anaerobic bio-reduction of azo dye assisted with lawsone-immobilized activated carbon. *J. Hazard. Mater.* **2018**, *347* (January), 423–430.
- 30. Lovley, D. R.;** Kashefi, K.; Vargas, M.; Tor, J. M.; Blunt-Harris, E. L. Reduction of humic substances and Fe(III) by hyperthermophilic microorganisms. *Chem. Geol.* **2000**, *169* (3–4), 289–298.
- 31. Lovley, D. R.;** Fraga, J. L.; Coates, J. D.; Blunt-Harris, E. L. Humics as an electron donor for anaerobic respiration. *Environ. Microbiol.* **1999**, *1* (1), 89–98.
- 32. Coates, J. D.;** Ellis, D. J.; Roden, E.; Gaw, K.; Blunt-Harris, E. L.; Lovley, D. R. Recovery of humics-reducing bacteria from a diversity of sedimentary environments. *Appl. Environ. Microbiol.* **1998**, *64* (4), 1504–1509.
- 33. Coates, J. D.;** Cole, K. A.; Chakraborty, R.; Connor, S. M. O.; Achenbach, L. A. Diversity and ubiquity of bacteria capable of utilizing humic substances as electron donors for anaerobic respiration diversity and ubiquity of bacteria capable of utilizing humic substances as electron donors for anaerobic respiration. *Appl. Environ. Microbiol.* **2002**, *68* (5), 2445–2452.
- 34. Lipczynska-Kochany, E.** Humic substances, their microbial interactions and effects on biological transformations of organic pollutants in water and soil: A review. *Chemosphere* **2018**, *202*, 420–437.
- 35. Cervantes, F. J.;** De Bok, F. A. M.; Duong-Dac, T.; Stams, A. J. M.; Lettinga, G.; Field, J. A. Reduction of humic substances by halo-respiring, sulphate-reducing and methanogenic microorganisms. *Environ. Microbiol.* **2002**, *4* (1), 51–57.
- 36. Bradley, P. M.;** Chapelle, F. H.; Lovley, D. R. Humic acids as electron acceptors for anaerobic microbial oxidation of vinyl chloride and dichloroethene. *Appl. Environ. Microbiol.* **1998**.
- 37. Cervantes, F. J.;** Velde, S.; Lettinga, G.; Field, J. a. Competition

- between methanogenesis and quinone respiration for ecologically important substrates in anaerobic consortia. *FEMS Microbiol. Ecol.* **2000**, *34* (2), 161–171.
- 38. Cervantes, F. J.;** Gutiérrez, C. H.; López, K. Y.; Estrada-Alvarado, M. I.; Meza-Escalante, E. R.; Texier, A.-C.; Cuervo, F.; Gómez, J. Contribution of quinone-reducing microorganisms to the anaerobic biodegradation of organic compounds under different redox conditions. *Biodegradation* **2008**, *19* (2), 235–246.
- 39. Holmes, D. E.;** Ueki, T.; Tang, H.; Zhou, J.; Smith, J. A.; Chaput, G.; Lovley, D. R. A Membrane-Bound Cytochrome Enables Methanosarcina acetivorans To Conserve Energy from Extracellular Electron Transfer. *MBio* **2019**, *10* (4), e00789-19.
- 40. Keller, J. K.;** Bridgham, S. D. Keller, Jason K., and Scott D. Bridgham. Pathways of anaerobic carbon cycling across an ombrotrophic-minerotrophic peatland gradient. *Limnol. Oceanogr.*, **2007**, *52* (1), 96–107. **2007**, *52* (1), 96–107.
- 41. Conrad, R.** Contribution of hydrogen to methane production and control of hydrogen concentrations in methanogenic soils and sediments. *FEMS Microbiology Ecology*. 1999.
- 42. Neubauer, S. C.;** Givler, K.; Valentine, S. K.; Megonigal, J. P. Seasonal patterns and plant-mediated controls of subsurface wetland biogeochemistry. *Ecology* **2005**, *86* (12), 3334–3344.
- 43. Keller, J. K.;** Weisenhorn, P. B.; Megonigal, J. P. Humic acids as electron acceptors in wetland decomposition. *Soil Biol. Biochem.* **2009**, *41* (7), 1518–1522.
- 44. Blodau, C.;** Deppe, M. Humic acid addition lowers methane release in peats of the Mer Bleue bog, Canada. *Soil Biol. Biochem.* **2012**, *52*, 96–98.
- 45. Aeschbacher, M.;** Vergari, D.; Schwarzenbach, R. P.; Sander, M. Electrochemical analysis of proton and electron transfer equilibria of the reducible moieties in humic acids. *Environ. Sci. Technol.* **2011**, *45* (19), 8385–8394.
- 46. Straub, K. L.;** Benz, M.; Schink, B. Iron metabolism in anoxic environments at near neutral pH. *FEMS Microbiol. Ecol.* **2000**, *34* (3), 181–186.
- 47. Smemo, K. A.;** Yavitt, J. B. Anaerobic oxidation of methane: An

- underappreciated aspect of methane cycling in peatland ecosystems? *Biogeosciences* **2011**, *8* (3), 779–793.
- 48. Gupta, V.**; Smemo, K. A.; Yavitt, J. B.; Basiliko, N. Active Methanotrophs in Two Contrasting North American Peatland Ecosystems Revealed Using DNA-SIP. *Microb. Ecol.* **2012**, *63* (2), 438–445.
- 49. Gupta, V.**; Smemo, K. A.; Yavitt, J. B.; Fowle, D.; Branfireun, B.; Basiliko, N. Stable isotopes reveal widespread anaerobic methane oxidation across latitude and peatland type. *Environ. Sci. Technol.* **2013**, *47* (15), 8273–8279.
- 50. Segarra, K. E. A.**; Schubotz, F.; Samarkin, V.; Yoshinaga, M. Y.; Hinrichs, K.-U.; Joye, S. B. High rates of anaerobic methane oxidation in freshwater wetlands reduce potential atmospheric methane emissions. *Nat. Commun.* **2015**, *6* (May), 7477.
- 51. Segarra, K. E. A.**; Comerford, C.; Slaughter, J.; Joye, S. B. Impact of electron acceptor availability on the anaerobic oxidation of methane in coastal freshwater and brackish wetland sediments. *Geochim. Cosmochim. Acta* **2013**, *115*, 15–30.
- 52. Knittel, K.**; Boetius, A. Anaerobic oxidation of methane: progress with an unknown process. *Annu. Rev. Microbiol.* **2009**, *63*, 311–334.
- 53. Scheller, S.**; Yu, H.; Chadwick, G. L.; McGlynn, S. E.; Orphan, V. J. Artificial electron acceptors decouple archaeal methane oxidation from sulfate reduction. *Science* (80-. ). **2016**, *351* (6274), 703–707.
- 54. Bai, Y.-N.**; Wang, X.-N.; Wu, J.; Lu, Y.-Z.; Fu, L.; Zhang, F.; Lau, T.-C.; Zeng, R. J. Humic substances as electron acceptors for anaerobic oxidation of methane driven by ANME-2d. *Water Res.* **2019**, *164*, 114935.
- 55. Haroon, M. F.**; Hu, S.; Shi, Y.; Imelfort, M.; Keller, J.; Hugenholtz, P.; Yuan, Z.; Tyson, G. W. Anaerobic oxidation of methane coupled to nitrate reduction in a novel archaeal lineage. *Nature* **2013**, *500* (7464), 567–570.
- 56. Ettwig, K. F.**; Zhu, B.; Speth, D.; Keltjens, J. T.; Jetten, M. S. M.; Kartal, B. Archaea catalyze iron-dependent anaerobic oxidation of methane. *Proc. Natl. Acad. Sci.* **2016**, *113* (45), 12792–12796.
- 57. Cui, M.**; Ma, A.; Qi, H.; Zhuang, X.; Zhuang, G. Anaerobic oxidation of methane: An “active” microbial process.



## CHAPTER I

- Microbiologypopen* **2015**, *4* (1), 1–11.
- 58. Cheng, C.;** Shen, X.; Xie, H.; Hu, Z.; Pavlostathis, S. G.; Zhang, J. Coupled methane and nitrous oxide biotransformation in freshwater wetland sediment microcosms. *Sci. Total Environ.* **2019**, *648*, 916–922.
- 59. Cassarini, C.;** Rene, E. R.; Bhattarai, S.; Esposito, G.; Lens, P. N. L. Anaerobic oxidation of methane coupled to thiosulfate reduction in a biotrickling filter. *Bioresour. Technol.* **2017**, *240*, 214–222.
- 60. Valenzuela, E. I.;** Avendaño, K. A.; Balagurusamy, N.; Arriaga, S.; Nieto-Delgado, C.; Thalasso, F.; Cervantes, F. J. Electron shuttling mediated by humic substances fuels anaerobic methane oxidation and carbon burial in wetland sediments. *Sci. Total Environ.* **2019**, *650*, 2674–2684.
- 61. He, Q.;** Yu, L.; Li, J.; He, D.; Cai, X.; Zhou, S. Electron shuttles enhance anaerobic oxidation of methane coupled to iron(III) reduction. *Sci. Total Environ.* **2019**, *688*, 664–672.
- 62. Lovley, D. R.;** Fraga, J. L.; Blunt-Harris, E. L.; Hayes, L. A.; Phillips, E. J. P.; Coates, J. D. Humic substances as a mediator for microbially catalyzed metal reduction. *Acta Hydrochim. Hydrobiol.* **1998**, *26* (3), 152–157.
- 63. White, G. F.;** Edwards, M. J.; Gomez-Perez, L.; Richardson, D. J.; Butt, J. N.; Clarke, T. A. *Mechanisms of Bacterial Extracellular Electron Exchange.*, 1st ed.; Elsevier Ltd., 2016; Vol. 68.
- 64. Lovley, D. R.** Syntrophy Goes Electric: Direct Interspecies Electron Transfer. *Annu. Rev. Microbiol.* **2017**, *71* (1), annurev-micro-030117-020420.
- 65. Shrestha, P. M.;** Rotaru, A. E. Plugging in or going wireless: Strategies for interspecies electron transfer. *Front. Microbiol.* **2014**, *5* (MAY), 1–8.
- 66. Liu, F.;** Rotaru, A. E.; Shrestha, P. M.; Malvankar, N. S.; Nevin, K. P.; Lovley, D. R. Promoting direct interspecies electron transfer with activated carbon. *Energy Environ. Sci.* **2012**, *5* (10), 8982–8989.
- 67. Heitmann, T.;** Blodau, C. Oxidation and incorporation of hydrogen sulfide by dissolved organic matter. *Chem. Geol.* **2006**, *235* (1–2), 12–20.
- 68. Urban, N. R.;** Ernst, K.; Bernasconi, S. Addition of sulfur to organic matter during early diagenesis of lake sediments. *Geochim. Cosmochim. Acta* **199**.

## CHAPTER II

# Anaerobic Methane Oxidation Driven by Microbial Reduction of Natural Organic Matter

### HIGHLIGHTS:

- The **anaerobic oxidation of methane (AOM)** was stoichiometrically linked to *anthraquinone-2,6-disulfonate (AQDS) reduction*.
- AOM was coupled to *Pahokee Peat* Humic Substances reduction (**~100 nmol cm<sup>-3</sup> day<sup>-1</sup>**).
- Archaeal and bacterial taxa **distinct to AOM putative microorganisms** were enriched under the humus-reducing/CH<sub>4</sub>-oxidizing conditions.
- The **global contribution** to CH<sub>4</sub> suppression by this novel process is estimated to be of the order of **1,300 Tg CH<sub>4</sub> year<sup>-1</sup>**.

### A modified version of this chapter has been published as:

Valenzuela, E. I., Prieto-Davó, A., López-Lozano, N. E., Hernández-Eligio, A., Vega-Alvarado, L., Juárez, K., et al. (2017). *Anaerobic methane oxidation driven by microbial reduction of natural organic matter in a tropical wetland*. Appl. Environ. Microbiol. 83, AEM.00645-17. doi:10.1128/AEM.00645-17.

## Abstract

Wetlands constitute the main natural source of methane on Earth due to their high content of *natural organic matter* (NOM), but key drivers such as electron acceptors supporting methanotrophic activities in these habitats are poorly understood. We performed anoxic incubations using freshly collected sediment along with water samples harvested from a tropical wetland, amended with  $^{13}\text{C}$ -methane (0.67 atm) to test the capacity of its microbial community to perform *anaerobic methane oxidation* (AOM) linked to the reduction of the humic fraction of its NOM. Collected evidence demonstrates that electron-accepting functional groups (e.g. quinones) present in NOM fueled AOM by serving as terminal electron acceptor. Indeed, while sulfate reduction was the predominant process accounting for up to 42.5% of the AOM activities, microbial reduction of NOM concomitantly occurred. Furthermore, enrichment of wetland sediment with external NOM provided complementary electron-accepting capacity, which reduction accounted for  $\sim 100$  nmol  $^{13}\text{C}$ - $\text{CH}_4$  oxidized  $\text{cm}^{-3} \text{d}^{-1}$ . Spectroscopic evidence showed that quinone moieties were heterogeneously distributed in the wetland sediment, and that their reduction occurred during the course of AOM. Moreover, an enrichment derived from wetland sediments performing AOM linked to NOM reduction stoichiometrically oxidized methane coupled to the reduction of the humic analogue, *anthraquinone-2,6-disulfonate* (AQDS). Microbial populations potentially involved in AOM coupled to microbial reduction of NOM were dominated by divergent biota from putative AOM-associated archaea. We estimate that this microbial process could potentially contribute to the suppression of up to 114 Tg  $\text{CH}_4 \text{yr}^{-1}$  in coastal wetlands and more than 1,300 Tg  $\text{yr}^{-1}$  considering the global wetland area.

## 2.1 Introduction

Microbial processes produce and consume methane ( $\text{CH}_4$ ) in anoxic sediments playing a crucial role in regulating Earth's climate. Virtually 90% of  $\text{CH}_4$  produced from marine environments is oxidized by microorganisms avoiding its release to the atmosphere <sup>1</sup>. *Anaerobic oxidation of methane* (AOM) associated with sulfate reduction was first discovered in marine environments <sup>2</sup>. More recently, AOM has also been linked to the microbial reduction of nitrate <sup>3,4</sup> and nitrite <sup>5</sup>, as well as Fe(III) and Mn(IV) oxides <sup>6-8</sup> in freshwater and marine environments. Wetlands are the largest natural source of  $\text{CH}_4$  <sup>9</sup>, contributing to about a third of global emissions <sup>10</sup>, but key drivers, such as electron acceptors fueling methanotrophic activities in these habitats, are poorly understood.  $\text{CH}_4$  emissions from wetlands have been strongly responsive to climate in the past and will likely continue to be responsive to anthropogenic-driven climate change in the future, predicting a large impact on global atmospheric  $\text{CH}_4$  concentration <sup>10</sup>. The traditional assumption is that aerobic methanotrophy dominates wetlands'  $\text{CH}_4$  cycling by oxidizing an estimated 40 to 70% of gross  $\text{CH}_4$  production in these ecosystems <sup>11</sup>. Recent findings <sup>12</sup> challenged this conjecture by providing evidence that AOM may consume up to 200 Tg  $\text{CH}_4$   $\text{yr}^{-1}$ , decreasing their potential  $\text{CH}_4$  emission by 50% in these habitats. Most AOM activities observed in wetlands have been related to sulfate reduction <sup>12,13</sup>, but other electron acceptors remain feasible. *Natural organic matter* (NOM), circumscribed to humic substances (HS) in many studies <sup>14</sup>, occurs at high concentrations in wetlands both in soluble and solid phases <sup>15</sup>. Recent evidence indicates that HS suppress methane production in different ecosystems <sup>16,17</sup>, yet the mechanisms involved are still enigmatic. HS can theoretically promote AOM as they can serve as terminal electron acceptors for microbial respiration <sup>18,19</sup> and have higher redox potential than sulfate <sup>20</sup>. However,

## CHAPTER II

compelling evidence demonstrating AOM driven by the microbial reduction of NOM present in anoxic environments remains elusive<sup>21,22</sup>.

We aimed to document  $^{13}\text{CH}_4$  anaerobic oxidation and the ongoing reduction of intrinsic electron acceptors, including the electron accepting fraction of NOM, by the biota of freshly sampled sediment from a coastal tropical wetland. We provide  $^{13}\text{CH}_4$  tracer studies and spectroscopic evidence demonstrating for the first time that AOM is linked to the microbial reduction of redox functional groups present in the NOM of this tropical marsh. Furthermore, we found evidence, based on 16s rRNA gene sequences, indicating that microbial populations potentially involved in AOM coupled to microbial reduction of NOM were dominated by divergent biota from putative AOM-associated microorganisms.

## 2.2 Materials and Methods

### 2.2.1 Sediment sampling and characterization

Sediment cores were collected from the tropical marsh *Sisal*, located in Yucatán Peninsula, south-eastern Mexico ( $21^{\circ}09'26''\text{N}$ ,  $90^{\circ}03'09''\text{W}$ ) in January 2016 (Fig. 2.1).



**Fig. 2.1 | Geographic localization of the sediment and water sampling point within the Yucatan Peninsula.** The Sisal wetland is a mangrove swamp located within the ports of Celestun and Sisal in southeastern Mexico. This coastal zone has a semi-arid climate, a high degree of karstification, and receives intermittent saltwater inputs from the ocean. The image was taken and modified from *Google Maps*, 2019.

Sediment cores with a depth of 15 cm were collected under a water column of approximately 70 cm. Water samples were also collected from the area of sediment sampling points to be used as liquid medium in anaerobic incubations. All sediment and water samples were sealed in hermetic flasks and were

## CHAPTER II

maintained in ice until arrival to the laboratory. Upon arrival, all sampled materials were stored at 4°C in a dark room until analysis and incubation. Sediment cores were opened and homogenized within an anaerobic chamber (atmosphere composed of N<sub>2</sub>/H<sub>2</sub> (95%/5%, v/v)) before characterization and incubation. No amendments (addition of chemicals, washing or exposure to air) were allowed on sediment and water samples in order to reflect the actual conditions prevailing *in situ* as closely as possible. Characterization of water and sediment samples is described in **Table 2.1**.

**Table 2.1 | Sediment and water characterization.**

|  | <b>Column water</b> | <b>Pore water</b> | <b>Sediment</b> |
|--|---------------------|-------------------|-----------------|
| <b>Sulfate (mM)</b>  | 2.81±0.4            | 6.7±0.8           | NA              |
| <b>Sulfide (mM)</b>  | 2.07±0.19           | 6.18±0.22         | NA              |
| <b>Nitrate (mM)</b>  | UD                  | 1.75±0.06         | NA              |
| <b>Nitrite (mM)</b>  | UD                  | UD                | NA              |
| <b>Total iron (mg g<sub>dry sediment</sub><sup>-1</sup>)</b>                   | UD                  | UD                | 0.26±0.02       |
| <b>Total manganese (mg g<sub>dry sediment</sub><sup>-1</sup>)</b>              | UD                  | UD                | 0.0067          |
| <b>TOC* (mg L<sup>-1</sup>)</b>  | 35.45±0.72          | 148.73±2.26       | NA              |
| <b>TIC** (mg L<sup>-1</sup>)</b>   | 39.85±1.05          | 185.07±0.68       | NA              |
| <b>TC (mg<sub>Carbon</sub> g<sub>dry sediment</sub><sup>-1</sup>)</b>          | NA                  | NA                | 80.35±4         |
| <b>TIC (mg<sub>Inorg. Carbon.</sub> g<sub>dry sediment</sub><sup>-1</sup>)</b> | NA                  | NA                | 43.97±2.1       |
| <b>Volatile solids (%)</b>   | NA                  | NA                | 11%             |
| <b>Sodium (mg L<sup>-1</sup>)</b>  | 2006.7±11.5         | 3914.37±37        | NA              |
| <b>Chloride (mg L<sup>-1</sup>)</b>  | 4361.11±<br>642.1   | 7506.24±607.9     | NA              |

UD, *undetectable*; NA, *not applicable*. \*total organic carbon measured in liquid phase, \*\*total inorganic carbon measured in liquid phase.

### 2.2.2 Sediment incubations

Water samples collected from sediment sampling points were thoroughly mixed before amendment with HS ( $2.5 \text{ g L}^{-1}$ ) by magnetic stirring. *Pahokee Peat* (Florida, Everglades) HS, purchased from the International Humic Substances Society, were employed as external NOM in sediment incubations. Humic-enriched water was flushed with  $\text{N}_2$  to blow away any dissolved oxygen. Portions of 15 mL were then distributed in 25-mL serological flasks. Sediment containers were opened inside an anaerobic chamber. Portions of 2.5 mL of wet sediment previously homogenized were then inoculated into each serological bottle. After sealing all bottles with rubber stoppers and aluminum rings inside the anaerobic chamber, they were flushed with  $\text{N}_2$ . Once anaerobic conditions were established, 5 mL of  $^{13}\text{C}$ -labeled methane were injected into each vial to reach a  $^{13}\text{CH}_4$  partial pressure of 0.67 atm in a headspace of 7.5 mL. Controls incubated in the absence of external HS were also prepared by following an identical protocol. Killed controls included chloroform at a concentration of 10% (v/v) to annihilate any microbial activity. Additional incubations were executed in the presence of the sulfate-reduction inhibitor, molybdate (25 mM), in the presence and in the absence of external NOM. All incubation bottles were statically placed in a dark room at  $28 \text{ }^\circ\text{C}$  (temperature prevailing at Sisal wetland at the sampling time). The pH remained at  $7.5 \pm 0.05$  throughout all incubations.



### 2.2.3 Enrichment incubations with AQDS

Incubations were commenced by inoculating 120-mL serological bottles with 10 g of volatile suspended solids (VSS) L<sup>-1</sup> of Sisal sediment. Prior inoculation, portions of 60 mL of artificial medium were distributed into the incubation bottles and flushed for 15 min with a mixture of N<sub>2</sub>:CO<sub>2</sub> (80%/20%, v/v) for stripping any dissolved oxygen from the medium. AQDS (>98.0% purity, TCI AMERICA Chemicals) was added at a concentration of 10 mM as terminal electron acceptor along with the following basal medium components (g L<sup>-1</sup>): NaHCO<sub>3</sub> (5), NH<sub>4</sub>Cl (0.3), K<sub>2</sub>HPO<sub>4</sub> (0.2), MgCl<sub>2</sub>·6H<sub>2</sub>O (0.03) and CaCl<sub>2</sub> (0.1). Trace elements were included in the medium by adding 1 mL L<sup>-1</sup> of a solution with the following composition (mg L<sup>-1</sup>): FeCl<sub>2</sub>·4H<sub>2</sub>O (2,000), H<sub>2</sub>BO<sub>3</sub> (50), ZnCl<sub>2</sub> (50), CuCl<sub>2</sub>·6H<sub>2</sub>O (90), MnCl<sub>2</sub>·4H<sub>2</sub>O (500), AlCl<sub>3</sub>·6H<sub>2</sub>O (90), CoCl<sub>2</sub>·6H<sub>2</sub>O (2000), NiCl<sub>2</sub>·6H<sub>2</sub>O (920), Na<sub>2</sub>SeO<sub>3</sub>·5H<sub>2</sub>O (162), (NH<sub>4</sub>)<sub>6</sub>Mo<sub>7</sub>O<sub>24</sub> (500), EDTA (1,000), Na<sub>2</sub>WO<sub>4</sub>·H<sub>2</sub>O (100) and 1 mL L<sup>-1</sup> of HCl at 36%. The final pH of the medium was 7.5 and no changes were observed throughout the incubation time. Once inoculation took place, microcosms were sealed with rubber stoppers and aluminum rings, and then flushed with the same N<sub>2</sub>:CO<sub>2</sub> mixture. After anoxic conditions were established, 1 ml of sodium sulfide stock solution was injected into each vial to reach a sulfide concentration of 0.1 g L<sup>-1</sup> in order to consume any traces of dissolved oxygen. Methane was provided into the microcosms by injecting 30 mL of CH<sub>4</sub> (99.9% purity, Praxair) reaching a partial pressure of methane of 0.54 atm. Subsequent incubations were performed after AQDS was reduced (converted to AH<sub>2</sub>QDS) coupled to anaerobic oxidation of methane (AOM). A new set of bottles containing basal medium with AQDS (10 mM) were inoculated within an anaerobic chamber by transferring 10 mL of slurry (sediment and medium) taken from previous incubations (**Fig. 2.2**). The following incubations were completed under the same experimental conditions.

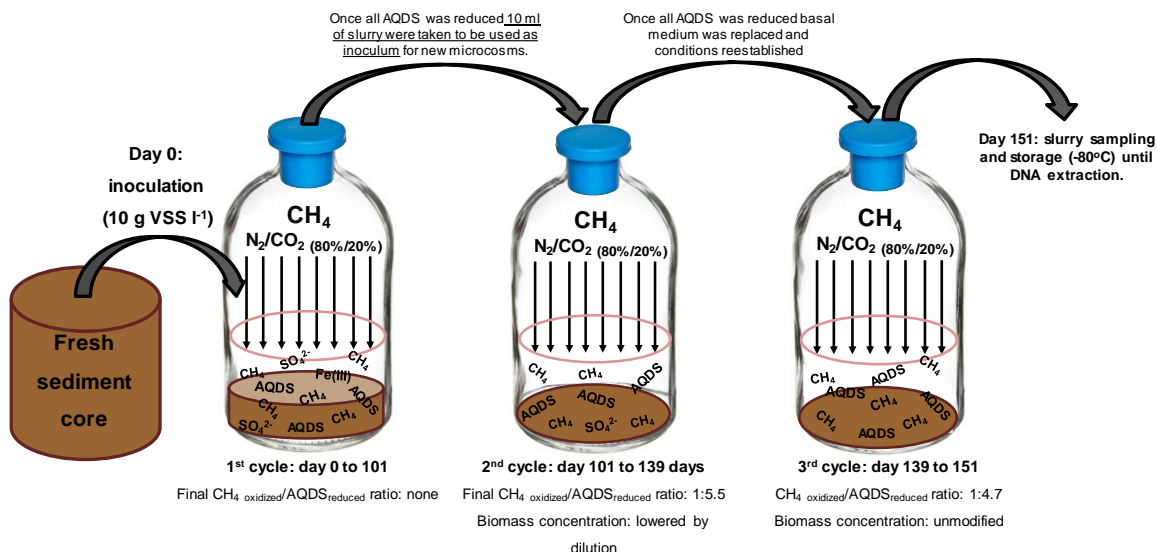


**Fig. 2.2 | Schematic representation of sequential incubation cycles for AQDS dependent methanotrophic activity.**

## 2.2.4 Analytical techniques

### 2.2.4.1 Isotopic carbon dioxide and methane measurements

Ions 16 (<sup>12</sup>CH<sub>4</sub>), 17 (<sup>13</sup>CH<sub>4</sub>), 44 (<sup>12</sup>CO<sub>2</sub>) and 45 (<sup>13</sup>CO<sub>2</sub>) were detected and quantified in a Gas Chromatograph Agilent Technologies 7890A coupled to a Mass Spectrometer (detector) Agilent Technologies 5975C, the ionization was achieved by electronic impact and quadrupole analyzer. For the analysis, a capillary column Agilent Technologies HP-PLOT/Q with a stationary phase of poly-styrene-di-vinyl-benzene (30 m × 0.320 mm × 20 μm) was employed as stationary phase using helium as carrier gas. The chromatographic method was as follows: the starting temperature was 70 °C which was held for 3 min, and then a ramp with an increase of 20 °C per min was implemented until 250 °C was reached and maintained for 1 min. The total time of the run had a duration of 13 min. The temperature of the injection port was 250 °C. The injection volume was 20 μl and there was only one

replicate of injection per bottle. The gas injected into the GC was taken directly from the headspace of the incubations and immediately injected in to the GC port. Methane calibration curves were made by injection of different methane (99.9% of purity) volumes into serological bottles under the same experimental conditions (atmosphere composition, pressure, temperature, and liquid volume).  $^{12}\text{CO}_2$  and  $^{13}\text{CO}_2$  curves were made using different dried sodium bicarbonate (99% purity, Sigma Aldrich) and sodium  $^{13}\text{C}$ -labelled carbonate (99 atom % $^{13}\text{C}$ , Sigma Aldrich) concentrations, respectively, in serological bottles which contained the same volume of wetland sediment and water used in incubations. Standards were incubated at room temperature for 12 hours until equilibrium with the gaseous phase was reached. The linear regression analysis of obtained measurements had a co-relation coefficient higher than 0.97.  $^{13}\text{CO}_2$  production rates were based on the maximum slope observed on linear regressions considering at least three sampling points.

#### **2.2.4.2 Methane quantification in AQDS enrichment**

Net methane consumption was assessed in terms of methane concentration measurements in the headspace of microcosms. These measurements were carried out by injecting 100  $\mu\text{l}$  of gas samples from the headspace of incubation bottles into a gas chromatograph (Agilent Technologies 6890M) equipped with a thermal conductivity detector, and a Hayesep D (Alltech, Deerfield, Illinois, USA) column with the following dimensions: 3.048 m  $\times$  3.185 m  $\times$  2.16 mm. Helium was employed as carrier gas at a flux of 12 mL  $\text{min}^{-1}$ . The temperature of injection port, oven and detector was 250, 60 and 250  $^{\circ}\text{C}$ , respectively. Calibration curves were made for each reaction volume used by injecting different methane concentrations into serological bottles under the same experimental conditions at which

microcosms were performed (atmosphere composition, pressure, temperature, and liquid volume).

#### **2.2.4.3 Determination of electron accepting functional groups in solid phase by XPS**

Sediment samples (solid fraction of microcosms) were dried under a constant nitrogen flow after incubation with methane. Once sediments became dried, bottles were open inside an anaerobic chamber with an atmosphere composed of N<sub>2</sub>/H<sub>2</sub> (95%/5%, v/v) and were triturated on an agate mortar. Samples were then kept under anaerobic conditions until analysis in an X-Ray Photoelectron Spectroscopy Analyzer PHI VersaProbe II (Physical Electronics, ULVAC-PHI). Two representative spectra were recorded per scanned sample.

#### **2.2.4.4 Determination of electron accepting functional groups in solid phase by Micro-ATR-FT-IR imaging**

Micro-ATR-FT-IR images were collected from each sample with a continuous scan spectrometer, Agilent 660 FT-IR interfaced to a 620-infrared microscope with a 32 × 32 FPA detector and Ge ATR objective for micro-ATR. Each pixel obtains a full IR spectrum or a total of 1024 spectra. Background spectra were collected from a clean ATR crystal (*i.e.*, without sample). The Ge crystal of the ATR microscope was lowered onto the surface of each sample for a contact area of approximately 100 × 100 μm. Spectra were collected by co-addition of 256 scans over a spectral range of 4000 to 900 cm<sup>-1</sup>, at a spectral resolution of 4 cm<sup>-1</sup>. In all images, a color scale bar is set within the software to reflect the relative concentration range, from low to high. Agilent Resolutions Pro was used for data acquisition and analysis.

#### **2.2.4.5 Determination of electron accepting functional groups in liquid phase by high resolution UV-Vis-NIR spectroscopy**

After each incubation cycle, liquid samples (1.5 mL) were taken in an anaerobic chamber with a disposable syringe and put into a quartz cell, which was sealed with plastic film in order to keep anoxic conditions during spectrometric analysis. Spectra were obtained in a Varian Cary 5000 UV-Vis (diffuse reflectance) spectrophotometer, equipped with an integrating sphere.

#### **2.2.4.6 Nitrite and nitrate determinations**

Nitrite and nitrate concentrations were measured according to spectrometric techniques established at Standard Methods <sup>44</sup>. Nitrate measurement is taken under acidic conditions at a wavelength of 275 nm and the value obtained is corrected for dissolved organic matter which has its maximum absorbance at 220 nm. Nitrite forms a purple complex through a reaction with sulfanilamide and N-(1-naphthyl) ethylene diamine, which presents its maximum absorbance at a wavelength of 543 nm. Samples were taken with a disposable syringe directly from the microcosms, injected into sealed quartz cuvettes or glass tubes (depending on the required lecture wavelength) and immediately taken to the spectrophotometer to avoid any reaction of the sample with atmospheric oxygen.

#### **2.2.4.7 Sulfate and sulfide determinations**

Samples were extracted from microcosms and immediately filtered through 0.22  $\mu\text{m}$  nitrocellulose membranes. Filtered samples were then diluted (1:10) with deionized water and processed in an Agilent Capillary Electrophoresis System

(Agilent Technologies) according to the methodology proposed by Soga & Ross <sup>45</sup>. Dissolved sulfide was measured by the spectrometric method proposed by Cord-Ruwisch <sup>46</sup>. Briefly, 100  $\mu\text{L}$  of sample were taken and immediately mixed in vortex with 4 mL of an acidic  $\text{CuSO}_4$  solution. Absorbance at 480 nm was immediately registered in a UV-VIS spectrophotometer (Thermo Spectronic) to avoid sulfide oxidation before measurements.

#### **2.2.4.8 Humic substances reduction and ferrous iron measurements**

Quantification of the reduction of electron-accepting functional groups in HS was performed according to Lovley *et al.*<sup>18</sup>. Slurry samples ( $\sim 500 \mu\text{L}$ ) were taken from microcosms with a disposable syringe while bottles were being manually shaken inside an anaerobic chamber. A portion of each sample (200  $\mu\text{L}$ ) was mixed with an equal volume of an acidic solution (HCl, 0.5 M) and allowed to stand for 30 min, while the same volume of sample was reacted with ferric citrate (20 mM) for 3 hours. After reaction with ferric citrate, samples were mildly re-suspended in a vortex and 200  $\mu\text{L}$  were left repose with the same volume of HCl solution for 30 min. Afterwards, each sample was centrifuged for 10 min at 10,000 g in a centrifuge Spectrafuge 16M and 200  $\mu\text{L}$  of supernatant were then recovered and reacted with a solution 0.2 g  $\text{L}^{-1}$  of 2,4,6-tris(2-pyridil)-1,3,5-triazine (ferrozine reagent). Ferrous iron produced due to chemical reduction of ferric citrate by reduced functional groups in HS, forms a purple complex along with ferrozine reagent, which has its maximum absorbance at 562 nm. The ferrozine solution was buffered with HEPES (50 mM). Once centrifuged samples were mixed with ferrozine solution, they were left reacting for 10 min before their measurement in a spectrometer Thermo Scientific Genesis 10 UV located inside an anaerobic chamber. All solutions

employed in this determination were bubbled with N<sub>2</sub> for 30 min to ensure the absence of dissolved oxygen.

#### **2.2.4.9 Total carbon (TC), total organic carbon (TOC) and total inorganic carbon (TIC) measurements**

Water samples were filtered through 0.22 µm nitrocellulose membranes and diluted with deionized water, while sediment samples were dried until constant weight. Both liquid and solid samples were analyzed in a Total Organic Carbon analyzer Shimadzu TOCVCS/TNM-1 equipped with a solids sampling port (SSM-5000A). Solid sample processing time was 6 min at 900°C using O<sub>2</sub> (500 mL min<sup>-1</sup>) with a purity of 99.9% as carrier gas, all samples were analyzed by triplicate.

#### **2.2.4.10 Total, volatile and fixed solids**

Total, fixed and volatile solids were measured by triplicate according to Standard Methods procedure <sup>44</sup>.

#### **2.2.4.11 Elemental composition**

Elemental composition of sediments was assessed by analyzing acid-extracts from 2 g of wet sediment. In the case of iron and manganese measurements in microcosms, supernatant samples were taken with disposable syringes, filtered and acidified prior analysis. Samples were then analyzed by *inductively coupled plasma optical emission spectrometry* (ICP-OES) in an equipment Varian 730-ES. The operational conditions were: potency 1 kW, auxiliary flow: 1.5 L min<sup>-1</sup>, net flow: 0.75

L min<sup>-1</sup>, sample taking delay: 30 s, and the number of measured replicates by sample was three. Argon was employed as carrier gas.

#### **2.2.4.12 DNA extraction, PCR amplification and Sequencing**

One microcosm for each selected treatment was randomly chosen at the end of the incubation period (30 days for experiments presented in **Fig. 2.3**, and 151 days for experiments depicted in **Fig. 2.10**). Before DNA extraction, liquid medium was decanted and extracted from the serological bottles. The total sediment was homogenized afterwards, and a subsample of 0.5 g was taken to proceed with DNA extraction. The remaining sediment and the other microcosms were used for material characterization. The total DNA was extracted from sediment samples using the Power Soil DNA extraction kit (MO BIO Laboratories, Carlsbad, CA, USA) following the protocol described by the manufacturer. DNA isolated from each sample was amplified using primers 341F and 785R, targeting the V3 and V4 regions of the 16s rRNA gene fused with Illumina adapter overhang nucleotide sequences<sup>47</sup>. The *polymerase chain reactions* (PCRs) were performed in 50 µL reactions using Phusion Taq polymerase (Thermo Scientific, USA) under the following conditions: denaturation at 98 °C for 60 s, followed by 5 cycles of amplification at 98 °C for 60 s, 50 °C for 30 s and 72 °C for 30 s, followed by 25 cycles of amplification at 98 °C for 60 s, 55 °C for 30 s and 72 °C for 30 s, followed by a final extension of 72 °C for 5 min. Two independent PCR reactions were performed for each sample. The products were indexed using Illumina's 16s Metagenomic Sequencing Library Preparation protocol and Nextera XT Index Kit v2 (Illumina, San Diego CA). Libraries were deep sequenced with the Illumina MiSeq sequencer.



### 2.2.4.13 Bioinformatics Analysis

An analysis of 16S rRNA gene libraries was carried out using Mothur open source software package (v 1.34.4) <sup>48</sup>. The high-quality sequence data were analyzed for potential chimeric reads using the UCHIME algorithm. Sequences containing homopolymer runs of 9 or more bases, those with more than one mismatch to the sequencing primer and Q-value average below 25 were eliminated. Group membership was determined prior to the trimming of the barcode and primer sequence. Sequences were aligned against the SILVA 123 16s/18s rRNA gene template using the *nearest alignment space termination* (NAST) algorithm and trimmed for the optimal alignment region. A pairwise distance matrix was calculated across the non-redundant sequence set, and reads were clustered into operational taxonomic units (OTUs) at 3% distance using the furthest neighbor method. The sequences and OTUs were categorized taxonomically using Mothur's Bayesian classifier and the SILVA 123 reference set. The sequences obtained have been submitted to NCBI GeneBank database.

### 2.2.4.14 Accession numbers

The accession numbers of sequences in this work were deposited in the GenBank sequence read archive under the BioProject with SRP094593 accession number.

## 2.3 Results

### 2.3.1 Kinetics of $^{13}\text{C}$ -methane oxidation and electron balances

Exponential phase of AOM was observed in microcosms over the first 15 days of incubation in the case of unamended sediment (free from external NOM addition). The methanotrophic rate in this experimental treatment was  $\sim 1.34 \mu\text{mol } ^{13}\text{C}$ -methane oxidized  $\text{cm}^{-3} \text{d}^{-1}$  (**Fig. 2.3**).

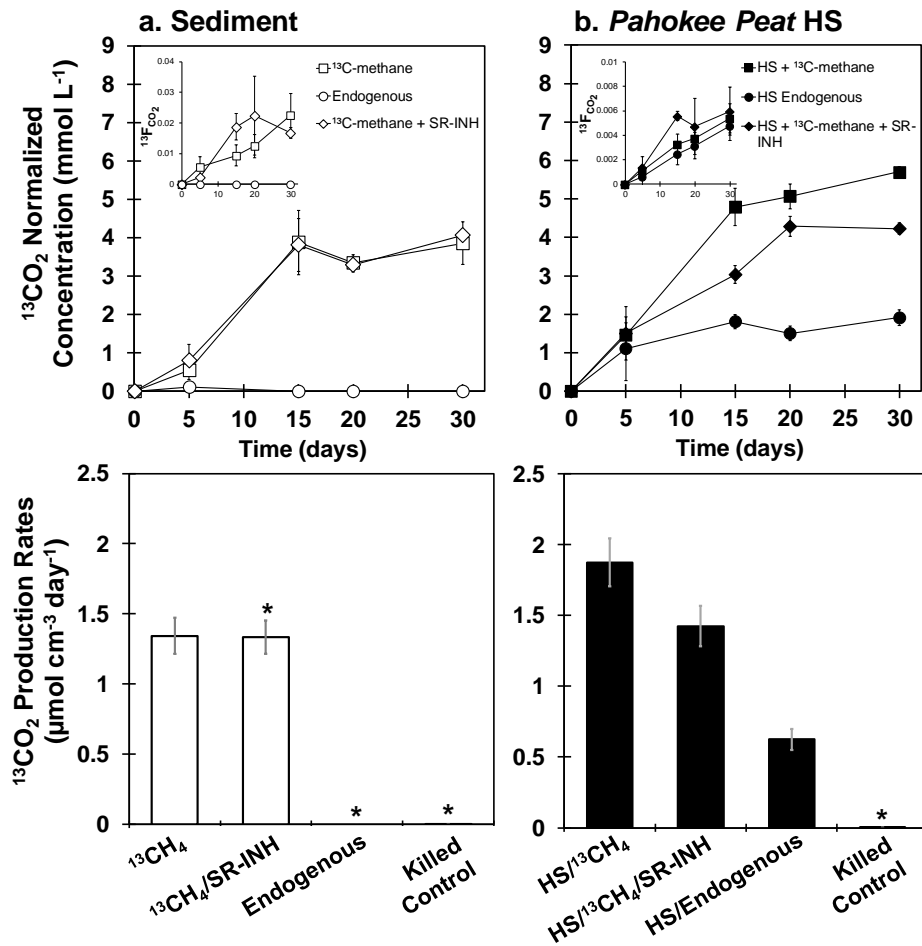


**Fig. 2.3** | Anaerobic methane oxidation measured as  $^{13}\text{CO}_2$  production in microcosms' headspace and  $^{13}\text{C}$  enrichment calculated as  $^{13}\text{FCO}_2$  ( $^{13}\text{CO}_2/^{13}\text{CO}_2 + ^{12}\text{CO}_2$ ). **Panel a** display the kinetics for incubations performed with unamended sediment. **Panel b** displays the kinetics for incubations performed with sediment

enriched with 2.5 g L<sup>-1</sup> of external NOM in the form of *Pahokee Peat* humic substances. Error bars represent the standard error among replicates (n = 4, or 3\*). *SR-INH* stands for sediment incubations performed with molybdate (25 mM) in order to inhibit sulfate reduction. <sup>13</sup>CO<sub>2</sub> production rates were based on the maximum slope observed on linear regressions considering at least three sampling points.

At the end of the exponential phase, sulfate and Fe(III) reduction accounted for 42.5% and 0.5% of <sup>13</sup>C-methane oxidized, respectively, while the role of nitrate was marginal (**Fig. 2.4** and **Table 2.2**).

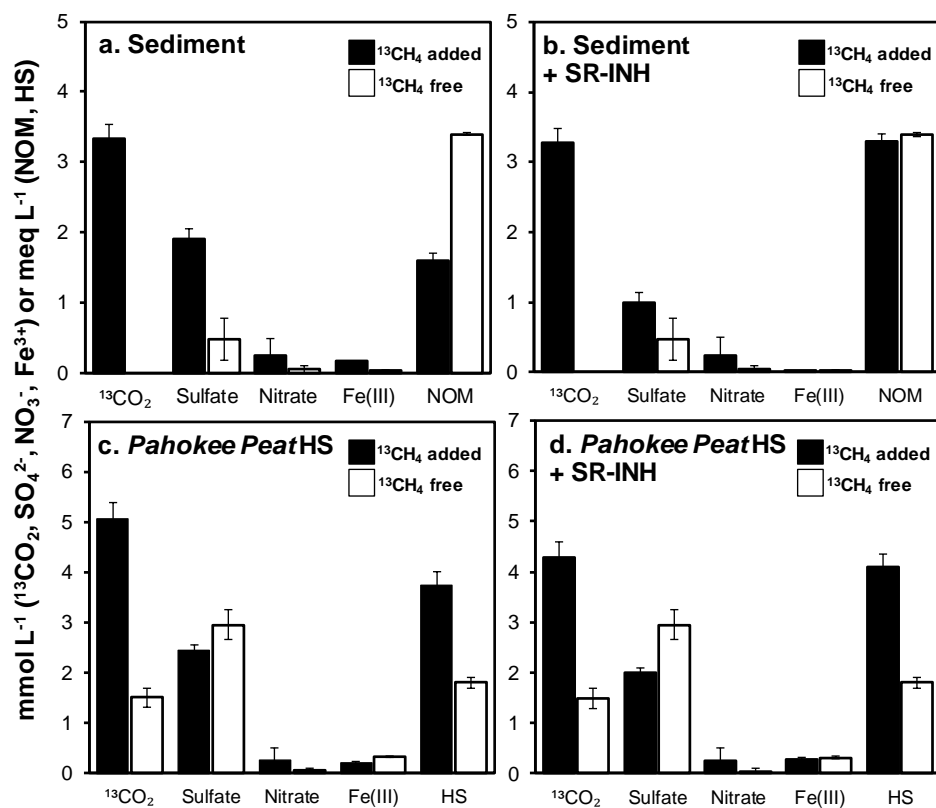


**Fig. 2.4** | Production of <sup>13</sup>CO<sub>2</sub> and reduction of intrinsic or added electron acceptors at the end of the exponential phase (20 days of incubation). Results in the absence and in the presence of external NOM as HS from *Pahokee Peat* are depicted in **Panels a, b** and **Panels c, d** respectively. SR-INH stands for controls amended with sulfate-

reduction inhibitor, sodium molybdate (25 mM). Error bars represent the standard error among replicates.  $^{13}\text{CO}_2$  produced was measured as described for **Fig. 2.1**. Quantification of nitrate reduction implies a decrease on their concentration at this sampling time, whereas Fe (III) reduction was quantified in terms of the ferrous iron produced. Reduction of NOM and HS was determined by the ferrozine technique. Error bars represent the standard error among replicates.

These unamended sediment microcosms exhibited a reduction in intrinsic NOM during the course of AOM, which was expected due to the high concentration of organic carbon in the tropical wetland, with the capacity to accept electrons (**Table 2.1, Fig. 2.4**). Nevertheless, large perturbation caused by endogenous NOM reduction in experimental controls lacking  $^{13}\text{C}$ -methane obstructed accurate assessment of AOM driven by this microbial process (**Fig. 2.3**). The large endogenous NOM reduction observed in these control experiments may be explained by concomitant methane production (and subsequent consumption) observed (**Fig. 2.5**), and by oxidation of labile organic matter present in the sediment (**Table 2.1**). Supplementary incubations spiked with the sulfate-reduction inhibitor, sodium molybdate (25 mM), showed decreased sulfate reducing activities (~50%, **Fig. 2.4**), while AOM rates remained high when compared against their non-inhibited counterparts (**Fig. 2.3**). Remarkably, when sulfate reduction was inhibited, the reduction of intrinsic NOM was doubled (from  $1.6 \pm 0.11$  to  $3.4 \pm 0.19$  milli-electron equivalents ( $\text{meq L}^{-1}$ )), implying that the reduction of redox functional groups in NOM was promoted when the utilization of sulfate was impeded.

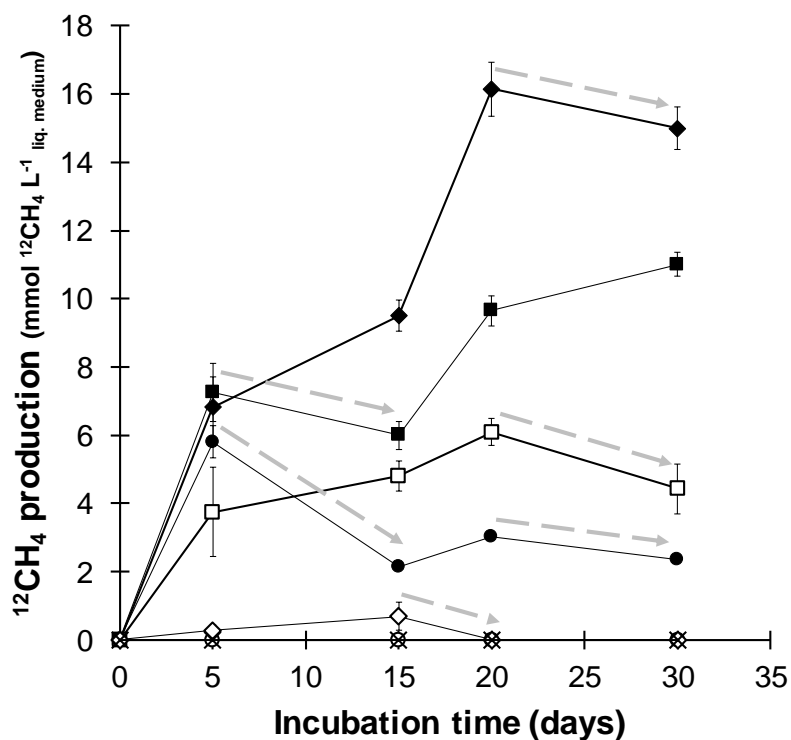


**Fig. 2.5 | Produced  $^{12}\text{CH}_4$  in wetland sediment microcosms.** Filled symbols represent experiments amended with external NOM as *Pahokee Peat* HS: squares (-■-) represent microcosms amended with  $^{13}\text{CH}_4$  (n=4), circles (-●-) represent  $^{13}\text{CH}_4$  free microcosms (endogenous controls, n=4) and diamonds (-◆-) represent sulfate-reduction inhibited controls (n=4). In the same way, open symbols represent  $^{13}\text{CH}_4$  added (-□-, n=4), endogenous (-○-, n=3) and sulfate-reduction inhibited controls (-◇-, n=3) without addition of external HS. Sterile controls are represented by crosses (-x-). Dashed arrows emphasize negative slopes, implying consumption of produced  $^{12}\text{CH}_4$  eventually contributing to substantial reduction of intrinsic and added electron acceptors. Error bars represent the standard error among replicates.

Further enrichment of wetland sediment with external NOM, in the form of HS derived from *Pahokee Peat* (Florida Everglades,  $2.5 \text{ g L}^{-1}$ ), provided

complementary electron accepting capacity, which significantly elicited AOM up to  $\sim 1.88 \mu\text{mol } ^{13}\text{C-methane oxidized cm}^{-3} \text{ d}^{-1}$  and extended the exponential phase to 20 days (**Fig. 2.3**). In this experimental treatment, electron balances revealed a methanotrophic activity responsible of  $\sim 100 \text{ nmol } ^{13}\text{C-CH}_4 \text{ oxidized cm}^{-3} \text{ d}^{-1}$  linked to microbial reduction of NOM (including both intrinsic and externally added as *Pahoee Peat* HS). As hypothesized before, consumption of intrinsically produced methane was confirmed by experimental controls enriched with HS from *Pahoee Peat* and incubated in the absence of  $^{13}\text{C-methane}$ , which showed significant consumption of  $^{12}\text{CH}_4$  (**Fig. 2.5**). This was also confirmed by increased  $^{12}\text{CO}_2$  production quantified, which was reflected on 2 to 4-fold lower enrichment of  $^{13}\text{CO}_2$  in HS enriched incubations as compared to unamended controls (see  $^{13}\text{FCO}_2$  values in **Fig. 2.3**). Reports <sup>23, 24</sup> indicate that methanotrophic microorganisms prefer to oxidize  $^{12}\text{CH}_4$  as compared to  $^{13}\text{CH}_4$ , which may partly explain our findings.

The role of sulfate reduction on AOM when wetland sediment was enriched with HS was not possible to assess (**Table 2.2**) due to large endogenous sulfate reduction elicited by degradation of the labile fraction of externally added NOM (**Fig. 2.4**), which also triggered methanogenesis in these microcosms. Since no significant differences in iron reduction were detected between microcosms with or without  $^{13}\text{CH}_4$  addition, the only microbial process clearly identified driving AOM in *Pahoee Peat* enriched sediments was the microbial reduction of HS (**Table 2.2**).

**Table 2.2 | Contribution of different electron acceptors on anaerobic oxidation of methane in wetland sediment incubations at the end of exponential phase (20 days of incubation)**

| Treatments                                | % of AOM linked to SO <sub>4</sub> <sup>2-</sup> reduction | % of AOM linked to Fe <sup>3+</sup> reduction | % of AOM linked to HS or NOM reduction |
|---|--|---|--|
| With <i>Pahokee Peat</i> HS               | -  | -   | 7±0.4                                  |
| With <i>Pahokee Peat</i> HS and molybdate | -  | -   | 10±0.5                                 |
| Sediment only                             | 42.5±2   | 0.46±0.05                                     | -                                      |
| Sediment and molybdate                    | 16±0.8   | -   | -                                      |

The percentages of <sup>13</sup>C-methane oxidation linked to the reduction of different electron acceptors in wetland sediment were quantified by dividing the amount of reduced terminal electron acceptors by the amount of <sup>13</sup>CH<sub>4</sub> oxidized (calculated from <sup>13</sup>CO<sub>2</sub> production), both corrected for endogenous controls. Stoichiometric relationships (1:1 for sulfate, and 1:8 for iron and HS or NOM) were considered.

### 2.3.2 Spectroscopic evidence on presence and reduction of redox-functional groups in NOM

Initial exploration of the solid phase NOM present in wetland sediment by micro-ATR-FTIR spectra, revealed the presence of electron accepting moieties both in unamended and in HS enriched wetland sediments.

By mapping of acquisition points at 1650-1620 cm<sup>-1</sup>, presence and heterogeneous distribution of quinone functional groups was evidenced in sediments confirming the presence of non-soluble electron accepting moieties classically attributed to humic-like materials (**Fig. 2.6a** and **b**).

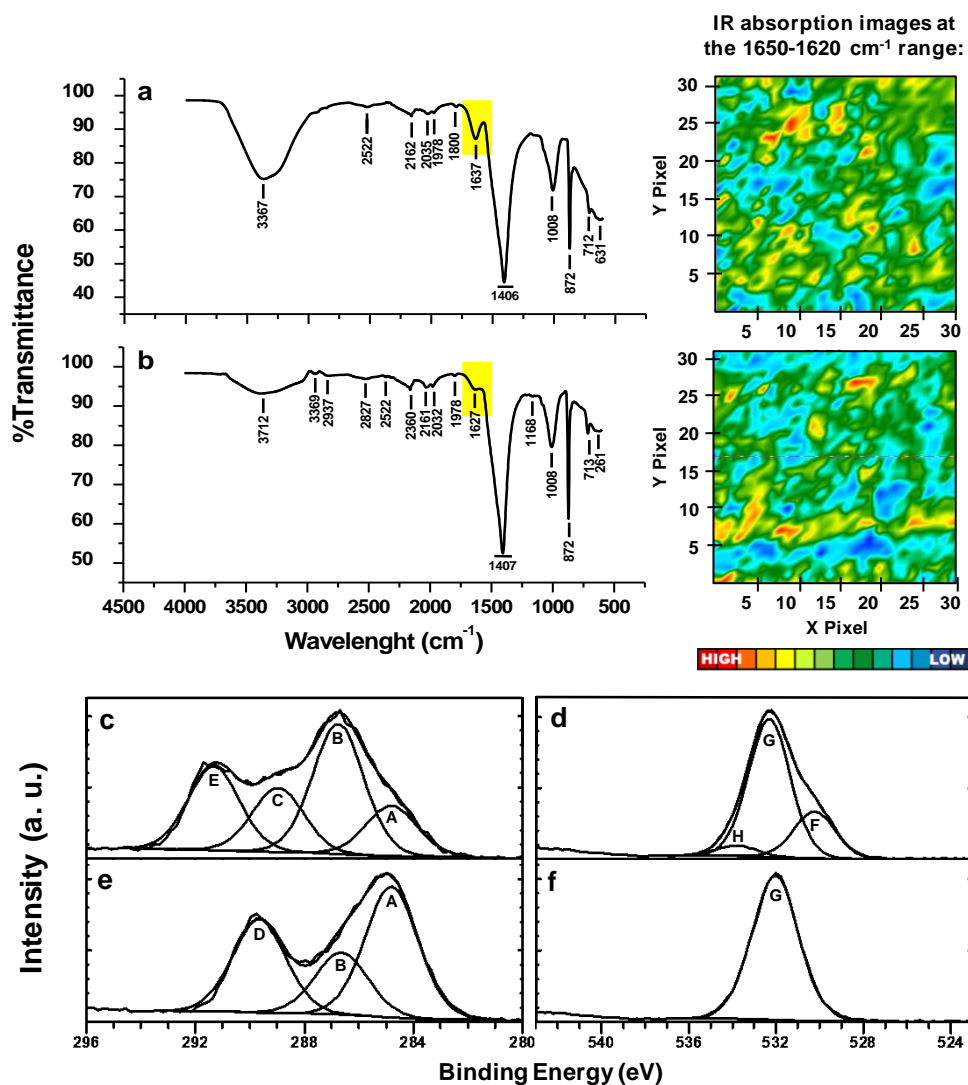


**Fig. 2.6 | Spectroscopic evidence of the presence of quinone moieties and their reduction in wetland sediment samples. Panels a and b depict the Micro-ATR-FTIR representative spectra taken from imaged areas generated after processing quinone functional groups ( $1650\text{-}1620\text{ cm}^{-1}$ ) of sediment samples before incubation in the absence and in the presence, respectively, of external NOM in the form of *Pahoee Peat* HS. Panels c and e portray XPS high resolution profiles of C1s, while d and f represent O1s signal. Panels c and d belong to sediment samples prior incubation, while panels e and f correspond to sediment samples after incubation with  $^{13}\text{C}$ -methane.**



Regions and components were corrected at 284.8 eV for the C-C adventitious carbon *A*; *B* and *G* components belong to C-O bond ( $\sim 286.6$  and  $\sim 532$  eV), *C* and *H* correspond to C=O functional group ( $\sim 288.9$  and  $\sim 533.3$  eV), *D* belongs to  $-\text{COOH}$  ( $\sim 289.6$ ), *E* is typical of the presence of carbonate ( $\sim 291$ ) and *F* suggests the occurrence of a metallic oxide ( $\sim 530$ ).

To further confirm this, we looked for double bonded carbon and oxygen (C=O) by use of *X-ray photoelectron spectra* (XPS), technique that supported the existence of quinone-like functional groups in unamended sediment and furthermore, provided evidence of the reduction of these moieties by showing the disappearance of the C=O signal from C1s and O1s high resolution spectra when comparing signals from sediment analyzed before and after incubation with  $^{13}\text{CH}_4$  in the absence of external HS (**Fig. 2.6c to f**). Another missing signal after the AOM process was that which corresponds to metallic oxides, evidenced by analysis of the O1s high resolution spectra (**Figure 2.6d and f**), which may imply reduction of intrinsic iron oxides that supported  $\sim 0.5\%$  of methanotrophy according to electron balances (**Table 2.2**). Further analysis of the liquid phase of pristine sediment microcosms also revealed the reduction of quinone-like moieties during the course of AOM (**Fig. 2.7**). Initial samples exhibited a well-defined and strong peak at  $1690\text{ cm}^{-1}$  associated with quinone moieties, while reduced samples, at the end of the incubation period, showed an increase in the signal related to phenolic groups ( $1660\text{ cm}^{-1}$ ). Additional signals of phenolic groups were detected after incubation with  $^{13}\text{CH}_4$  and *Pahokee Peat* by spectral signals detected around  $2260\text{-}2500\text{ cm}^{-1}$ .

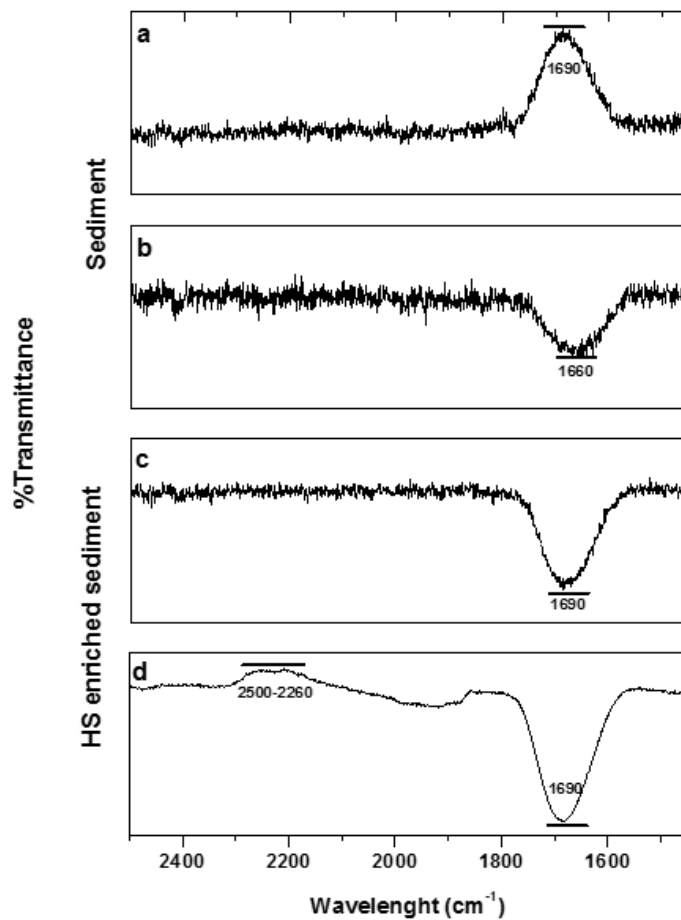


**Fig. 2.7 | High performance Ultraviolet-Visible-Near Infrared spectra obtained from liquid samples before and after incubation with <sup>13</sup>CH<sub>4</sub>. Panels a and c depict spectra obtained before incubation with <sup>13</sup>CH<sub>4</sub>, while panels b and d show spectra obtained after incubation with <sup>13</sup>CH<sub>4</sub>.**

### 2.3.3 Microbial communities performing AOM

According to 16S rRNA gene sequences from wetland sediment samples performing AOM, anaerobic methanotrophic archaea (ANME), which are traditionally linked to anaerobic methanotrophy under sulfate-reducing<sup>2, 26</sup>, Fe(III)-reducing<sup>6, 8</sup>, and artificial electron acceptor-reducing conditions<sup>27</sup>, were barely detected in our experiments, with ANME-1b and ANME-3 representing less than 0.5% and 0.2%, respectively, from the archaeal community in all experimental treatments (Fig. 5). The only abundant *Euryarchaeota* members detected were affiliated to an unclassified genus of the *Marine Benthic Group D* family (MBGD and DHVEG-1), which accounted for 18 to 23% of the archaeal biota in all treatments. Outside of the *Euryarchaeota* phylum, members from the newly named *Bathyarchaeota* lineage (formerly known as *Miscellaneous Crenarchaeotic Group*) were another cluster of microorganisms that remained in high percentages (from 8 to 14%) in all treatments. Two genera from the *Thaumarchaeota* phylum, one belonging to the pMC2A209 class, and the other from the *Marine Benthic Group B* (MBG-B) were also consistently present in all sediment samples showing AOM, the latter one increasing its proportion up to 12% when sulfate reduction was inhibited (Fig. 2.8).

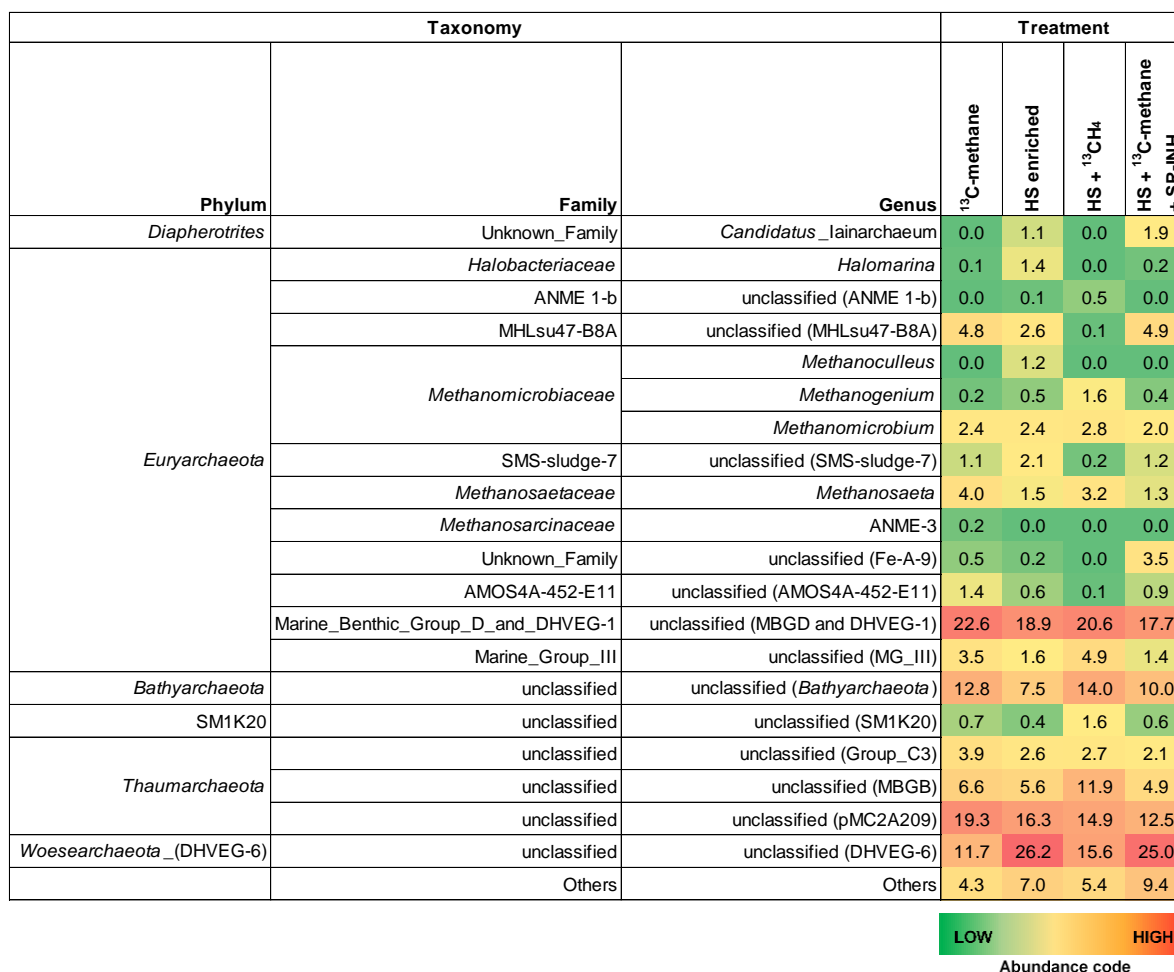


**Fig. 2.8 | Archaeal composition in wetland sediment samples performing AOM.** Most abundant archaeal genera detected, based on 16s rRNA amplicon gene libraries, on selected experimental treatments shown in **Fig. 2.3** at the end of the incubation period (30 days).

From the bacterial counterpart, the most abundant bacteria in two of the treatments was a genus of *Oceanimonas* from *Aeromonadaceae* family (*Gammaproteobacteria*), whose presence was diminished when sulfate reduction was inhibited and when <sup>13</sup>CH<sub>4</sub> was absent, suggesting that this microorganism might have been involved in sulfate-dependent AOM. Other evident changes in the bacterial community included the increase of *Clostridia* and *Bacilli* members when

external NOM was supplied (Fig. 2.9), which agrees with their capacity to reduce HS<sup>28</sup>.

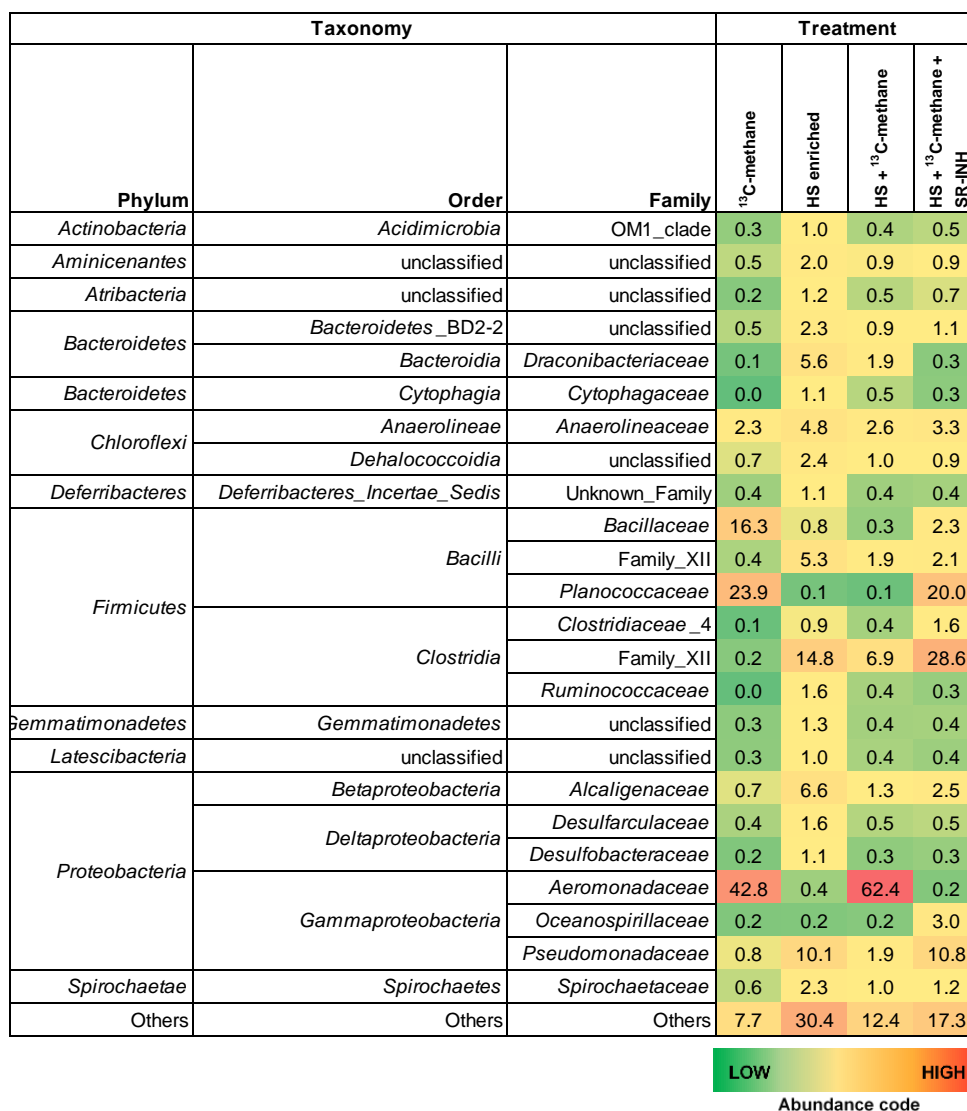
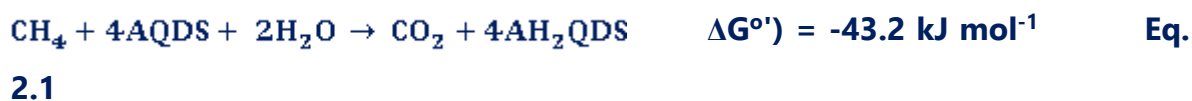


**Fig. 2.9 | Bacterial community composition in wetland sediment samples performing AOM based on 16s rRNA gene libraries obtained by MiSeq ILLUMINA technology.** HS stands for humic substances, as reference for added *Pahokee Peat* enriched microcosms, SR-INH stands for sulfate-reduction inhibited, as reference for those treatments spiked with sodium molybdate.

### 2.3.4 AOM linked to AQDS reduction

In order to confirm the capacity of the sediment biota to channel  $^{13}\text{C}$ -methane derived electrons to quinone groups, the humic analogue, anthraquinone-2,6-disulfonate (AQDS), was added as an electron acceptor to the artificial basal medium for sediment enrichments (**Fig. 2.2**). AQDS reduction and methane consumption were observed since the first enrichment cycle, although no clear relationship between net methane consumption and  $\text{AH}_2\text{QDS}$  production was observed due to high concentrations of intrinsic electron donors and acceptors (data not shown). Nevertheless, during the third incubation cycle, net AOM was observed within 11 days, which corresponded to a final ratio of oxidized methane/reduced AQDS of 1:4.7 corrected for endogenous controls, which is very close to the stoichiometric 1:4 according to the following equation (**Eq. 2.1** and **Fig. 2.10**):



Analysis of 16s rRNA gene sequences from enriched sediment sampled at the end of the third cycle of AQDS-dependent AOM activity (**Fig. 2.1**) displayed a significant decrease on the diversity of the microbial community evidenced by a decrease in Shannon index, from 5.52 in freshly sampled sediment to 3.56 after enrichment with  $\text{CH}_4$  and AQDS.

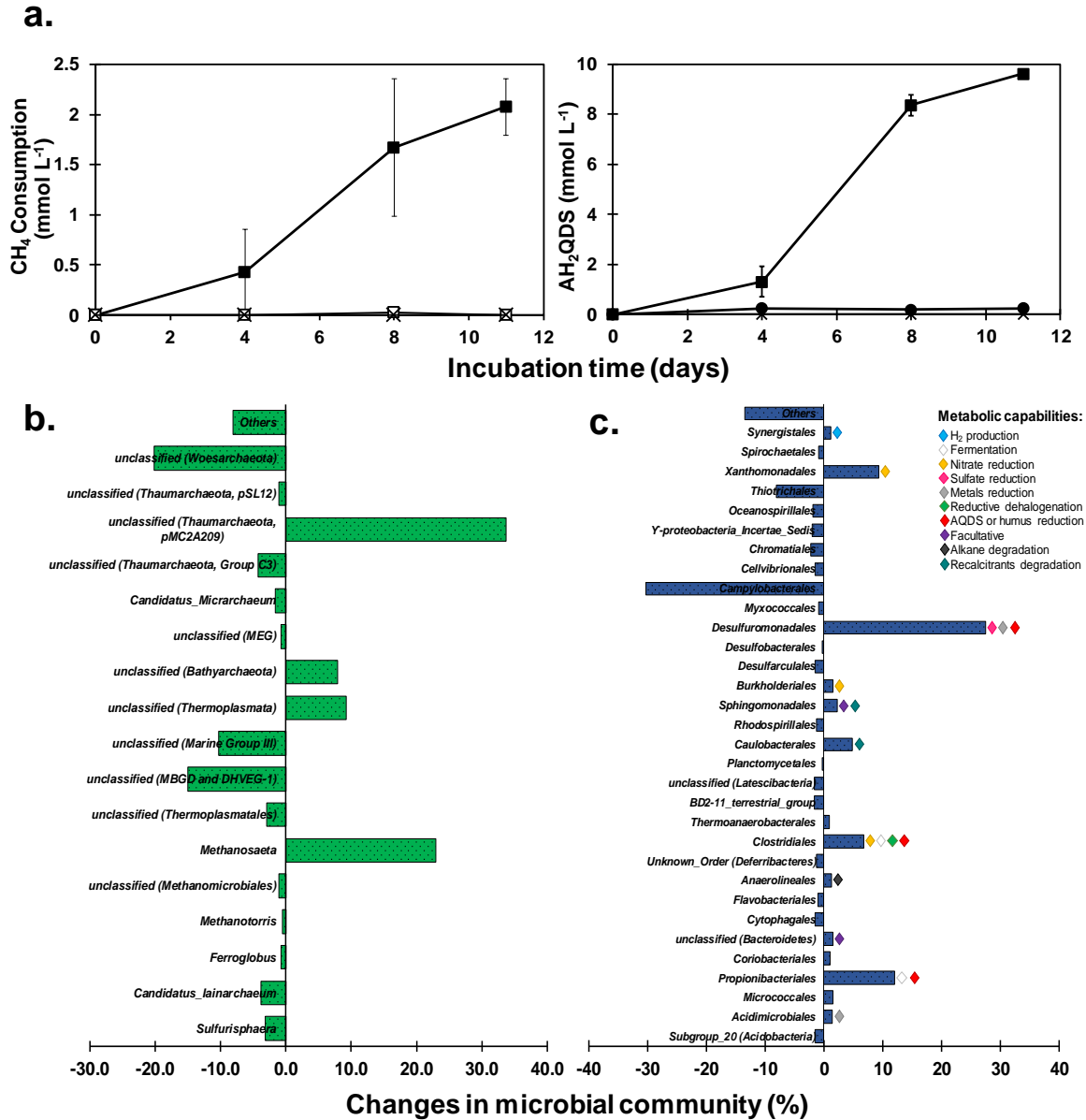


**Fig. 2.10 | AOM with AQDS as electron acceptor by an enrichment derived from wetland sediment. Panel a:** Kinetics of methane consumption linked to AQDS reduction (to AH<sub>2</sub>QDS) observed during the last 11 days of the entire enrichment process lasting 151 days: filled squares (-■-) represent microcosms including CH<sub>4</sub> as electron donor and AQDS as electron acceptor (complete experiments, n=3), open squares (-□-) represent controls without electron acceptor provided (without AQDS control, n=3), solid circles (-●-) represent CH<sub>4</sub>-free microcosms (endogenous controls, n=3), and

## CHAPTER II

crosses (-x-) represent heat killed controls (sterile controls, n=2). Error bars represent the standard error among replicates. **Panels b** and **c** depict microbial community changes at the end of the enrichment (151 days of incubation) at the phylum level based on Illumina sequencing of 16s rRNA V3-V4 regions. Fresh sediment composition was used as a reference.

Significant increments and decreases of specific groups of archaea and bacteria did occur in this enrichment (**Fig. 2.10b** and **c**). From the archaeal fraction, the pMC2A209 class from the *Thaumarchaeota* and the *Methanosaeta* genera were archaeal clusters that significantly increased their presence in the AQDS enrichment (34% and 23%, respectively). Also, in the AQDS enrichment, the *Bathyarchaeota* phylum previously detected in wetland sediments, both in the presence and in the absence of external NOM, significantly increased its proportion in the archaeal community (around 10% respect to the original composition), suggesting potential metabolic arrangements to thrive under AQDS-dependent AOM conditions (**Fig. 2.10b**). Humus-reducing bacteria that proliferated throughout the five months of enrichment included genera from the *Desulfuromonadales*<sup>29,30</sup>, *Clostridiales*<sup>14,28</sup> and *Propionibacteriales*<sup>31</sup> orders in 27%, 7%, and 12%, respectively, with respect to the original composition (**Fig. 2.9**).



## 2.4 Discussion

### 2.4.1 NOM as terminal electron acceptor fueling AOM in wetland sediment

Although the complex composition of the studied wetland sediment challenged efforts to elucidate the microbial processes responsible for the high methanotrophic activities quantified, the present study provides multiple lines of evidence demonstrating that electron-accepting functional groups present in its NOM fueled AOM by serving as terminal electron acceptor. Indeed, while sulfate reduction was the predominant process accounting for up to 42.5% of AOM activities, microbial reduction of NOM concomitantly occurred. Furthermore, enrichment of wetland sediment with external NOM, as *Pahokee Peat* HS, significantly promoted AOM with a quantified amount of  $\sim 100 \text{ nmol } ^{13}\text{C-CH}_4$  oxidized  $\text{cm}^{-3} \text{ d}^{-1}$  attributed to this microbial process. Spectroscopic evidence also demonstrated that quinone moieties, main redox functional groups in HS<sup>19</sup>, were heterogeneously distributed in the studied wetland sediment and that their reduction occurred during the course of AOM. Moreover, an enrichment derived from wetland sediments performing AOM linked to NOM reduction stoichiometrically oxidized methane coupled to AQDS. Sediment incubations performed in the presence of the sulfate reduction inhibitor, molybdate, further confirmed the role of HS in AOM. Certainly, even though sulfate-reducing activities significantly decreased in the presence of molybdate, AOM activities remained high, while microbial reduction of NOM was doubled under these conditions. These interesting findings suggest that methanotrophic microorganisms performing sulfate-dependent AOM might have directed electrons derived from AOM towards NOM when sulfate reduction became blocked as has been suggested based on experiments performed under artificial conditions<sup>27</sup>.

### 2.4.2 Microbial communities in wetland sediments performing AOM

Archaeal clusters consistently found in wetland sediment incubations performing AOM included members from the MBG-D family, which have already been proposed as players in metal-dependent AOM<sup>6</sup>, thus their presence agrees with evidence indicating AOM linked to iron reduction observed in some experimental controls (**Table 2.2**). Additionally, these microorganisms were not found in the AQDS enrichment, probably due to depletion of intrinsic ferric iron throughout the incubation cycles. Archaea constantly present amongst fresh sediment incubation and AQDS enrichment were those from the pMC2A209 class and the *Bathyarchaeota* phylum. To our knowledge, the pMC2A209 class of archaea has not been related to AOM, but its close partners from the MBG-B class have been consistently found in environments in which AOM occurs<sup>32-35</sup>. In fact, *Thaumarchaeota* members, including the MBG-B, have been found in consortia performing AOM in the absence of ANME clades<sup>36</sup>. Interestingly, the pMC2A209 cluster seemed to duplicate its proportion up to 12% when sulfate reduction was inhibited (by molybdate), which might suggest that the impediment of sulfate reduction enhanced its activity promoting AOM coupled to NOM reduction. Respect to the *Bathyarchaeota* phylum, increasing evidence suggests that this lineage might be involved in the methane cycle. Recently, it has been demonstrated that this cluster possesses the necessary genetic elements to express the enzymatic machinery required for methane production, and potentially methane consumption<sup>37</sup>. Additionally, Saxton and colleagues have found abundant *Bathyarchaeota* representation in a fulvic acids rich deep sediment that oxidizes methane uncoupled from sulfate reduction<sup>22</sup>. Unexpectedly, a very low percentage within the archaeal population was identified as members from the ANME type archaea, even though it would be expected to find ANME-2 members since it is the

only ANME subgroup with proven capability to derive electrons extracellularly towards humus and its analogues under artificial conditions<sup>27</sup>. Our microcosms, both in fresh sediment as well as in the AQDS long-term enrichment, showed a barely detectable number of copies of ANME-1b and ANME-3 sequences retrieved by the methodology employed, suggesting a low presence of ANME microorganisms in the ecosystem studied.

Regarding the bacterial composition, while *Clostridia*, *Bacilli* and *Gammaproteobacteria* were significantly represented within the fresh sediment performing AOM (**Fig. 2.9**), the AQDS enrichment (**Fig. 2.10**) exhibited the most significant increase in *Deltaproteobacteria* of the *Desulfuromonadales* order, which includes several humus-reducing microorganisms<sup>14</sup>. Since a wide diversity of microorganisms have been proven to reduce humus analogues or HS, we do not rule out that diverse bacterial clusters could have participated in partnership with detected archaea to jointly performed AOM coupled to NOM reduction. Nevertheless, humus-reducing bacteria possess metabolic versatility and capability to reduce miscellaneous electron acceptors, which makes it difficult to come to conclusions about their participation in our experiments. Further investigation must be done to unravel the potential involvement of humus-reducing bacteria in AOM.

## 2.5 Ecological significance

To our knowledge this is the first report of AOM coupled to microbial reduction of NOM, which constitutes a missing link within the carbon cycle. HS frequently contribute up to 80% of soil NOM and up to 50% of dissolved NOM in aquatic environments. While the labile fraction of NOM promotes methanogenesis in anaerobic environments, the slowly decomposing humic portion may serve as an important barricade to prevent methane emissions in organotrophic ecosystems by serving as terminal electron acceptor driving AOM (**Fig. 2.11**).

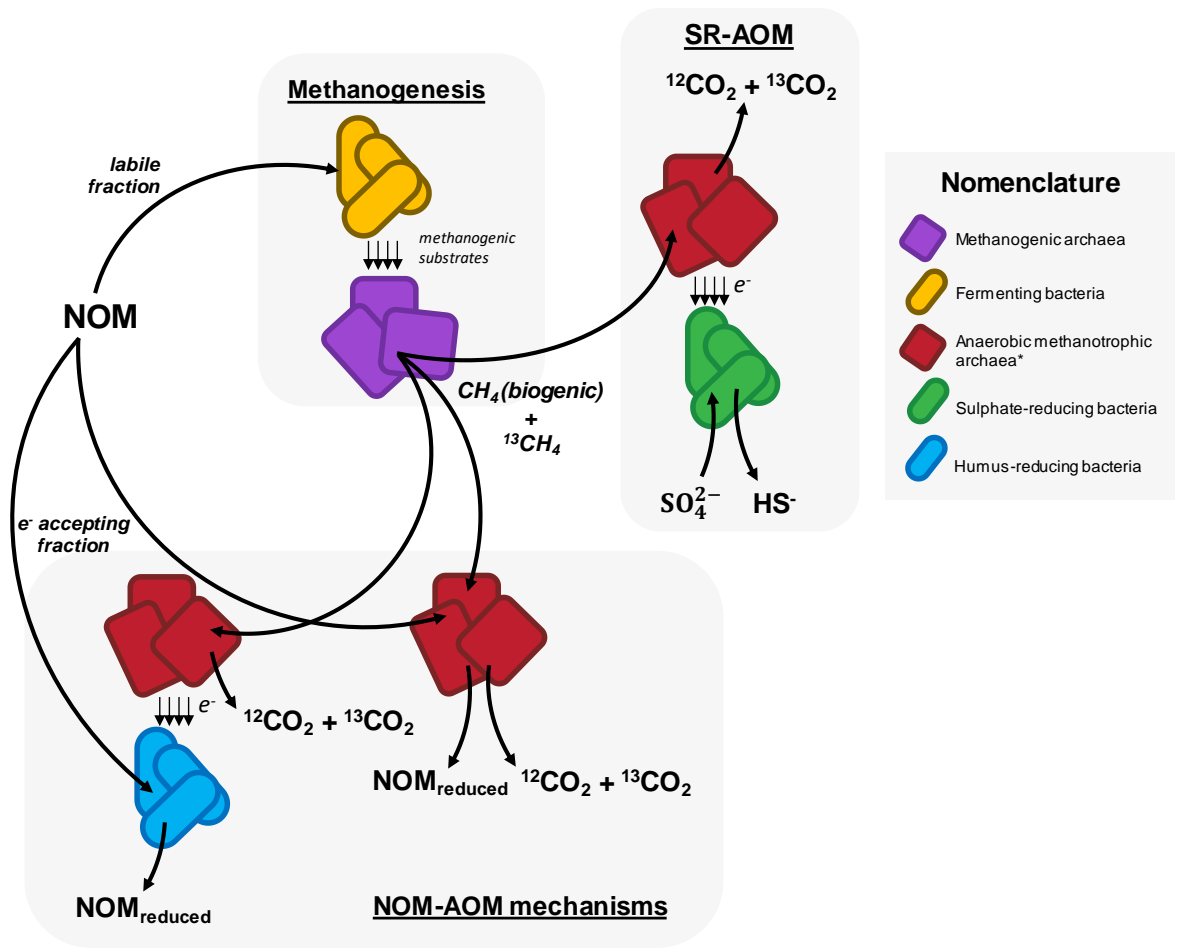


**Fig. 2.11 | Schematic representation of methane generation and consumption by wetland sediment biota.** While a fraction of NOM may serve as electron acceptor to support AOM (NOM-AOM) and decouple sulfate-reduction dependent AOM (SR-AOM), depending on its chemical properties, a labile fraction of NOM could also be degraded following the methanogenesis pathway by a fermenting and methanogenic fraction of the consortia. Equilibrium between these three phenomena must be tightly dependent on thermodynamic conditions, concentration of chemical species, and composition of microbial community. \*Anaerobic methanotrophic archaea are considered in a broader perspective than ANME clades from *Euryarchaeota* phylum.

## CHAPTER II

As an example, considering the maximum AOM driven by microbial reduction of NOM measured in humic enriched sediments, and the global area of coastal wetlands<sup>38, 39</sup>, we approximate that this microbial process consumes up to 114 Tg CH<sub>4</sub> yr<sup>-1</sup>. Considering the global wetland area<sup>10</sup>, we anticipate methane suppression of more than 1,300 Tg yr<sup>-1</sup> according to the following calculations:

The maximum measured AOM activity linked to microbial reduction of NOM was 100 nmol <sup>13</sup>C-CH<sub>4</sub> oxidized cm<sup>-3</sup> d<sup>-1</sup> (**Fig. 2.3** and **Fig. 2.4**). This activity was calculated based on quantified NOM reduction linked to AOM (corrected for the endogenous control lacking <sup>13</sup>CH<sub>4</sub>), which was then divided by 8 (number of electrons derived from the oxidation of <sup>13</sup>CH<sub>4</sub> to <sup>13</sup>CO<sub>2</sub>). Considering that AOM activities prevail within the top 40 cm from wetland sediments<sup>12</sup> and a global coastal wetland area of 48.9 Mha<sup>49</sup>, the total coastal wetland volume in which AOM occurs is:

The estimated total coastal wetland volume for AOM would be = 40 cm × 48.9 × 10<sup>6</sup> ha × (1 cm<sup>2</sup>/10<sup>-8</sup> ha)

Therefore,

Total coastal wetland volume for AOM = 1.956 × 10<sup>17</sup> cm<sup>3</sup>

Considering this total volume of coastal wetland, methane consumption by microbial reduction of NOM in coastal ecosystems is:

100 nmol CH<sub>4</sub> cm<sup>-3</sup> d<sup>-1</sup> × (16 ng CH<sub>4</sub>/1 nmol CH<sub>4</sub>) × (1 Tg CH<sub>4</sub>/ 10<sup>21</sup> ng CH<sub>4</sub>) × 1.956 × 10<sup>17</sup> cm<sup>3</sup> × (365 d/yr)

Therefore,

Total methane consumption in coastal wetlands by NOM reduction = 114.23 Tg CH<sub>4</sub> yr<sup>-1</sup>

Considering the global wetlands area of 570 Mha, the calculated methane suppression by this microbial process can be as follows:

Global wetlands volume for AOM = 40 cm × 570 × 10<sup>6</sup> ha × (1 cm<sup>2</sup>/10<sup>-8</sup> ha)

## CHAPTER II

Global wetlands volume for AOM =  $2.28 \times 10^{18} \text{ cm}^3$

Considering this volume for global wetlands<sup>10</sup>, methane consumption by microbial reduction of NOM in wetlands is:

$$100 \text{ nmol CH}_4 \text{ cm}^{-3} \text{ d}^{-1} \times (16 \text{ ng CH}_4 / 1 \text{ nmol CH}_4) \times (1 \text{ Tg CH}_4 / 10^{21} \text{ ng CH}_4) \times 2.28 \times 10^{18} \text{ cm}^3 \times (365 \text{ d/yr})$$

Therefore,

$$\text{Total methane consumption in wetlands by NOM reduction} = \underline{\underline{1,331.5 \text{ Tg CH}_4 \text{ yr}^{-1}}}$$

Accordingly, NOM-driven AOM may be more prominent in organotrophic sites with poor sulfate content, such as peatlands, swamps and organotrophic lakes. This premise is supported by suppression of methanogenesis by HS observed in different ecosystems<sup>16, 17</sup> and by the widespread AOM activity reported across many peatland types<sup>40-42</sup>. The potential role of HS is further emphasized because their electron accepting capacity is fully recycled in recurrently anoxic environments. Thus, the suppression of methanogenesis by HS estimated to be of the order of  $190,000 \text{ mol CH}_4 \text{ km}^{-2} \text{ yr}^{-1}$  may be much larger than previously considered.

## 2.6 References

1. **Reeburgh WS.** 2007. Oceanic methane biogeochemistry. *Chem Rev* 107:486–513.
2. **Boetius A,** Ravensschlag K, Schubert CJ, Rickert D, Widdel F, Gieseke A, Amann R, Jørgensen BB, Witte U, Pfannkuche O. 2000. A marine microbial consortium apparently mediating anaerobic oxidation of methane. *Nature* 407:623–626.
3. **Raghoebarsing A,** Pol a, van de Pas-Schoonen K, Smolders A, Ettwig K, Rijpstra W, Schouten S, Damste J, Op den Camp H, Jetten M, Strous M. 2006. A microbial consortium couples anaerobic methane oxidation to denitrification RID B-9395-2011 *Nature* 440:918–921.
4. **Deutzmann JS,** Stief P, Brandes J, Schink B. 2014. Anaerobic methane oxidation coupled to denitrification is the dominant methane sink in a deep lake. *Proc Natl Acad Sci U S A* 111:18273–18278.
5. **Ettwig KF,** Butler MK, Le Paslier D, Pelletier E, Mangenot S, Kuypers MMM, Schreiber F, Dutilh BE, Zedelius J, de Beer D, Gloerich J, Wessels HJCT, van Alen T, Luesken F, Wu ML, van de Pas-Schoonen KT, Op den Camp HJM, Janssen-Megens EM, Francoijs K-J, Stunnenberg H, Weissenbach J, Jetten MSM, Strous M. 2010. Nitrite-driven anaerobic methane oxidation by oxygenic bacteria. *Nature* 464:543–8.
6. **Beal EJ,** House CH, Orphan VJ. 2009. Manganese- and iron-dependent marine methane oxidation. *Science* 325:184–7.
7. **Egger M,** Rasigraf O, Sapart CJ, Jilbert T, Jetten MSM, Röckmann T, Van Der Veen C, Bânda N, Kartal B, Ettwig KF, Slomp CP. 2015. Iron-mediated anaerobic oxidation of methane in brackish coastal sediments. *Environ Sci Technol* 49:277–283.
8. **Ettwig KF,** Zhu B, Speth D, Keltjens JT, Jetten MSM, Kartal B. 2016. Archaea catalyze iron-dependent anaerobic oxidation of methane. *Proc Natl Acad Sci U S A* 113:12792–12796.
9. **Walter AKM,** Macintyre S. 2016. Nocturnal escape route for marsh gas. *Nature* 535:363–365.

10. **Bridgham SD**, Cadillo-Quiroz H, Keller JK, Zhuang Q. 2013. Methane emissions from wetlands: biogeochemical, microbial, and modeling perspectives from local to global scales. *Glob Chang Biol* 19:1325–46.
11. **Megonigal JP**, Hines ME, Visscher PT. 2004. Anaerobic Metabolism: Linkages to Trace Gases and Aerobic Processes. *Biogeochemistry* 317–424.
12. **Segarra KEA**, Schubotz F, Samarkin V, Yoshinaga MY, Hinrichs K-U, Joye SB. 2015. High rates of anaerobic methane oxidation in freshwater wetlands reduce potential atmospheric methane emissions. *Nat Commun* 6:7477.
13. **Segarra KEA**, Comerford C, Slaughter J, Joye SB. 2013. Impact of electron acceptor availability on the anaerobic oxidation of methane in coastal freshwater and brackish wetland sediments. *Geochim Cosmochim Acta* 115:15–30.
14. **Martinez CM**, Alvarez LH, Celis LB, Cervantes FJ. 2013. Humus-reducing microorganisms and their valuable contribution in environmental processes. *Appl Microbiol Biotechnol* 97:10293–308.
15. **Lehmann J**, Kleber M. 2015. The contentious nature of soil organic matter. *Nature* 528:60–8.
16. **Blodau C**, Deppe M. 2012. Humic acid addition lowers methane release in peats of the Mer Bleue bog, Canada. *Soil Biol Biochem* 52:96–98.
17. **Miller KE**, Lai CT, Friedman ES, Angenent LT, Lipson DA. 2015. Methane suppression by iron and humic acids in soils of the Arctic Coastal Plain. *Soil Biol Biochem* 83:176–183.
18. **Lovley DR**, Coates JD, Blunt-Harris EL, Phillips EJP, Woodward JC. 1996. Humic Substances as Electron acceptors for Microbial Respiration. *Nature* 17:428-437.
19. **Scott DT**, Mcknight DM, Blunt-Harris EL, Kolesar SE, Lovley DR. 1998. Quinone moieties act as electron acceptors in the reduction of humic substances by humics-reducing microorganisms. *Environ Sci Technol* 32:2984–2989.
20. **Straub KL**, Benz M, Schink B. 2000. Iron metabolism in anoxic environments at near neutral pH. *FEMS Microbiol Ecol* 34:181–186.



- 21. Timmers PH**, Suarez-Zuluaga DA, van Rossem M, Diender M, Stams AJ, Plugge CM. **2015**. Anaerobic oxidation of methane associated with sulfate reduction in a natural freshwater gas source. *ISME J* 10:1–13.
- 22. Saxton MA**, Samarkin VA, Schutte CA, Bowles MW, Madigan MT, Cadieux SB, Pratt LM, Joye SB. **2016**. Biogeochemical and 16S rRNA gene sequence evidence supports a novel mode of anaerobic methanotrophy in permanently ice-covered Lake Fryxell, Antarctica. *Limnol Oceanogr* 61:S119–S130.
- 23. Alperin MJ**. **1988**. Carbon and hydrogen isotope fractionation resulting from anaerobic methane oxidation. *Biogeochem Cycles* 2:279–288.
- 24. Martens CS**, Albert DB, Alperin MJ. **1999**. Stable isotope tracing of anaerobic methane oxidation in the gassy sediments of Eckernforde Bay German Baltic Sea. *Am J Sci* 299: 589–610.
- 25. Socrates G**. **2004**. Infrared and Raman characteristic group frequencies. *Infrared and Raman characteristic group frequencies*.
- 26. Orphan VJ**, House CH, Hinrichs K-U, McKeegan KD, DeLong EF. **2002**. Multiple archaeal groups mediate methane oxidation in anoxic cold seep sediments. *Proc Natl Acad Sci U S A* 99:7663–7668.
- 27. Scheller S**, Yu H, Chadwick GL, Mcdlynn SE. **2016**. Artificial electron acceptors decouple archaeal methane oxidation from sulfate reduction. *Science* (80- ) 351:703–707.
- 28. Xi B**, Zhao X, He X, Huang C, Tan W, Gao R, Zhang H, Li D. **2016**. Successions and diversity of humic-reducing microorganisms and their association with physical-chemical parameters during composting. *Bioresour Technol* 219:204–211.
- 29. Coates JD**, Cole KA, Chakraborty R, Connor SMO, Achenbach LA. **2002**. Diversity and ubiquity of bacteria capable of utilizing humic substances as electron donors for anaerobic respiration diversity and ubiquity of bacteria capable of utilizing humic substances as electron donors for anaerobic respiration. *Appl Environ Microbiol* 68:2445–2452.
- 30. Lovley DR**, Fraga JL, Blunt-Harris EL, Hayes LA, Phillips EJP,

- Coates JD. 1998. Humic substances as a mediator for microbially catalyzed metal reduction. *Acta Hydrochim Hydrobiol* 26:152–157.
- 31. Benz M**, Schink B, Brune A. **1998**. Humic acid reduction by *Propionibacterium freudenreichii* and other fermenting bacteria. *Appl Environ Microbiol* 64:4507–4512.
- 32. Glass JB**, Yu H, Steele J a, Dawson KS, Sun S, Chourey K, Pan C, Hettich RL, Orphan VJ. **2014**. Geochemical, metagenomic and metaproteomic insights into trace metal utilization by methane-oxidizing microbial consortia in sulphidic marine sediments. *Environ Microbiol* 16:1592–611.
- 33. Knittel K**, Lösekann T, Boetius A, Kort R, Amann R, Lo T. **2005**. Diversity and Distribution of Methanotrophic Archaea at Cold Seeps Diversity and Distribution of Methanotrophic Archaea at Cold Seeps †. *Appl Environ Microbiol* 71:467–479.
- 34. Schubert CJ**, Vazquez F, L??sekann-Behrens T, Knittel K, Tonolla M, Boetius A. **2011**. Evidence for anaerobic oxidation of methane in sediments of a freshwater system (Lago di Cadagno). *FEMS Microbiol Ecol* 76:26–38.
- 35. Yoshinaga MY**, Lazar CS, Elvert M, Lin YS, Zhu C, Heuer VB, Teske A, Hinrichs KU. **2015**. Possible roles of uncultured archaea in carbon cycling in methane-seep sediments. *Geochim Cosmochim Acta* 164:35–52.
- 36. Biddle JF**, Lipp JS, Lever MA, Lloyd KG, Sørensen KB, Anderson R, Fredricks HF, Elvert M, Kelly TJ, Schrag DP, Sogin ML, Brenchley JE, Teske A, House CH, Hinrichs K-U. **2006**. Heterotrophic Archaea dominate sedimentary subsurface ecosystems off Peru. *Proc Natl Acad Sci U S A* 103:3846–3851.
- 37. Evans PN**, Parks DH, Chadwick GL, Robbins SJ, Orphan VJ, Golding SD, Tyson GW. **2015**. Methane metabolism in the archaeal phylum Bathyarchaeota revealed by genome-centric metagenomics. *Science* 350:434–8.
- 38. Keller**, Jason K. & Medvedeff C, A. **2016**. Soil organic matter, p. 165–188. In *Wetland soils: genesis, hydrology, landscapes, and classifications* Vepraskas,. Taylor and Francis Group.

- 39. Pendleton L**, Donato DC, Murray BC, Crooks S, Jenkins WA, Sifleet S, Craft C, Fourqurean JW, Kauffman JB, Marbà N, Megonigal P, Pidgeon E, Herr D, Gordon D, Baldera A. **2012**. Estimating Global “Blue Carbon” Emissions from Conversion and Degradation of Vegetated Coastal Ecosystems. *PLoS One* 7: e43542.
- 40. Gupta V**, Smemo KA, Yavitt JB, Basiliko N. **2012**. Active Methanotrophs in Two Contrasting North American Peatland Ecosystems Revealed Using DNA-SIP. *Microb Ecol* 63:438–445.
- 41. Smemo KA**, Yavitt JB. 2007. Evidence for Anaerobic CH<sub>4</sub> Oxidation in Freshwater Peatlands. *Geomicrobiol J* 24:583–597.
- 42. Smemo KA**, Yavitt JB. **2011**. Anaerobic oxidation of methane: An underappreciated aspect of methane cycling in peatland ecosystems? *Biogeosciences* 8:779–793.
- 43. Klüpfel L**, Piepenbrock A, Kappler A, Sander M. **2014**. Humic substances as fully regenerable electron acceptors in recurrently anoxic environments. *Nat Geosci* 7:195–200.
- 44. APHA/AWWA/WEF**. **2012**. *Standard Methods for the Examination of Water and Wastewater Standard Methods*.
- 45. Soga T**, Ross GA. **1999**. Simultaneous determination of inorganic anions, organic acids and metal cations by capillary electrophoresis. *J Chromatogr A* 834:65–71.
- 46. Cord-Ruwisch R**. **1985**. A quick method for the determination of dissolved and precipitated sulfides in cultures of sulfate-reducing bacteria. *J Microbiol Methods* 4:33–36.
- 47. Klindworth A**, Pruesse E, Schweer T, Peplies J, Quast C, Horn M, Glöckner FO. **2013**. Evaluation of general 16S ribosomal RNA gene PCR primers for classical and next-generation sequencing-based diversity studies. *Nucleic Acids Res* 41:1–11.
- 48. Schloss PD**, Westcott SL, Ryabin T, Hall JR, Hartmann M, Hollister EB, Lesniewski RA, Oakley BB, Parks DH, Robinson CJ, Sahl JW, Stres B, Thallinger GG, Van Horn DJ, Weber CF. **2009**. Introducing mothur: Open-source, platform-independent, community-supported software for describing and comparing microbial communities. *Appl Environ Microbiol* 75:7537–754.

## CHAPTER II

- 49. Pendleton L, Donato DC, Murray BC, Crooks S, Jenkins WA, Sifleet S, Craft C, Fourqurean JW, Kauffman JB, Marbà N, Megonigal P, Pidgeon E, Herr D, Gordon D, Baldera A. 2012.** Estimating global “blue carbon” emissions from conversion and degradation of vegetated coastal ecosystems. *PLoS One* 7, e43542.

## CHAPTER III

# Electron Shuttling Mediated by Humic Substances Fuels Anaerobic Methane Oxidation and Carbon Burial

### HIGHLIGHTS

- **Elusive mechanisms** for the **anaerobic oxidation of methane (AOM)** in a tropical wetland were explored.
- Humus promoted net AOM with a **poorly reactive iron oxide (goethite)** as the electron sink.
- **Humus-driven electron shuttling** enhanced **carbon sequestration** as inert minerals (iron and calcium carbonates).
- The **environmental significance** of humus electron shuttling in AOM is discussed.

**A modified version of this chapter has been published as:**

**Valenzuela, E. I.**, Avendaño, K. A., Balagurusamy, N., Arriaga, S., Nieto-Delgado, C., Thalasso, F., et al. (2019). *Electron shuttling mediated by humic substances fuels anaerobic methane oxidation and carbon burial in wetland sediments*. **Sci. Total Environ.** **650**, 2674–2684. doi:10.1016/J.SCITOTENV.2018.09.388.

## Abstract

Key pathways for the *anaerobic oxidation of methane* (AOM) have remained elusive, particularly in organic rich ecosystems. In this work, the occurrence of AOM driven by humus-catalyzed dissimilatory iron reduction was investigated in sediments from a coastal mangrove swamp. Anoxic sediment incubations supplied with both *goethite* ( $\alpha$ -FeOOH) and *leonardite* (humic substances (HS)) displayed an average AOM rate of  $10.7 \pm 0.8 \mu\text{mol CH}_4 \text{ cm}^{-3} \text{ day}^{-1}$ , which was 7 and 3 times faster than that measured in incubations containing only goethite or HS, respectively. Additional incubations performed with  $^{13}\text{C}$ -methane displayed *Pahoee Peat* HS-catalyzed carbonate precipitation linked to  $^{13}\text{CH}_4$  oxidation and *ferrhydrite* reduction ( $\sim 1.3 \mu\text{mol carbonate cm}^{-3} \text{ day}^{-1}$ ). These results highlight the role of HS on mitigating greenhouse gases released from wetlands, not only by mediating the AOM process, but also by enhancing carbon sequestration as inert minerals (*calcite*, *aragonite* and *siderite*).

### 3.1 Introduction

Wetlands are complex ecosystems characterized by the flooding of soils and are important in global carbon dynamics because of their large soil carbon pools and potential for carbon sequestration in peat formation, sediment deposition, and plant biomass. These ecosystems, commonly classified as bogs, marshes and swamps, represent the largest biogenic source of greenhouse gases, particularly methane ( $\text{CH}_4$ ), and growing evidence suggests that these emissions are climate sensitive; thus, future  $\text{CH}_4$  wetland budgeting will be tightly controlled by global warming<sup>1-3</sup>. The net amount of  $\text{CH}_4$  released to the atmosphere from wetlands is estimated to be one third of the global  $\text{CH}_4$  budget ( $\sim 164 \text{ Tg yr}^{-1}$ )<sup>4</sup>, and is the result of the balance between methanogenesis (microbial generation of  $\text{CH}_4$ ), and methanotrophy (biological oxidation of  $\text{CH}_4$ )<sup>5</sup>, with the latter process being promoted by the reduction of molecular oxygen<sup>6</sup> or an alternative electron acceptor (sulfate, nitrate/nitrite, oxidized metals, humic material)<sup>7,8</sup>. Due to limited oxygen availability induced by flooding conditions, anaerobic oxidation of methane (AOM) constitutes a key  $\text{CH}_4$  sink in wetlands with the potential to exert outstanding impact on global biogeochemical carbon cycling<sup>9</sup>. After decades of elusiveness, AOM in wetlands has been linked to the reduction of sulfate<sup>9,10</sup>, nitrate/nitrite<sup>11-14</sup>, and recently to the electron-accepting fraction of natural organic matter (NOM), also known as *humus* or *humic substances* (HS)<sup>8</sup>. HS is the term traditionally employed to denote the recalcitrant fraction of NOM with redox activity (capability to accept or donate electrons)<sup>15-17</sup>, which has also been referred to as *organic acids*<sup>18</sup>. Once HS are reduced by microbial activity, they can be chemically re-oxidized, either by molecular oxygen<sup>19</sup> or oxidized compounds, such as metallic oxides<sup>20,21</sup> promoting further oxidation of pollutants. Due to their abundance on Earth and availability in both terrestrial and aquatic environments,

the oxidized forms of iron, which at near neutral pH values prevail in the form of crystalline minerals, are the most important metals with the capacity to re-oxidize HS in natural ecosystems<sup>20</sup>. To date, iron-dependent AOM has been reported in several aquatic ecosystems including marine sediments<sup>22–25</sup>, a polluted aquifer<sup>26</sup>, and freshwater lakes<sup>27,28</sup> by means of isotopic tracing and biogeochemical profiling<sup>29</sup>. Nevertheless, the role of HS on this reaction has not been demonstrated despite the fact that electron shuttling reactions (involving both metals and sulfurous compounds) have been previously demonstrated to play key roles in the dynamics of anaerobic degradation of organic molecules<sup>20,30,31</sup>. The occurrence of *humus-mediated* iron-dependent AOM, first hypothesized almost a decade ago<sup>32</sup>, would represent an unrevealed methane sink that could have huge biogeochemical and ecological implications, since the net amount of CH<sub>4</sub> mitigated by ferric iron and HS in organotrophic ecosystems may be much higher than previously considered due to the redox interactions involved<sup>20,33,34</sup>. Until now, it has been estimated that AOM contributes to reduce freshwater wetlands emission by 200 Tg of methane per year<sup>9</sup>.

Given the recent evidence on the potential role of HS as an electron acceptor in the AOM<sup>8,35</sup>, we aimed to provide biogeochemical insight into the role of humus-catalyzed reduction of iron oxides in the AOM in wetland sediments. To this end, we studied the addition of two widespread mineral forms of ferric iron, and two sources of external HS on the methanotrophic activity carried out by the biota of a coastal wetland sediment, which previously showed AOM activity linked to the reduction of HS and their analogues<sup>8</sup>. Three scenarios were considered: **1)** a long-term incubation in which intrinsic electron acceptors allowed substantial rates of net AOM with a highly crystalline iron oxide (*e.g.* goethite) as terminal electron acceptor (TEA), **2)** an incubation cycle in which the biogeochemical conditions prevailing in the sampled site were preserved, and **3)** an incubation under artificial



conditions using destructive sampling to minimize the interference related to the biogeochemical complexity of natural samples. The reduction of different external electron acceptors (two sources of HS and two iron oxides of different reactivity) was correlated to AOM both as  $^{13}\text{C}$  enrichment and net  $^{13}\text{C}$ - and  $^{12}\text{C}$ -methane consumption.

## 3.2 Materials and Methods

### 3.2.1 Wetland description and sediment sampling

The *Sisal* wetland (**Fig. 2.1**) is a mangrove swamp located within the ports of Celestun and Sisal in the Yucatán Peninsula, southeastern Mexico ( $21^{\circ}09'26''\text{N}$ ,  $90^{\circ}03'09''\text{W}$ ). This coastal zone has a semi-arid climate and presents a high degree of karstification of sediments, which are mainly composed of tertiary carbonates subject to constant dissolution. Due to intermittent saltwater inputs from the ocean (which reach 40 km inland)<sup>36</sup>, this water reservoir possesses significant levels of salinity, which can vary seasonally depending on the rainfall regime. Wetland sediment samples were collected in January 2016, the depth of the sampled cores being 15 cm. Sediment cores were harvested under a water column of approximately 70 cm. Water samples from the top of the sampling point were also collected. All samples were sealed in hermetic flasks and maintained in ice until their arrival to the laboratory where they were then stored at  $4^{\circ}\text{C}$  in a dark room. Before performing the incubation assays, sediment and water samples were chemically characterized. The characteristics of sediment and water samples are provided in **Chapter II (Table 2.1)**.

## 3.2.2 Microcosms set-up

### 3.2.2.1 Long-term incubations

#### 3.2.2.1.1 Inoculation and first incubation cycle

A wetland sediment core was homogenized inside of an anaerobic chamber (COY 14500; atmosphere composed of N<sub>2</sub>/H<sub>2</sub>, 95%/5%, v/v) and 2 g of wetland sediment were inoculated into 120 mL serological flasks. Subsequently, 30 mL of anoxic artificial basal medium with the following composition (in g L<sup>-1</sup>): NH<sub>4</sub>Cl (0.3), K<sub>2</sub>HPO<sub>4</sub> (0.2), MgCl<sub>2</sub>·6H<sub>2</sub>O (0.03), CaCl<sub>2</sub> (0.1), NaCl (3), and 1 mL L<sup>-1</sup> of a trace metals solution previously described<sup>8</sup>, were provided as liquid medium. In order to provide the different experimental conditions, the artificial basal medium was enriched with the following electron acceptors in different experimental treatments: 5000 mg L<sup>-1</sup> of bulk leonardite (catalogue number from International Humic Substances Society: BS104L), 50 mmol L<sup>-1</sup> of chemically synthesized goethite<sup>37</sup>, a combination of both, or none (*unamended sediment* control). Six flasks were inoculated under each experimental condition and afterwards they were sealed with air-tight rubber stoppers and aluminum caps and flushed with a mixture of N<sub>2</sub>:CO<sub>2</sub> (80%/20% [vol/vol]) for 10 min. Before initial headspace measurements and incubation at 28 °C in the dark, three flasks from each experimental treatment were spiked with 30 mL of CH<sub>4</sub> (99% purity; Praxair), reaching a partial pressure of ~0.39 atm (on a 90 mL headspace), while the remaining three were left with a N<sub>2</sub>:CO<sub>2</sub> atmosphere to serve as *endogenous* controls. *Killed* controls (amended with the same concentrations of electron acceptors (leonardite and goethite) were also prepared by autoclaving the sealed microcosms three times at 120° C for 21 min and then spiked with the same volume of CH<sub>4</sub>.

### 3.2.2.1.2 Second incubation cycle

After 65 days of incubation, microcosms were opened inside the anaerobic chamber, where they were decanted to replace the old liquid medium with freshly prepared basal medium enriched with the same electron acceptors at the following concentrations: 2500 mg L<sup>-1</sup> of leonardite, 50 mmol L<sup>-1</sup> of goethite, the combination of both, or none. Afterwards, the bottles were thoroughly shaken and 50% of the content of each microcosm (15 mL of slurry) was transferred into new serological flasks, which were then complemented with the respective electron acceptor-enriched basal medium to reach a final volume of 30 mL. Once outside the anaerobic chamber, microcosms were flushed with a mixture of N<sub>2</sub>:CO<sub>2</sub> (80%/20% [vol/vol]) for 10 min, and methane was spiked into the correspondent microcosms following the same procedures previously described in **Section 3.2.2.1.1**.

### 3.2.2.2 Incubations with <sup>13</sup>C-methane

Serological flasks (25 mL) were inoculated with 1 cm<sup>3</sup> of homogenized sediment on the inside of the previously described anaerobic chamber. Once inoculated, 15 mL of water collected from the sampling-point (water column) were provided as a liquid medium, then the flasks were sealed with air-tight rubber stoppers and aluminum caps (no external electron acceptor or methane were added at this point). Once outside the anaerobic chamber, anoxic conditions were established by flushing the bottle's headspace with N<sub>2</sub> (Ultra High Purity; Praxair, Mexico) for 5 min. Afterwards, the flasks were incubated at 28°C in the dark. After 10 days of pre-incubation under these conditions, the flasks were opened inside the anaerobic chamber and the following electron acceptors were added to six

flasks per treatment to start the first incubation cycle: 500 mg L<sup>-1</sup> of *Pahokee Peat* humic substances (PPHS, catalogue number from International Humic Substances Society: 1S103H), chemically synthesized 2-line ferrihydrite<sup>37</sup> (50 mmol L<sup>-1</sup>), a combination of both, or none (unamended sediment control). After amendment with the electron acceptors, all flasks were sealed again as previously described, removed from the anaerobic chamber and flushed with N<sub>2</sub> for 5 min. After 12 hours of incubation at 28°C in the dark, to allow carbonate equilibrium, three of the six flasks were spiked with 2.5 mL of <sup>13</sup>CH<sub>4</sub> (<sup>13</sup>CH<sub>4</sub>, Sigma Aldrich, 99 atom. % <sup>13</sup>C), which renders a methane partial pressure of ~0.28 atm. (on a 9-mL headspace), while the remaining three were left with a N<sub>2</sub> atmosphere to serve as *endogenous* controls. Immediately after <sup>13</sup>CH<sub>4</sub> amendment, initial gaseous measurements were made for every flask, including the endogenous controls. *Killed* controls (amended with the same concentrations of ferrihydrite, PPHS and the same volume of <sup>13</sup>CH<sub>4</sub>) were also prepared by autoclaving the sealed microcosms three times at 120° C for 21 min and by the subsequent addition of 10% v/v of anhydrous chloroform.

### 3.2.2.3 Destructive sampling incubations

After the incubation period performed under quasi natural conditions (described in **Section 3.2.2.2**) lasting 21 days, a second incubation cycle was started under artificial conditions, which involved a *destructive sampling* regime. For this second stage, 15-mL serological flasks were supplied with 7 mL of artificial basal medium previously described. The artificial basal medium was amended with the same external electron acceptors, as in the previous cycle, at the following concentrations: 2500 mg L<sup>-1</sup> for PPHS, 50 mmol L<sup>-1</sup> for chemically synthesized 2-line

ferrihydrite<sup>37</sup>. Furthermore, a treatment including both PPHS and 2-line ferrihydrite, as well as killed and *unamended* sediment controls lacking any electron acceptor, were also considered in this incubation cycle. After inoculation with 0.16 mL of slurry taken from the previous microcosms (mixture of sediment and water column), the flasks were sealed inside the anaerobic chamber and the headspace was flushed for 5 min with N<sub>2</sub>. The final headspace volume was 6 mL, which was spiked with 1 mL of <sup>13</sup>CH<sub>4</sub> to reach ~0.17 atm of <sup>13</sup>CH<sub>4</sub> partial pressure. A total of 90 vials belonging to 5 experimental treatments (described above) were prepared, and a complete set involving triplicates for each experimental treatment was destroyed by the addition of strong-acid. In the first three sampling-points, each microcosm was acidified by injecting 500 µL of HCl 3N with a disposable syringe, while during the last two measurements, the same volume of concentrated HCl (37%) was employed. After acidification, the flasks were thoroughly shaken and left for 12 hours at 28°C in the dark prior to CO<sub>2</sub> (<sup>12</sup>CO<sub>2</sub> and <sup>13</sup>CO<sub>2</sub>) and Fe<sup>2+</sup> measurements.

### 3.2.3 Chemical determinations

Sulfate, sulfide, nitrate and nitrite were measured by previously reported standard methodologies<sup>8,38–40</sup>. For the first two experiments (described in **Sections 3.2.2.1 & 3.2.2.2**), ferrous iron measurements were made by acid extraction from slurry sub-samples taken over time from the microcosms with disposable syringes. Afterwards, the extracted ferrous iron was measured using the ferrozine technique in a spectrophotometer located inside of an anaerobic chamber (COY 14500, atmosphere: N<sub>2</sub> (95%)/H<sub>2</sub> (5%))<sup>8,41</sup>. For the incubation cycle involving artificial conditions and destructive sampling (**Section 3.2.2.3**), vials were sacrificed for iron extraction from the flasks' entire content at the acid concentrations previously

described and then iron was quantified following the same methodology. The reduction of humic material in the form of intrinsic NOM or added HS was assessed as the amount of ferrous iron produced by the reaction of ferric citrate with slurry taken from the microcosms under anoxic conditions; the ferrous iron released was then measured using the ferrozine technique<sup>16,41</sup> and corrected for intrinsic ferrous iron detected ( $\text{Fe}^{2+}$  measured in samples after acid treatment). Unlabeled methane (employed to assess net  $\text{CH}_4$  oxidation in the long-term incubations) was measured by injecting 100  $\mu\text{L}$  from the headspace of incubation flasks into a Gas Chromatograph (GS) Agilent Technologies 6890M equipped with a thermal conductivity detector and a HayeSep D column (Alltech, Deerfield, IL, USA). The temperatures of the injection port, oven, and detector were 250, 60, and 250°C, respectively.  $\text{N}_2$  was employed as a carrier gas at a flux of 12  $\text{mL min}^{-1}$ . Methane and carbon dioxide isotopes were measured in a Gas Chromatograph Agilent Technologies 7890A coupled to an Agilent Technologies Mass Spectrometer 5975C. The ionization was carried out by electronic impact, quadrupole analyzer and a capillary column Agilent Technologies HP-PLOT/Q with a stationary phase of poly-styrene-di-vinyl-benzene, using helium as carrier gas<sup>8</sup>.

### **3.2.4 Mineral characterization of the sediment**

Sediment samples were analyzed by X-Ray diffraction (XRD, Bruker D8 Advance) and Environmental Scanning Electron Microscopy (ESEM, QUANTA FEG-250) combined with Energy Dispersive Spectroscopy (EDS). At the end of the second incubation cycle, selected experimental units from each treatment were opened inside an anaerobic chamber and sediment samples were dried under a  $\text{N}_2/\text{H}_2$  atmosphere (95:5%). Samples for ESEM analysis were observed without affecting particle morphologic characteristics. XRD analysis was made after the

trituration of dried sediment on an agate mortar. The patterns obtained ( $2\theta = 10^\circ$  to  $80^\circ$ , step = 10 s, step size =  $0.02^\circ$ ) were compared against data from the International Center of Diffraction Data (ICDD) PDF-4 database.

### 3.3 Calculations

#### 3.3.1 Fractional enrichment of $^{13}\text{CO}_2$

Labeled carbon dioxide ( $^{13}\text{CO}_2$ ) enrichment is denoted as its fraction with respect to the total  $\text{CO}_2$  quantified at the headspace ( $^{12}\text{CO}_2 + ^{13}\text{CO}_2$ ) and is referred to as  $^{13}\text{F}_{\text{CO}_2}$  throughout the text (**Eq. 3.1**).

$$^{13}\text{F}_{\text{CO}_2} = \frac{^{13}\text{CO}_2}{^{12}\text{CO}_2 + ^{13}\text{CO}_2} \quad \text{Eq. 3.1}$$

The  $^{13}\text{F}_{\text{CO}_2}$  data shown were normalized by subtraction of the initial value, which was measured after 12 hours of incubation before  $^{13}\text{CH}_4$  addition (described in the Microcosms set-up section) and is denoted as  $^{13}\text{F}'_{\text{CO}_2}$  (**Eq. 3.2**).

$$^{13}\text{F}'_{\text{CO}_2} = ^{13}\text{F}_{\text{CO}_2}(\text{actual}) - ^{13}\text{F}_{\text{CO}_2}(\text{initial}) \quad \text{Eq. 3.2}$$

#### 3.3.2 Electron balances

The percentage of net  $^{13}\text{CH}_4$  anaerobic oxidation explained by the reduction of intrinsic and added electron acceptors was calculated as follows (**Eq. 3.3**):

$$\% \text{ of AOM} = \frac{EA_{\text{reduced}}^* (\text{in the presence of } ^{13}\text{CH}_4) - EA_{\text{reduced}}^{**} (\text{in the endogenous controls}^{***})}{\frac{EA \text{ stoichiometric value}^{***}}{^{13}\text{CH}_4 \text{ oxidized}}} \times 100$$

#### Eq. 3.3

Where  $^*EA$  stands for electron acceptor,  $^{**}endogenous \ controls$  refer to microcosms lacking added  $^{13}\text{CH}_4$ , and  $^{***}EA \ stoichiometric \ value$  is 1 for sulfate, 8 for ferric iron according to the respective reactions of methane oxidation<sup>7,8</sup> and 8

for reduced humic material considering the electron equivalents measured via ferric citrate reduction.

### 3.3.3 AOM assessment via carbonate precipitation

The percentage of net  $^{13}\text{CH}_4$  oxidation linked to ferrihydrite reduction, or PPHS-catalyzed ferrihydrite reduction, was calculated by comparing the amount of  $^{13}\text{CO}_3^{2-}$  precipitated due to  $\text{Fe}^{2+}$  exclusively produced in the presence of  $^{13}\text{CH}_4$  and considering the  $\text{FeCO}_3$  precipitation stoichiometry. The calculations were as follows:

The amount of  $^{13}\text{C}$ -carbon dioxide not quantified due to precipitation with ferrous iron was employed to perform an electron balance considering the stoichiometry of the Fe-dependent AOM reaction, as well as the amount of net  $^{13}\text{CH}_4$  oxidized. The calculations were as follows:

- Since the precipitation of one mole of  $^{13}\text{CO}_2$  requires of 1 mole of  $\text{Fe}^{2+}$  produced (stoichiometry 1:1), and the oxidation of a  $^{13}\text{CH}_4$  molecule requires 8  $\text{Fe}^{3+}$  molecules (stoichiometry 1:8), we can estimate the amount of  $^{13}\text{CH}_4$  oxidized due to iron reduction by knowing the difference in iron precipitation triggered by the presence of methane with respect to that determined in the endogenous controls (lacking methane):

**a) Only ferrihydrite controls:**

$$^{13}\text{CO}_3^{2-} \text{ precipitated (not quantified)} = \text{Fe}^{2+} \text{ precipitation due to } ^{13}\text{CH}_4 \text{ oxidation}$$

$$\text{Fe}^{2+} \text{ precipitation due to } ^{13}\text{CH}_4 \text{ oxidation} = \text{Fe}_{\text{ferrihydrite}}^{2+} - \text{Fe}_{\text{ferrihydrite} + ^{18}\text{CH}_4}^{2+}$$

$$\% \text{ of net } ^{13}\text{CH}_4 \text{ oxidized responded by Fe}^{3+} \text{ reduction} = \frac{^{18}\text{CO}_3^{2-} \text{ precipitated}}{^{18}\text{CH}_4 \text{ oxidized}} \times 100$$

Following the same basis:

**b) Pahokee Peat Humic Substances + Ferrihydrite controls:**



## CHAPTER III

$^{13}\text{CO}_3^{2-}$  precipitated (not quantified) =  $\text{Fe}^{2+}$  precipitation due to  $^{13}\text{CH}_4$  oxidation and PPHS  $e^-$  shut.

$\text{Fe}_2^{2+}$  precipitation due to  $^{13}\text{CH}_4$  ox. and PPHS presence and  $e^-$  shuttling

$$= \text{Fe}_{\text{PPHS} + \text{ferrihydrite}}^{2+} - \text{Fe}_{\text{PPHS} + \text{ferrihydrite} + ^{18}\text{CH}_4}^{2+}$$

% of net

$$^{13}\text{CH}_4 \text{ oxidized responded by PPHS - mediated } \text{Fe}^{3+} \text{ reduction} = \frac{^{18}\text{CO}_3^{2-} \text{ precipitated}}{^{18}\text{CH}_4 \text{ oxidized}} \times 100$$

## 3.4 Results

### 3.4.1 Net CH<sub>4</sub> oxidation linked to goethite reduction mediated by HS

After an initial incubation period of 65 days (data not shown, see [Section 3.2.2.1.2](#)), AOM was observed associated to leonardite or goethite reduction in a 24-day subsequent period ([Fig. 3.1](#)).

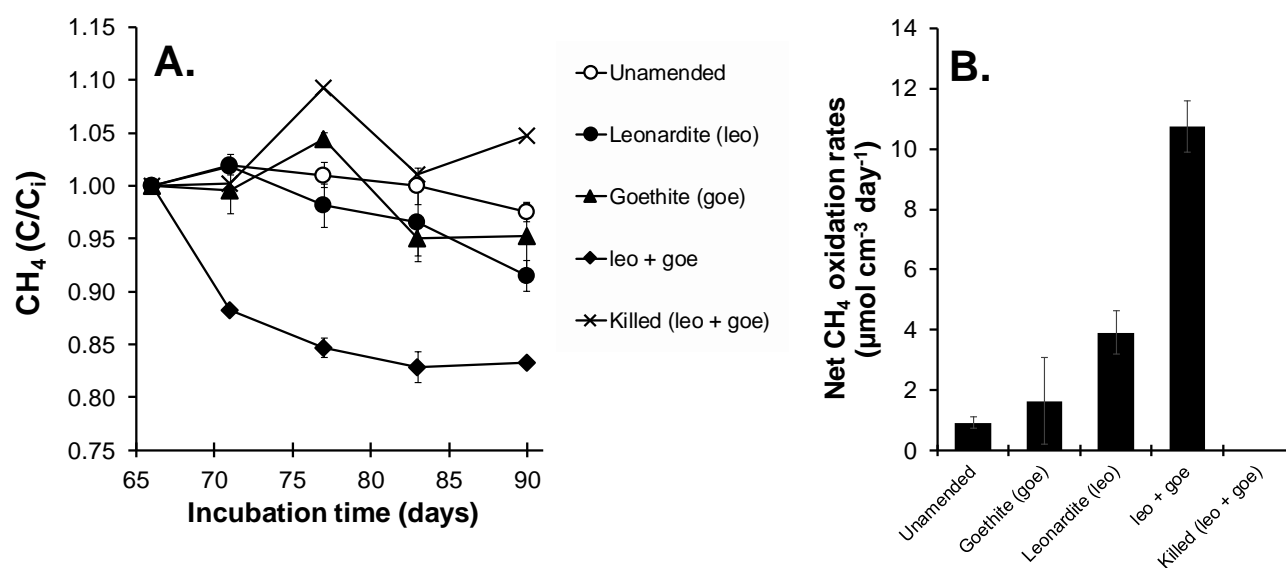


**Fig 3.1 | Net anaerobic methane oxidation linked to leonardite-mediated reduction of goethite.** Panel A depicts the normalized kinetics of methane consumption during the second incubation cycle ( $C$ , methane concentration overtime;  $C_i$ , initial methane concentration). The calculated rates of AOM are shown in Panel B. Data represent average from triplicate incubations  $\pm$  standard error.

Substantial CH<sub>4</sub> consumption ( $10.7 \pm 0.8 \mu\text{mol cm}^{-3} \text{ day}^{-1}$ ) was promoted by the presence of both leonardite and goethite into the microcosms ([Fig. 3.1A](#)). The reaction rates under these conditions were approximately 7 and 3 times higher than those observed in microcosms enriched only with either goethite ( $1.6 \pm 1.4$

$\mu\text{mol cm}^{-3} \text{ day}^{-1}$ ) or leonardite ( $3.9 \pm 0.7 \mu\text{mol cm}^{-3} \text{ day}^{-1}$ ), respectively (**Fig. 3.1B**). Moreover, quantification of the milli-electron equivalents (meq) accepted by leonardite and goethite due to  $\text{CH}_4$  oxidation after 24 days of active methanotrophy, revealed a gain of  $0.098 \pm 0.015$  and  $0.58 \pm 0.042 \text{ meq L}^{-1}$ , corrected for endogenous controls lacking added methane, which accounts for  $\sim 3.4$  and 10% of the total methane consumption observed in the leonardite and leonardite/goethite treatments, respectively (**Table 3.1**).

**Table 3.1 | Number of milli-electron equivalents ( $\text{meq L}^{-1}$ ) derived from methane oxidation, linked to leonardite and goethite reduction.**

| <b>2<sup>nd</sup> incubation cycle (29 days)</b>             | <b>Unamended</b> | <b>Leonardite (leo)</b> | <b>Goethite (goe)</b> | <b>leo + goe</b> | <b>Killed (leo + goe)</b> |
|--|------------------|-------------------------|-----------------------|------------------|---------------------------|
| <b>Recovered electrons (<math>\text{meq L}^{-1}</math>)*</b> | 0                | $0.098 \pm 0.015$       | 0                     | $0.58 \pm 0.042$ | 0                         |
| <b>AOM percentage explained by EA reduction (%)</b>          | 0                | 3.38                    | 0                     | 10.02            | 0                         |

\* $\text{meq L}^{-1}$  values were corrected for endogenous controls lacking added methane. The standard error for biological triplicates is shown.

No clear methane consumption could be linked to goethite reduction in the absence of leonardite (**Fig. 3.1B**), emphasizing the importance of this electron shuttle to promote AOM linked to goethite reduction.

### 3.4.2 Incubations with $^{13}\text{CH}_4$ to assess AOM linked to HS and ferrihydrite reduction

Further incubations, amended with  $^{13}\text{CH}_4$  as electron donor, were performed to assess the capacity of the biota of the wetland sediment to achieve AOM with PPHS as electron acceptor or as electron shuttle with ferrihydrite as the TEA. AOM was documented as both net  $^{13}\text{CH}_4$  consumption and  $^{13}\text{CO}_2$  enrichment in the microcosm's headspace. In all experimental conditions, a net  $^{13}\text{CH}_4$  consumption was observed together with a transient enrichment in  $^{13}\text{CO}_2$  (**Fig. 3.2**). Wetland sediment incubated without any external electron acceptor displayed one of the shortest periods of net  $^{13}\text{CH}_4$  consumption (3 days) with a maximum rate of  $1.15 \pm 0.63 \mu\text{mol}^{13}\text{CH}_4 \text{ cm}^{-3} \text{ day}^{-1}$  (**Fig. 3.2A**). Meanwhile, microcosms enriched with PPHS showed a shorter lag phase (2 days), as compared to the unamended control, and a  $^{13}\text{CH}_4$  consumption rate of  $0.83 \pm 0.1 \mu\text{mol}^{13}\text{CH}_4 \text{ cm}^{-3} \text{ day}^{-1}$  during an extended active period (9 days, **Fig. 3.2B**). Furthermore, an increase in  $^{13}\text{F}'_{\text{CO}_2}$  in this treatment occurred in parallel to net methane consumption.  $^{13}\text{CO}_2$  enrichment (over  $^{12}\text{CO}_2$ ) in sediment incubations enriched with PPHS is remarkable since it has been observed that  $^{12}\text{CO}_2$  originating from the decomposition of the labile fraction of external HS can mask labeled carbon dioxide production leading to underestimation of AOM <sup>8</sup>.

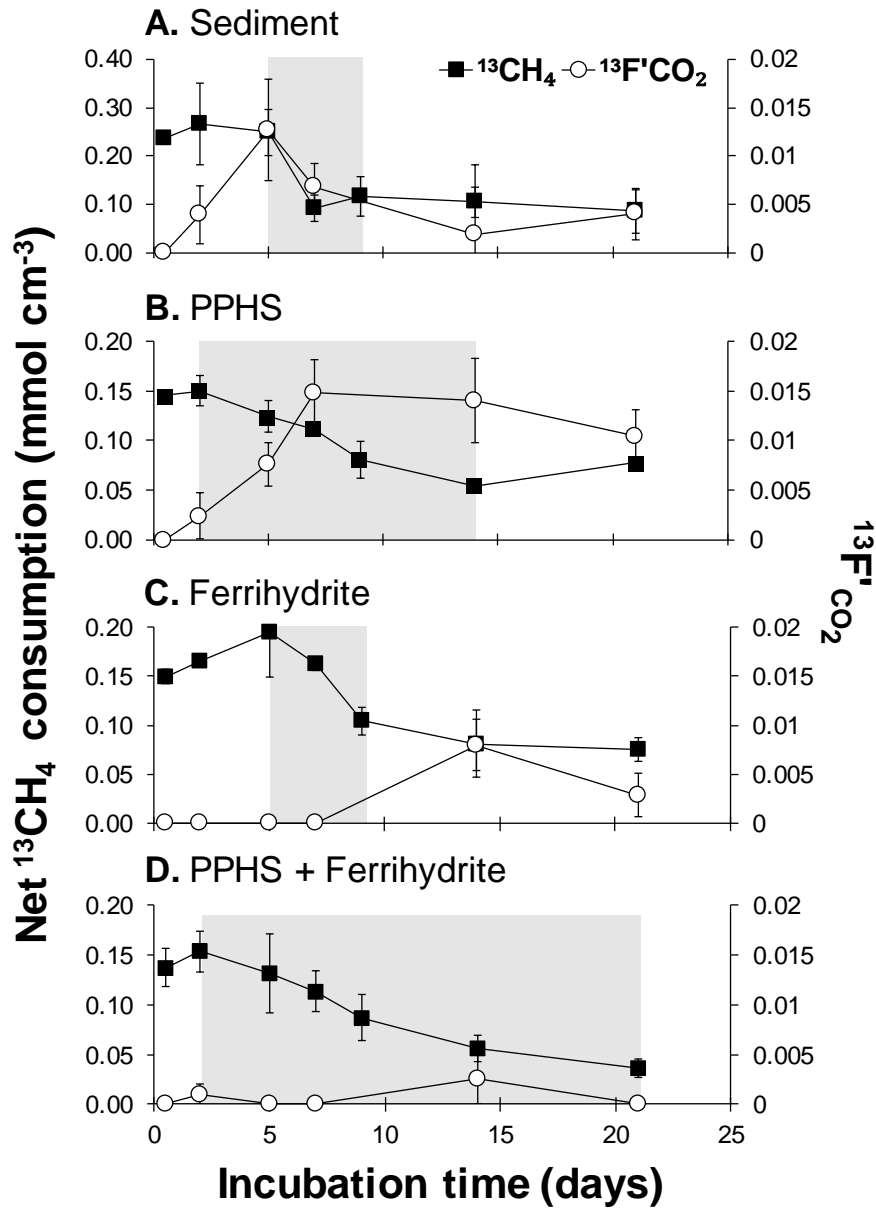


**Fig. 3.2 | Net  $^{13}\text{C}$ -methane consumption and  $^{13}\text{C}$ -carbon dioxide enrichment.** Filled squares depict net  $^{13}\text{CH}_4$  consumption per cubic centimeter of wetland sediment over time, and open dots display normalized headspace  $^{13}\text{C}$ -carbon dioxide enrichment in terms of  $^{13}\text{F}'\text{CO}_2$ . Gray areas depict the period of maximum  $^{13}\text{CH}_4$  consumption rates, which were based on the maximum slope obtained by linear regressions per experimental unit. Endogenous controls (lacking added  $^{13}\text{CH}_4$ , exhibited decreasing

negative  $^{13}\text{F}'\text{CO}_2$  values over the incubation time (see Fig. 3.3), while killed controls displayed insignificant changes in  $^{13}\text{CH}_4$  concentrations and null  $^{13}\text{CO}_2$  enrichment over time. Data represent average from triplicate incubations  $\pm$  standard error.

Despite these facts,  $^{13}\text{F}'\text{CO}_2$  values were always higher in PPHS enriched treatment when compared against those observed in the absence of PPHS (Fig. 3.2A and B). This is an indication of HS functioning as TEA for achieving AOM<sup>8,35</sup>.

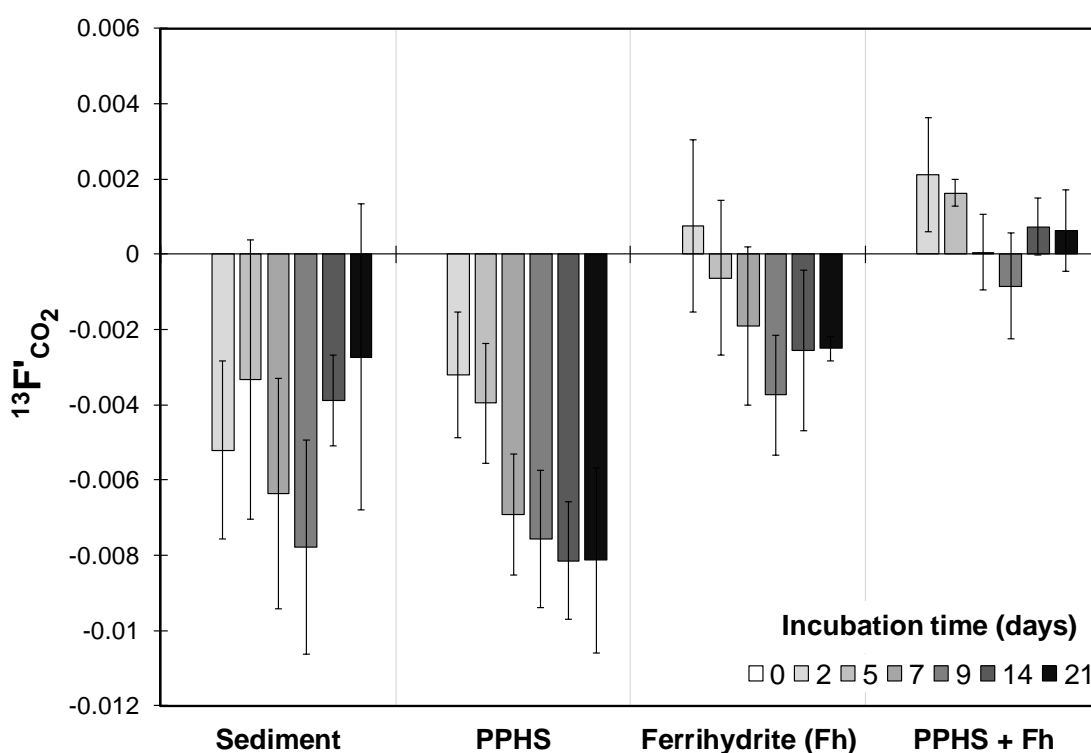


Fig. 3.3 |  $^{13}\text{F}'\text{CO}_2$  values for the endogenous controls (lacking added  $^{13}\text{CH}_4$ ) incubated under quasi-natural conditions.

Compared to unamended sediment controls, incubations enriched with ferrihydrite also displayed a long lag phase, as well as a short net AOM period (3 days) with a

maximum rate of  $1.26 \pm 0.4 \mu\text{mol}^{13}\text{CH}_4 \text{ cm}^{-3} \text{ day}^{-1}$  (**Fig. 3.2C**). Furthermore,  $^{13}\text{F}_{\text{CO}_2}$  values for this treatment were lower than those observed in unamended controls. It is well known that carbonate precipitates with divalent ions at circumneutral pH values, resulting in the formation of authigenic minerals<sup>22,42,43</sup>, therefore interfering with  $^{13}\text{CO}_2$  detection due to carbonates deposition.

Microcosms amended with both ferrihydrite and PPHS exhibited the longest net AOM period (19 days), after 2 days of lag phase (**Fig. 3.2D**). The average maximum AOM rate for this treatment was  $0.64 \pm 0.16 \mu\text{mol}^{13}\text{CH}_4 \text{ cm}^{-3} \text{ day}^{-1}$  and exhibited the lowest  $^{13}\text{CH}_4$  concentrations amongst all experimental treatments at the end of the incubation cycle ( $7.4 \pm 1 \text{ mmol CH}_4 \text{ cm}^{-3}$ ); however, complementary evidence of this high methanotrophic activity was disabled by poor detection of  $^{13}\text{CO}_2$ , which was the most affected amongst all treatments, presumably due to increased ferrous iron production and subsequent  $\text{FeCO}_3$  formation (**Fig. 3.2D**). Killed controls including both ferrihydrite and PPHS displayed neither  $^{13}\text{CH}_4$  consumption nor  $^{13}\text{CO}_2$  production; therefore, chemical reactions masking AOM activities can be ruled out. Endogenous controls (lacking added  $^{13}\text{CH}_4$ ) displayed decreasing  $^{13}\text{F}_{\text{CO}_2}$  values over time, suggesting the prevalence of  $^{12}\text{CO}_2$  production from intrinsic organic substrates present in the sediment (**Fig. 3.3**).

### **3.4.2.1 Reduction of electron acceptors**

#### **3.4.2.1.1 Reduction of intrinsic NOM and added PPHS**

Humic material was one of the electron acceptors added to microcosms (in the form of PPHS) and intrinsically present in the wetland sediment (as NOM) with the potential to support AOM (**Eq. 3.4**).



\*standard *Gibbs* free energy range calculated using -200 to +300  $E_0'$ (mV) values for HS <sup>44</sup>

Sediment incubations without the addition of any external electron acceptor displayed the reduction of intrinsic NOM, but quantified values were not significantly higher than those measured in the control lacking added  $^{13}\text{CH}_4$  (**Table 3.2, Fig. 3.4**).

**Table 3.2 | Reduction of intrinsic and added electron acceptors at the end of the 21-days incubation cycle under quasi natural conditions.**

| Treatment           | NOM/PPHS reduction (meq L <sup>-1</sup> ) <sup>†</sup> |                            |                                      | Intrinsic iron/Ferrihydrite reduction (mmol L <sup>-1</sup> ) <sup>††</sup> |                            |                                      | Sulfate reduction (mmol L <sup>-1</sup> ) <sup>†††</sup> |                            |                                      |
|---------------------|--|----------------------------|--------------------------------------|---|----------------------------|--------------------------------------|--|----------------------------|--------------------------------------|
|                     | with $^{13}\text{CH}_4$                                | without $^{13}\text{CH}_4$ | AOM explained by EA <sup>†</sup> (%) | with $^{13}\text{CH}_4$   | without $^{13}\text{CH}_4$ | AOM explained by EA <sup>†</sup> (%) | with $^{13}\text{CH}_4$                                  | without $^{13}\text{CH}_4$ | AOM explained by EA <sup>†</sup> (%) |
| Unamended sediment  | 2.7±0.3  | 2.6±0.1                    | 0                                    | 2.7±0.2   | 2.6±0.1                    | 0                                    | 0.4±0.2  | 0.5±0.2                    | 0                                    |
| PPHS                | 3.3±0.3  | 2.7±0.3                    | ~3%                                  | 3.2±0.8   | 2.6±0.03                   | 0                                    | 0.2±0.2  | 0.1±0.1                    | 0                                    |
| Ferrihydrite        | -  | -                          | -                                    | 2.2±0.3   | 3.5±0.1                    | *                                    | 0.1±0.1  | 0.1±0.04                   | 0                                    |
| PPHS + Ferrihydrite | -  | -                          | -                                    | 3.1±0.2   | 6.9±1.1                    | *                                    | 0.5±0.2  | 0.8±0.3                    | 0                                    |
| Killed              | 0  | 0                          | 0                                    | 0   | 0                          | 0                                    | 0  | 0                          | 0                                    |

<sup>†</sup>NOM/PPHS reduction was assessed as milli-electron equivalents recovered via reaction with ferric citrate. <sup>††</sup>Fe(III) reduction was quantified in terms of the ferrous iron produced. <sup>†††</sup>Quantification of sulfate reduction implies a decrease in sulfate concentration. <sup>†</sup>EA stands for *electron acceptor* \*Electron balances hindered by poor recovery of ferrous iron precipitated as  $^{13}\text{C}$ -carbonates. Data represent average values ± standard error (n = 3).



However, addition of 500 mg L<sup>-1</sup> of PPHS as complementary electron acceptor promoted AOM linked to its reduction, which was based on electron balances corrected for endogenous controls lacking added <sup>13</sup>CH<sub>4</sub>. This process accounted for ~3% of the <sup>13</sup>CH<sub>4</sub> oxidized at the end of the incubation period, which corresponds to ~1.67 μmol of <sup>13</sup>CH<sub>4</sub> oxidized per cm<sup>3</sup> of wetland sediment (**Table 3.2**).

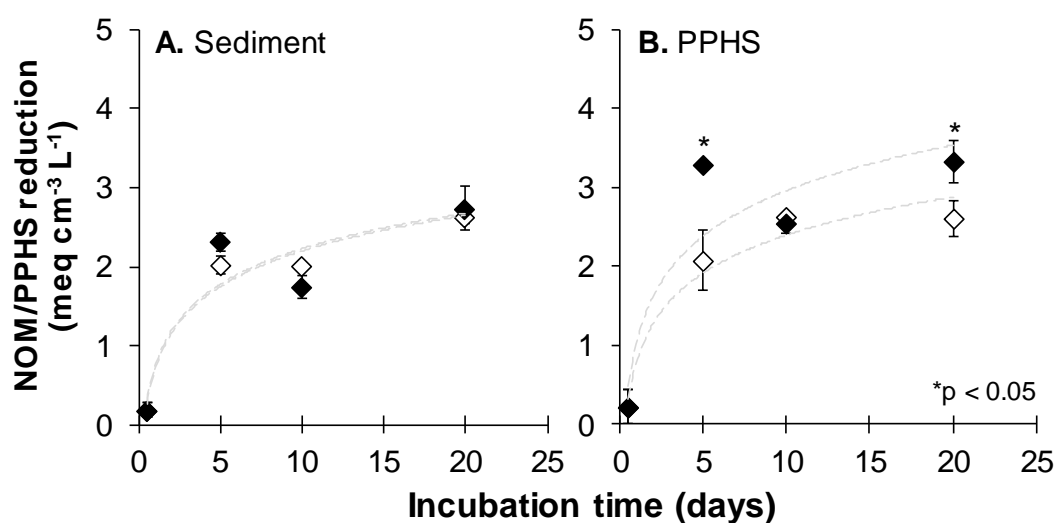


**Fig. 3.4 | Microbial reduction of intrinsic NOM and the mixture of intrinsic NOM/*Pahoee Peat* humic substances.** Empty symbols depict endogenous controls, while <sup>13</sup>CH<sub>4</sub> spiked microcosms are represented by the filled ones. Bars represent the standard error obtained from triplicate incubations and statistically significant differences (one-way ANOVA) are marked with asterisks.

### 3.4.2.1.2 Ferrihydrite reduction

Quantification of ferrous iron in incubations performed with unamended sediment revealed the production of up to  $\sim 0.04$  mmol of  $\text{Fe}^{2+}$   $\text{cm}^{-3}$  regardless the presence of  $^{13}\text{C}$ -methane, which indicates the reduction of intrinsic iron minerals present in the wetland sediment (**Fig. 3.5**).

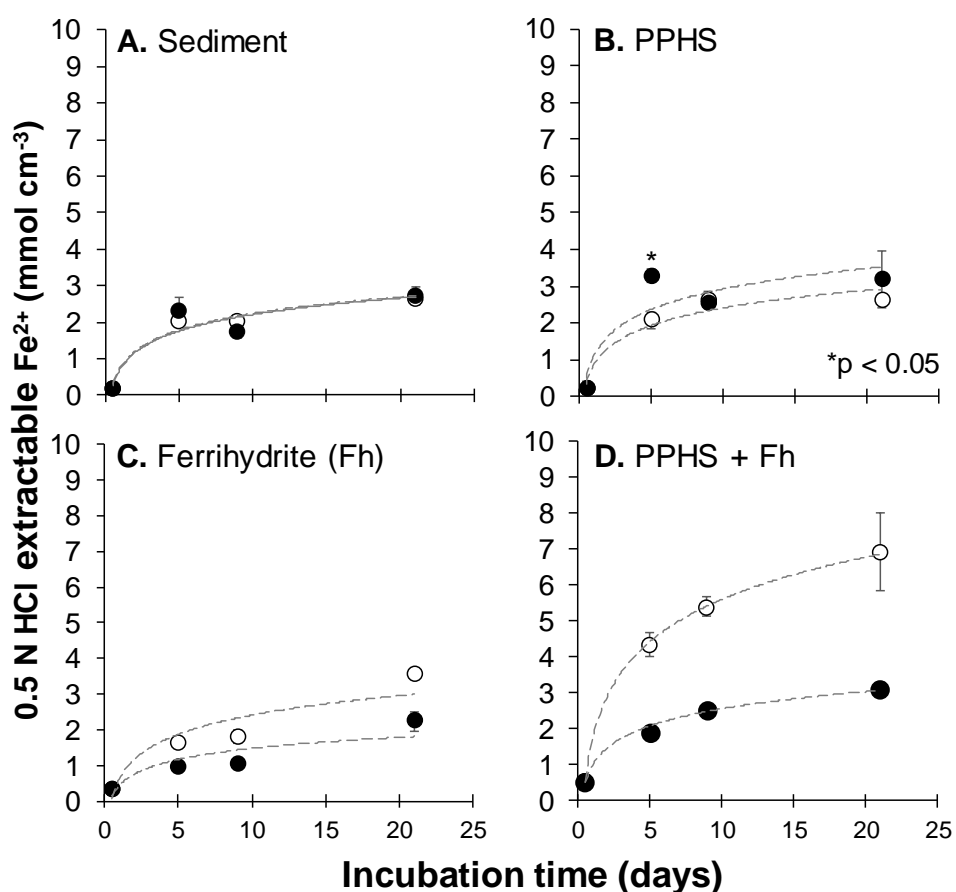
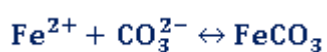


**Fig. 3.5** | Acid extractable ferrous iron measured by the ferrozine technique over time. Empty symbols depict endogenous controls, while  $^{13}\text{CH}_4$  spiked microcosms are represented by the filled ones. Bars represent the standard error obtained from triplicate

incubations and statistically significant differences (one-way ANOVA) are marked with asterisks.

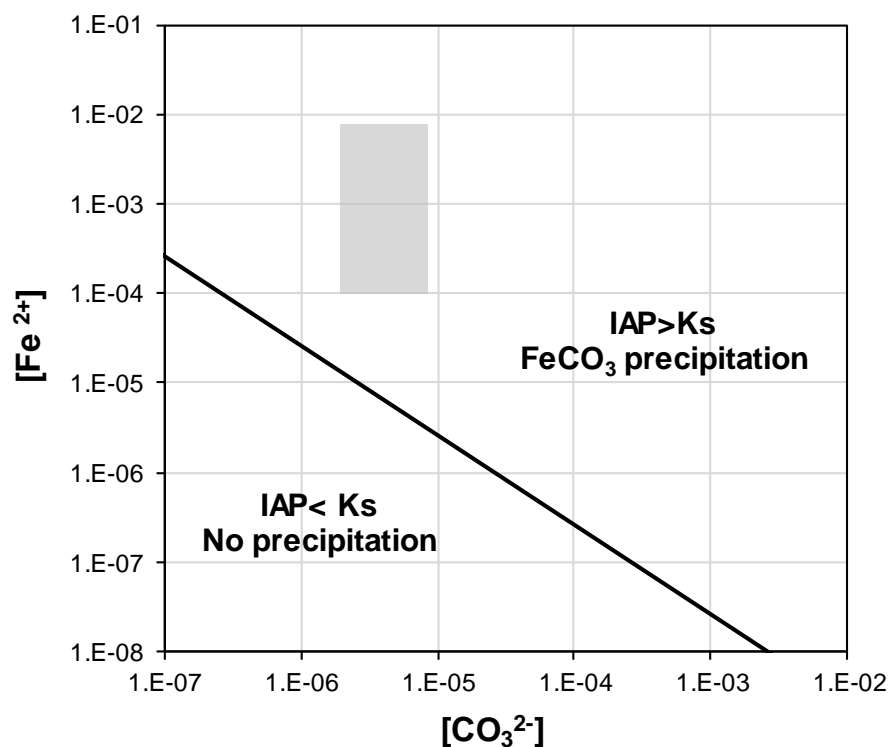
For microcosms enriched with PPHS, ~10% of the observed AOM activity could be explained by the quantified iron reduction on the 5<sup>th</sup> day of incubation, thus displaying the positive effect of PPHS on net AOM with intrinsic iron as TEA (**Fig. 3.5**). Nevertheless, this evidence could not be sustained overtime. Thus, AOM linked to the reduction of intrinsic ferric minerals could not be documented at the end of the incubation period (**Table 3.2**). Experimental treatments containing ferrihydrite or PPHS/ferrihydrite showed lower Fe<sup>2+</sup> concentrations with respect to their endogenous controls lacking added <sup>13</sup>CH<sub>4</sub> (**Table 3.2, Fig. 3.5**). Since this effect was only triggered by <sup>13</sup>CH<sub>4</sub> amendment, <sup>13</sup>C-carbonates originated from AOM linked to ferric iron reduction might have induced major Fe<sup>2+</sup> precipitation producing minerals, which could not be solubilized by the experimental protocol employed here.

Siderite precipitation is possible if both Fe<sup>2+</sup> and CO<sub>3</sub><sup>2-</sup> concentration reach the saturation levels according to **Eq 3.5**. Based on Fe<sup>2+</sup> extractions (**Fig. 3.5**), ferrous ion concentration ranged from 6.9x10<sup>-3</sup> M to 1.2x10<sup>-6</sup> M (pH=7). Under these considerations, the saturation level for siderite precipitation was always favorable for the solid formation (**Fig. 3.6**). It has widely been reported that iron extraction is frequently affected by the complex geochemical composition of natural samples <sup>45</sup>, which has often impeded the stoichiometric demonstration of iron dependent AOM <sup>22,35</sup> (**Eq. 3.5**).



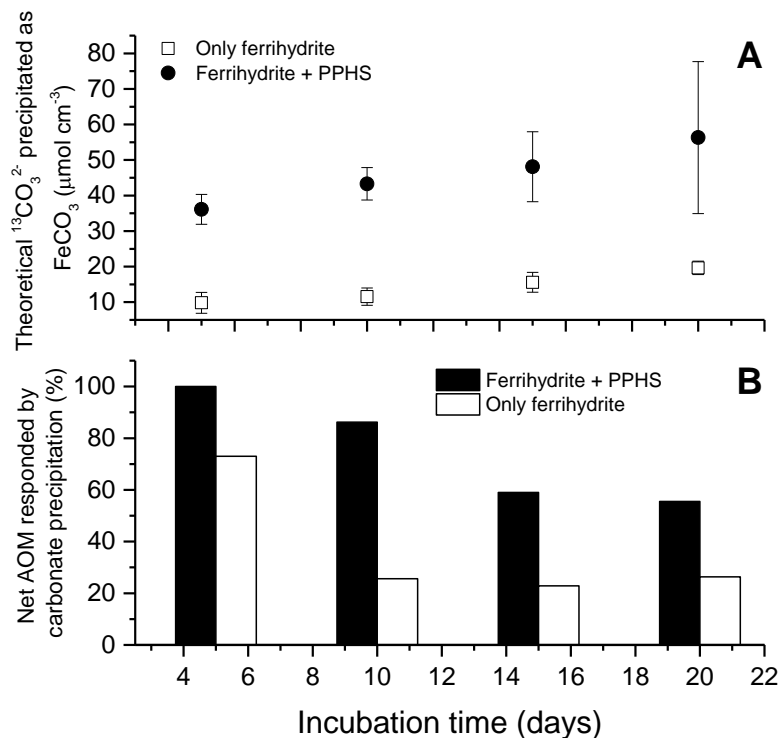
$$\log K_{sp} = -10.6$$

**Eq. 3.5**



**Fig. 3.6 | Solubility diagram for siderite.** Solid line indicates the solid-liquid equilibrium condition ( $IAP=K_s$ , where  $IAP=[Fe^{2+}][CO_3^{2-}]$ ) for  $FeCO_3$  precipitation. Shaded area indicates the iron and carbonate concentration range prevailing in all incubation samples from the kinetics of  $^{13}CH_4$  oxidation discussed in **Figure 3.2**, confirming precipitation of siderite.

In agreement with this observation, as shown in **Fig. 3.2C and 3.2D**, no  $^{13}CO_2$  headspace enrichment ( $^{13}F'_{CO_2}$ ) was detected preventing the assessment of total methanotrophic activity in terms of  $^{13}CO_2$  accumulated. Nevertheless, by employing data from **Fig. 3.2** and **Fig. 3.5** (calculations showed in **Section 3.3.3**), we could indirectly attribute the oxidation of  $\sim 19.6 \mu mol^{13}CH_4 cm^{-3}$  to ferrihydrite reduction at the end of the incubation cycle (**Eq. 3.3**). This AOM activity accounts for approximately  $\sim 26\%$  of the total methane oxidized in ferrihydrite amended microcosms (**Fig. 3.7**).

**Eq. 3.6**

**Fig. 3.7** | Effect of ferrihydrite reduction, mediated by Pahokee Peat humic substances, on anaerobic methane oxidation assessed as ferrous iron carbonates precipitation (calculations showed in Section 3.3.3). **Panel A** depicts the calculated carbonate concentration per cubic centimeter of wetland sediment, while **Panel B** portrays the percentage of net anaerobic oxidation of  $^{13}\text{CH}_4$  explained by the theoretical  $^{13}\text{C}$ -carbonate produced. Data represent average from triplicate incubations  $\pm$  standard error.

The interplay between ferrihydrite and PPHS triggered higher precipitation of  $\text{Fe}^{2+}$  presumably due to major  $^{13}\text{CO}_3^{2-}$  production (**Table 3.2** and **Fig. 3.5**). Through

these assumptions and calculations, we could estimate the oxidation of  $\sim 56.3 \mu\text{mol}^{13}\text{CH}_4 \text{ cm}^{-3}$  that accounts for  $\sim 56\%$  of the total amount of  $^{13}\text{CH}_4$  consumed during the entire incubation period (**Fig. 3.7**). Overall, net AOM driven by the electron-shuttling capacity of PPHS yielded higher amounts of oxidized methane, which were presumably buried as carbonate minerals in the wetland sediment. These rates of  $^{13}\text{CO}_3^{2-}$  precipitation, were almost twice as fast in the presence of both PPHS and ferrihydrite than those observed in the incubations that contained only ferrihydrite ( $\sim 1.3$  vs  $\sim 0.67 \mu\text{mol carbonate cm}^{-3} \text{ day}^{-1}$ , respectively) (**Fig. 3.7**).

#### **3.4.2.1.3 Sulfate reduction**

After the pre-incubation period, initial sulfate concentrations averaged  $2.3 \pm 0.1 \text{ mmol L}^{-1}$ , which derived from sediment pore water along with the wetland's water column employed as liquid phase in the incubations (**Table 2.1**). All experimental treatments displayed sulfate-reducing activity, but not directly linked to AOM because controls lacking added  $^{13}\text{CH}_4$  showed the same or even higher sulfate-reducing activities.

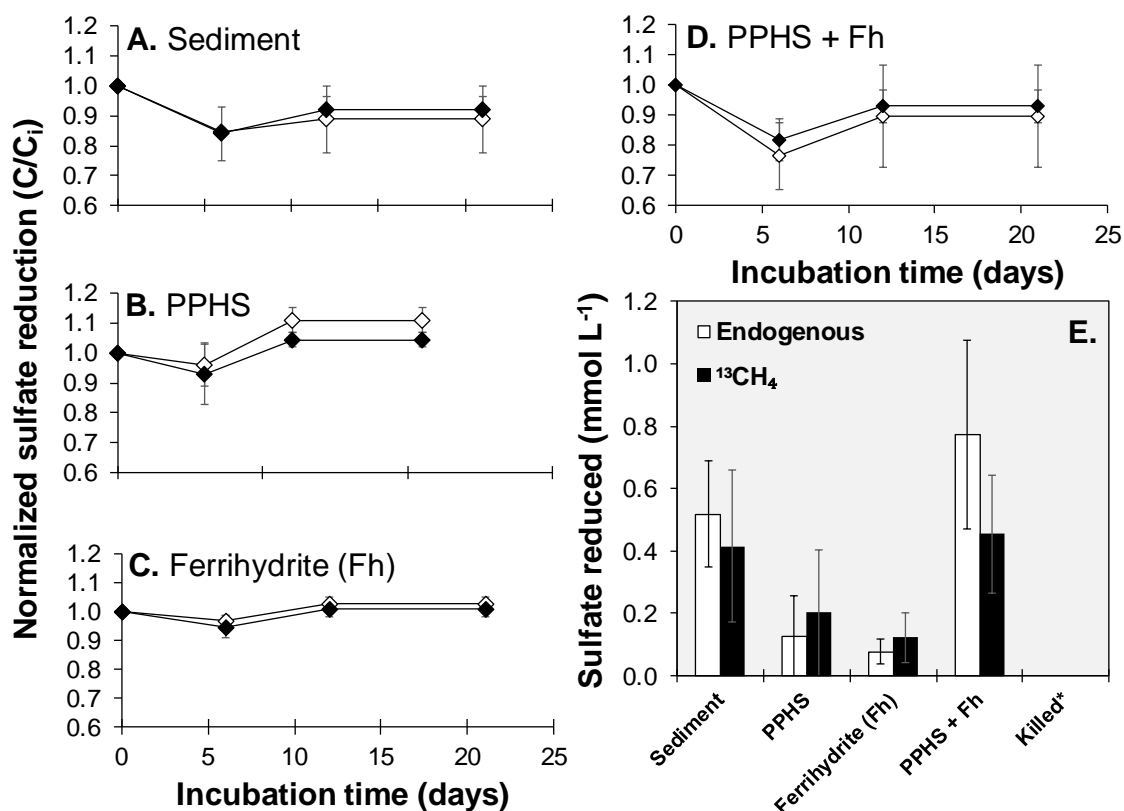


**Fig. 3.8. | Sulfate consumption over incubation time.** Panels A to D depict normalized sulfate consumption over time (conc./initial conc.), initial concentration for all microcosms was  $2.3 \pm 0.1 \text{ mmol L}^{-1}$ . Panel E displays net sulfate reduction in the absence and presence of  $^{13}\text{CH}_4$  methane after 21 days of the incubation period. Error bars for all graphs are defined as standard errors of three experimental replicates.

Thus, it was impossible to attribute any  $^{13}\text{CH}_4$  consumption to sulfate-dependent AOM (SR-AOM, Eq. 7) via electron balances (Table 3.2, Fig. 3.7).



$$\Delta G' \text{ (kJ mol}^{-1}\text{)} = -16.6$$

Eq. 7

### 3.4.3 AOM assessment under artificial conditions and destructive sampling

To test the hypothesis on the humus-catalyzed iron-dependent AOM and subsequent precipitation of iron carbonates, an incubation cycle consisting of a set of destructible experimental units was carried out. AOM activities readily started in all experimental treatments as evidenced by an immediate  $^{13}\text{CO}_2$  enrichment (Fig. 3.9). As expected, the lowest  $^{13}\text{C}$  enrichment was obtained in unamended sediment incubations ( $\sim 3\%$ ), while the presence of PPHS, ferrihydrite or both promoted further  $^{13}\text{C}$  enrichment by  $\sim 2.3\%$ ,  $6.5\%$  and  $9.6\%$  with respect to unamended controls, respectively (Fig. 3.9A).

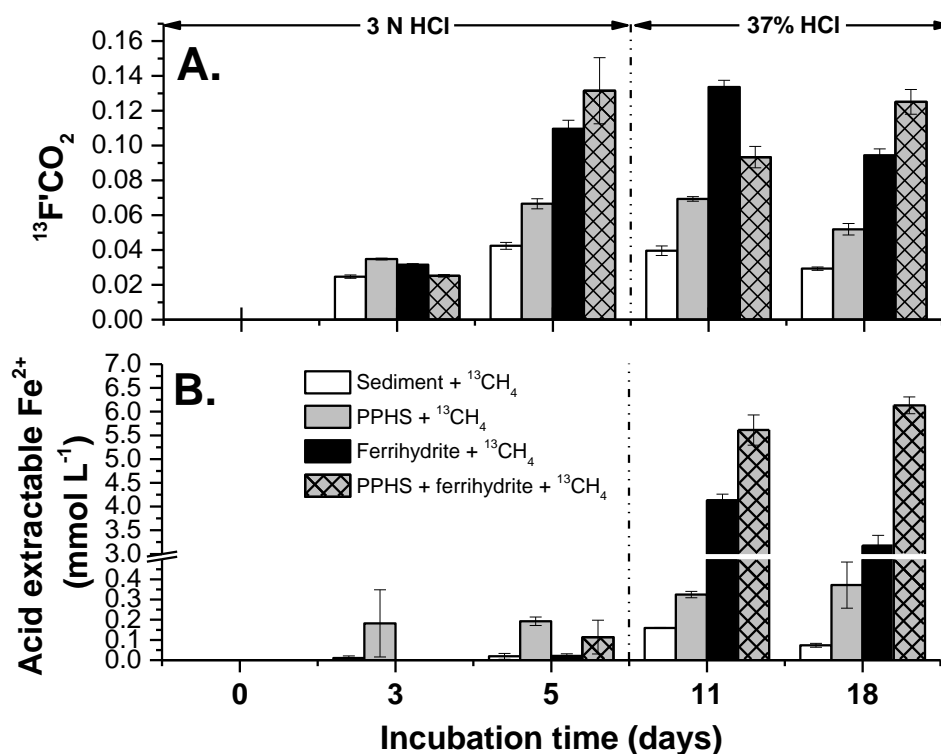


Fig. 3.9 | Evidence of AOM mediated by Pahokee Peat humic substances with ferrihydrite as terminal electron acceptor. Panel A depicts  $^{13}\text{CO}_2$  enrichment over time



denoted as  $^{13}\text{F}'\text{CO}_2$ , while **Panel B** depicts the total ferrous iron concentrations extracted via destructive sampling employing hydrochloric acid at concentrations of 3N (left) and 37% (right). Data represent average from triplicate incubations  $\pm$  standard error ( $n=3$ ).

The experimental treatment containing both PPHS and ferrihydrite showed a decrease in the  $^{13}\text{F}'\text{CO}_2$  ratio, as compared to the experimental treatment containing only ferrihydrite, after 11 days of incubation. This may be explained by significant  $^{12}\text{CO}_2$  production elicited by mineralization of the labile fraction of PPHS which would have temporarily served as a source of  $^{12}\text{CO}_2$ . Subsequently (after 18 days of incubation), the  $^{13}\text{F}'\text{CO}_2$  value rose again; thus, by the end of the experiment,  $^{13}\text{CO}_2$  enrichment was higher in the presence of both PPHS and ferrihydrite than the level observed with either ferrihydrite or PPHS alone.

As seen in **Fig. 3.9A**, the application of 3M HCl as dissolution agent efficiently induced  $\text{CO}_2$  displacement towards the gaseous phase allowing accurate  $^{13}\text{F}'\text{CO}_2$  calculations. Nevertheless, quantified  $\text{Fe}^{2+}$  under these conditions did not agree with the AOM activity observed (**Fig. 3.9B**). However, further acidification of samples (performed with HCl 37%) on subsequent monitoring days yielded higher amounts of ferrous iron due to solubilization of stable iron-containing minerals. This evidence suggests that, on one hand, a fraction of the carbonate produced in the AOM process might have precipitated as calcium carbonate, which is easily dissolved, while, on the other hand, a second fraction might have involved the precipitation of ferrous iron carbonate, which is more difficult to dissolve (**Equations 3.5, 3.8 & 3.9**).

### 3.4.4 Mineral characterization of wetland sediment performing AOM

XRD analysis of dried sediments, collected at the end of the incubation period, showed typical spectral signals associated to calcium carbonate ( $\text{CaCO}_3$ ) minerals, such as *calcite* and *aragonite*, while the only mineral detected involving ferrous iron was the iron carbonate ( $\text{FeCO}_3$ ) known as *siderite* (**Fig. 3.11**). Although sulfate-reducing activity was observed during the first incubation cycle, iron sulfides were not detected by diffractograms obtained by XRD analysis, which was expected due to the absence of black precipitates that typically originate when biogenic sulfide is produced in the presence of iron<sup>46</sup>, nevertheless biogenic FeS can be amorphous and therefore not detected by XRD. Overall, these lines of evidence confirm that the fate of  $^{13}\text{CH}_4$  carbon was the production of carbonate particles of different composition and solubility, being calcite and aragonite (**Eq. 8** and **9**) the most vulnerable to solubilization by the acidification method employed during the first sampling days of the assay (**Fig. 3.9**).

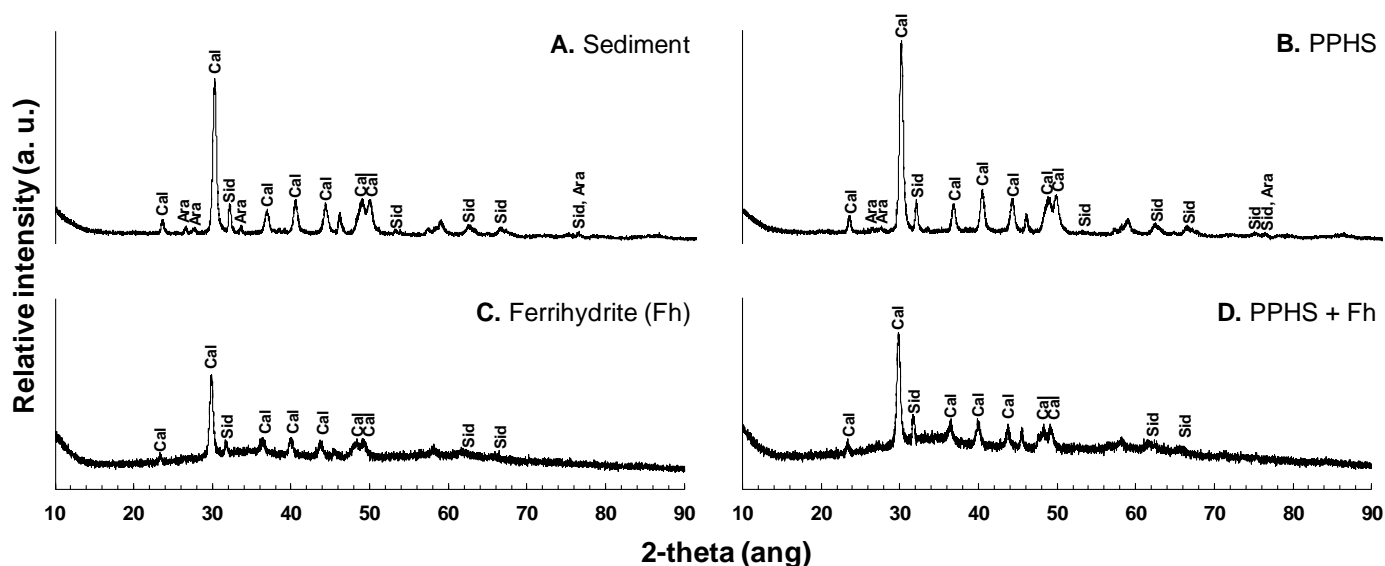


**Fig. 3.10** | XRD diffractograms displaying the mineral phases found after incubation under the experimental conditions tested. *Cal* stands for calcite (00-005-0586), *Ara* stands for aragonite (00-005-0453) and *Sid* stands for siderite (00-008-0133).



An exploration of unamended sediment by ESEM-EDS allowed the identification of intrinsic iron solids in the form of prism-like particles (**Fig. 3.12A**), while an EDS analysis revealed minerals containing iron and oxygen (**Fig. 3.13B**).

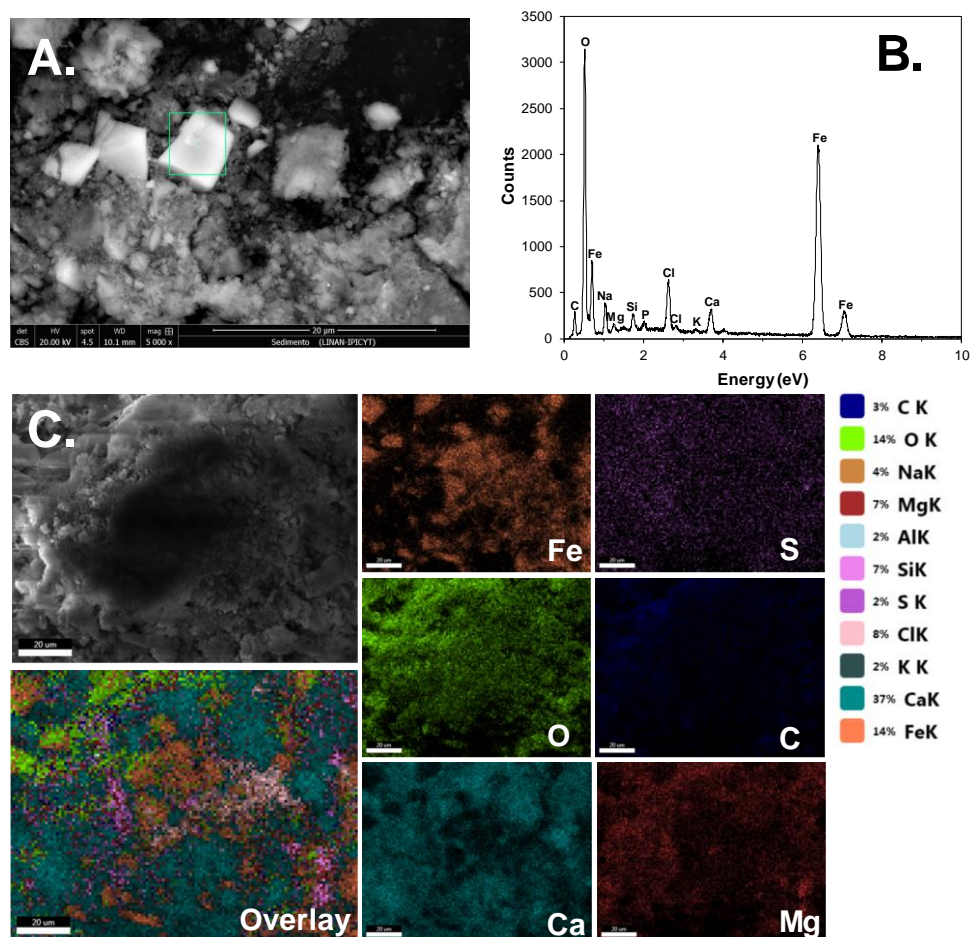


**Fig. 3.11 | ESEM-EDS exploration of wetland sediment after incubation. Panel A** shows cubic and prism-like iron oxide particles found in unamended sediment incubations, whose respective EDS is shown at **Panel B**. **Panel C** displays the mapping of the 10 most abundant chemical elements detected in the mineral clusters formed by the end of the incubation period in the PPHS/ferrihydrate treatment.

These results suggest the presence of oxidized iron minerals, which might have partially fueled AOM in PPHS-enriched treatments (**Fig. 3.2B** and **3.5**). Additionally, analyses from sediment of this experimental treatment, as well as unamended sediment, confirmed the presence of siderite, hence supporting the prevalence of

iron-mediated AOM even without the addition of chemically synthesized ferrihydrite in microcosms enriched with PPHS (**Fig. 3.5**). SEM observation of the PPHS/ferrihydrite enriched sediment, conducted at the end of the incubation period, also revealed the predominance of iron (~14%) and calcium (~37%) rich areas of apparent mineral clusters, which agrees with the precipitation of carbonates (**Fig. 3.12C**).

### 3.4 Discussion

Wetlands constitute the main natural source of atmospheric CH<sub>4</sub><sup>47</sup>; despite this, there are still significant knowledge gaps regarding the microbial processes serving as CH<sub>4</sub> sinks in these organotrophic environments<sup>34</sup>. The aim of the present study was to elucidate the role of humic substances on mitigating CH<sub>4</sub> release from wetland sediments by promoting AOM through their electron shuttling capacity towards Fe(III)-bearing minerals. Several lines of evidence revealed how two sources of humic substances and two distinct Fe(III) oxides influenced not only the anaerobic oxidation of CH<sub>4</sub>, but also the production and fate of the carbonate coming from this microbial process. Net methane oxidation elicited by leonardite and goethite was observed after a long-term incubation test (**Fig. 3.1**). These results show that long incubation periods are needed to be able to explicitly link the anaerobic net CH<sub>4</sub> consumption to goethite reduction, which is most likely due to the need for absence of indigenous electron acceptors (such as sulfate) and labile organic molecules, which at initial incubation phases lead to overall net CH<sub>4</sub> production. Furthermore, tracer analysis with <sup>13</sup>CH<sub>4</sub> demonstrated that the combination of PPHS and ferrihydrite fueled <sup>13</sup>CH<sub>4</sub> oxidation as well as production of <sup>13</sup>CO<sub>2</sub>, which was subsequently precipitated as authigenic carbonate minerals. Such precipitation phenomenon was strongly affected by PPHS eliciting the

production of both Fe(II) and  $^{13}\text{CO}_2$  (**Fig. 3.2** and **3.7**), which supports a model of carbon burial similar to that observed in the seafloor in which sulfate-dependent AOM takes place <sup>48-50</sup>.

Previous reports addressing the occurrence of AOM in wetlands have been able to link this process to the reduction of conventional electron acceptors, such as sulfate, nitrate or nitrite; however, the role of humic substances either as TEA or as electron shuttle has not been evaluated in these studies <sup>9,10,51</sup>. Further studies testing the effect of humic and/or metal oxides on AOM, have not distinguished any significant effect of these electron acceptors on AOM neither in terms of  $\text{CO}_2$  production nor in net  $\text{CH}_4$  depletion <sup>52,53</sup>. In contrast to these reports, the present study provides evidence demonstrating how the redox-active fraction of NOM (e. g. humic substances) promotes AOM when Fe(III) oxides serve as the TEA, and how complex chemical and biological reactions concomitantly occur during this process determining the fate of both  $\text{CH}_4$  and the  $\text{CO}_2$  derived from AOM (**Fig. 3.12**).

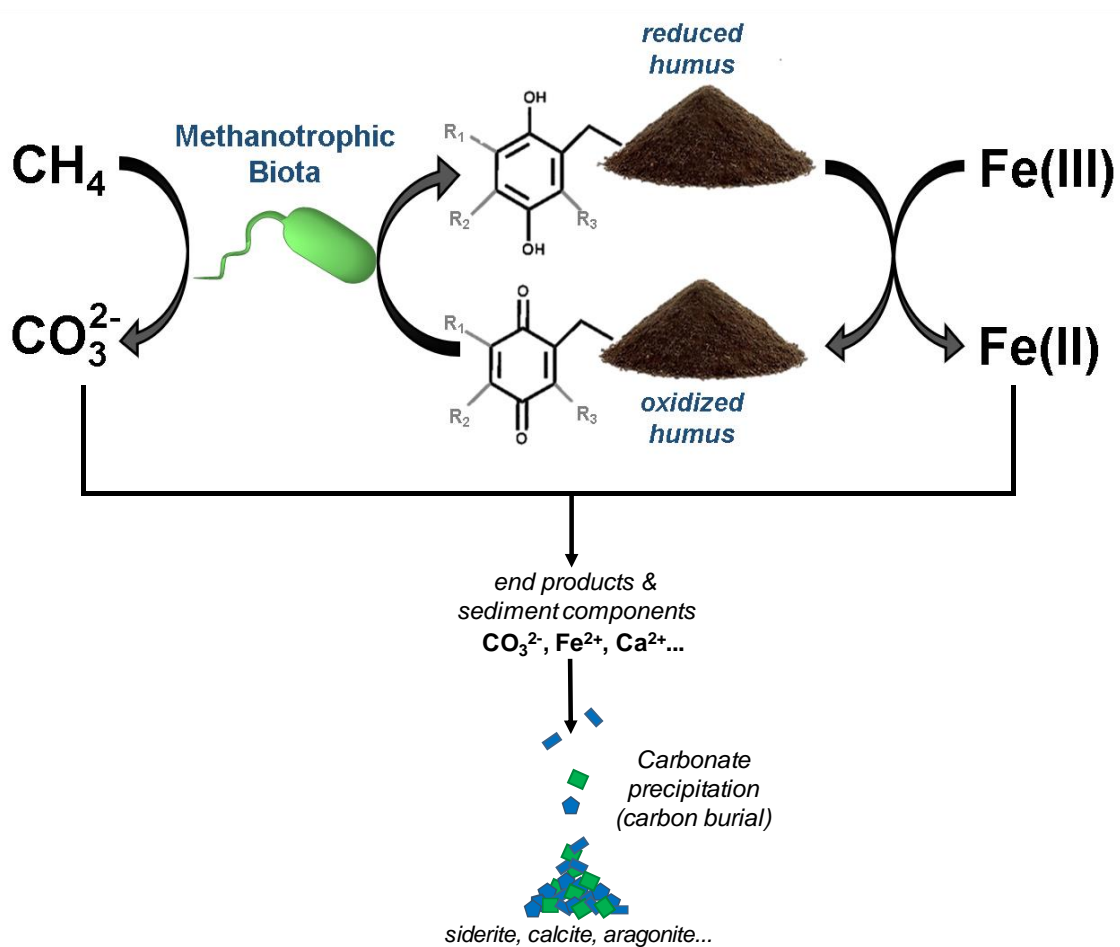


**Fig. 3.12 | Schematic representation of methane consumption by wetland sediment biota with humic substances as electron shuttle and Fe (III) as the TEA.** While  $\text{CH}_4$  is mineralized, electrons derived from this biologically catalyzed reaction are transferred to redox functional moieties in humus. Reduced humus is then regenerated to its oxidized state by chemical oxidation with Fe (III) solid oxides as TEA (see Smemo and Yavitt, 2011). Because of the geochemical context in which this reaction may take place, carbonate and ferrous iron produced concomitantly may precipitate as authigenic carbonate minerals, which will also be influenced by other environmental factors, such as the presence of divalent ions (e. g. calcium and magnesium).

Remarkably, even in the presence of sulfate as an available intrinsic electron acceptor, humus-mediated iron reduction was the only microbial process linked to  $^{13}\text{CH}_4$  oxidation (**Table 3.2, Fig. 3.8**). This implied that, under the experimental conditions tested, sulfate reduction did not play a role sustaining AOM activities. However, we cannot rule out the possibility of a cryptic sulfur cycle taking place, since the recycling of sulfurous compounds (e.g. sulfide) could hypothetically be responsible for the increased oxidation of electron donors, which may include  $\text{CH}_4$  <sup>30,31,54,55</sup>. Yet, the potential role of this cryptic sulfur cycle in  $\text{CH}_4$  consuming processes must be addressed in future studies.

### 3.5 Conclusions

The present study provides evidence indicating that the electron accepting fraction of NOM significantly contributes to AOM activities in wetland sediments by functioning as electron shuttle towards the reduction of Fe(III) minerals. Previously, it has been demonstrated that humic substances can serve as the terminal electron acceptor for AOM. In this work, we provide further insight on the important role of humus on mitigating  $\text{CH}_4$  emissions from organotrophic ecosystems, but further mechanisms by which they can mitigate these emissions remain feasible and should be addressed in future studies. Our findings suggest that important amounts of  $\text{CO}_2$  coming from the AOM process can be buried into wetland sediments due to collateral chemical phenomena promoted by humic substances. Hence, the biological and chemical phenomena discussed here are proposed as key players affecting carbon dynamics in wetlands. This information should be considered in future studies of  $\text{CH}_4$  sinks in organotrophic environments since it may have huge implications on wetlands  $\text{CH}_4$  budgeting and therefore on global climate change.



### 3.6 References

1. **Arneth, A.**, Harrison, S. P., Zaehle, S., Tsigaridis, K., Menon, S., Bartlein, P. J., Feichter, J., Korhola, A., Kulmala, M., O'Donnell, D., *et al.* Terrestrial biogeochemical feedbacks in the climate system. *Nat. Geosci.* **2010**, *3* (8), 525–532.
2. **Davidson, E. A.**, Janssens, I. A. Temperature sensitivity of soil carbon decomposition and feedbacks to climate change. *Nature* **2006**, *440* (7081), 165–173.
3. **Bridgham, S. D.**, Megonigal, J. P., Keller, J. K., Bliss, N. B., Trettin, C. The Carbon Balance of North American Wetlands. *Wetlands* **2006**, *26* (4), 889–916.
4. **Bridgham, S. D.**, Cadillo-Quiroz, H.; Keller, J. K.; Zhuang, Q. Methane emissions from wetlands: biogeochemical, microbial, and modeling perspectives from local to global scales. *Glob. Chang. Biol.* **2013**, *19* (5), 1325–1346.
5. **Kirschke, S.**, Bousquet, P., Ciais, P., Saunois, M., Canadell, J. G., Dlugokencky, E. J., Bergamaschi, P., Bergmann, D., Blake, D. R., Bruhwiler, L., *et al.* Three decades of global methane sources and sinks. *Nat. Geosci.* **2013**, *6* (10), 813–823.
6. **Trotsenko, Y. A.**, Murrell, J. C. Metabolic aspects of aerobic obligate methanotrophy. *Adv. Appl. Microbiol.* **2008**, *63* (07), 183–229.
7. **Cui, M.**, Ma, A., Qi, H., Zhuang, X., Zhuang, G. Anaerobic oxidation of methane: An “active” microbial process. *Microbiologyopen* **2015**, *4* (1), 1–11.
8. **Valenzuela, E. I.**; Prieto-Davó, A.; López-Lozano, N. E.; Hernández-Eligio, A.; Vega-Alvarado, L.; Juárez, K.; García-González, A. S.; López, M. G.; Cervantes, F. J. Anaerobic methane oxidation driven by microbial reduction of natural organic matter in a tropical wetland. *Appl. Environ. Microbiol.* **2017**, *83* (11), AEM.00645-17.
9. **Segarra, K. E. A.**, Schubotz, F., Samarkin, V., Yoshinaga, M. Y., Hinrichs, K. U., Joye, S. B. High rates of anaerobic methane oxidation in freshwater wetlands reduce potential atmospheric methane emissions. *Nat.*

*Commun.* **2015**, *6* (May), 7477.

**10. Segarra, K. E. A.**, Comerford, C., Slaughter, J., Joye, S. B. Impact of electron acceptor availability on the anaerobic oxidation of methane in coastal freshwater and brackish wetland sediments. *Geochim. Cosmochim. Acta* **2013**, *115*, 15–30.

**11. Hu, B. L.**, Shen, L.D., Lian, X., Zhu, Q., Liu, S., Huang, Q., He, Z.F., Geng, S., Cheng, DQ., Lou, L.P., Evidence for nitrite-dependent anaerobic methane oxidation as a previously overlooked microbial methane sink in wetlands. *Proc. Natl. Acad. Sci. U. S. A.* **2014**, *111* (12), 4495–4500.

**12. Shen, L. D.**, Wu, H. S., Gao, Z. Q. Distribution and environmental significance of nitrite-dependent anaerobic methane-oxidising bacteria in natural ecosystems. *Appl. Microbiol. Biotechnol.* **2014**, *99* (1), 133–142.

**13. Shen, L.**, Wu, H., Liu, X., Li, J. Cooccurrence and potential role of nitrite- and nitrate-dependent methanotrophs in freshwater marsh sediments. *Water Res.* **2017**, *123*, 162–172.

**14. Zhu, B.**, van Dijk, G., Fritz, C., Smolders, A. J. P., Pol, A., Jetten, M.

S. M., Ettwig, K. F. Anaerobic oxidation of methane in a minerotrophic peatland: Enrichment of nitrite-dependent methane-oxidizing bacteria. *Appl. Environ. Microbiol.* **2012**, *78* (24), 8657–8665.

**15. Stevenson, F. J.** Humus Chemistry: Genesis, Composition, Reactions. *Nature* **1983**, *303* (30), 835–836.

**16. Lovley, D. R.**, Coates, J. D., Blunt-Harris, E. L., Phillips, E. J. P., Woodward, J. C. Humic substances as electron acceptors for microbial respiration. *Nature*. **1996**, pp 445–448.

**17. Lovley, D. R.**, Fraga, J. L., Coates, J. D., Blunt-Harris, E. L. Humics as an electron donor for anaerobic respiration. *Environ. Microbiol.* **1999**, *1* (1), 89–98.

**18. Lehmann, J.**, Kleber, M. The contentious nature of soil organic matter. *Nature* **2015**, *528* (7580), 60–68.

**19 Klüpfel, L.**, Piepenbrock, A., Kappler, A., Sander, M. Humic substances as fully regenerable electron acceptors in recurrently anoxic environments. *Nat. Geosci.* **2014**, *7* (February), 195–200.

20. **Lovley, D. R.**, Fraga, J. L., Blunt-Harris, E. L., Hayes, L. A., Phillips, E. J. P., Coates, J. D. Humic substances as a mediator for microbially catalyzed metal reduction. *Acta Hydrochim. Hydrobiol.* **1998**, *26* (3), 152–157.
21. **Scott, D. T.**, Mcknight, D. M., Blunt-Harris, E. L., Kolesar, S. E., Lovley, D. R. Quinone moieties act as electron acceptors in the reduction of humic substances by humics-reducing microorganisms. *Environ. Sci. Technol.* **1998**, *32* (19), 2984–2989.
22. **Beal, E. J.**, House, C. H., Orphan, V. J. Manganese- and iron-dependent marine methane oxidation. *Science* **2009**, *325* (5937), 184–187.
23. **Egger, M.**, Rasigraf, O., Sapart, C. J., Jilbert, T., Jetten, M. S. M., Röckmann, T., Van Der Veen, C., Bânda, N., Kartal, B., Ettwig, K. F., *et al.* Iron-mediated anaerobic oxidation of methane in brackish coastal sediments. *Environ. Sci. Technol.* **2015**, *49* (1), 277–283.
24. **Wankel, S. D.**, Adams, M. M., Johnston, D. T., Hansel, C. M., Joye, S. B., Girguis, P. R. Anaerobic methane oxidation in metalliferous hydrothermal sediments: Influence on carbon flux and decoupling from sulfate reduction. *Environ. Microbiol.* **2012**, *14* (10), 2726–2740.
25. **Riedinger, N.**, Formolo, M. J., Lyons, T. W., Henkel, S., Beck, A., Kasten, S. An inorganic geochemical argument for coupled anaerobic oxidation of methane and iron reduction in marine sediments. *Geobiology* **2014**, *12* (2), 172–181.
26. **Amos, R. T.**, Bekins, B. A., Cozzarelli, I. M., Voytek, M. A., Kirshtein, J. D., Jones, E. J. P., Blowes, D. W. Evidence for iron-mediated anaerobic methane oxidation in a crude oil-contaminated aquifer. *Geobiology* **2012**, *10* (6), 506–517.
27. **Nordi, K. Á.**, Thamdrup, B., Schubert, C. J. Anaerobic oxidation of methane in an iron-rich Danish freshwater lake sediment. *Limnol. Oceanogr.* **2013**, *58* (2), 546–554.
28. **Bar-Or, I.**, Elvert, M., Eckert, W., Kushmaro, A., Vigderovich, H., Zhu, Q., Ben-Dov, E., Sivan, O. Iron-Coupled Anaerobic Oxidation of Methane Performed by a Mixed Bacterial-Archaeal Community Based on Poorly Reactive Minerals. *Environ. Sci.*

- Technol.* **2017**, *7*;51 (21), 12293–12301.
- 29. He, Z.**, Zhang, Q., Feng, Y., Luo, H., Pan, X., Michael, G. Microbiological and environmental significance of metal-dependent anaerobic oxidation of methane. *Sci. Total Environ.* **2018**, *610–611*, 759–768.
- 30. Heitmann, T.**, Goldhammer, T., Beer, J., Blodau, C. Electron transfer of dissolved organic matter and its potential significance for anaerobic respiration in a northern bog. *Glob. Chang. Biol.* **2007**, *13* (8), 1771–1785.
- 31. Heitmann, T.**, Blodau, C. Oxidation and incorporation of hydrogen sulfide by dissolved organic matter. *Chem. Geol.* **2006**, *235* (1–2), 12–20.
- 32. Smemo, K. A.**, Yavitt, J. B. Anaerobic oxidation of methane: An underappreciated aspect of methane cycling in peatland ecosystems? *Biogeosciences* **2011**, *8* (3), 779–793.
- 33. Martinez, C. M.**, Alvarez, L. H., Celis, L. B., Cervantes, F. J. Humus-reducing microorganisms and their valuable contribution in environmental processes. *Appl. Microbiol. Biotechnol.* **2013**, *97* (24), 10293–10308.
- 34. Reed, D. C.**, Deemer, B. R., van Grinsven, S., Harrison, J. A. Are elusive anaerobic pathways key methane sinks in eutrophic lakes and reservoirs? *Biogeochemistry* **2017**, *134* (1–2), 29–39.
- 35. Scheller, S.**, Yu, H., Chadwick, G. L., Mcglynn, S. E. Artificial electron acceptors decouple archaeal methane oxidation from sulfate reduction. *Science (80-. )*. **2016**, *351* (6274), 703–707.
- 36. Batllori-Sampedro, E.**, Febles-Patron, J. L., Diaz-Sosa, J. Landscape change in Yucatan's northwest coastal wetlands (1948-1991). *Hum. Ecol. Rev.* **1999**, *6* (1), 8–20.
- 37. Cornell, R.M.**, Schwertmann, U. The iron oxides: structure, properties, reactions, occurrence and uses. *Mineral. Mag.* **2003**, *61* (408), 741.
- 38. Soga, T.**, Ross, G. A. Simultaneous determination of inorganic anions, organic acids and metal cations by capillary electrophoresis. *J. Chromatogr. A* **1999**, *834* (1–2), 65–71.
- 39. Cord-Ruwisch, R. A.**, Quick method for the determination of dissolved and precipitated sulfides in cultures of sulfate-reducing bacteria. *J. Microbiol. Methods* **1985**, *4* (1), 33–36.

40. **APHA/AWWA/WEF.** *Standard Methods for the Examination of Water and Wastewater*; 2012.
41. **Stookey, L. L.** Ferrozine - A new spectrophotometric reagent for iron. *Anal. Chem.* **1970**, *42* (7), 779–781.
42. **Fu, L.**, Li, S. W., Ding, Z. W., Ding, J., Lu, Y. Z., Zeng, R. J. Iron reduction in the DAMO/Shewanella oneidensis MR-1 coculture system and the fate of Fe(II). *Water Res.* **2016**, *88*, 808–815.
43. **Kappler, A.**, Wuestner, M. L., Ruecker, A., Harter, J., Halama, M., Behrens, S. Biochar as an Electron Shuttle between Bacteria and Fe(III) Minerals. *Environ. Sci. Technol. Lett.* **2014**, *1* (8), 339–344.
44. **Straub, K. L.**, Benz, M., Schink, B. Iron metabolism in anoxic environments at near neutral pH. *FEMS Microbiol. Ecol.* **2000**, *34* (3), 181–186.
45. **Schaedler, F.**, Kappler, A., Schmidt, C. A Revised Iron Extraction Protocol for Environmental Samples Rich in Nitrite and Carbonate. *Geomicrobiol. J.* **2018**, *35* (1), 23–30.
46. **Hansel, C. M.**, Lentini, C. J., Tang, Y., Johnston, D. T., Wankel, S. D., Jardine, P. M. Dominance of sulfur-fueled iron oxide reduction in low-sulfate freshwater sediments. *ISME J.* **2015**, *9* (11), 1–13.
47. **Shindell, D. T.**, Walter, B. P., Faluvegi, G. Impacts of climate change on methane emissions from wetlands. *Geophys. Res. Lett.* **2004**, *31* (21).
48. **Li, J.**, Peng, X., Bai, S., Chen, Z., Van Nostrand, J. D. Biogeochemical processes controlling authigenic carbonate formation within the sediment column from the Okinawa Trough. *Geochim. Cosmochim. Acta* **2018**, *222*, 363–382.
49. **Zeng, Z.**, Tice, M. M. Promotion and nucleation of carbonate precipitation during microbial iron reduction. *Geobiology* **2014**, *12* (4), 362–371.
50. **Peng, X.**, Guo, Z., Chen, S., Sun, Z., Xu, H., Ta, K., Zhang, J., Zhang, L., Li, J., Du, M. Formation of carbonate pipes in the northern Okinawa Trough linked to strong sulfate exhaustion and iron supply. *Geochim. Cosmochim. Acta* **2017**, *205*, 1–13.
51. **Smemo, K. A.**, Yavitt, J. B. Evidence for anaerobic CH<sub>4</sub> oxidation in freshwater peatlands. *Geomicrobiol. J.* **2007**, *24* (7–8), 583–597.
52. **Saxton, M. A.**, Samarkin, V. A.,

Schutte, C. A., Bowles, M. W., Madigan, M. T., Cadieux, S. B., Pratt, L. M., Joye, S. B. Biogeochemical and 16S rRNA gene sequence evidence supports a novel mode of anaerobic methanotrophy in permanently ice-covered Lake Fryxell, Antarctica. *Limnol. Oceanogr.* **2016**, *61*, S119–S130.

**53. Timmers, P. H.**, Suarez-Zuluaga, D. A., van Rossem, M., Diender, M., Stams, A. J., Plugge, C. M. Anaerobic oxidation of methane associated with sulfate reduction in a natural freshwater gas source. *ISME J.*

**2015**, *10* (6), 1–13.

**54. Pester, M.**, Knorr, K. H., Friedrich, M. W., Wagner, M., Loy, A. Sulfate-reducing microorganisms in wetlands - fameless actors in carbon cycling and climate change. *Front. Microbiol.* **2012**, *3* (FEB), 1–19.

**55. Holmkvist, L.**, Ferdelman, T. G., Jørgensen, B. B. A cryptic sulfur cycle driven by iron in the methane zone of marine sediment (Aarhus Bay, Denmark). *Geochim. Cosmochim. Acta* **2011**, *75* (12), 3581–3590

## CHAPTER IV

# Humic Substances Mediate Anaerobic Methane Oxidation Linked to Nitrous Oxide Reduction in Wetland Sediments

### HIGHLIGHTS

- Reduced *Pahokee Peat Humic Substances* (PPHS) served as the **electron donor** for **microbial N<sub>2</sub>O reduction**.
- The ***anaerobic oxidation of methane (AOM)*** was linked to **N<sub>2</sub>O reduction** due to extracellular electron transport mediated by PPHS.
- **Methanocellaceae, Methanomicrobiaceae and Acinetobacter** were the microbial taxa potentially fueling the CH<sub>4</sub> and N<sub>2</sub>O consuming process.
- The implications of **inter-species electron transport processes mediated by quinones** in greenhouse gas consuming processes is discussed.

**A modified version of this chapter has been submitted as:**

**Valenzuela, E. I.,** Padilla-Loma, C., Gómez-Hernández, N., López-Lozano, N. E., Casas-Flores, S. Cervantes, F. J. *Humic Substances Mediate Anaerobic Methane Oxidation Linked to Nitrous Oxide Reduction in Wetland Sediments.* (in revision)

## Abstract

Humic substances (HS) are redox-active organic molecules, which play pivotal roles in several biogeochemical cycles due to their electron-transferring capacity involving multiple abiotic and microbial transformations. Based on the redox properties of HS, and the metabolic capabilities of microorganisms to reduce and oxidize them, we hypothesized that they could mediate *anaerobic methane oxidation* (AOM) coupled to the reduction of nitrous oxide (N<sub>2</sub>O) in wetland sediments. This study provides several lines of evidence indicating the coupling between AOM and the reduction of N<sub>2</sub>O through an extracellular electron transfer mechanism mediated by HS. We found that the microbiota of a wetland sediment collected from Sisal (Yucatán Peninsula, southeastern Mexico) was able to reduce N<sub>2</sub>O ( $4.61 \pm 0.5 \mu\text{mol N}_2\text{O g}_{\text{sed.}}^{-1} \text{ day}^{-1}$ ) when reduced HS were provided as electron donor in a close stoichiometric relationship. Furthermore, simultaneous <sup>13</sup>CH<sub>4</sub> oxidation ( $1.28 \pm 0.14 \mu\text{mol } ^{13}\text{CO}_2 \text{ g}_{\text{sed.}}^{-1} \text{ day}^{-1}$ ) and N<sub>2</sub>O reduction ( $25.23 \pm 0.46 \mu\text{mol N}_2\text{O g}_{\text{sed.}}^{-1} \text{ day}^{-1}$ ) occurred, which was highly dependent on the presence of HS as an extracellular electron shuttle. Electron balances further confirmed the stoichiometric coupling between AOM and N<sub>2</sub>O reduction in wetland sediment incubations amended with HS. Taxonomic characterization based on 16S rRNA genomic libraries sequencing and cloning of the *nosZ* gene revealed *Acinetobacter* (a  $\gamma$ -proteobacteria), the Rice Cluster I from the *Methanocellaceae* and an uncultured archaeon from *Methanomicrobiaceae* as the microbes potentially involved in AOM linked to N<sub>2</sub>O reduction mediated by HS. These findings suggest that HS may play an important role to prevent the emission of greenhouse gases (CH<sub>4</sub> and N<sub>2</sub>O) from wetland sediments.



## 4.1 Introduction

Greenhouse gases (GHG) constitute the main agents causing global warming (GW), one of the biggest threats to our environment and thus to life <sup>1</sup>. Due to their wide range of energy absorption, molecules such as carbon dioxide (CO<sub>2</sub>), methane (CH<sub>4</sub>) and nitrous oxide (N<sub>2</sub>O) have raised the Earth's temperature by trapping excessive amounts of infrared radiation into the atmosphere, thus boosting the natural greenhouse effect <sup>2</sup>. Although much evidence has been collected regarding the anthropogenic component of climate change <sup>3</sup>, large amounts of GHGs are released from natural sources since several ecosystems naturally produce such molecules <sup>4</sup>. As an example, water bodies are responsible for the emission of great amounts of GHG, such as CH<sub>4</sub> and N<sub>2</sub>O <sup>3</sup>. For instance, up to 37% of the global CH<sub>4</sub> emission is estimated to be released from natural sources, with around 200 Tg CH<sub>4</sub> year<sup>-1</sup> coming from water bodies (mostly from wetlands and the oceans), in the case of N<sub>2</sub>O, 5.4 Tg N year<sup>-1</sup> are estimated to be released from the same source (64% of the global input) <sup>5</sup>. Further, it is expected that the amount of GHG emitted by water bodies is going to be affected by the current increase in the Earth's temperature, which implies that natural and anthropogenic processes will exacerbate GW <sup>6</sup>. Due to these reasons, a complete understanding of the key drivers governing the natural GHG dynamics is required to predict and prevent future scenarios of GW <sup>7</sup>. GHG emissions by water bodies are mainly triggered by microbial activity given that some of these molecules are either end products (*i.e.* CO<sub>2</sub> and CH<sub>4</sub>) or intermediates (*i.e.* N<sub>2</sub>O) of the metabolism of microbes <sup>8</sup>. Anaerobic degradation of *natural organic matter* (NOM) by microorganisms, which involves the methanogenesis process, constitutes a pivotal source for CO<sub>2</sub> and CH<sub>4</sub> emission from aquatic ecosystems <sup>9-11</sup>. In the same fashion, N<sub>2</sub>O is produced by anaerobic microbes in nitrogen-rich environments due to an incomplete

denitrification process<sup>12</sup>. Collectively, CH<sub>4</sub> and N<sub>2</sub>O are two of the most hazardous GHGs, both because of their high GW potential (25 and 300 times higher than that of CO<sub>2</sub>, respectively), and because of their long residence time in the Earth's atmosphere (12 and 114 years, respectively)<sup>13,14</sup>. As a counterpart of these microbial sources of GHG emission, there are several mechanisms for CH<sub>4</sub> and N<sub>2</sub>O microbial uptake, which have been extensively described. Regarding CH<sub>4</sub>, after assuming for decades that only aerobic microbes could oxidize this very stable compound (via a monooxygenase activation), several inorganic terminal electron acceptors (TEAs) have been reported to support anaerobic methane oxidation (AOM) by specialized anaerobic microorganisms. These TEAs include sulfate (SO<sub>4</sub><sup>2-</sup>), nitrate and nitrite (NO<sub>3</sub><sup>-</sup>, NO<sub>2</sub><sup>-</sup>), as well as metallic oxides of iron and manganese (Fe(III) & Mn(IV))<sup>15-17</sup>. Recently, the redox-active fraction of the continuously decaying NOM, commonly referred to as *humic substances* (HS)<sup>18</sup>, as well as their structural analogues (*e.g.* quinones), have also been found to be suitable oxidants for achieving AOM<sup>19-21</sup>. Moreover, HS can promote AOM not only by acting as TEA, but also by shuttling electrons derived from AMO towards metallic oxides reduction<sup>22,23</sup>. For N<sub>2</sub>O microbial depletion, there is only one known process, which consists of its reduction to molecular nitrogen (N<sub>2</sub>). This transformation is achieved by *nosZ* gene (*nitrous oxide reductase*) bearing microorganisms, which might not be mandatorily denitrifiers<sup>24</sup>. Regularly, the source of electrons for this reaction comes from labile molecules in NOM. Additionally, it has been reported that CH<sub>4</sub> could serve as an electron donor for this reaction, implying the existence of microorganisms capable of coupling the simultaneous consumption of two GHGs<sup>25</sup>. However, the underlying mechanisms and the main environmental drivers of this process remain unknown. Taking into account the previous evidence showing that reduced HS could serve as electron donor for denitrification<sup>26,27</sup>, and that HS could drive AOM by serving as TEA<sup>20</sup>, we aimed to decipher if HS could mediate AOM

linked to N<sub>2</sub>O reduction via an inter-species electron transfer (IET). This hypothesis is supported by the previous evidence about HS and other quinone-containing materials (such as biochar or activated carbon) linking the oxidation of reduced compounds to the reduction of oxidized molecules, which a single microorganism could not accomplish due to metabolic limitations<sup>28,29</sup>.

## 4.2 Materials and Methods

### 4.2.1 Wetland and sediment sampling description

The Sisal wetland is a mangrove swamp located in the Yucatán Peninsula (southeastern Mexico) within the ports of Celestun and Sisal (21°09'26"N, 90°03'09"W). Wetland sediment cores were collected under a water column of approximately 70 cm, in January 2016. The depth of the sampled cores was 15 cm. All sediment samples were sealed in hermetic flasks, which were maintained in ice until their arrival to the laboratory where they were then stored at 4°C in a dark room. Before performing the incubation assays, sediment and its pore water were chemically characterized. These characteristics have previously been reported elsewhere<sup>20,22</sup>.

### 4.2.2 Microcosms set-up

#### 4.2.2.1 Kinetics of N<sub>2</sub>O reduction

An initial evaluation of the capacity of the wetland sediment biota to employ reduced *Pahokee Peat* humic substances (PPHS, catalogue number from the IHSS: 1S103H) as electron donors for N<sub>2</sub>O reduction was performed. To this end, serum bottles (25 mL) were inoculated with previously homogenized wetland sediment (1 g), and 15 mL of basal medium enriched with PPHS at a concentration of 1 g L<sup>-1</sup> were employed. The composition of the basal medium has been reported

## CHAPTER IV

previously<sup>20,30</sup>. Controls lacking PPHS were also included, as well as PPHS enriched killed controls, which were prepared by autoclaving (3 cycles) and subsequent addition of anhydrous chloroform (99%, Sigma-Aldrich) at a concentration of 10% v/v. All microcosms were incubated under anoxic conditions for 2 months. Hydrogen (H<sub>2</sub>) was provided as electron donor to achieve PPHS reduction (these treatments are referred to as *PPHS<sub>red</sub>*). The headspace of all microcosms was flushed with argon (99.9% purity, Praxair) for 10 min, and then H<sub>2</sub> was provided to a partial pressure of 0.67 atm with disposable syringes (supply of H<sub>2</sub> was done three times during the reduction process). After this period, all bottles were flushed with Ar for 10 min to remove the remaining H<sub>2</sub> and then the electrons stored as *PPHS<sub>red</sub>* were measured by the ferrozine technique<sup>20,31</sup>.

After these measurements, a control containing the same amount of oxidized PPHS was prepared without passing through the reduction process (referred to as *PPHS<sub>ox</sub>*). The concentrated PPHS stock was prepared by dissolving PPHS in fresh basal medium and magnetically stirring overnight. Dissolved oxygen was flushed away from the stock solution by purging with Ar for 1 hour. To begin the N<sub>2</sub>O reduction experiment, 4 mL of N<sub>2</sub>O were spiked to all microcosms except to those *PPHS<sub>red</sub>* bottles serving as endogenous controls; afterwards, the zero-time gaseous measurements were done, and the incubation period was started by placing all bottles in a dark room at 28°C without shaking.

#### 4.2.2.2 Kinetics of simultaneous N<sub>2</sub>O and <sup>13</sup>CH<sub>4</sub> consumption

Homogenized wetland sediment (1 g) was inoculated into 25 mL serum bottles containing 15 mL of the anoxic basal medium previously described. Afterwards, the headspace of each bottle was flushed with argon gas (Ar) for 10 min. All microcosms were then pre-incubated in a dark room at 28°C for approximately 30 days. The purpose of this initial incubation was to deplete endogenous electron acceptors and donors, such as organic molecules, sulfate and metals. After this period, microcosms were taken inside an anoxic chamber (COY 14500; atmosphere composed of N<sub>2</sub>/H<sub>2</sub>, 95%/5% v/v) to replace the liquid phase by freshly prepared anoxic basal medium enriched with 500 mg L<sup>-1</sup> of PPHS. Control incubations were filled with regular basal medium lacking PPHS. Once the basal medium was replaced, all microcosms were sealed with rubber stoppers and aluminum crimps, taken outside the anaerobic chamber and their atmosphere was flushed with Ar for 10 min. Once these anoxic microcosms were prepared, 2 mL of <sup>13</sup>CH<sub>4</sub> (99 atom. %, Sigma Aldrich) and/or 4 mL of N<sub>2</sub>O (99.9 % purity, Sigma Aldrich) were injected into the bottles' headspace using plastic disposable syringes. Endogenous controls were left without addition of GHG, while sterile controls were prepared as described above.

The first incubation cycle in which microbial <sup>13</sup>CH<sub>4</sub> oxidation and N<sub>2</sub>O reduction was observed lasted 9 days. After this period, microcosms were supplied with new basal medium inside the anaerobic chamber and then flushed with Ar for 10 min. <sup>13</sup>CH<sub>4</sub> and N<sub>2</sub>O were spiked again, and a second incubation cycle (9 days) was started.

## 4.2.3 Analytical techniques

### 4.2.3.1 Sulfate, sulfide, nitrate and nitrite measurements

The concentrations of  $\text{SO}_4^{2-}$ ,  $\text{HS}^-$ ,  $\text{NO}_3^{2-}$  and  $\text{NO}_2^-$  were measured according to standard methodologies previously established<sup>32-34</sup>. A detailed description of these methodologies and their modifications can be found in Rios-Del Toro et al., 2018.

### 4.2.3.2 Isotopic carbon dioxide and nitrous oxide determinations

Simultaneous quantification of  $^{13}\text{CO}_2$  production from  $^{13}\text{CH}_4$  oxidation and  $\text{N}_2\text{O}$  consumption was conducted by mass spectrometry (MS) (Agilent Technologies 5977A Series MSD) complemented by 7890B gas chromatograph (GC). Separation was achieved with a HP-PLOT/Q + PT capillary column (30 m x 0.320 mm ID x 0.20  $\mu\text{m}$ ) from Agilent Technologies. Helium was used as carrier gas at 0.2655 mL/min. The chromatographic method was as follows: the starting temperature was 70°C, and then a ramp with an increase of 20°C per min was implemented for 3 min. The temperatures of injector and MS source were maintained at 250 and 230 °C, respectively. The injection volume was 20  $\mu\text{L}$  and there was only one replicate of injection per sample. The gas injected into the gas chromatograph was manually taken directly from the headspace of the incubations and immediately injected into the GC port.

### **4.2.3.3 Quantification of electron-donating capacity in slurry samples**

The reduction of humic material in the form of PPHS or intrinsic NOM was assessed as the amount of ferrous iron produced by the reaction of ferric citrate with slurry taken from the microcosms under anoxic conditions. The ferrous iron released was then measured by the ferrozine technique<sup>31</sup> and corrected for intrinsic ferrous iron detected ( $\text{Fe}^{2+}$  measured in samples after acid treatment without addition of ferric citrate)<sup>36</sup>. These measurements were performed in a spectrophotometer located inside the COY 14500 anaerobic chamber previously described. Further details on this methodology have been previously described<sup>20</sup>.

## **4.2.4 Molecular analysis**

### **4.2.4.1 DNA extraction and pooling**

Two replicates for each experimental treatment were sacrificed at the end of the incubation periods for DNA extraction. Bottles were vigorously shaken and then 500  $\mu\text{L}$  of slurry were taken with sterile disposable syringes to extract DNA using the PowerSoil DNA extraction kit (Mo Bio Laboratories, Carlsbad, CA, USA) according to the protocol described by the manufacturer. For the *nosZ* cloning procedure, DNA pools of each experimental replicate were created by mixing equal volumes of DNA from the two experimental replicates, for the construction of the 16s genomic libraries. DNA was processed in an independent manner in order to obtain parallel sequencing results for each experimental replicate.

#### 4.2.4.2 *nosZ* cloning

DNA pools created for each experimental treatment were used to amplify the *nosZ* gene using the primers nosZF and nosZR (1162-1178 and 1889-1907 positions of the *nosZ* gene of *P. denitrificans* PD1222) proposed by Jones et al. (2013). PCR was performed in 25  $\mu$ L reaction mixtures using a Taq DNA Polymerase (ThermoFisher Scientific, USA) under the following conditions: denaturation at 95 °C for 5 min, followed by 40 cycles of amplification at 95 °C for 30 s, 48 °C for 60 s, 72 °C for 60 s, and finished with 72 °C for 10 min. The size of the PCR products was verified by electrophoresis in a 2% agarose gel stained with ethidium bromide. PCR products were cleaned using the Wizard SV Gel and PCR Clean-Up system (Promega) and then cloned into the pGEM T-easy vector (Promega) following the manufacturers recommendations. Ligation products were used to transform chemically competent *Escherichia coli* TOP 10F' cells by electroporation using an ECM 360 electroporator under the following conditions: 2500 V voltage, 0200 $\Omega$  resistance and 0025 $\mu$ F capacitance. Recombinant plasmids were extracted by alkaline extraction as described by Birnboim (1983)<sup>37</sup> and sequenced by the Sanger reaction in an ABI sequencer (Applied Biosystems).

#### 4.2.4.3 Genomic libraries construction and Sequencing

DNA isolated from each experimental replicate was amplified using primers targeting the 16s rRNA gene of Bacteria (V3–V4 region, 341F-805R) and Archaea (340F-1000R)<sup>38</sup>, both fused with Illumina adapter overhang nucleotide sequences. PCRs for bacterial 16 s RNA region were performed in 25  $\mu$ L reaction mixtures using Invitrogen HF Platinum Taq Polymerase (Thermo Fisher Scientific, USA) under the following conditions: denaturation at 95 °C for 90 s, followed by 30 cycles of



amplification at 95 °C for 15 s, 57 °C for 30 s, 72 °C for 30 s, 80 °C for 30 s and finished with 95 °C for 15 s and 60 °C for 10 s. PCRs for archaeal 16 s RNA region were performed under the conditions reported by Gantner et al., 2011<sup>38</sup>. PCR products were indexed using Nextera XT Index Kit v2 (Illumina, San Diego, CA) according to the Illumina's 16s Metagenomic Sequencing Library Preparation protocol. Libraries were further sequenced by single end with Illumina MiSeq sequencer.

#### **4.2.4.4 *nosZ* bioinformatic analysis**

Sequenced *nosZ* clones were checked for quality, cleaned and then screened using the *blastx* tool (nucleotide to protein) of the NCBI database (<http://blast.ncbi.nlm.nih.gov/>).

#### **4.2.4.5 16s bioinformatic analysis**

Mothur open source software (v 1.34.4) was used for analysis of 16s rRNA libraries<sup>39</sup>. Sequences with a length less than 500 bp, homopolymer runs of eight or more bases, those with more than one mismatch to the sequencing primer and Q-value average below 25 were discarded. The potential occurrence of chimeric sequences was analyzed using UCHIME algorithm. Group membership was determined prior to trimming of the barcode and primer sequence. Sequences were aligned against the SILVA v. 132 16S rRNA gene database, using the nearest alignment space termination (NAST) algorithm. Group membership was determined prior to trimming of the barcode and primer sequence. A distance matrix was calculated across the set of non-redundant sequences and the readings were grouped into operational taxonomic units (OTUs) with a similarity threshold of 97%. Mothur's Bayesian classifier and the SILVA 132 reference set were used to

taxonomically categorize the sequences. Taxonomic assignments were made with a confidence threshold greater than 80% of bootstrap value.

#### 4.2.5 Accession numbers

The accession numbers of sequences in this work were deposited in the GenBank sequence read archive under the BioProject with PRJNA576687 accession number.

#### 4.2.6 Electron balance calculations

The amount of  $^{13}\text{CO}_2$  produced due to the PPHS driven synergistic activity of  $\text{CH}_4$  oxidizers and  $\text{N}_2\text{O}$  reducers was calculated as follows:

- mM of  $^{13}\text{CO}_2$  produced in the PPHS/ $\text{N}_2\text{O}/^{13}\text{CH}_4$  treatment – mM of  $^{13}\text{CO}_2$  produced in the  $\text{N}_2\text{O}/^{13}\text{CH}_4$  treatment =  **$^{13}\text{CO}_2$  produced due to  $\text{N}_2\text{O}$  reduction**

The electron milli-equivalents (meq) derived from this reaction were calculated as follows considering the stoichiometric relationship of  $\text{CH}_4$  oxidation with  $\text{N}_2\text{O}$  as terminal electron acceptor.

- ( $^{13}\text{CO}_2$  produced due to  $\text{N}_2\text{O}$  reduction) \* 8 = **meq obtained from  $^{13}\text{CH}_4$  oxidation**

Where 8 equals the amount of electrons obtained from the complete oxidation of  $^{13}\text{CH}_4$  to  $^{13}\text{CO}_2$ .

The amount of  $\text{N}_2\text{O}$  consumed due to the PPHS driven synergistic activity of  $\text{CH}_4$  oxidizers and  $\text{N}_2\text{O}$  reducers was calculated as follows:

- mM of  $\text{N}_2\text{O}$  consumed in the PPHS/ $\text{N}_2\text{O}/^{13}\text{CH}_4$  treatment – mM of  $\text{N}_2\text{O}$  consumed in the  $\text{N}_2\text{O}/^{13}\text{CH}_4$  treatment =  **$\text{N}_2\text{O}$  consumed due to  $^{13}\text{CH}_4$  oxidation**

## CHAPTER IV

The electron milli-equivalents (meq) required for this reaction were calculated as follows considering the stoichiometric relationship of CH<sub>4</sub> oxidation with N<sub>2</sub>O as terminal electron acceptor.

$$- (\text{N}_2\text{O consumed due to } ^{13}\text{CH}_4 \text{ oxidation}) * 2 = \underline{\text{meq required for N}_2\text{O reduction}}$$

Where 2 equals the number of electrons needed for the reduction of N<sub>2</sub>O to N<sub>2</sub>. If the coupling of the oxidation and reduction reactions were 100%, then the relationship

$$- \text{meq obtained from } ^{13}\text{CH}_4 \text{ oxidation/meq required for N}_2\text{O reduction}$$

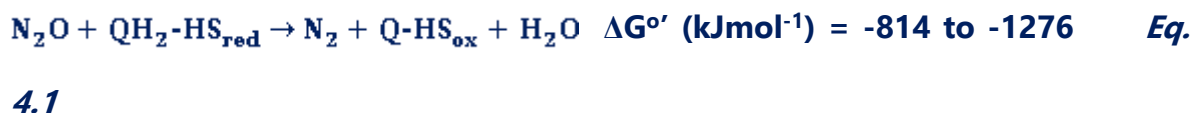
should be 1.

These calculations were done for each experimental replicate at each experimental sampling point. The triplicate results were averaged and then a linear regression analysis was made for all the sampling points throughout the incubation period.

## 4.3 Results

### 4.3.1 Kinetics of N<sub>2</sub>O reduction with reduced PPHS as electron donor

The wetland sediment microbiota achieved N<sub>2</sub>O reducing activities of up to 4.61±0.5 μmol g sed.<sup>-1</sup> day<sup>-1</sup> in incubations enriched with HS<sub>red</sub> (reduced PPHS) during 12 days of incubation (**Fig. 4.1A**). This N<sub>2</sub>O reducing activity was linked to the oxidation of 0.75±0.27 milli-equivalents (meq) L<sup>-1</sup> derived from HS<sub>red</sub>, which was calculated by the loss on their EDC through the same incubation period (**Fig. 4.1B**). Considering quinones/hydroquinones as the main redox groups in HS<sup>40</sup>, the stoichiometry of N<sub>2</sub>O reduction coupled to hydroquinones oxidation can be considered as follows:



Where QH<sub>2</sub>-HS<sub>red</sub> refers to reducing equivalents stored as hydroquinones in HS<sub>red</sub> (2 reducing equivalents per hydroquinone moiety) and Q-HS<sub>ox</sub> represents quinone equivalents produced as oxidized HS during the oxidation of QH<sub>2</sub>-HS<sub>red</sub>. The ratio oxidized QH<sub>2</sub>-HS<sub>red</sub>:reduced N<sub>2</sub>O obtained at the end of the experiments was approximately 1.1 (corrected for the HS<sub>red</sub> oxidation quantified in controls lacking N<sub>2</sub>O and for the N<sub>2</sub>O reduction measured in controls amended with HS<sub>ox</sub>, respectively, **Fig. 4.1**), which is in agreement with the expected stoichiometric value (**Eq. 4.1**). As seen in **Fig. 4.1B**, quantification of the intrinsic EDC present in the wetland sediment (incubated without external HS), accounted for 75% of the N<sub>2</sub>O reduction observed in these controls (1.3 stoichiometric relationship). In agreement with this, substantial N<sub>2</sub>O reduction occurred in sediment incubations spiked with

HS<sub>ox</sub> (2.84  $\mu\text{mol g}_{\text{sed.}}^{-1} \text{ day}^{-1}$ ), which was significantly higher than that measured in the absence of added HS ( $0.68 \pm 0.35 \mu\text{mol g}_{\text{sed.}}^{-1} \text{ day}^{-1}$ ). Sediment incubations enriched with HS<sub>red</sub>, but lacking added N<sub>2</sub>O (*endogenous* controls) did not show any significant loss on the initial EDC (including both HS<sub>red</sub> and reduced intrinsic NOM), suggesting that N<sub>2</sub>O was the only TEA fueling microbial HS<sub>red</sub> oxidation (**Fig. 4.1B**). *Killed* controls including both HS<sub>red</sub> and N<sub>2</sub>O did not show any activity validating the biological nature of these redox processes.

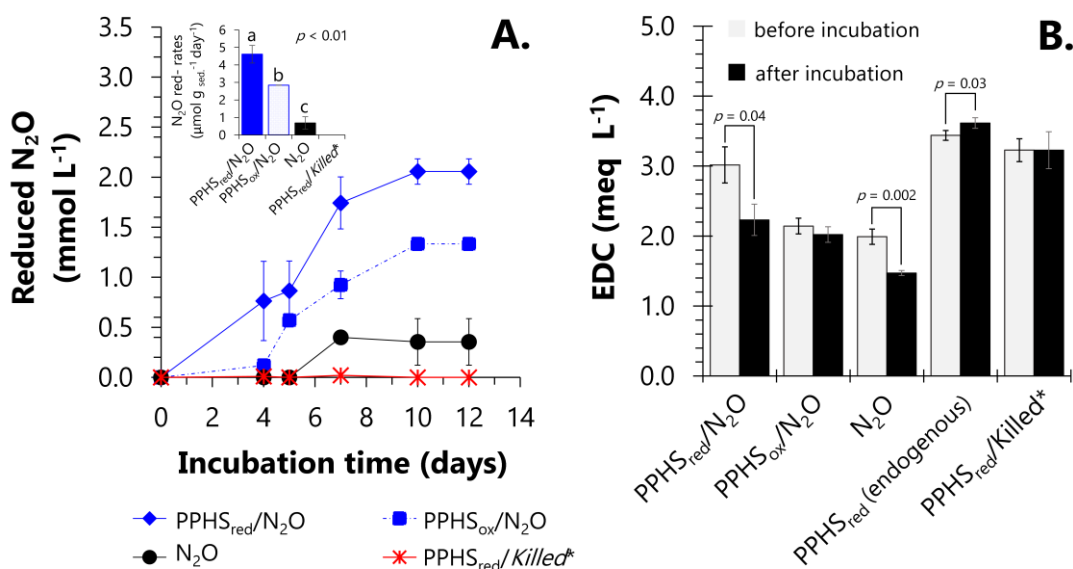


**Fig. 4.1 | Nitrous oxide reduction linked to re-oxidation of reduced functional groups in *Pahokee Peat* Humic Substances (PPHS<sub>red</sub>).** Panel A depicts the normalized (concentration – initial concentration, C–C<sub>i</sub>) kinetics of N<sub>2</sub>O reduction. The inset shows the maximum rates of N<sub>2</sub>O reduction based on the linear regressions of at least three sampling points during the days of highest activity. Statistically different groups (rates) are represented with letters obtained via a one-way ANOVA and the Duncan *post hoc* test (95% percent confidence interval). Panel B shows changes on the electron donating capacity (EDC) of PPHS before and after incubation with or without N<sub>2</sub>O after

12 days of incubation. Significant changes in EDC after incubation are denoted with  $p$  values ( $< 0.05$ ) which were evaluated through a Student's  $t$ -test (95% percent confidence interval, degrees of freedom = 4). Data represent the average from triplicate incubations  $\pm$  standard error. \**Killed* controls contained the same concentration of  $N_2O$  as in the main experimental treatments ( $3.23 \pm 0.03 \text{ mmol L}^{-1}$ ). Endogenous controls were incubated in the absence of  $N_2O$ .

### 4.3.2 AOM linked to $N_2O$ reduction mediated by HS

#### 4.3.2.1 $N_2O$ reduction rates

After the conditioning pre-incubation cycle, intended to exhaust intrinsic electron donors and acceptors present in the wetland sediment,  $N_2O$  reduction was documented in two subsequent incubation periods (referred to as 1<sup>st</sup> and 2<sup>nd</sup> incubation cycles). During the 1<sup>st</sup> cycle, high  $N_2O$  reduction rates were observed only in microcosms enriched with HS ( $0.23 \pm 0.03$  and  $0.15 \pm 0.03 \text{ mmol } N_2O \text{ g}_{\text{sed.}}^{-1} \text{ day}^{-1}$ ) in the presence and in the absence of  $^{13}CH_4$ , respectively). These treatments displayed nearly complete depletion of the supplied  $N_2O$  within the first three days of incubation. However, this denitrifying activity was mainly fueled by the oxidation of labile organic compounds originally present in the wetland sediment. Thus, the role of PPHS as redox mediator linking AOM to  $N_2O$  reduction was not conclusive in the 1<sup>st</sup> cycle (**Fig. 4.2**).

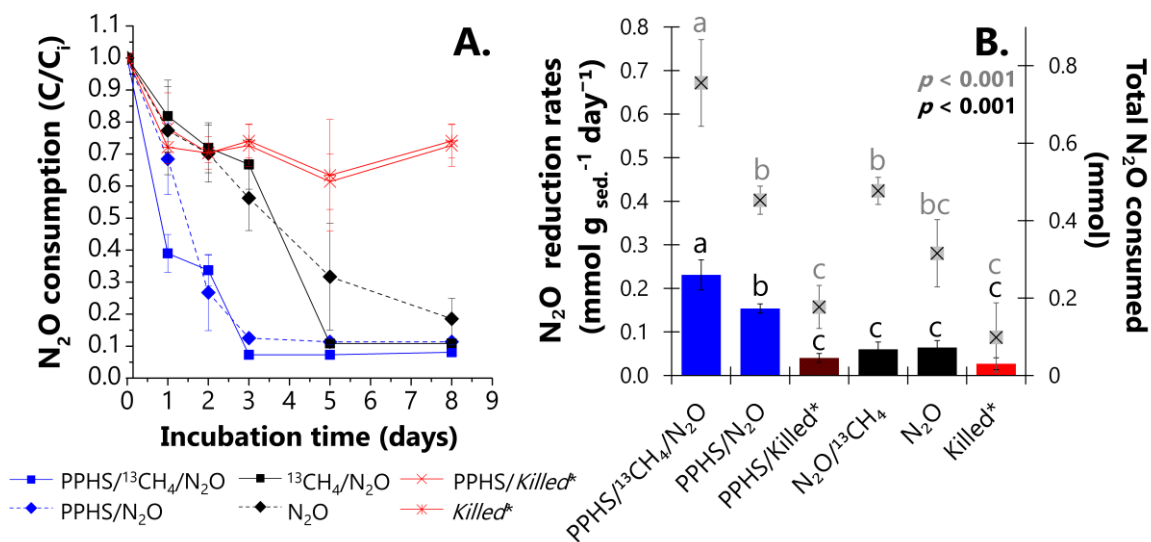


**Fig. 4.2 | Nitrous oxide reduction promoted by Pahokee Peat Humic Substances (PPHS) acting as electron shuttle and <sup>13</sup>CH<sub>4</sub> as electron donor. Panel A** depicts the normalized (concentration / initial concentration, C/C<sub>i</sub>) kinetics of N<sub>2</sub>O consumption with and without PPHS as electron shuttle. **Panel B** shows the rates (bars, left axis) and net amount of N<sub>2</sub>O depleted (× symbols, right axis) after 8 days of incubation. Statistically different groups (rates) are represented with letters obtained via a one-way ANOVA and the Duncan *post hoc* test (95% percent confidence interval). Data represent the average from triplicate incubations ± standard error. \**Killed* controls contain the same concentration of <sup>13</sup>CH<sub>4</sub> and N<sub>2</sub>O as in the main experimental treatments. N<sub>2</sub>O consumption rates (**Panel B**) were based on the maximum slope observed on linear regressions considering at least three sampling points.

Nevertheless, throughout the 2<sup>nd</sup> incubation cycle (**Fig. 4.3**), the importance of PPHS fueling the consumption of both GHGs was explicitly shown by ~30% more N<sub>2</sub>O reduced in the treatment containing <sup>13</sup>CH<sub>4</sub> as electron donor. The maximum reduction rate observed in this treatment was 25.53±0.46 μmol N<sub>2</sub>O g

$\text{sed.}^{-1} \text{ day}^{-1}$  (15% higher than those rates observed in the experimental controls containing PPHS but lacking  $^{13}\text{CH}_4$  ( $22.11 \pm 0.2 \mu\text{mol N}_2\text{O g sed.}^{-1} \text{ day}^{-1}$ ).

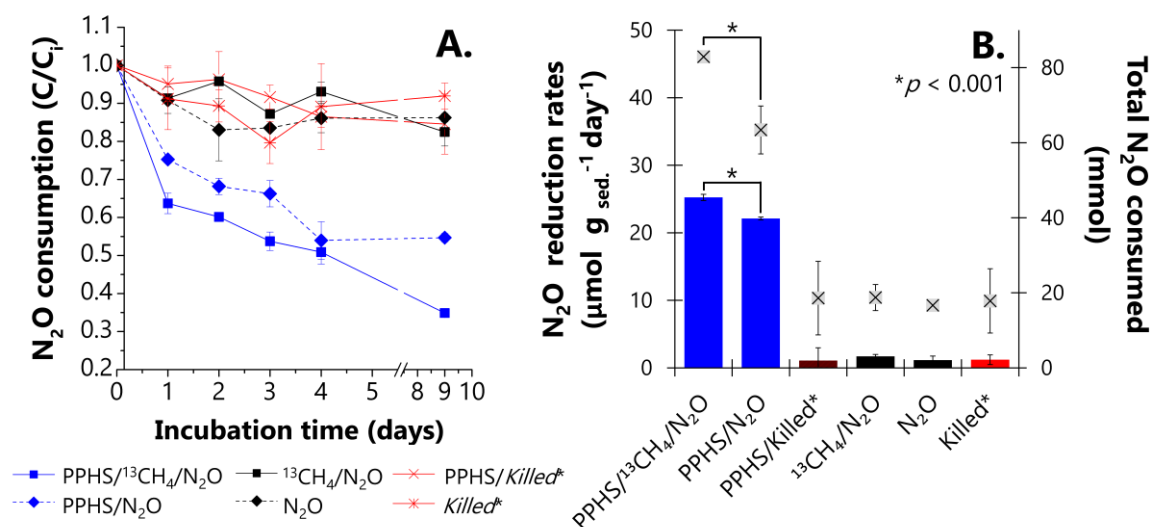


**Fig. 4.3 | Nitrous oxide reduction promoted by *Pahokee Peat* Humic Substances (PPHS) acting as electron shuttle and  $^{13}\text{CH}_4$  as electron donor. Panel A** depicts the normalized (concentration / initial concentration,  $C/C_i$ ) kinetics of  $\text{N}_2\text{O}$  consumption with and without PPHS as electron shuttle. **Panel B** shows the rates (bars, left axis) and net amount of  $\text{N}_2\text{O}$  depleted ( $\times$  symbols, right axis) after 9 days of incubation. Statistically different groups (rates) are represented with letters obtained via a one-way ANOVA and the Duncan *post hoc* test (95% percent confidence interval). Significant changes in EDC after incubation are denoted with  $p$  values ( $< 0.05$ ) which were evaluated through a Student's *t*-test (95% percent confidence interval, degrees of freedom = 4). Data represent the average from triplicate incubations  $\pm$  standard error. \**Killed* controls contain the same concentration of  $^{13}\text{CH}_4$  ( $\sim 4 \text{ mmol L}^{-1}$ ) and  $\text{N}_2\text{O}$  ( $6.6 \pm 0.4 \text{ mmol L}^{-1}$ ) as in the main experimental treatments.  $\text{N}_2\text{O}$  consumption rates (**Panel B**) were based on the maximum slope observed on linear regressions considering at least three sampling points.



Marginal rates of N<sub>2</sub>O depletion ( $1.7 \pm 0.3$  and  $1.16 \pm 0.6$   $\mu\text{mol N}_2\text{O g}_{\text{sed.}}^{-1} \text{day}^{-1}$ ) were observed with and without <sup>13</sup>CH<sub>4</sub> addition, respectively, in microcosms lacking PPHS, which were in fact very similar to the activity observed in *killed* controls (**Fig. 4.3B**). Moreover, high N<sub>2</sub>O reduction was only observed in incubations amended with PPHS or with PPHS/<sup>13</sup>CH<sub>4</sub> (**Fig. 4.3A**).

#### 4.3.2.2 AOM and its coupling with N<sub>2</sub>O reduction

Supplementary evidence demonstrating the coupling between AOM and N<sub>2</sub>O reduction was obtained by quantifying the amount of <sup>13</sup>CO<sub>2</sub> derived from <sup>13</sup>CH<sub>4</sub> oxidation in all experimental conditions (**Fig. 4.4**). During the 2<sup>nd</sup> incubation cycle, <sup>13</sup>CO<sub>2</sub> production was only detected in sediment incubations containing both PPHS and N<sub>2</sub>O ( $1.28 \pm 0.14$   $\mu\text{mol } ^{13}\text{CO}_2 \text{ g}_{\text{sed.}}^{-1} \text{day}^{-1}$ , **Fig. 4.4A**). Furthermore, reducing equivalents originated from AOM and quantified as <sup>13</sup>CO<sub>2</sub> were highly correlated (84%) with the amount of reduced N<sub>2</sub>O (corrected for endogenous controls) through the entire incubation cycle (**Fig. 4.4B**). This correlation was calculated considering the following stoichiometry:



No <sup>13</sup>CO<sub>2</sub> production was observed in experimental treatments lacking PPHS or N<sub>2</sub>O further emphasizing the role of HS as electron shuttles for coupling AOM to N<sub>2</sub>O reduction (**Fig. 4.4A**).

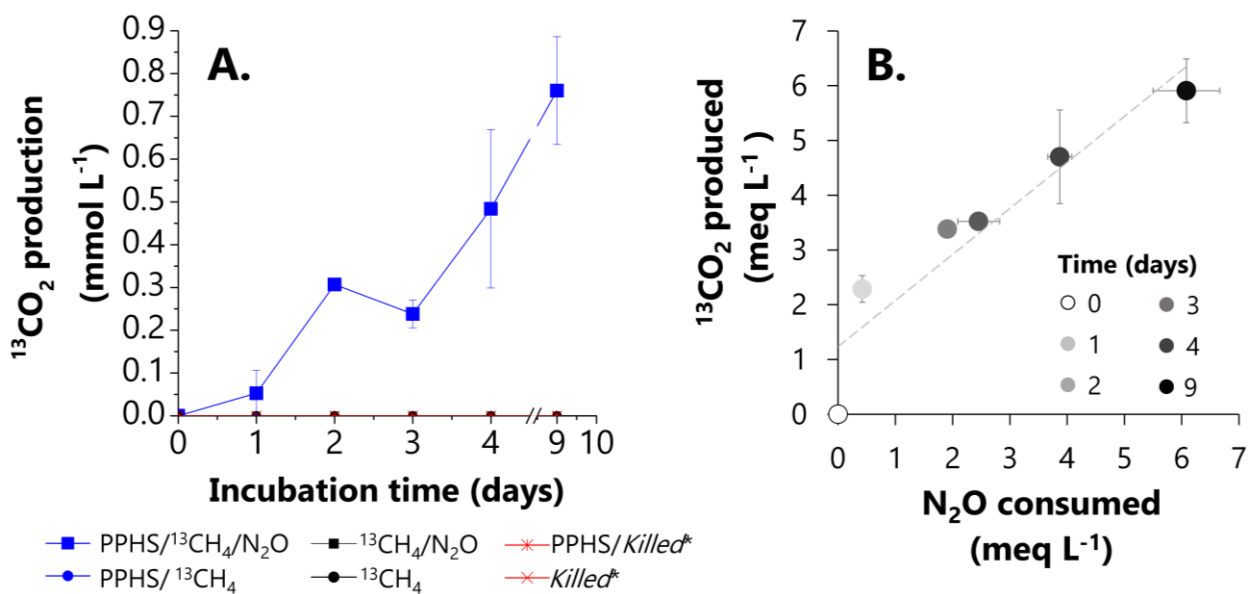


**Fig. 4.4** | Anaerobic  $^{13}\text{CH}_4$  oxidation measured as  $^{13}\text{CO}_2$  production and its relationship with  $\text{N}_2\text{O}$  reduction in the presence of *Pahokee Peat* Humic Substances (PPHS). **Panel A** depicts the produced  $^{13}\text{CO}_2$  from AOM  $\text{N}_2\text{O}$  reduction via electron shuttling mediated by PPHS. **Panel B** shows an electron balance correlating the produced  $^{13}\text{CO}_2$  with reduced  $\text{N}_2\text{O}$  in terms of reducing milli-equivalents (meq). Data represent the average from triplicate incubations  $\pm$  standard error.

### 4.3.2.3 PPHS redox pattern during AOM linked to N<sub>2</sub>O reduction

The redox state of PPHS was monitored during the observed AOM linked to N<sub>2</sub>O reduction in the 2<sup>nd</sup> cycle of incubation (**Fig. 4.5**).

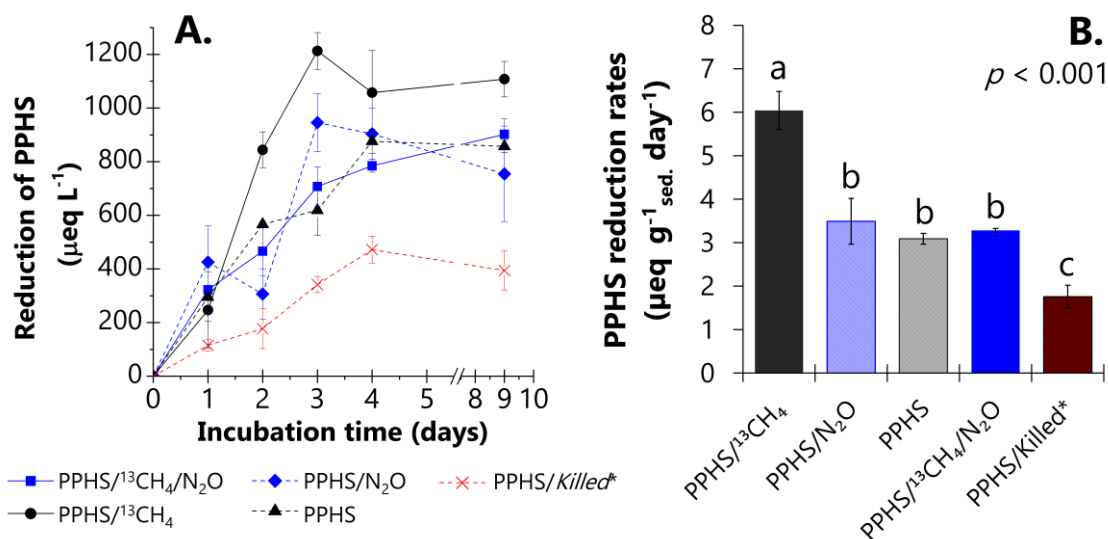
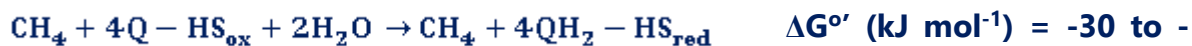


**Fig. 4.5** | Reduction of *Pahokee Peat* Humic Substances (PPHS) under the different experimental conditions during the incubation time. **Panel A** shows the reduction of PPHS during incubation period in. **Panel B** compares the rates of PPHS reduction among the different experimental treatments. Data represent the average from triplicate incubations  $\pm$  standard error. \**Killed* controls contained the same concentrations of <sup>13</sup>CH<sub>4</sub> ( $\sim 4$  mmol L<sup>-1</sup>) and N<sub>2</sub>O ( $6.6 \pm 0.4$  mmol L<sup>-1</sup>) as in the main experimental treatments. PPHS reduction rates (**Panel B**) were based on the maximum slope observed on linear regressions considering at least three sampling points.

As expected, microcosms containing <sup>13</sup>CH<sub>4</sub> and PPHS, but lacking N<sub>2</sub>O, displayed the maximum rates of PPHS reduction ( $6.04 \pm 0.4$  µeq g<sub>sed.</sub><sup>-1</sup> day<sup>-1</sup>, **Fig.**

4.5A), while endogenous controls incubated in the absence of  $^{13}\text{CH}_4$  showed PPHS reduction rates ~42% lower than the former experimental treatment. These findings confirm the utilization of  $^{13}\text{CH}_4$  as electron donor by humus-reducing microorganisms (humus-driven AOM, Eq. 4.3).



416.5 Eq. 4.3

Moreover, microcosms amended with both  $^{13}\text{CH}_4$  and  $\text{N}_2\text{O}$  in the presence of PPHS displayed the lowest PPHS reduction rates among all experimental treatments ( $3.28 \pm 0.04 \mu\text{eq g}_{\text{sed.}}^{-1} \text{ day}^{-1}$ ). (Fig. 4.5B). This confirms that  $\text{HS}_{\text{red}}$  produced via AOM are re-oxidized to  $\text{HS}_{\text{ox}}$  coupled to  $\text{N}_2\text{O}$  reduction (Fig. 4.6).

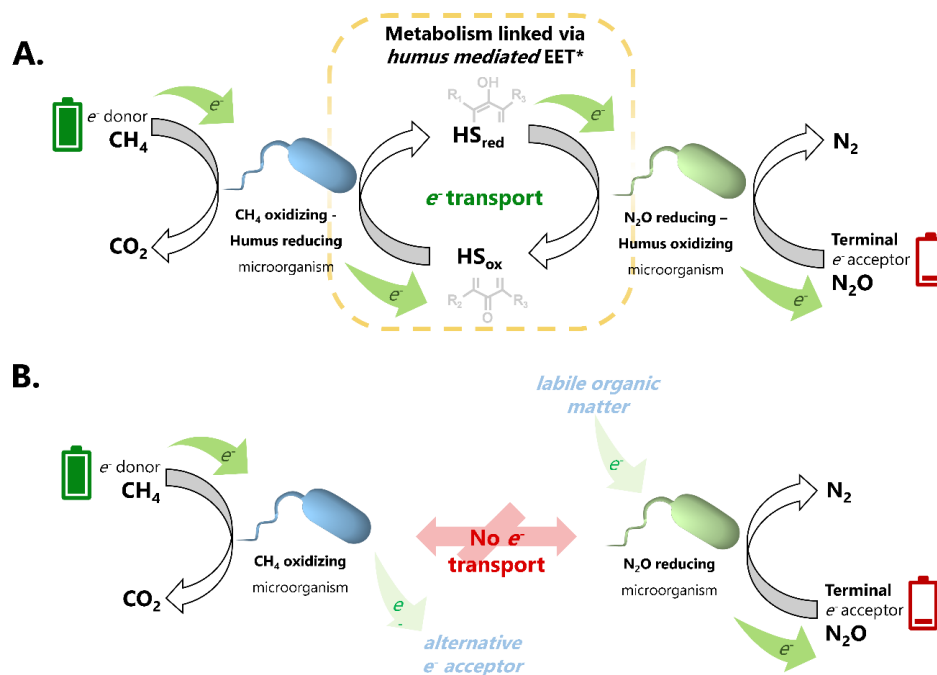


Fig. 4.6 | Schematic representation of anaerobic  $\text{CH}_4$  oxidation linked to  $\text{N}_2\text{O}$  reduction mediated by the electron shuttling capacity of humic substances (HS).

**Panel A** illustrates the extracellular electron transfer process promoted by HS, which links the metabolic capabilities of anaerobic methane oxidizing and nitrous oxide reducing microbes. Full (green) batteries are a representation of the high content of reducing equivalents in CH<sub>4</sub>, which are taken by anaerobic methane oxidizing-humus reducing microorganisms and then taken from the reduced redox-active moieties (hydroquinones) by humus oxidizing-nitrous oxide-reducing microbes to reduce N<sub>2</sub>O, represented by an energy depleted (red) battery, into inert N<sub>2</sub>. In the absence of HS (**Panel B**), each process consuming CH<sub>4</sub> and N<sub>2</sub>O could be independently fueled by an alternative electron donor or electron acceptor present at the wetland sediments (displayed in attenuated colors).

#### 4.3.2.4 Microbial communities potentially involved in AOM linked to N<sub>2</sub>O reduction

##### 4.3.2.4.1 Bacterial taxa

According to 16S rRNA gene sequences performed at end of the incubation cycles, some bacterial groups considerably increased their abundance within the whole bacterial community under the selective conditions established in each experimental treatment (**Fig. 4.7**). The most noticeable feature in the bacterial community in sediment incubations in which PPHS mediated AOM linked to N<sub>2</sub>O reduction was the enrichment of a member of the *Moraxellaceae* family, identified as an *Acinetobacter* phylotype (accounting for 43% of the bacterial community, Fig. 6A). The most predominant taxon observed in the remaining experimental treatments belongs to  $\gamma$ -Proteobacteria. However, the abundance of this member of *Pseudomonas* did not show any relationship with the presence of PPHS, CH<sub>4</sub> or N<sub>2</sub>O during the experiments (**Fig. 4.7A**).

Additional bacterial groups, which were noticeably abundant in the  $^{13}\text{CH}_4/\text{N}_2\text{O}/\text{PPHS}$  experimental treatment (Fig. 4.7B) belonged to the families *Alteromonadaceae* ( $\gamma$ -Proteobacteria), *Burkholderiaceae* and *Caulobacteraceae* from the  $\alpha$ -Proteobacteria, *Erysipelotrichaceae* and the Family XII from the Firmicutes, as well as *Sulfurovaceae* from the Epsilonbacteraeota phylum (formerly  $\epsilon$ -Proteobacteria).

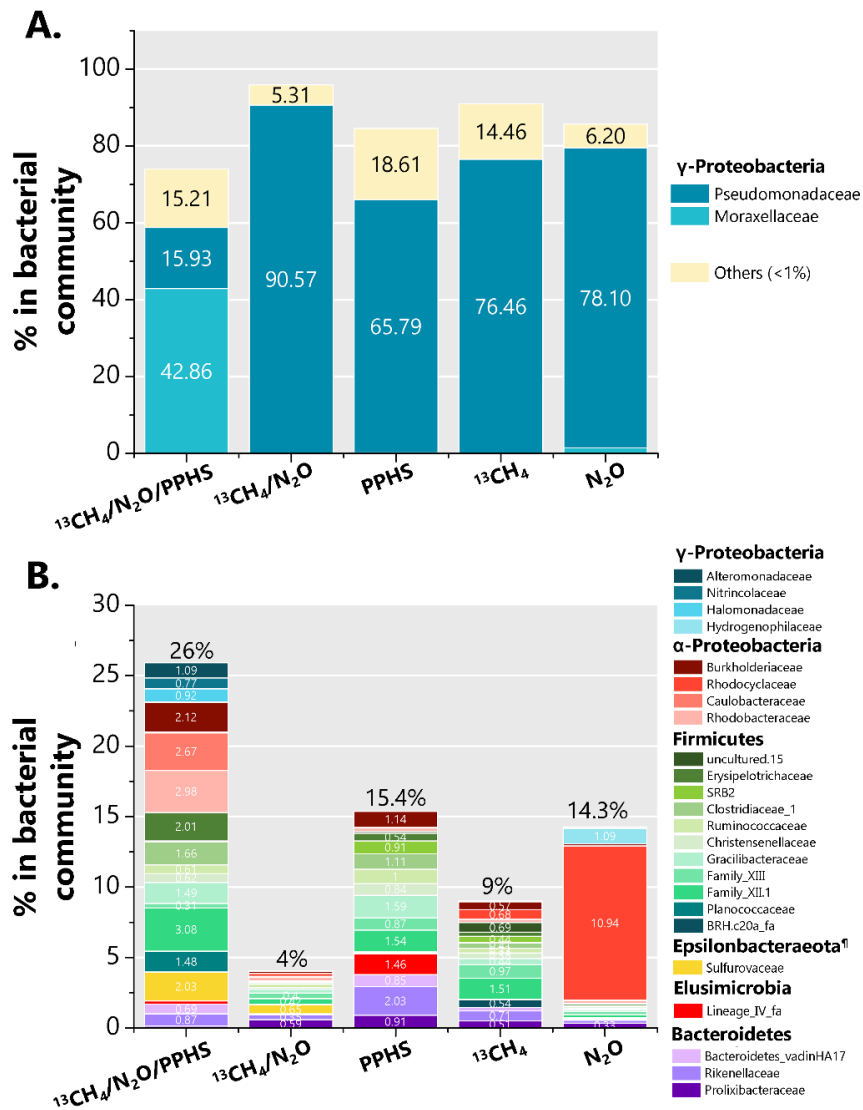
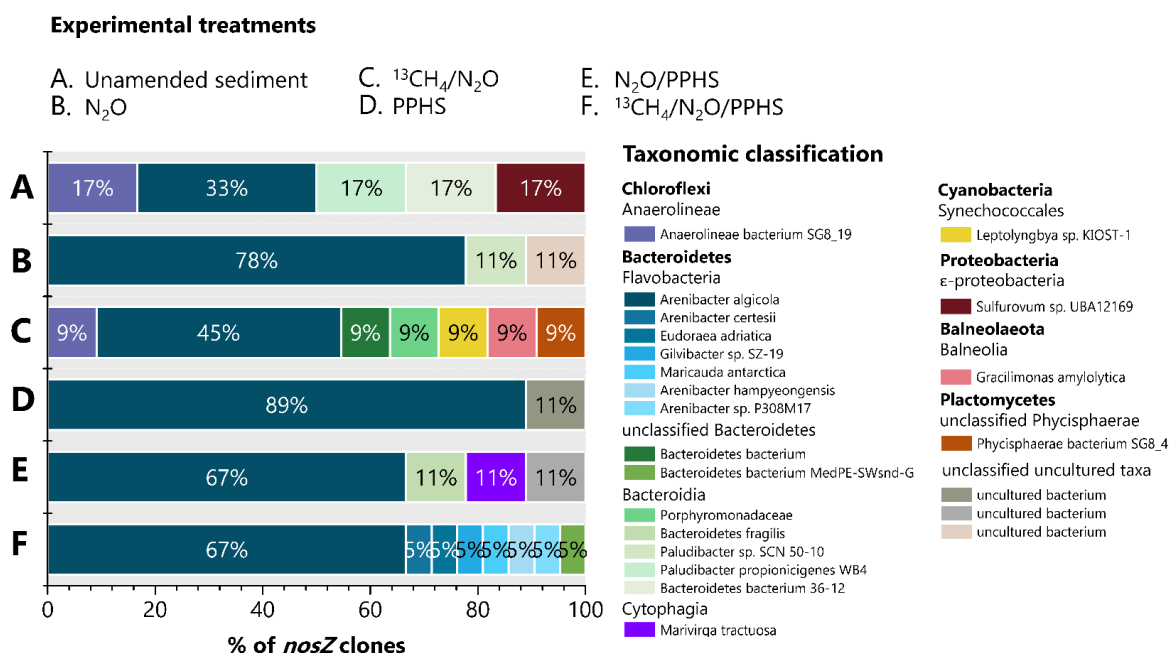


Fig. 4.7 | Composition of the bacterial communities found in selected experimental treatments at the end of the incubation period. Panel A displays those microbial taxa,

which predominated the bacterial communities at the family level (>40%) as well as the summarized fraction of all families which percentage in the whole bacterial community was lower than 1%. **Panel B** displays all bacterial families which percentage in the bacterial community was higher than 1%. All data represent the average from two or three (<sup>13</sup>CH<sub>4</sub>/N<sub>2</sub>O treatment) genomic libraries sequenced. Each library coming from an independent DNA sample extracted from one biological replicate. <sup>†</sup>The Epsilonbacteraeota were formerly known as the ε class of the Proteobacteria phylum.

Further analysis was performed by cloning of the *nosZ* gene, indicative of *nitrous oxide reductase* (**Fig. 4.8**), to identify potential N<sub>2</sub>O reducers involved in AOM linked to N<sub>2</sub>O reduction. Results revealed that *nosZ* genes were affiliated to Bacteroidetes and Proteobacteria (α & ε) phyla (also confirmed by the 16s rRNA library sequencing, **Fig. 4.7B**).



**Fig. 4.8 | *nosZ* gene diversity found by cloning at the end of the incubation period.**

Additionally, sequences belonging to members of Chloroflexi, Cyanobacteria, Balneolaeota, and the Planctomycetes phyla, as well as non-classified sequences belonging to *uncultured bacteria* were also identified. Among the categorized *nosZ* genes within Bacteroidetes, the most represented taxa were affiliated to *Arenibacter* phylotypes, mainly *A. algicola* (Fig. 4.8).

#### 4.3.2.4.2 Archaeal taxa

Sequencing of archaeal 16s rRNA genomic libraries displayed high percentages of two families of the Euryarchaeota phylum in the  $^{13}\text{CH}_4/\text{N}_2\text{O}/\text{PPHS}$  treatment with respect to the experimental controls (Fig. 4.9). *Methanocellaceae* and *Methanomicrobiaceae* families (99.2% and 94.3% dominated by the Rice Cluster I (RC-I) genera and an *uncultured* phylotype, respectively (Fig. 4.9B)) were highly abundant as compared to the experimental control conditions. In the case of *Methanocellaceae* family, its abundance was remarkably higher (12.7%) than that found in the controls (0.06 to 1.8%), while *Methanomicrobiaceae* family approximately doubled its proportion with respect to the controls (22.3% vs 7.3 to 12.4%, Fig. 4.9A). Furthermore, important members of the archaeal community in all treatments include the Bathyarchaeota phylum (~20%), Marine Benthic Group D and DHVEG family (6 – 27%) as previously reported for this wetland sediment<sup>20</sup>. Previously reported AOM-performing archaea were marginally detected in the archaeal communities of the wetland sediment. For instance, ANME-1 was only detected in the  $^{13}\text{CH}_4/\text{N}_2\text{O}/\text{PPHS}$  treatment in a 0.07% proportion of the archaeal community, while the abundance of ANME-3 ranged 0.05 to 0.11% in all experimental treatments. Moreover, *Candidatus Methanoperedens nitroreducens*, which has been related to AOM under denitrifying conditions<sup>41</sup> was not perceived.



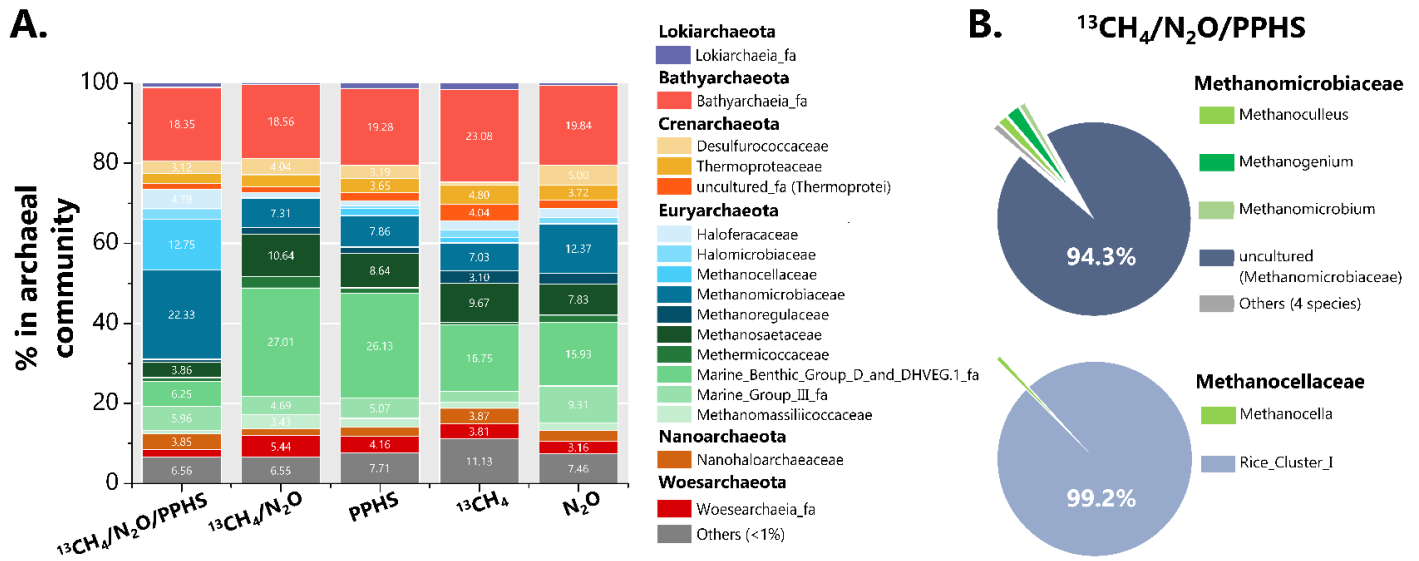


**Fig. 4.9 | Composition of the archaeal communities found in selected experimental treatments at the end of the incubation period. Panel A** shows the distribution of the whole bacterial sequences obtained through archaeal 16s ILLUMINA sequencing at family level amongst the experimental treatments. **Panel B** displays the analysis of Methanomicrobiaceae and Methanocellaceae in the  $^{13}\text{CH}_4/\text{N}_2\text{O}/\text{PPHS}$  treatment at the genera level. All data represent the average from two genomic libraries sequenced. Each library came from an independent DNA sample extracted from an experimental replicate.

## 4.4 Discussion

### 4.4.1 Redox active moieties in humus suppress the emission of GHGs from organotrophic environments

Microbial decomposition of NOM releases huge amounts of GHGs, such as CO<sub>2</sub> and CH<sub>4</sub>, from organic-rich environments. For instance, wetlands produce a third of the global methane emissions on Earth equivalent to ~164 Tg year<sup>-1</sup> <sup>42,43</sup>. Furthermore, incomplete denitrification coupled to the oxidation of this NOM also produces significant levels of N<sub>2</sub>O in nitrogen-rich ecosystems. Accumulation of these powerful GHGs is a serious threat since they are associated with global warming. Therefore, identification of processes governing the fluxes of GHGs in natural environments is of vital relevance.

Although biodegradation of the labile fraction of NOM produces large amounts of GHGs, there are several reports indicating that redox functional groups in NOM suppress the emission of methane in organotrophic environments <sup>20,44,45</sup>. Indeed, humus-reducing microorganisms out-compete methanogens for several organic substrates, thus decreasing the production of methane <sup>30</sup>. Moreover, methanogens, such as *Methanospirillum hungatie* and *Methanosarcina acetivorans*, are able to divert the electron flow from methanogenesis toward the reduction of HS during the oxidation of different substrates <sup>46,47</sup>. More recently, AOM linked to the reduction of HS has been reported in wetland sediments and it is estimated that this microbial process prevents the emission of 1300 Tg CH<sub>4</sub> year<sup>-1</sup> considering the global extension of wetlands<sup>20</sup>. Furthermore, electron shuttling mediated by HS fuels AOM coupled to ferric iron reduction, which concomitantly triggers carbon

sequestration as inert minerals (*calcite*, *aragonite* and *siderite*) produced during the process<sup>22</sup>.

The present study provides additional evidence of the important contribution of HS to suppress the emission of GHGs in wetland sediments. AOM linked to N<sub>2</sub>O reduction is a thermodynamically feasible reaction (see **Eq. 4.2**). Nevertheless, poor solubility of CH<sub>4</sub> and N<sub>2</sub>O in aquatic environments may be an important regulator of the process in natural ecosystems. In fact, the process was not detected in our incubations when no external HS were supplied. In contrast, PPHS-amended incubations showed parallel AOM and N<sub>2</sub>O reduction (Fig. 4.3 and 4.4) and electron balance confirmed the high correlation between both processes (Fig. 4.4). These results confirmed the theoretical feasibility for this process to occur in nature, which according to our calculations, is possible for the whole range of redox potentials ( $E^{\circ}$ ) proposed for HS (-300 to +300 mV, Eq. 1) <sup>48,49</sup>.

HS are more soluble than CH<sub>4</sub> and N<sub>2</sub>O and are plenty of redox functional groups, such as quinone moieties<sup>40,50</sup>. Therefore, it is expected that they may significantly contribute to link the C and N cycles by this mechanism. HS have previously been reported to link the C and N biogeochemical cycles by anaerobic ammonium oxidation coupled to microbial reduction of NOM in marine sediments <sup>51</sup>.

The current knowledge on anaerobic methanotrophic microorganisms that are able to link the C and the N cycles through AOM driven by oxidized N compounds, describes the mandatory utilization of NO<sub>3</sub><sup>-</sup> (by *Candidatus Methanoperedens nitroreducens*, an ANME-2d affiliated archaeon) or NO<sub>2</sub><sup>-</sup> (by *Candidatus Methyloirabilis oxyfera*, a bacterium) as TEA <sup>41,52</sup>. Nevertheless, there are no kinetic or genetic studies showing that these microbes could use N<sub>2</sub>O as TEA, either by themselves or by a syntrophic relationship with another microbial partner in order to oxidize CH<sub>4</sub>.

A previous study demonstrating the simultaneous consumption of CH<sub>4</sub> and N<sub>2</sub>O in an artificial wetland proved that this coupled process stimulated the activity of aerobic methanotrophs<sup>25</sup>. However, no parallel stimulation of *nosZ* enzymatic activity could be identified; consequently, the mechanisms for the coupling reaction remained unknown. In the present work, we provide several clues indicating that HS can mediate the coupling between the methanotrophs and N<sub>2</sub>O reducers, which would expand the metabolic capabilities of the microbial communities in wetland sediments (**Fig. 4.6**).

#### 4.4.2 Microbial communities potentially involved

The wide diversity of bacteria found at the end of the incubation period agreed with previous reports listing the highly taxonomical diversity of denitrifying and non-denitrifying N<sub>2</sub>O reducers found in several ecosystems<sup>53,54</sup>. Although the miscellaneous composition of known N<sub>2</sub>O reducers detected in the wetland sediment already showed the high potential of its microbial community to suppress N<sub>2</sub>O emissions, the presence of a  $\gamma$ -proteobacteria phylotype from the *Acinetobacter* genera stood out due to its high enrichment under the <sup>13</sup>CH<sub>4</sub>/N<sub>2</sub>O/PPHS conditions (**Fig. 4.7A**). Previous studies, have shown the involvement of *Acinetobacter* species in the N cycle due to their capacity to accomplish heterotrophic nitrification-aerobic denitrification<sup>55,56</sup>, whilst other species have been reported as heterotrophic and autotrophic denitrifiers<sup>57,58</sup>. Reports by Su and colleagues, (2015, 2016), showed how *Acinetobacter sp.* strain SZ28 was able to accomplish NO<sub>3</sub><sup>-</sup> and N<sub>2</sub>O reduction coupled to Mn<sup>2+</sup>, Fe<sup>2+</sup> and S<sup>2-</sup> oxidation<sup>59,60</sup>. These authors also documented the capacity of strain SZ28 to employ several organic compounds, including HS, as an energy source. Thus, based on the body of evidence demonstrating the respiratory and metabolic versatility of

*Acinetobacter* species, we hypothesize that some species of this microbial taxon could have been potentially involved in N<sub>2</sub>O reduction using reduced redox groups in PPHS<sub>red</sub> as electron donor. Nevertheless, we cannot dismiss the potential involvement of other N<sub>2</sub>O reducers in the process since the diversity of microbes possessing this feature is as wide as the diversity of humus-oxidizing microorganisms<sup>61,62</sup>; however, future research must be done in order to isolate and characterize the microorganisms conducting this process.

From the archaeal counterpart, only two taxa showed considerable increases within the microbial community in the complete treatment including <sup>13</sup>CH<sub>4</sub>/N<sub>2</sub>O/PPHS: an uncultured genus of the *Methanomicrobiaceae* family, and the RC-I genus from the *Methanocellaceae* (**Fig. 4.9A and B**). By using H<sub>2</sub>, formate, and CO<sub>2</sub> as substrates for methanogenesis<sup>63</sup>, the RC-I cluster has been proposed as the most important archaea controlling CH<sub>4</sub> emissions from paddy soils<sup>64,65</sup>. Despite this, no methanogenic activity was detected in our incubations under any of the experimental conditions tested. Archaeal members of the RC-I cluster have previously been detected in wetland and marsh ecosystems<sup>66,67</sup>, as well as in rice paddies. These organotrophic systems contain high amounts of endlessly decomposing NOM, which prevail under anoxic conditions due to flooding, thus creating the proper niche for microbes to perform the redox reactions involved in HS supporting AOM coupled to N<sub>2</sub>O reduction (**Fig. 4.6**). Although to the best of our knowledge, the RC-I archaeal group has not been reported to perform either AOM or humus-reducing activities, Bao and colleagues (2016) showed how NO<sub>3</sub><sup>-</sup> addition promoted a positive response in RC-I archaea in terms of the expression of the *mcrA* gene (indicative of methanogenesis and/or methanotrophy)<sup>68</sup>. This effect was also linked to diminished CH<sub>4</sub> production and given the evidence provided in the present study, a possible connection involving the RC-I type of archaea between denitrification and methanotrophy must be addressed in future studies.

Regarding the uncultured *Methanomicrobiaceae* phylotype, which comprised ~20% of the total archaeal community, in addition to the numerous reports on its role as CH<sub>4</sub> producer<sup>69</sup>, a recent study showed that the *Methanobacterium* genera, which also belongs to the *Methanomicrobiaceae* family, drove AOM coupled to ferrihydrite reduction with HS as electron shuttle<sup>21</sup>. These authors demonstrated how this microorganism oxidized CH<sub>4</sub> to propionate and proposed that this intermediate was then taken by a bacterial partner (potentially a *Desulfovibrio* species) to produce siderite (a ferrous iron carbonate). Previous reports have described the syntrophic activity of anaerobic methanotrophic archaea in partnership with bacteria to reduce TEAs, such as SO<sub>4</sub><sup>2-</sup><sup>70</sup>. Here, we propose a novel syntrophic process mediated by HS in which the RC-I cluster and/or an uncultured member of the *Methanomicrobiaceae* family could have coupled metabolic capabilities with a bacterial member, such as *Acinetobacter*, to perform AOM linked to N<sub>2</sub>O reduction via an EET mechanism mediated by HS (**Fig. 4.6**).

## 4.5 Conclusions

The present study showed several lines of evidence indicating that HS mediate an EET process in which AOM is linked to N<sub>2</sub>O reduction in coastal wetland sediments. These results further emphasize the relevant role that HS could play to prevent the emission of GHGs from organotrophic environments and provide insights into the potential of their redox active groups as a metabolic linking agent for connecting the C and N cycles.

## 4.6 References

1. **Gerald A. Meehl**; Claudia Tebaldi. More Intense, More Frequent, and Longer Lasting Heat Waves in the 21st Century. *Science* (80-. ). **2004**, 305 (5686), 994–997.
2. **Hansen, J.**; Sato, M.; Ruedy, R. Radiative forcing and climate response. *J. Geophys. Res. Atmos.* **1997**, 102 (D6), 6831–6864.
3. **Crowley, T. J.** Causes of climate change over the past 1000 years. *Science* (80-. ). **2000**, 289 (5477), 270–277.
4. **Bousquet, P.**; Ciais, P.; Miller, J. B.; Dlugokencky, E. J.; Hauglustaine, D. A.; Prigent, C.; Van Der Werf, G. R.; Peylin, P.; Brunke, E. G.; Carouge, C.; et al. Contribution of anthropogenic and natural sources to atmospheric methane variability. *Nature* **2006**, 443 (7110), 439–443.
5. **EPA.** Methane and nitrous oxide emissions from natural sources, United States Environmental Protection Agency (EPA) Report. United States Environ. Prot. Agency **2010**, No. April, 1–194.
6. **Comyn-Platt, E.**; Hayman, G.; Huntingford, C.; Chadburn, S. E.; Burke, E. J.; Harper, A. B.; Collins, W. J.; Webber, C. P.; Powell, T.; Cox, P. M.; et al. Carbon budgets for 1.5 and 2 °C targets lowered by natural wetland and permafrost feedbacks. *Nat. Geosci.* **2018**, 1–6.
7. **Kirschke, S.**; Bousquet, P.; Ciais, P.; Saunois, M.; Canadell, J. G.; Dlugokencky, E. J.; Bergamaschi, P.; Bergmann, D.; Blake, D. R.; Bruhwiler, L.; et al. Three decades of global methane sources and sinks. *Nat. Geosci.* **2013**, 6 (10), 813–823.
8. **Singh, B. K.**; Bardgett, R. D.; Smith, P.; Reay, D. S. Microorganisms and climate change: Terrestrial feedbacks and mitigation options. *Nat. Rev. Microbiol.* **2010**, 8 (11), 779–790.
9. **Laruelle, G. G.**; Lauerwald, R.; Pfeil, B.; Regnier, P. Global Biogeochemical Cycles. *Global Biogeochem. Cycles* **2014**, 1199–1214.
10. **Gougoulias, C.**; Clark, J. M.; Shaw, L. J. The role of soil microbes in the global carbon cycle: Tracking the below-ground microbial processing of plant-derived carbon for manipulating carbon dynamics in agricultural systems. *J. Sci.*

*Food Agric.* **2014**, 94 (12), 2362–2371.

**11. Lever, M. A.** A New Era of Methanogenesis *Research. Trends Microbiol.* **2016**, 24 (2), 84–86.

**12. Philippot, L.;** Hallin, S.; Schloter, M. Ecology of Denitrifying Prokaryotes in Agricultural Soil. *Adv. Agron.* **2007**, 96 (07), 249–305.

**13. U.S. EPA.** Methane and Nitrous Oxide Emissions From Natural Sources. United States Environmental Protection Agency. 2010, p 194.

**14. Meinshausen, M.;** Smith, S. J.; Calvin, K.; Daniel, J. S.; Kainuma, M. L. T.; Lamarque, J.; Matsumoto, K.; Montzka, S. A.; Raper, S. C. B.; Riahi, K.; et al. The RCP greenhouse gas concentrations and their extensions from 1765 to 2300. *Clim. Change* **2011**, 109 (1), 213–241.

**15. Bhattarai, S.;** Cassarini, C.; Lens, P. N. L. Physiology and Distribution of Archaeal Methanotrophs That Couple Anaerobic Oxidation of Methane with Sulfate. *Microbiol. Mol. Biol. Reviews*, **2019**, No. July, 1–31.

**16. Welte, C. U.;** Rasigraf, O.; Vaksmaa, A.; Versantvoort, W.; Arshad, A.; Op den Camp, H. J. M.; Jetten, M.

S. M.; Lüke, C.; Reimann, J. Nitrate- and nitrite-dependent anaerobic oxidation of methane. *Environ. Microbiol. Rep.* **2016**, 00, 1–15.

**17. He, Z.;** Zhang, Q.; Feng, Y.; Luo, H.; Pan, X.; Michael, G. Microbiological and environmental significance of metal-dependent anaerobic oxidation of methane. *Sci. Total Environ.* **2018**, 610–611, 759–768.

**18. Lehmann, J.;** Kleber, M. The contentious nature of soil organic matter. *Nature* **2015**, 528 (7580), 60–68.

**19. Scheller, S.;** Yu, H.; Chadwick, G. L.; McGlynn, S. E.; Orphan, V. J. Artificial electron acceptors decouple archaeal methane oxidation from sulfate reduction. *Science* (80-. ). **2016**, 351 (6274), 703–707.

**20. Valenzuela, E. I.;** Prieto-Davó, A.; López-Lozano, N. E.; Hernández-Eligio, A.; Vega-Alvarado, L.; Juárez, K.; García-González, A. S.; López, M. G.; Cervantes, F. J. Anaerobic Methane Oxidation Driven by Microbial Reduction of Natural Organic Matter in a Tropical Wetland. *Appl. Environ. Microbiol.* **2017**, 83 (11), AEM.00645-17.

**21. Bai, Y.-N.;** Wang, X.-N.; Wu, J.; Lu,



- Y.-Z.; Fu, L.; Zhang, F.; Lau, T.-C.; Zeng, R. J. Humic substances as electron acceptors for anaerobic oxidation of methane driven by ANME-2d. *Water Res.* **2019**, 164, 114935.
- 22. Valenzuela, E. I.**; Avendaño, K. A.; Balagurusamy, N.; Arriaga, S.; Nieto-Delgado, C.; Thalasso, F.; Cervantes, F. J. Electron shuttling mediated by humic substances fuels anaerobic methane oxidation and carbon burial in wetland sediments. *Sci. Total Environ.* **2019**, 650, 2674–2684.
- 23. He, Q.**; Yu, L.; Li, J.; He, D.; Cai, X.; Zhou, S. Electron shuttles enhance anaerobic oxidation of methane coupled to iron(III) reduction. *Sci. Total Environ.* **2019**, 688, 664–672.
- 24. Hallin, S.**; Philippot, L.; Sanford, R. A.; Jones, C. M. Genomics and Ecology of Novel N<sub>2</sub>O-Reducing Microorganisms. *Trends Microbiol.* **2017**, xx (August), 1–13.
- 25. Cheng, C.**; Shen, X.; Xie, H.; Hu, Z.; Pavlostathis, S. G.; Zhang, J. Coupled methane and nitrous oxide biotransformation in freshwater wetland sediment microcosms. *Sci. Total Environ.* **2019**, 648, 916–922.
- 26. Aranda-Tamaura, C.**; Estrada-Alvarado, M. I.; Texier, A. C.; Cuervo, F.; Gómez, J.; Cervantes, F. J. Effects of different quinoid redox mediators on the removal of sulphide and nitrate via denitrification. *Chemosphere* **2007**, 69 (11), 1722–1727.
- 27. van Trump Ian J., I. J.**; Wrighton, K. C.; Thrash, J. C.; Weber, K. A.; Andersen, G. L.; Coates, J. D. Humic acid-oxidizing, nitrate-reducing bacteria in agricultural soils. *MBio* **2011**, 2 (4), 1–9.
- 28. Liu, F.**; Rotaru, A. E.; Shrestha, P. M.; Malvankar, N. S.; Nevin, K. P.; Lovley, D. R. Promoting direct interspecies electron transfer with activated carbon. *Energy Environ. Sci.* **2012**, 5 (10), 8982–8989.
- 29. Lovley, D. R.** Happy together: microbial communities that hook up to swap electrons. *ISME J.* **2016**, 1–10.
- 30. Cervantes, F. J.**; Velde, S.; Lettinga, G.; Field, J. a. Competition between methanogenesis and quinone respiration for ecologically important substrates in anaerobic consortia. *FEMS Microbiol. Ecol.* **2000**, 34 (2), 161–171.
- 31. Lovley, D. R.**; Coates, J. D.; Blunt-Harris, E. L.; Phillips, E. J. P.; Woodward, J. C. Humic substances as

- electron acceptors for microbial respiration. *Nature*. **1996**, pp 445–448.
- 32. Cord-Ruwisch, R.** A quick method for the determination of dissolved and precipitated sulfides in cultures of sulfate-reducing bacteria. *J. Microbiol. Methods* **1985**, 4 (1), 33–36.
- 33. Soga, T.;** Ross, G. A. Simultaneous determination of inorganic anions, organic acids and metal cations by capillary electrophoresis. *J. Chromatogr. A* **1999**, 834 (1–2), 65–71.
- 34. APHA/AWWA/WEF.** Standard Methods for the Examination of Water and Wastewater; **2012**.
- 35. Rios-Del Toro, E. E.;** Valenzuela, E. I.; López-Lozano, N. E.; Cortés-Martínez, M. G.; Sánchez-Rodríguez, M. A.; Calvario-Martínez, O.; Sánchez-Carrillo, S.; Cervantes, F. J. Anaerobic ammonium oxidation linked to sulfate and ferric iron reduction fuels nitrogen loss in marine sediments. *Biodegradation*. **2018**.
- 36. Stookey, L. L.** Ferrozine---a new spectrophotometric reagent for iron. *Anal. Chem.* **1970**, 42 (7), 779–781.
- 37. Birnboim, H. C.** A Rapid Alkaline Extraction Method for the Isolation of Plasmid DNA. *Methods Enzymol.* **1983**.
- 38. Gantner, S.;** Andersson, A. F.; Alonso-Sáez, L.; Bertilsson, S. Novel primers for 16S rRNA-based archaeal community analyses in environmental samples. *J. Microbiol. Methods* **2011**, 84 (1), 12–18.
- 39. Kozich, J. J.;** Westcott, S. L.; Baxter, N. T.; Highlander, S. K.; Schloss, P. D. Development of a dual-index sequencing strategy and curation pipeline for analyzing amplicon sequence data on the miseq illumina sequencing platform. *Appl. Environ. Microbiol.* **2013**.
- 40. Scott, D. T.;** Mcknight, D. M.; Blunt-Harris, E. L.; Kolesar, S. E.; Lovley, D. R. Quinone moieties act as electron acceptors in the reduction of humic substances by humics-reducing microorganisms. *Environ. Sci. Technol.* **1998**, 32 (19), 2984–2989.
- 41. Haroon, M. F.;** Hu, S.; Shi, Y.; Imelfort, M.; Keller, J.; Hugenholtz, P.; Yuan, Z.; Tyson, G. W. Anaerobic oxidation of methane coupled to nitrate reduction in a novel archaeal lineage. *Nature* **2013**, 500 (7464), 567–570.
- 42. Saunois, M.;** Bousquet, P.; Poulter, B.; Peregon, A.; Ciais, P.; Canadell, J. G.; Dlugokencky, E. J.; Etiope, G.;

- Bastviken, D.; Houweling, S.; et al. The global methane budget 2000-2012. *Earth Syst. Sci. Data* **2016**, 8 (2), 697–751.
- 43. Bridgham, S. D.**; Cadillo-Quiroz, H.; Keller, J. K.; Zhuang, Q. Methane emissions from wetlands: biogeochemical, microbial, and modeling perspectives from local to global scales. *Glob. Chang. Biol.* **2013**, 19 (5), 1325–1346.
- 44. Keller, J. K.**; Weisenhorn, P. B.; Megonigal, J. P. Humic acids as electron acceptors in wetland decomposition. *Soil Biol. Biochem.* **2009**, 41 (7), 1518–1522.
- 45. Keller, J. K.** & Medvedeff, C.; A. Soil organic matter. In *Wetland soils: genesis, hydrology, landscapes, and classifications*; Taylor and Francis Group, **2016**; Vol. 3, pp 165–188.
- 46. Cervantes, F. J.**; De Bok, F. A. M.; Duong-Dac, T.; Stams, A. J. M.; Lettinga, G.; Field, J. A. Reduction of humic substances by halorespiring, sulphate-reducing and methanogenic microorganisms. *Environ. Microbiol.* **2002**, 4 (1), 51–57.
- 47. Holmes, D. E.**; Ueki, T.; Tang, H.; Zhou, J.; Smith, J. A.; Chaput, G.; Lovley, D. R. A Membrane-Bound Cytochrome Enables Methanosarcina acetivorans To Conserve Energy from Extracellular Electron Transfer. *MBio* **2019**, 10 (4), e00789-19.
- 48. Aeschbacher, M.**; Sander, M.; Schwarzenbach, R. P. Novel electrochemical approach to assess the redox properties of humic substances. *Environ. Sci. Technol.* **2010**, 44 (1), 87–93.
- 49. Straub, K. L.**; Benz, M.; Schink, B. Iron metabolism in anoxic environments at near neutral pH. *FEMS Microbiol. Ecol.* **2000**, 34 (3), 181–186.
- 50. Hernández-Montoya, V.**; Alvarez, L. H.; Montes-Morán, M. a.; Cervantes, F. J. Reduction of quinone and non-quinone redox functional groups in different humic acid samples by *Geobacter sulfurreducens*. *Geoderma* **2012**, 183–184, 25–31.
- 51. Rios-Del Toro, E. E.**; Valenzuela, E. I.; Ramírez, J. E.; López-Lozano, N. E.; Cervantes, F. J. Anaerobic Ammonium Oxidation Linked to Microbial Reduction of Natural Organic Matter in Marine Sediments. *Environ. Sci. Technol. Lett.* **2018**, acs.estlett.8b00330.
- 52. Ettwig, K. F.**; Butler, M. K.; Le

- Paslier, D.; Pelletier, E.; Mangenot, S.; Kuypers, M. M. M.; Schreiber, F.; Dutilh, B. E.; Zedelius, J.; de Beer, D.; et al. Nitrite-driven anaerobic methane oxidation by oxygenic bacteria. *Nature* **2010**, 464 (7288), 543–548.
- 53. Hallin, S.;** Philippot, L.; Löffler, F. E.; Sanford, R. A.; Jones, C. M. Genomics and Ecology of Novel N<sub>2</sub>O-Reducing Microorganisms. *Trends Microbiol.* **2018**, 26 (1), 43–55.
- 54. Conthe, M.;** Wittorf, L.; Kuenen, J. G.; Kleerebezem, R.; Van Loosdrecht, M. C. M.; Hallin, S. Life on N<sub>2</sub>O: Deciphering the ecophysiology of N<sub>2</sub>O respiring bacterial communities in a continuous culture. *ISME J.* **2018**, 12 (4), 1142–1153.
- 55. Wen, G.;** Wang, T.; Li, K.; Wang, H.; Wang, J.; Huang, T. Aerobic denitrification performance of strain *Acinetobacter johnsonii* WGX-9 using different natural organic matter as carbon source: Effect of molecular weight. *Water Res.* **2019**, 164, 114956.
- 56. Chen, S.;** He, S.; Wu, C.; Du, D. Characteristics of heterotrophic nitrification and aerobic denitrification bacterium *Acinetobacter* sp. T1 and its application for pig farm wastewater treatment. *J. Biosci. Bioeng.* **2019**, 127 (2), 201–205.
- 57. Pishgar, R.;** Dominic, J. A.; Sheng, Z.; Tay, J. H. Denitrification performance and microbial versatility in response to different selection pressures. *Bioresour. Technol.* **2019**, 281 (December 2018), 72–83.
- 58. Lee, D. J.;** Pan, X.; Wang, A.; Ho, K. L. Facultative autotrophic denitrifiers in denitrifying sulfide removal granules. *Bioresour. Technol.* **2013**, 132, 356–360.
- 59. Su, J. F.;** Zheng, S. C.; Huang, T. lin; Ma, F.; Shao, S. C.; Yang, S. F.; Zhang, L. na. Characterization of the anaerobic denitrification bacterium *Acinetobacter* sp. SZ28 and its application for groundwater treatment. *Bioresour. Technol.* **2015**, 192, 654–659.
- 60. Su, J. F.;** Zheng, S. C.; Huang, T. L.; Ma, F.; Shao, S. C.; Yang, S. F.; Zhang, L. N. Simultaneous Removal of Mn(II) and Nitrate by the Manganese-Oxidizing Bacterium *Acinetobacter* sp. SZ28 in Anaerobic Conditions. *Geomicrobiol. J.* **2016**, 33 (7), 586–591.
- 61. Martinez, C. M.;** Alvarez, L. H.;

- Celis, L. B.; Cervantes, F. J. Humus-reducing microorganisms and their valuable contribution in environmental processes. *Appl. Microbiol. Biotechnol.* **2013**, 97 (24), 10293–10308.
- 62. Lovley, D. R.;** Fraga, J. L.; Coates, J. D.; Blunt-Harris, E. L. Humics as an electron donor for anaerobic respiration. *Environ. Microbiol.* **1999**, 1 (1), 89–98.
- 63. Hunger, S.;** Schmidt, O.; Hilgarth, M.; Horn, M. A.; Kolb, S.; Conrad, R.; Drake, H. L. Competing formate- and carbon dioxide-utilizing prokaryotes in an anoxic methane-emitting fen soil. *Appl. Environ. Microbiol.* **2011**, 77 (11), 3773–3785.
- 64. Großkopf, R.;** Stubner, S.; Liesack, W. Novel euryarchaeotal lineages detected on rice roots and in the anoxic bulk soil of flooded rice microcosms. *Appl. Environ. Microbiol.* **1998**, 64 (12), 4983–4989.
- 65. Erkel, C.;** Kube, M.; Reinhardt, R.; Liesack, W. *Science*. **2004**, 1482 (1997), 2004–2007.
- 66. Xiao, L.;** Xie, B.; Liu, J.; Zhang, H.; Han, G.; Wang, O.; Liu, F. Stimulation of long-term ammonium nitrogen deposition on methanogenesis by Methanocellaceae in a coastal wetland. *Sci. Total Environ.* **2017**, 595, 337–343.
- 67. Lin, Y.;** Liu, D.; Yuan, J.; Ye, G.; Ding, W. Methanogenic community was stable in two contrasting freshwater marshes exposed to elevated atmospheric CO<sub>2</sub>. *Front. Microbiol.* **2017**, 8 (MAY), 1–12.
- 68. Bao, Q.;** Huang, Y.; Wang, F.; Nie, S.; Nicol, G. W.; Yao, H.; Ding, L. Effect of nitrogen fertilizer and/or rice straw amendment on methanogenic archaeal communities and methane production from a rice paddy soil. *Appl. Microbiol. Biotechnol.* **2016**, 100 (13), 5989–5998.
- 69. Kröber, M.;** Bekel, T.; Diaz, N. N.; Goesmann, A.; Jaenicke, S.; Krause, L.; Miller, D.; Runte, K. J.; Viehöver, P.; Pühler, A.; et al. Phylogenetic characterization of a biogas plant microbial community integrating clone library 16S-rDNA sequences and metagenome sequence data obtained by 454-pyrosequencing. *J. Biotechnol.* **2009**, 142 (1), 38–49.
- 70. Boetius, A.;** Ravensschlag, K.; Schubert, C. J.; Rickert, D.; Widdel, F.; Gieseke, A.; Amann, R.; Jørgensen, B. B.; Witte, U.; Pfannkuche, O. A marine

## CHAPTER IV

microbial consortium apparently methane. *Nature* **2000**, 407 (6804),  
mediating anaerobic oxidation of 623–626.

## CHAPTER V

# Assessing the Effect of Sulfur/Organic Matter Interactions in the Methane Dynamics of a Coastal Wetland Sediment

### HIGHLIGHTS:

- **S cycling** by oxidized humic substances produced **elemental sulfur, thiosulfate** and **S incorporation to organic matter**.
- Sulfate and humus addition to wetland sediment **suppressed methanogenesis**.
- **Humus-driven AOM** was the predominant mechanism for CH<sub>4</sub> oxidation.
- **AOM was inhibited by sulfide** as a competing electron donor.

### Manuscript in preparation:

**Valenzuela, E. I.**, Kappler A., Cervantes, F. J. *Assessing the effect of Sulfur/Organic Matter interactions in the CH<sub>4</sub> dynamics of a coastal wetland sediment*. (in preparation).

## Abstract

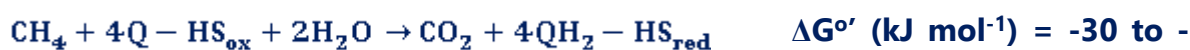
Organic matter decomposition at natural ecosystems, leads to the formation of one of the most important redox-active molecules in organotrophic environments, the complex, yet versatile, *humic substances* (HS). By participating in microbial reactions, this redox-moieties rich class of material, link biogeochemical cycles by serving as electron sink, source, or shuttle for ecologically relevant processes. It has been suggested that on their oxidized state, HS could receive electrons from reduced sulfur (S) species (e.g. sulfide) provoking a cryptic S cycle, which would provide additional oxidized S compounds that would suppress methanogenesis and/or provide intermediates, which could stimulate the *anaerobic oxidation of methane* (AOM). In this work, by performing wetland sediment incubations, we demonstrate that while methanogenesis suppression occurred due to the extended electron-accepting capacity provided by sulfate, AOM was preferentially driven by humus-reducing microbes. Furthermore, this humus-dependent methanotrophy was negatively affected by sulfate reduction due to the chemical reduction of HS redox moieties and the incorporation of S into the organic humic structure. Altogether, our results provide new clues into the intricate processes linking C and S cycles in organic-rich environments, which can have important implications on the net emissions of the important greenhouse gases, CH<sub>4</sub> and CO<sub>2</sub>.



## 5.1 Introduction

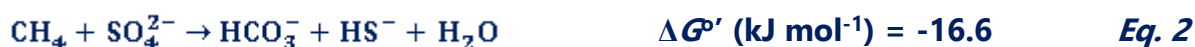
In aquatic and terrestrial ecosystems, the redox-active fraction of the incessantly decomposing *natural organic matter* (NOM), traditionally known as *humus* or *humic substances* (HS), takes part of several natural transformations by driving numerous redox processes<sup>1,2</sup>. These chemical and biological reactions are inherently located within several biogeochemical cycles, thus they play critical roles regulating matter and energy fluxes on natural environments<sup>3,4</sup>. The electron transferring moieties in NOM, mainly comprised by quinones<sup>5</sup>, can fuel the oxidation of many reduced organic and inorganic compounds by functioning as the terminal electron acceptor (TEA) in the *humus-reducing microorganisms'* (HRM) respiratory chain<sup>5-7</sup>. By employing such respiratory way, several mechanisms conducted by HRM can prevent the emission of important greenhouse gases, such as methane (CH<sub>4</sub>). Cervantes and colleagues (2000), observed the prevention of methanogenesis when quinones reduction became the preferred pathway for anaerobic decomposition, suggesting that HRM outcompeted methanogens over common substrates<sup>8</sup>. Subsequent studies also proved how methanogenesis was reduced due to the greater thermodynamic feasibility of HS reduction over that of methanogenesis<sup>9</sup>. Subsequently, Keller and colleagues (2009), validated how *humic acids* (a fraction of HS) served as TEA for organic matter decomposition in wetland sediments, which led to CO<sub>2</sub>:CH<sub>4</sub> production ratios greater than the commonly expected value of one<sup>10</sup>; discovery that was then supported by additional evidence obtained by Blodau and Deppe (2012)<sup>11</sup>. Abiotically, HS can also contribute to CO<sub>2</sub>:CH<sub>4</sub> ratios higher than 1 by promoting the cycling of alternative TEAs, such as sulfur compounds via a HS supported sulfide oxidation. Such recycling would further sustain biological S reducing mechanisms, such as sulfate or thiosulfate reducing activity, which could outcompete methanogenesis due to the more

favorable thermodynamics<sup>12,13</sup>. More recently, supplementary mechanisms by which HRM can suppress CH<sub>4</sub> emission have been discovered after years of remaining elusive and involve HS serving as the TEA for *anaerobic methane oxidation* (AOM)<sup>14,15</sup> or as electron shuttle for the dissimilatory reduction of oxidized iron minerals<sup>16,17</sup>. Such processes, firstly hypothesized by Blodau and Deppe (2012), consist of the microbial uptake of CH<sub>4</sub> as electron donor while HS are microbially reduced, and it is possible due to the wide range of redox potential that HS present (+300 to -300 mV)<sup>18,19</sup>, as well as to the great respiratory versatility that anaerobic methanotrophic microorganisms display (**Eq. 1**)<sup>20</sup>.



#### 416.5 Eq. 1

Considering that NOM can co-exist with other electron acceptors in most environments, there is little information describing how competing processes, such as sulfate (SO<sub>4</sub><sup>2-</sup>) and HS/NOM-reduction could affect CH<sub>4</sub> cycling in natural settings. Sulfate dependent AOM (SR-AOM, **Eq. 2**) is the most common anaerobic process depleting CH<sub>4</sub> in marine environments and it has also been detected in some freshwater settings<sup>14,21,22</sup>.



However, it is not clear if the presence of NOM could boost SR-AOM by triggering a cryptic cycling of S, which is highly possible as it has already been demonstrated to happen when iron oxides are present<sup>23</sup>, and considering that in the same way oxidized HS can lead to the production of oxidized S cycle intermediates, for instance thiosulfate,<sup>12,24,25</sup> which has been demonstrated to be suitable for microorganisms to perform AOM (**Eq. 3**)<sup>26</sup>. Thus, in this work we aimed to elucidate the possibility of a cryptic S cycle elicited by a HS and the effect on the

methanogenic and methanotrophic activities by using sediments from a coastal wetland, which microbiota has been proven to perform AOM employing several TEAs (*Sisal*/wetland, Yucatan Peninsula, southeastern Mexico)<sup>14</sup>.

## 5.2 Materials and Methods

### 5.2.1 Chemical assay

#### 5.2.1.1 Microcosms set-up

*Pahokee Peat* HS (PPHS, catalogue number from International Humic Substances Society: 1S103H) were dissolved overnight by magnetic stirring in the same basal medium employed to perform the biological experiments, the medium composition has been previously described elsewhere<sup>14</sup>. Three final different concentrations were employed: 50, 200 and 500 mg L<sup>-1</sup>. Basal medium without added PPHS was also prepared to use as control. All media were then flushed with N<sub>2</sub> for 1 hour to get rid of any dissolved oxygen, anoxically closed, and then introduced into a glove-box (100% N<sub>2</sub> atmosphere) to anoxically dispense 75 mL of each solution in 110 mL serum flasks. After all flasks were sealed with rubber stoppers and aluminum rings, they were taken out of the glove-box, their atmosphere was replaced by a mixture of N<sub>2</sub>:CO<sub>2</sub> (90/10%) during 10 min, and then bicarbonate was provided as buffer from a concentrated anoxic stock to a final concentration of 60 mM (final pH = 7.5). Sulfide was provided to the correspondent treatments from a concentrated anoxic stock to reach a final concentration of 2 mM. Dissolved sulfide concentration after equilibrium with the microcosm's headspace was ~1.3 mM, which agreed with the initial almost neutral pH. The experimental design was as follows: 50 mg<sub>PPHS</sub> L<sup>-1</sup> + sulfide, 200 mg<sub>PPHS</sub> L<sup>-1</sup> + sulfide, 500 mg<sub>PPHS</sub> L<sup>-1</sup> + sulfide, 500 mg PPHS L<sup>-1</sup> (without sulfide), and sulfide (without PPHS). All experimental treatments were carried out with six replicates,

wrapped in aluminum foil to avoid photoreactions, and incubated at 28°C in an oven located on the inside of a glove-box.

### 5.2.1.2 Microcosms sampling

Based on preliminary assays, the time between each sampling point was determined to be 2 hours. On each sampling point, aliquots to determine sulfide, thiosulfate, elemental sulfur and the electron shuttling capacity of PPHS, were taken with disposable syringes. All sampling was performed inside of a glove-box.

#### 5.2.1.2.1 Sulfide

Samples for dissolved sulfide determinations (100 µL) were fixed on acid 2% Zn-acetate according to the protocol described by Cline<sup>27</sup>. Fixed samples were collected during the experiment running time and preserved at 4°C until measurement.

#### 5.2.1.2.2 Sulfate and Thiosulfate

1 mL samples were taken and placed on Eppendorf tubes. Afterwards, 75 µL of concentrated Zn-acetate (200 g L<sup>-1</sup>) were used to precipitate the remaining dissolved sulfide and avoid additional formation of sulfur products coming from further oxidation not associated with the electron-accepting capacity of PPHS. Under these conditions, after reaction with Zn-acetate, all remaining sulfide would precipitate as *smithsonite*, *sphalerite*, Zn<sub>3</sub>(PO<sub>4</sub>)<sub>2</sub>·4H<sub>2</sub>O (s). After reaction, the tubes were centrifuged at 10000 RPM x 10 min, the supernatant was taken from the tubes and preserved frozen until analysis.

#### 5.2.1.2.3 Zero-valent (elemental) Sulfur

2 mL samples were taken and immediately fixed with 75 µL of Zn-acetate (200 g L<sup>-1</sup>). The samples were readily frozen and preserved at -20°C until filtration

with polytetrafluoroethylene membrane filters and extraction with methanol prior to analysis.

#### **5.2.1.2.4 Electron Shuttling Capacity of PPHS**

2 mL samples were taken and injected into anoxic glass vials sealed with rubber stoppers and aluminum rings containing 70  $\mu\text{L}$  of Zn-acetate ( $200 \text{ g L}^{-1}$ ). As previously mentioned, precipitation of sulfide with Zn would avoid further reaction of dissolved sulfide with PPHS while the redox-state of PPHS achieved during the incubation time would be preserved to be quantified afterwards by reaction with ferric citrate<sup>7,14</sup>.

#### **5.2.1.3 Assessing of Anaerobic Oxidation of Methane**

Serological flasks (110 mL) were inoculated with 2  $\text{cm}^3$  of homogenized sediment inside a glove-box. The wetland sediment employed was sampled from *Sisal* wetland, located in the Yucatán Peninsula, south-eastern Mexico on April 2018. 80 mL of the same basal medium employed in the chemical tests previously described. Up to this point, no extrinsic electron donors or acceptors were added to the experiments. The bottles were tight-sealed with rubber stoppers and aluminum rings. Once outside the glove-box the microcosms headspace was replaced by  $\text{N}_2:\text{CO}_2$  and bicarbonate was provided as buffer in the same fashion previously described. The bottles were then stored in the dark at  $28^\circ\text{C}$  for the next 15 days as a pre-incubation cycle.

After the pre-incubation cycle, bottles were open on the inside of the glove-box, and the basal medium was replaced by fresh anoxic PPHS enriched medium ( $500 \text{ mg L}^{-1}$ ) or by medium lacking HS to run in parallel as controls. Once outside the glove-box, the headspace was replaced by  $\text{N}_2:\text{CO}_2$ ; afterwards, the headspace pressure was equilibrated with the atmosphere and then 20 mL of pure  $\text{CH}_4$  was injected to the flask's headspace. Flasks were incubated over night at room

temperature to let the gas reach equilibrium with the liquid phase, and the next morning, initial CH<sub>4</sub> measurements were performed. Sterile controls including PPHS were made by autoclaving three times. The final experimental set-up was as follows: PPHS + sulfate + CH<sub>4</sub> (*complete treatment*), PPHS + CH<sub>4</sub> (*humus reducing conditions*), sulfate + CH<sub>4</sub> (*sulfate reducing conditions*), only CH<sub>4</sub> (control), PPHS + sulfate (*endogenous control*), PPHS (*endogenous control*), sulfate (*endogenous control*) and controls including only sediment without addition of any electron acceptor nor donor. Sulfate was provided to the correspondent treatments from an anoxic concentrated stock up to a final concentration of 2 mM.

After 20 days of incubation (from now on called *1<sup>st</sup> incubation cycle*), the remaining CH<sub>4</sub> was removed from the flasks headspace by flushing with N<sub>2</sub>. The flasks were then put inside the glove-box and the basal medium was replaced by fresh anoxic medium enriched with 1000 mg L<sup>-1</sup> of PPHS. PPHS were excluded again in the correspondent controls and sulfate was provided in the same way as previously described. The 2<sup>nd</sup> cycle of incubation began after injecting CH<sub>4</sub> again under the same procedure described before at 28°C in the dark.

## 5.2.2 Analytical techniques

### 5.2.2.1 Sulfur species determinations

Sulfate and thiosulfate were analyzed with a Metrohm 883Basic Ion Chromatography instrument equipped with a Metrohm 863 compact autosampler and a Metrosepp A supp 250/4.0 and a MetroseppRP2 guard/3.5 column and precolumn, respectively. The eluent employed was a mixture of Na<sub>2</sub>CO<sub>3</sub> 1 mM, NaHCO<sub>3</sub> 4 mM and 5% acetone. Sulfide was measured with a modified version of

the spectrometric proposed by Cline<sup>27</sup>. Briefly, 200  $\mu\text{L}$  of Zn-acetate preserved samples were made react with N,N-dimethyl-p-phenyl-diamine and  $\text{NH}_4\text{Fe(III)SO}_4$  under highly acidic conditions. The blue coloration produced after 10 min reaction was measured at 664 nm in a microplate reader (FlashScan 550, Analytic Jena, Germany). Elemental sulfur was analyzed by HPLC after derivatization with methanol according to the protocol described by Lohmayer and colleagues<sup>28</sup>.

### **5.2.2.2 Methane determinations**

Changes in methane concentrations in the microcosm's headspace were measured by injecting 100  $\mu\text{L}$  of the headspace gas into a gas chromatograph (GC) (SRI 8610C; SRI Instruments, Torrence, USA) equipped with a packed column (0.3-m HaySep-D packed Teflon; Restek, Bellefonte, USA) at 42  $^\circ\text{C}$ , a thermal conductivity detector (TCD) at 111  $^\circ\text{C}$ , and a flame ionization detector (FID) and with  $\text{N}_2$  as the carrier gas.

### **5.2.2.3 Reduction of the functional moieties of PPHS**

The reduction of the HS's functional groups with capacity to accept electrons was measured by the protocol proposed by Lovely and colleagues<sup>7</sup> with some modifications<sup>14</sup>.

### **5.2.2.4 Analysis of sediment post-incubation**

Leak of sulfur compounds by incorporation into organic matter was explored by analysis of freeze-dried organic content of the microcosms by Fourier-transform

## CHAPTER V

infrared spectroscopy (FTIR). KBr pellets with approximately 1% (v/v) of the freeze-dried PPHS sample (after reaction with HS<sup>-</sup> and PPHS without reaction as control) were made and analyzed in a Bruker VERTEX 80v instrument using as a blank KBr pellets without PPHS sample. Data were collected in a range of 4500–370 cm<sup>-1</sup> at a resolution of 4cm<sup>-1</sup> with 100 scans for each sample.



## 5.3 Results

### 5.3.1 Sulfide oxidation by Pahokee Peat Humic Substances

All experimental treatments showed decreases in dissolved sulfide ( $\text{HS}^-$ ) concentrations within 8 hours of chemical reaction (Fig. 5.1A).

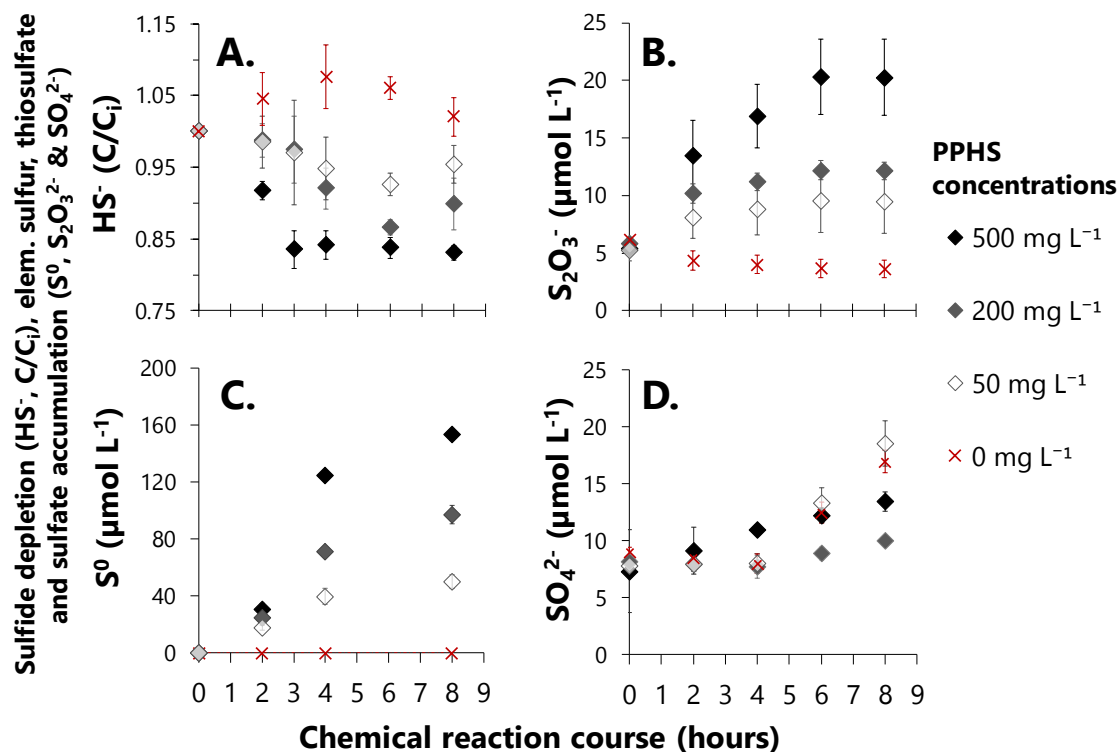
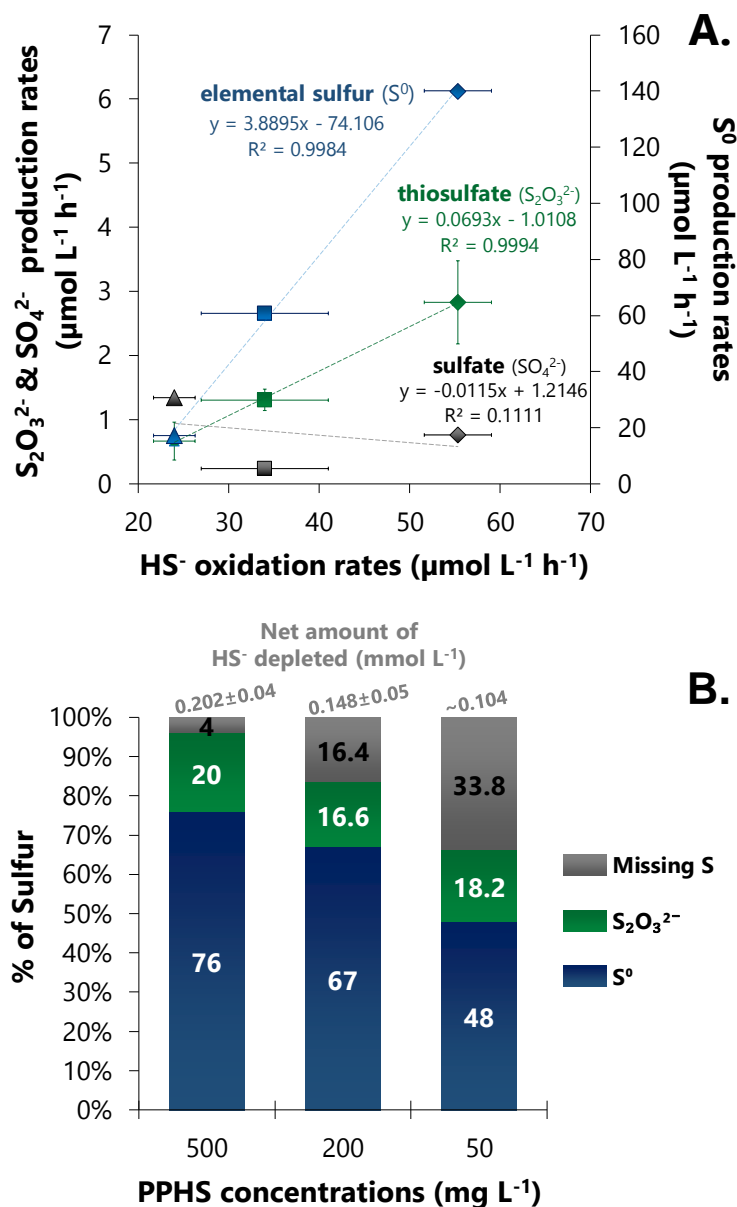


Fig. 5.1 | Transformation of dissolved sulfide ( $\text{HS}^-$ ) upon reaction with *Pahokee Peat* Humic substances and formation of oxidized products. Panel A, displays the normalized ( $C/C_1$ ) decrease on dissolved  $\text{HS}^-$  concentrations over time. The formation of elemental sulfur ( $\text{S}^0$ ), thiosulfate ( $\text{S}_2\text{O}_3^{2-}$ ) and sulfate ( $\text{SO}_4^{2-}$ ) is shown in Panels B to D, respectively. All data represents the mean and standard error values from experimental triplicates.

Initial  $\text{HS}^-$  concentrations after equilibrium with the microcosms' headspace were  $\sim 1.3 \text{ mmol L}^{-1}$ , which agreed with the initial pH of the system ( $\sim 7.5$ ).  $\text{HS}^-$  transformation was significantly affected by the distinct concentrations of PPHS (**Fig. 5.1**). After 8 hours of chemical transformation of dissolved  $\text{HS}^-$ , the amounts of this electron donor consumed at the end of the incubation period were: 0.104,  $0.148 \pm 0.05$  and  $0.202 \pm 0.04 \text{ mmol L}^{-1}$  for assays amended with 50, 200 and 500  $\text{mg L}^{-1}$ , respectively (**Fig. 5.2B**). These results confirm that the oxidizing power of PPHS imposed a linear effect on the extent of  $\text{HS}^-$  oxidation as it has been previously reported with other sources of humic material, such as *Pahoee Peat* Reference Humic Acid (from the IHSS, # catalogue: 1R103H)<sup>12</sup> and Sigma Aldrich Humic Acids<sup>24,25</sup>. Elemental sulfur ( $\text{S}^0$ ), thiosulfate ( $\text{S}_2\text{O}_3^{2-}$ ) and sulfate ( $\text{SO}_4^{2-}$ ) were detected over time on the micromolar scale (**Figs. 5.1B, C & D**). However, only the rates of  $\text{S}^0$  and  $\text{S}_2\text{O}_3^{2-}$  formation were explicitly linked to the kinetics of dissolved sulfide transformation and to the PPHS concentration (**Fig. 5.2A**). As previously reported,  $\text{HS}^-$  oxidation with PPHS as the electron acceptor mainly produced elemental sulfur and thiosulfate as the main products<sup>12,24,25</sup>. Although sulfate was also detected in all the assays (**Fig. 5.1D**), its rate of production was not related to PPHS concentrations and it was even detected in those controls lacking humic material (**Fig. 5.2A**).



**Fig. 5.2 | Analysis of products coming from dissolved sulfide ( $\text{HS}^-$ ) transformation by PPHS. Panel A** shows the correlation between the rates of dissolved  $\text{HS}^-$  consumption and the rates for  $\text{S}^0$ ,  $\text{S}_2\text{O}_3^{2-}$  and  $\text{SO}_4^{2-}$  production. **Panel B** displays a sulfur mass balance considering the amounts of sulfide transformed and the sulfur compounds, which rates of production correlated with the rates of  $\text{HS}^-$  consumption (elemental sulfur and thiosulfate). All data represents the mean and standard error values of triplicates.

This agrees with the study by Heitmann and Blodau, in which  $\text{SO}_4^{2-}$  was detected, but it was related to the presence of oxygen traces<sup>12</sup>. A sulfur mass balance made for those products which rates of production correlated with sulfide consumption ( $\text{S}^0$  and  $\text{S}_2\text{O}_3^{2-}$ ), revealed that in the presence of 500 mg PPHS  $\text{L}^{-1}$ ,  $\text{S}^0$  and  $\text{S}_2\text{O}_3^{2-}$  accounted for the 76 and 20% of the transformed dissolved sulfide, respectively. These percentages diminished to 67% and 16% in incubations performed with 200 mg PPHS  $\text{L}^{-1}$ , and to 48% and to 18% for those conducted with 50 mg PPHS  $\text{L}^{-1}$ , respectively (**Fig. 5.2B**).

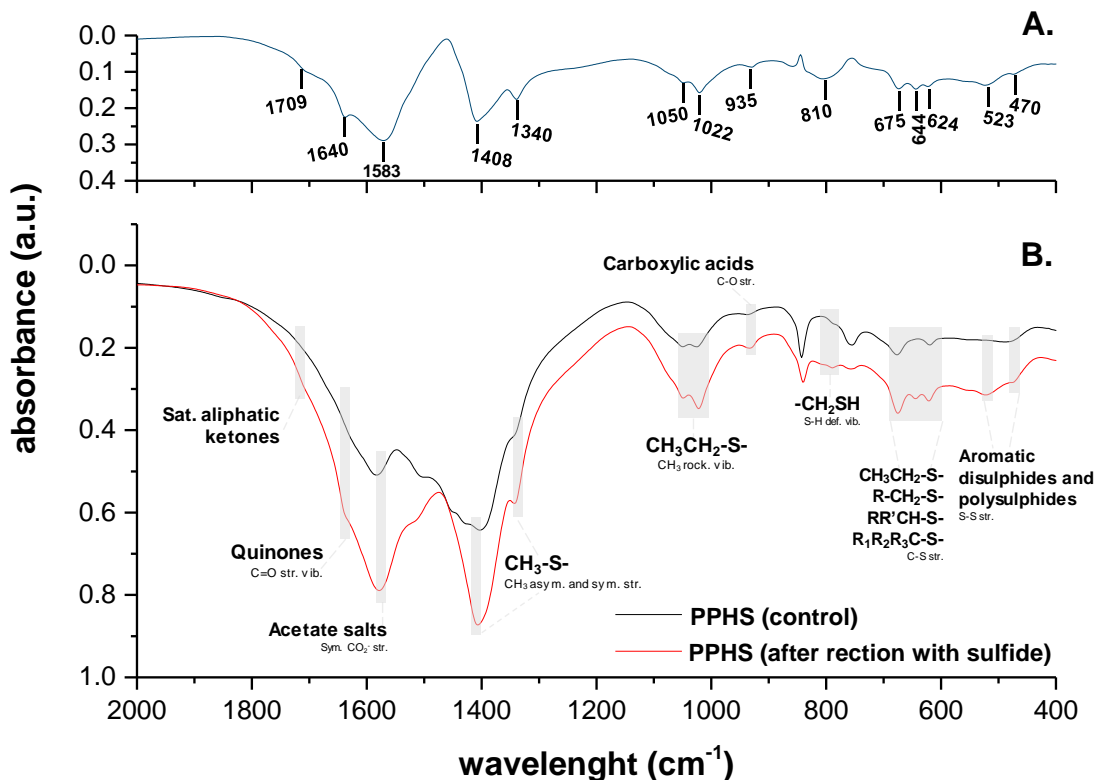


**Fig. 5.3 | Fourier-transformed infrared (FTIR) spectra of PPHS after reaction with sulfide. Panel A** displays the changes in intensity of peaks determined by using the PPHS control to correct the base line. The signals which intensity increased after

reaction with sulfide are marked with a shadow at **Panel B**, in which the spectra obtained for both treatments are shown.

According to previous research, the remaining sulfur missing in the mass balance could potentially be integrated into HS by forming *organosulfur* compounds ( $S_{org}$ )<sup>29-31</sup>. This was confirmed by FTIR analysis of PPHS after reaction with sulfur. The FTIR spectra revealed that sulfur was partially incorporated into the humic material by forming bonds with carbonaceous functional groups (**Fig. 5.3**). According to these observations, the percentage of S missing in the mass balance shown in **Figure 5.2B** might be responded by this S that was transformed into organosulfur compounds. However, this was not quantitatively proven since it was far from the aim of this work. A summary comparing the results obtained from this study with previous reports on sulfur oxidation by HS and analogues is shown in **Table 5.1**.

### 5.3.2 Methane dynamics as affected by PPHS and/or Sulfate

Wetland sediment incubations displayed distinct dynamics of CH<sub>4</sub> consumption and production as affected by PPHS and sulfate in an independent manner or jointly. At the beginning of the 1<sup>st</sup> incubation cycle, a short period of CH<sub>4</sub> production had place in all biologically active treatments (**Figure 5.4**). Subsequently, net CH<sub>4</sub> consumption started and different rates of AOM were observed depending on the presence of the different electron acceptors (**Fig. 5.4A** and **B**, left panels). During the 1<sup>st</sup> incubation period, the highest rates AOM were observed in the PPHS + SO<sub>4</sub><sup>2-</sup> treatment ( $18.6 \pm 4.2 \mu\text{mol CH}_4 \text{ L}^{-1} \text{ cm}^{-3} \text{ sed. day}^{-1}$ ). These consumption rates were 3.2-times higher than in the treatment containing only SO<sub>4</sub><sup>2-</sup> ( $5.7 \pm 2.16 \mu\text{mol CH}_4 \text{ L}^{-1} \text{ cm}^{-3} \text{ sed. day}^{-1}$ ) and 1.7-times higher than in the

## CHAPTER V

treatment containing only PPHS ( $10.67 \pm 1.7 \mu\text{mol CH}_4 \text{ L}^{-1} \text{ cm}^{-3} \text{ sed. day}^{-1}$ ). The null effect of  $\text{SO}_4^{2-}$  by itself on AOM was also evidenced since the rate of methanotrophy in the control lacking any electron acceptor was not significantly different than in this treatment ( $6.7 \pm 1.7 \mu\text{mol CH}_4 \text{ L}^{-1} \text{ day}^{-1}$ ).

**Table 5.1 | Comparison of reports regarding dissolved sulfide (HS<sup>-</sup>) oxidation by humic substances or model quinones.**

| Source of humic material or analogue                                    | Background  | pH        | Fraction of HS employed              | Inorganic products  | S <sub>org</sub> <sup>*</sup> formation                | Reference                               |
|---|---|-----------|--------------------------------------|---|--|---|
| Juglone <sup>**</sup>   | Deionized water                                   | 7 to 12.5 | -                                    | Not evaluated   | Aryl-thiocompounds                                     | Perlinger et al, 2002 <sup>29</sup> .   |
| Humic Acid<br><i>Pahoee Peat</i><br>(IHSS <sup>***</sup> , 1R103H)      | Deionized water.                                  | 6         | Soluble fraction (filtered, 0.22 μm) | S <sub>2</sub> O <sub>3</sub> <sup>2-</sup> , background presence of SO <sub>4</sub> <sup>2-</sup> .                  | Aryl-polysulfide                                       | Heitmann & Blodau, 2006 <sup>12</sup> . |
| Sigma Aldrich Humic Acids   | Deionized water.                                  | 6         | Soluble fraction (filtered, 0.45 μm) | S <sup>0</sup> and S <sub>2</sub> O <sub>3</sub> <sup>2-</sup> .  | Thiols, organic di- and polysulfides, and heterocycles | Yu et al, 2015 <sup>25</sup> .          |
| Sigma Aldrich Humic Acids   | Deionized water.                                  | 7         | Soluble fraction (filtered, 0.45 μm) | Not evaluated   | Not evaluated  | Yu <i>et al</i> , 2016 <sup>24</sup> .  |
| <i>Pahoee Peat</i><br>Humic Substances<br>(IHSS <sup>**</sup> , 1S103H) | Bicarbonate buffered basal medium <sup>14</sup> . | 7.5       | Unfiltered suspension.               | S <sup>0</sup> , S <sub>2</sub> O <sub>3</sub> <sup>2-</sup> , background presence of SO <sub>4</sub> <sup>2-</sup> . | Several C-S bonds (see <b>Fig. 5.3</b> ).              | This study.                             |

<sup>\*</sup>Organic sulfur, <sup>\*\*</sup>5-hydroxy-1,4-naphthoquinone, <sup>\*\*\*</sup>International Humic Substances Society.

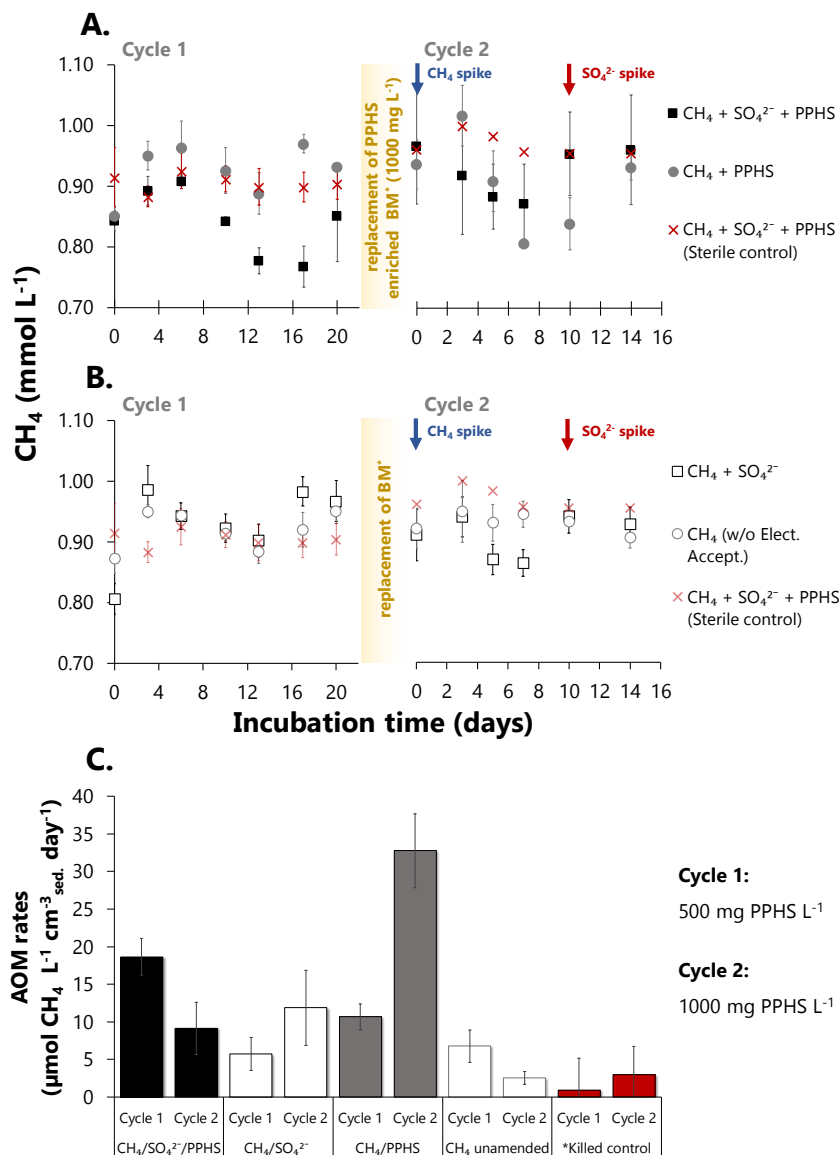


**Fig. 5.4** | Anaerobic methane oxidation performed by wetland sediment microbiota as affected by sulfate ( $\text{SO}_4^{2-}$ ), *Pahokee Peat* Humic Substances (PPHS), both, and none. **Panel A** displays the pattern of  $\text{CH}_4$  concentrations through time in experiments enriched with  $500 \text{ mg L}^{-1}$  of PPHS during the 1<sup>st</sup> incubation cycle (left panel) and  $1000 \text{ mg L}^{-1}$  during the 2<sup>nd</sup> cycle (right panel). **Panel B** displays the pattern of  $\text{CH}_4$  concentrations in absence of PPHS. \*BM stands out for *basal medium*. BM replacement is indicated by yellow letters. Spiking of a new concentration of  $\text{CH}_4$  into the microcosm's headspace at the beginning of the 2<sup>nd</sup> incubation cycle is depicted by a



blue arrow. Spiking with a concentrated solution of  $\text{SO}_4^{2-}$  is depicted by a red arrow. **Panel C** displays the maximum rates of  $\text{CH}_4$  consumption, which were obtained by calculating the linear regression of at least three points of each independent experimental replicate per treatment. All data represents the mean and standard error values of triplicates.

After 12 days of incubation, all treatments stopped consuming  $\text{CH}_4$ , except for that including both electron acceptors in which  $\text{CH}_4$  consumption lasted 16 days. Afterwards, all treatments (except for the sterile controls) started producing  $\text{CH}_4$  as a signal of the depletion of electron acceptors suitable to keep sustaining AOM activities (**Fig. 5.4A** and **B** left panels).

On the 2<sup>nd</sup> incubation cycle, initial methanogenic activity only lasted three days and it did not happen in the treatment containing both electron acceptors (**Fig. 5.4**, right panels). Surprisingly, the highest rates of  $\text{CH}_4$  consumption during this degradation cycle were observed in the treatment containing PPHS as the only electron acceptor ( $32.7 \pm 5 \mu\text{mol L}^{-1} \text{cm}^{-3} \text{sed. day}^{-1}$ ), which was 2.7-, 3.6- and 13-times higher than the rates observed in incubations amended with  $\text{SO}_4^{2-}$  ( $11.8 \pm 5 \mu\text{mol L}^{-1} \text{cm}^{-3} \text{sed. day}^{-1}$ ), PPHS +  $\text{SO}_4^{2-}$  ( $9.1 \pm 3.5 \mu\text{mol L}^{-1} \text{cm}^{-3} \text{sed. day}^{-1}$ ), and without external *electron acceptor* ( $2.5 \pm 0.85 \mu\text{mol L}^{-1} \text{cm}^{-3} \text{sed. day}^{-1}$ ), respectively (**Fig. 5.4C**). As previously hinted in the 1<sup>st</sup> incubation cycle, the role of  $\text{SO}_4^{2-}$  as electron acceptor to drive  $\text{CH}_4$  consumption was much lower than expected. In fact, in the 2<sup>nd</sup> cycle, there was no evidence of an accumulative positive effect on AOM when both  $\text{SO}_4^{2-}$  and PPHS were present. In contrast,  $\text{SO}_4^{2-}$  had a negative effect on  $\text{CH}_4$  consumption when PPHS were present since the  $\text{CH}_4$  consumption rates were much higher when PPHS were the only available electron acceptor. Further evidence supporting this observation was the lack of effect in terms of stimulation of AOM by spiking  $\text{SO}_4^{2-}$  to a final concentration of  $4 \text{ mmol L}^{-1}$  on day 10 of the 2<sup>nd</sup>

incubation cycle (**Fig. 5.3A** and **B**, right panels). Tracking of CH<sub>4</sub> production on those microcosms used as *endogenous controls* (lacking added CH<sub>4</sub>), revealed that both electron acceptors PPHS and SO<sub>4</sub><sup>2-</sup>, in combination or by themselves, had a positive effect suppressing methanogenesis as it has been previously reported (**Fig. 5.4**).

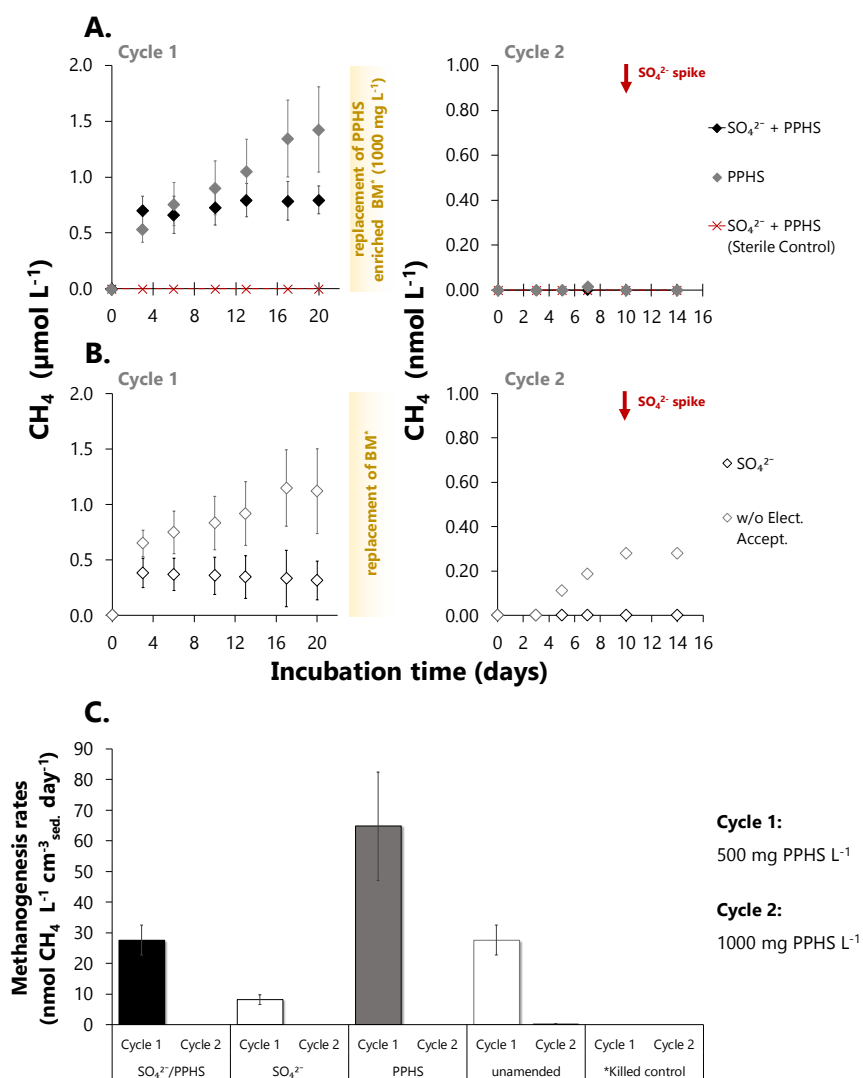


**Fig. 5.5** | Effect of the different electron acceptors on methanogenesis. Panel A displays the pattern of CH<sub>4</sub> concentrations through time in experiments enriched with 500 mg L<sup>-1</sup> of PPHS during the 1<sup>st</sup> incubation cycle (left panel) and 1000 mg L<sup>-1</sup> during

the 2<sup>nd</sup> cycle (right panel). **Panel B** displays the pattern of CH<sub>4</sub> concentrations in absence of PPHS. \*BM stands out for *basal medium*. BM replacement is indicated by yellow letters. Spiking with a concentrated solution of SO<sub>4</sub><sup>2-</sup> is depicted by a red arrow. **Panel C** displays the maximum rates of CH<sub>4</sub> production, which were obtained by calculating the linear regression of at least three points of each independent experimental replicate per treatment. All data represents the mean and standard error values of triplicates.

Endogenous microcosms (lacking added CH<sub>4</sub>), showed methanogenesis suppression in the presence of sulfate during the 1<sup>st</sup> incubation cycle, as well as in presence and in the absence of PPHS (Fig. 5.5A and B, left panels). During the 2<sup>nd</sup> incubation cycle, the same effect was observed in the presence of 1000 mg L<sup>-1</sup> of PPHS in which organic matter intrinsic to the wetland sediment was nearly depleted (**Fig. 5.5**, right panels). In this cycle, CH<sub>4</sub> was produced at the nanomolar scale only in those controls that did not include any external electron acceptor (**Fig. 5.1B**, right panel).

### 5.3.3 Electron acceptors driving AOM

As previously deduced by the null effect of  $\text{SO}_4^{2-}$  on the rates of AOM, no significant sulfate reduction occurred, based both on in terms of sulfate depletion and  $\text{HS}^-$  production in the microcosms (**Figure 5.6**).

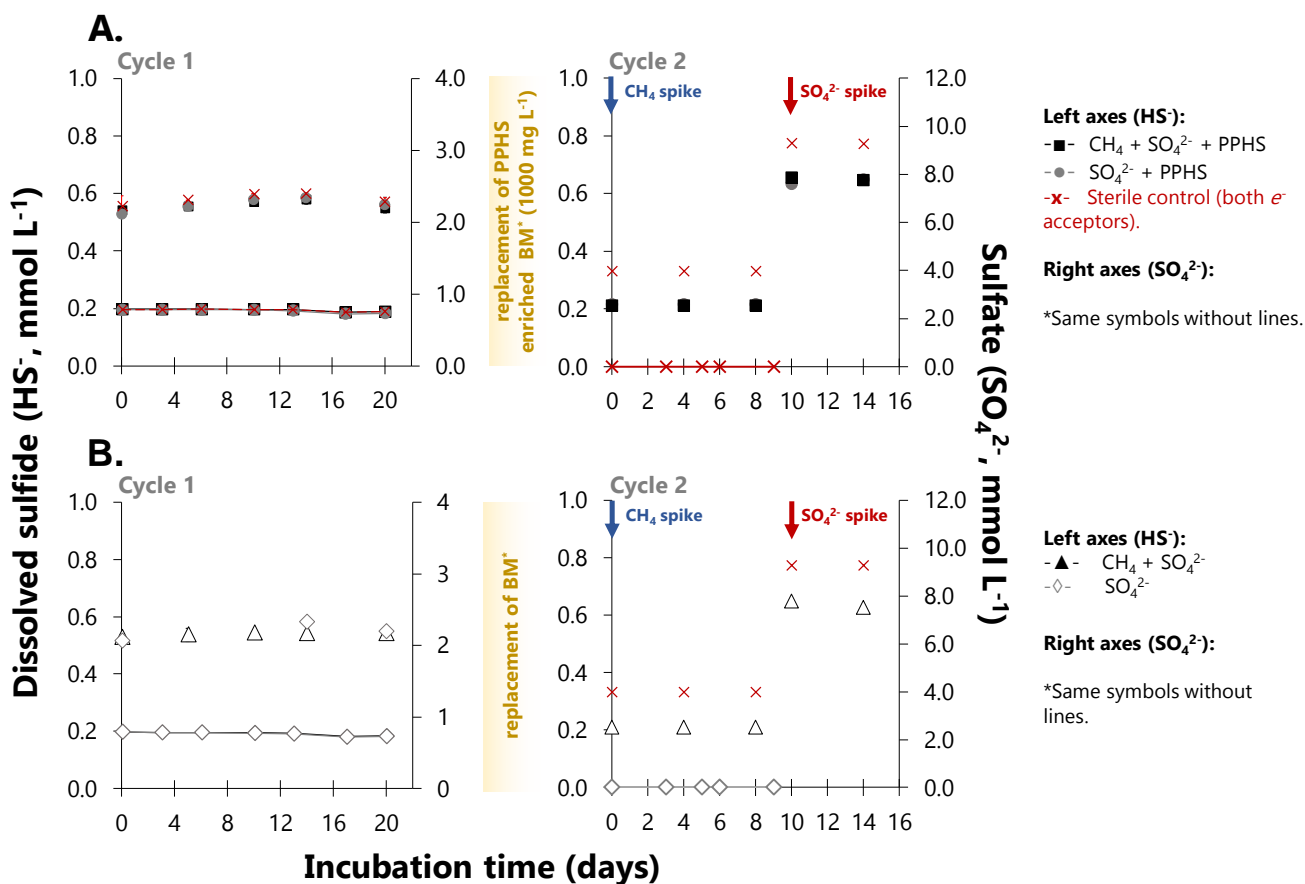


**Fig. 5.6 | Sulfate ( $\text{SO}_4^{2-}$ ) reduction and dissolved sulfide ( $\text{HS}^-$ ) production.**  $\text{SO}_4^{2-}$  concentrations over time are depicted with symbols without connecting lines while  $\text{HS}^-$  concentrations are depicted with lone connected symbols. **Panel A** displays  $\text{SO}_4^{2-}$  and  $\text{HS}^-$  concentrations through time in experiments enriched with  $500 \text{ mg L}^{-1}$  of PPHS during the 1<sup>st</sup> incubation cycle (left panel) and  $1000 \text{ mg L}^{-1}$  during the 2<sup>nd</sup> incubation

cycle (right panel). **Panel B** displays  $\text{CH}_4$  concentrations in the absence of PPHS. \*BM stands out for *basal medium*. BM replacement is indicated by yellow letters. Spiking with a concentrated solution of  $\text{SO}_4^{2-}$  is depicted by a red arrow. All data represents the mean and standard error values of triplicates.

On the other hand, reduction of PPHS was in fact affected by the presence of  $\text{CH}_4$  in the 1<sup>st</sup> incubation cycle, suggesting its role as the main terminal electron acceptor fueling methanotrophy<sup>14,15</sup> (**Fig. 5.7A**). However, in the 2<sup>nd</sup> incubation cycle, the highest reduction of PPHS was detected in microcosms including  $\text{SO}_4^{2-}$ , which implies sulfate reducing processes may have affected the redox state of PPHS (**Fig. 7B**).

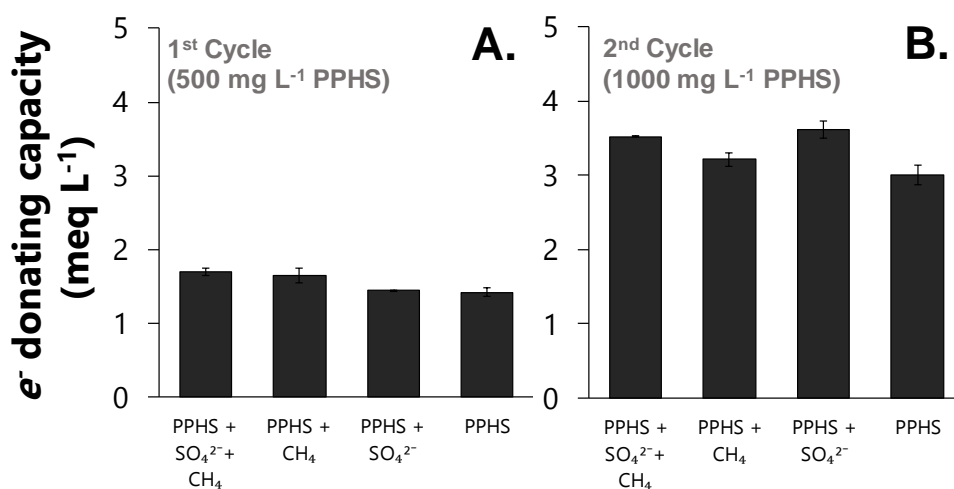


**Fig. 5.7 | Electron donating capacity of Pahokee Peat Humic Substances (PPHS) at the end of each incubation cycle. Panel A** displays the electron donating capacity of PPHS after the 1<sup>st</sup> incubation cycle in which 500 mg L<sup>-1</sup> of PPHS were employed as electron acceptor in the presence and in the absence of sulfate ( $\text{SO}_4^{2-}$ ). **Panel B** displays the same parameter after the 2<sup>nd</sup> incubation cycle in which 1000 mg L<sup>-1</sup> of PPHS were employed. All values are corrected for the sediment and PPHS intrinsic Fe(II) content and depict the mean and standard error values of triplicates.

## 5.4 Discussion

### 5.4.1 Oxidation of dissolved sulfide with Pahokee Peat Humic substances as electron acceptor

Chemical set-ups testing the capability of PPHS to oxidize sulfide under anaerobic conditions displayed the formation elemental sulfur and thiosulfate as the main inorganic products, which agrees with previous reports (**Fig. 5.1**, **Table 5.1**). From the latter, thiosulfate has been proven to be able to sustain AOM activities,<sup>26</sup> thus confirming the potential of a cryptic cycling of S driven by PPHS to extend S-dependent AOM activities. Calculations revealed that the amount of sulfur missing to close the S mass balance increased when the concentration of dissolved sulfide decreased from 500 to 50 mg of PPHS L<sup>-1</sup> at a fixed value of dissolved sulfide (**Fig. 5.2B**). Therefore, it is conceivable that high concentrations of PPHS supported the kinetically more favored reaction of S<sup>0</sup> formation and then quickly depleted the electron accepting capacity of the redox moieties in PPHS. In contrast, at lower PPHS concentrations, more S was incorporated into its organic structure, the formation of several kinds of C-S chemical bonds was observed by FTIR analysis (**Fig. 5.3**), thus suggesting the fate of S to its incorporation into the HS structure, which has been also observed in previous reports (**Table 5.1**).

### 5.4.2 Methanotrophic and methanogenic activities affected by sulfate and Pahokee Peat Humic Substances as electron acceptors

Experiments to assess AOM activities with sulfate and PPHS as terminal electron acceptors, showed that PPHS reduction was the preferred pathway to sustain the methanotrophic activities (**Figures 5.4**) while sulfate neither stimulated methane consumption nor produced any traceable reaction byproducts (**Figure 5.6**). Nonetheless, supporting previous findings, sulfate's presence suppressed methanogenesis presumably due to the more thermodynamical feasibility that sulfate-reducing processes have over methanogenesis<sup>32</sup> (**Figure 5.5**). Interestingly,  $\text{SO}_4^{2-}$  presence seemed to affect the redox-state of PPHS at the end of the 2<sup>nd</sup> incubation cycle by reducing them more than controls lacking sulfate (**Fig. 5.7B**). The only mechanism by which this could be possible is the initial reduction of sulfate into dissolved sulfide, a strong electron donor, which would then chemically reduce the functional groups in PPHS as observed in our chemical set-ups. Taking into consideration the low electron accepting capacity that HS usually present, even low concentrations of sulfide present in the wetland sediment, which may have been originated from heterotrophic sulfate-reducing processes, would be enough to quickly deplete the electron-accepting capacity of PPHS. Then, if AOM was mainly driven by the oxidized groups of PPHS, any transformation that sulfate-reducing processes may trigger on these functional moieties may be the reason why on the 2<sup>nd</sup> incubation cycle the rates of AOM were higher in those microcosms containing only PPHS and not in the set ups containing both electron acceptors, resulting in a counter intuitive result from that expected from the cryptic S cycling favoring AOM.

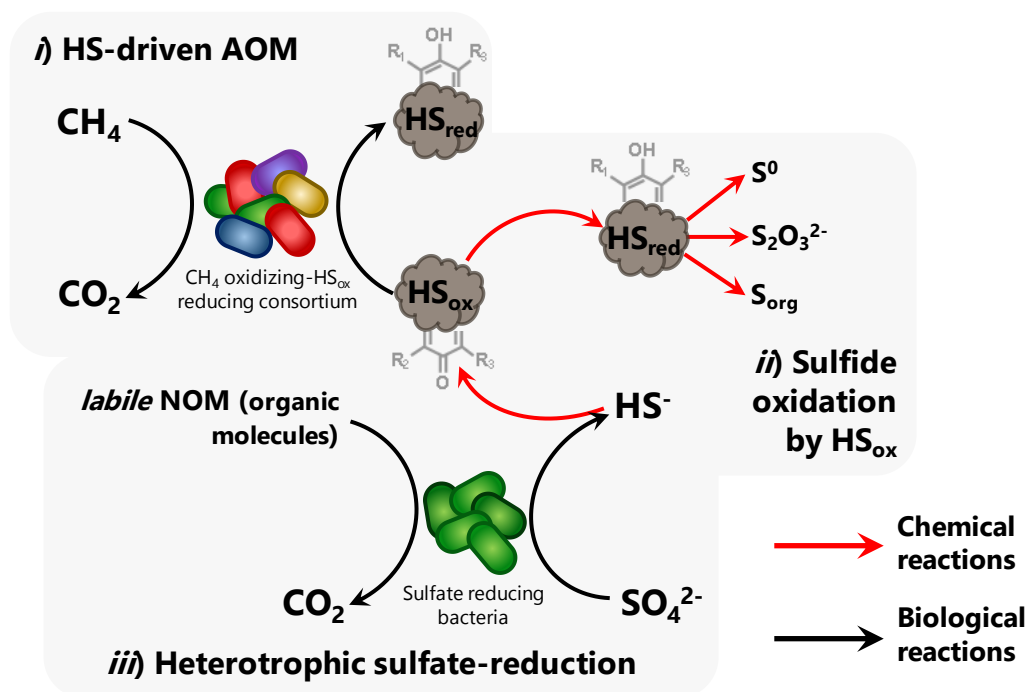


**Fig. 5.8 | Sulfur cycling by Humic Substances (HS) and the effect on anaerobic methane oxidation (AOM).** Proposed inter connection of the S and C cycles affecting CH<sub>4</sub> consumption by the microbiota of the wetland sediment tested. While indeed *Pahokee Peat* HS (PPHS) induced the oxidation of dissolved sulfide into inorganic and organic products (ii) these reactions apparently competed with HS-dependent AOM (i) for the redox moieties in PPHS to be reduced. Since no linking between AOM and sulfate reduction to sulfide was observed, sulfide production was apparently fueled by heterotrophic sulfate reducing processes, which might have employed labile organic molecules intrinsically present in the wetland sediment as electron donor (iii).

## 5.5 Conclusions

The present study shows evidence demonstrating that inorganic electron donors, such as dissolved sulfide, may be oxidized by the functional moieties in NOM producing sulfurous intermediates like thiosulfate and elemental sulfur.



Although sulfate decreased methane production rates, it was not identified as a product of sulfide oxidation by NOM. Surprisingly, the redox reactions involving NOM, which produce partially oxidized S products, negatively affected AOM rates presumably due to a competition between the chemical reaction with sulfide and the microbial reduction of HS by CH<sub>4</sub> oxidizers for the electron-accepting moieties in NOM. This could be due to a predominance of humus-reducing/CH<sub>4</sub> oxidizing microorganisms instead of sulfate reducers.

## 5.6 References

1. **MacCarthy, P.** The principles of humic substances: An introduction to the first principle. In *Humic Substances*; 2007.
2. **Martinez, C. M.;** Alvarez, L. H.; Celis, L. B.; Cervantes, F. J. Humus-reducing microorganisms and their valuable contribution in environmental processes. *Appl. Microbiol. Biotechnol.* **2013**, *97* (24), 10293–10308.
3. **Lehmann, J.;** Kleber, M. The contentious nature of soil organic matter. *Nature* **2015**, *528* (7580), 60–68.
4. **Stevenson, F. J.** Humus Chemistry: Genesis, Composition, Reactions. *Nature* **1983**, *303* (30), 835–836.
5. **Scott, D. T.;** Mcknight, D. M.; Blunt-Harris, E. L.; Kolesar, S. E.; Lovley, D. R. Quinone moieties act as electron acceptors in the reduction of humic substances by humics-reducing microorganisms. *Environ. Sci. Technol.* **1998**, *32* (19), 2984–2989.
6. **Coates, J. D.;** Cole, K. A.; Chakraborty, R.; Connor, S. M. O.; Achenbach, L. A. Diversity and ubiquity of bacteria capable of utilizing humic substances as electron donors for anaerobic respiration diversity and ubiquity of bacteria capable of utilizing humic substances as electron donors for anaerobic respiration. *Appl. Environ. Microbiol.* **2002**, *68* (5), 2445–2452.
7. **Lovley, D. R.;** Coates, J. D.; Blunt-Harris, E. L.; Phillips, E. J. P.; Woodward, J. C. Humic substances as electron acceptors for microbial

respiration. *Nature*. 1996, pp 445–448.

**8. Cervantes, F. J.;** Velde, S.; Lettinga, G.; Field, J. a. Competition between methanogenesis and quinone respiration for ecologically important substrates in anaerobic consortia. *FEMS Microbiol. Ecol.* **2000**, *34* (2), 161–171.

**9. Cervantes, F. J.;** Gutiérrez, C. H.; López, K. Y.; Estrada-Alvarado, M. I.; Meza-Escalante, E. R.; Texier, A.-C.; Cuervo, F.; Gómez, J. Contribution of quinone-reducing microorganisms to the anaerobic biodegradation of organic compounds under different redox conditions. *Biodegradation* **2008**, *19* (2), 235–246.

**10. Keller, J. K.;** Weisenhorn, P. B.; Megonigal, J. P. Humic acids as electron acceptors in wetland decomposition. *Soil Biol. Biochem.* **2009**, *41* (7), 1518–1522.

**11. Blodau, C.;** Deppe, M. Humic acid addition lowers methane release in peats of the Mer Bleue bog, Canada. *Soil Biol. Biochem.* **2012**, *52*, 96–98.

**12. Heitmann, T.;** Blodau, C. Oxidation and incorporation of hydrogen sulfide by dissolved organic matter. *Chem. Geol.* **2006**, *235* (1–2), 12–20.

**13. Heitmann, T.;** Goldhammer, T.;

Beer, J.; Blodau, C. Electron transfer of dissolved organic matter and its potential significance for anaerobic respiration in a northern bog. *Glob. Chang. Biol.* **2007**, *13* (8), 1771–1785.

**14. Valenzuela, E. I.;** Prieto-Davó, A.; López-Lozano, N. E.; Hernández-Eligio, A.; Vega-Alvarado, L.; Juárez, K.; García-González, A. S.; López, M. G.; Cervantes, F. J. Anaerobic Methane Oxidation Driven by Microbial Reduction of Natural Organic Matter in a Tropical Wetland. *Appl. Environ. Microbiol.* **2017**, *83* (11), AEM.00645-17.

15. Bai, Y.-N.; Wang, X.-N.; Wu, J.; Lu, Y.-Z.; Fu, L.; Zhang, F.; Lau, T.-C.; Zeng, R. J. Humic substances as electron acceptors for anaerobic oxidation of methane driven by ANME-2d. *Water Res.* **2019**, *164*, 114935.

**16. Valenzuela, E. I.;** Avendaño, K. A.; Balagurusamy, N.; Arriaga, S.; Nieto-Delgado, C.; Thalasso, F.; Cervantes, F. J. Electron shuttling mediated by humic substances fuels anaerobic methane oxidation and carbon burial in wetland sediments. *Sci. Total Environ.* **2019**, *650*, 2674–2684.

**17. He, Q.;** Yu, L.; Li, J.; He, D.; Cai, X.; Zhou, S. Electron shuttles enhance

anaerobic oxidation of methane coupled to iron(III) reduction. *Sci. Total Environ.* **2019**, *688*, 664–672.

**18. Straub, K. L.;** Benz, M.; Schink, B. Iron metabolism in anoxic environments at near neutral pH. *FEMS Microbiol. Ecol.* **2000**, *34* (3), 181–186.

**19. Aeschbacher, M.;** Vergari, D.; Schwarzenbach, R. P.; Sander, M. Electrochemical analysis of proton and electron transfer equilibria of the reducible moieties in humic acids. *Environ. Sci. Technol.* **2011**, *45* (19), 8385–8394.

**20. Scheller, S.;** Yu, H.; Chadwick, G. L.; McGlynn, S. E.; Orphan, V. J. Artificial electron acceptors decouple archaeal methane oxidation from sulfate reduction. *Science (80-. )*. **2016**, *351* (6274), 703–707.

**21. Bhattarai, S.;** Cassarini, C.; Lens, P. N. L. Physiology and Distribution of Archaeal Methanotrophs That Couple Anaerobic Oxidation of Methane with Sulfate. **2019**, No. July, 1–31.

**22. Timmers, P. H.;** Suarez-Zuluaga, D. A.; van Rossem, M.; Diender, M.; Stams, A. J.; Plugge, C. M. Anaerobic oxidation of methane associated with sulfate reduction in a natural freshwater

gas source. *ISME J.* **2015**, *10* (6), 1–13.

**23. Holmkvist, L.;** Ferdelman, T. G.; Jørgensen, B. B. A cryptic sulfur cycle driven by iron in the methane zone of marine sediment (Aarhus Bay, Denmark). *Geochim. Cosmochim. Acta* **2011**, *75* (12), 3581–3599.

**24. Yu, Z. G.;** Orsetti, S.; Haderlein, S. B.; Knorr, K. H. Electron Transfer Between Sulfide and Humic Acid: Electrochemical Evaluation of the Reactivity of Sigma-Aldrich Humic Acid Toward Sulfide. *Aquat. Geochemistry* **2016**, *22* (2), 117–130.

**25. Yu, Z. G.;** Peiffer, S.; Göttlicher, J.; Knorr, K. H. Electron transfer budgets and kinetics of abiotic oxidation and incorporation of aqueous sulfide by dissolved organic matter. *Environ. Sci. Technol.* **2015**, *49* (9), 5441–5449.

**26. Cassarini, C.;** Rene, E. R.; Bhattarai, S.; Esposito, G.; Lens, P. N. L. Anaerobic oxidation of methane coupled to thiosulfate reduction in a biotrickling filter. *Bioresour. Technol.* **2017**, *240*, 214–222.

**27. Cline, J. D.** Spectrophotometric Determination of Hydrogen Sulfide in Natural Waters. *Limnol. Oceanogr.*

1969, *14* (3), 454–458.

**28. Lohmayer, R.;** Kappler, A.; Lösekann-Behrens, T.; Planer-Friedrich, B. Sulfur species as redox partners and electron shuttles for ferrihydrite reduction by *Sulfurospirillum deleyianum*. *Appl. Environ. Microbiol.* **2014**, *80* (10), 3141–3149.

**29. Perlinger, J. A.;** Kalluri, V. M.; Venkatapathy, R.; Angst, W. Addition of hydrogen sulfide to juglone. *Environ. Sci. Technol.* **2002**, *36* (12), 2663–2669.

**30. Urban, N. R.;** Ernst, K.; Bernasconi, S. Addition of sulfur to organic matter

during early diagenesis of lake sediments. *Geochim. Cosmochim. Acta* **1999**.

**31. Henneke, E.;** Luther, G. W.; De Lange, G. J.; Hoefs, J. Sulphur speciation in anoxic hypersaline sediments from the eastern Mediterranean Sea. *Geochim. Cosmochim. Acta* **1997**.

**32. Pester, M.;** Knorr, K. H.; Friedrich, M. W.; Wagner, M.; Loy, A. Sulfate-reducing microorganisms in wetlands - fameless actors in carbon cycling and climate change. *Front. Microbiol.* **2012**, *3* (FEB), 1–19.

## CHAPTER VI

# General Discussion, Perspectives and Concluding Remarks

### HIGHLIGHTS

- The contribution of this thesis to **20 years of research on humic substances (HS)** fueled microbial reactions is discussed.
- **Emerging research questions** regarding HS mediated greenhouse gas consuming processes are presented.
- **Biotechnological applications** exploiting the metabolic capabilities of HS-reducing, CH<sub>4</sub>-oxidizing microbes are proposed.

## 6.1 Introduction

In this thesis, several mechanisms involving the participation of the redox-active fraction of natural organic matter (NOM), *a.k.a. humic substances* (HS), in mediating chemical and biological processes, which suppress the emission of greenhouse gases (GHG) were demonstrated. Employing sediments collected from a coastal wetland (*Sisal*/wetland), it was evidenced the occurrence of methane ( $\text{CH}_4$ ) and sulfide oxidation, as well as iron oxide (ferrihydrite and goethite) and nitrous oxide reduction, fueled by the reduction or oxidation of the redox moieties of external (*Pahokee Peat* Humic Substances) and intrinsic NOM. This study pinpoints the necessity of further studying NOM-driven microbial mechanisms, as well as the chemical reactions, which could affect these processes. This is particularly relevant considering the high diversity of microbes with a variety of metabolic capacities that may imprint a direct effect in the emission of GHG not only in wetlands, but also in a variety of ecosystems in which NOM is abundant. In the process of obtaining the scientific contributions presented in this thesis, several collateral processes in which humus played a key role were identified: 1) the production of  $\text{CH}_4$  elicited by the often considered entirely recalcitrant humic substances (HS); 2) the apparently null contribution of methanotrophy putative archaea (ANME) to carry out AOM in the *Sisal* wetland sediments; 3) the sequestration of carbon in the form of iron carbonates elicited by the electron shuttling capacity of HS for iron-dependent AOM; and 4) the competitive effect that a cryptic cycling of sulfur would have on humus-driven AOM. All these complex phenomena, often contradicting the current paradigms and in a counterintuitive manner, demonstrated how NOM can overlap several biogeochemical cycles by functioning as a linking agent by forming networks of chemical and biologically mediated reactions with ultimate consequences on the net amount of greenhouse gases emitted to the atmosphere.

This general discussion is focused on the novel mechanisms contributing to mitigate GHG emissions driven by the redox moieties in NOM. Furthermore, the remaining knowledge gaps that must be addressed in future studies, as well as the potential for applying GHG consuming/HS-reducing or -oxidizing microbes in biotechnological developments will be discussed.

## **6.2 Relevance of Humic Substances in Processes Consuming Greenhouse Gases**

Nowadays, given the current environmental concern about the increase in the temperature of the Earth (global warming), much attention has been given to deciphering the contribution of anthropogenic and natural processes in the emission of GHG to the atmosphere. Given that GHG are the main responsible for trapping excessive amounts of radiation into the atmosphere<sup>1</sup>, elucidating the trends that the increase of these molecules will have in the near future is of pivotal relevance considering the several negative effects that global warming is thought to have in the flora, fauna and life in general<sup>2</sup>.

Natural GHG release is mostly constituted by emissions coming from ecosystems, predominantly water bodies<sup>3</sup>. Since GHG, such as CH<sub>4</sub>, CO<sub>2</sub> and N<sub>2</sub>O, are produced in the anoxic sediments of these water systems by microbes<sup>3,4</sup>, elucidating the characteristics of these microorganisms is highly relevant. This will contribute to extrapolate these data and making approximations on the amount of naturally produced gases, which are released. Moreover, the information will also be relevant for exploring the application of these microbes in engineered systems as well as to develop strategies to lessen this natural emissions<sup>5</sup>.

The microbial counterpart for GHG production, the microbial consumption of GHG, has been subject of study during more than a century. For instance, CH<sub>4</sub>

microbial consumption was discovered to be performed aerobically by methane oxidizing bacteria (MOB). These bacteria rely on the use of monooxygenase enzymes to accomplish the activation of such a stable hydrocarbon. These discoveries were made in the early 1900's<sup>6</sup>. However, several decades passed until the paradigm of the O<sub>2</sub> dependent oxidation of CH<sub>4</sub> being the only possible process to biologically mineralize this potent GHG was broken. The discovery of the process, nowadays known as the anaerobic oxidation of methane (AOM), emerged from geochemical observations in marine sediments during the late 70's<sup>7</sup>.

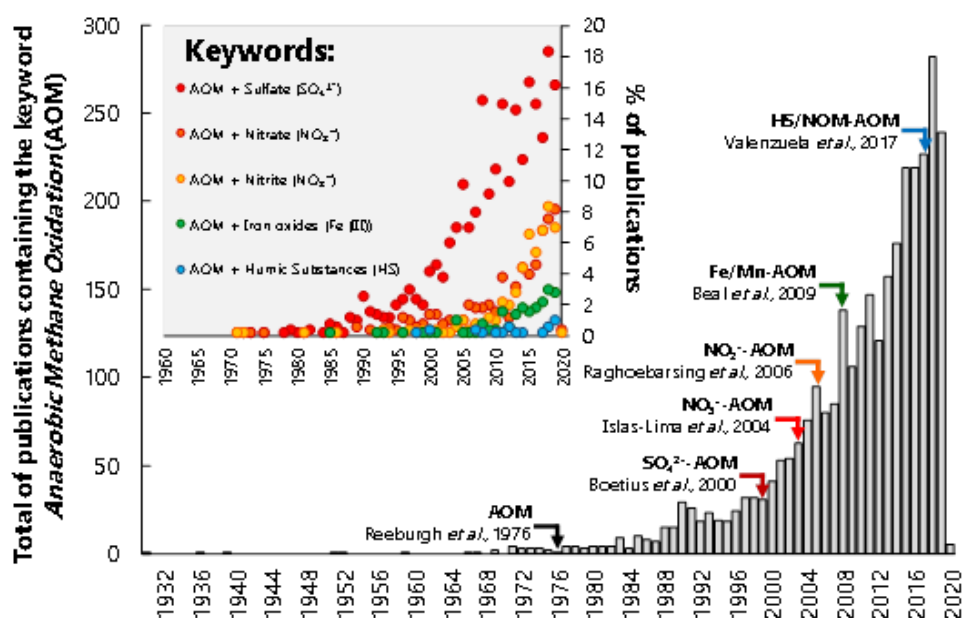


**Fig. 6.1 | SCOPUS based search on the scientific interest in the Anaerobic Oxidation of Methane process.** The total number of scientific papers published per year in which anaerobic oxidation of methane (AOM) is used as a keyword is shown in bars. The insert represents the percentage of papers in which AOM and keywords referring to the main electron acceptors driving this process in natural environments are present in the literature. Calculations were as follows: % = (# of papers with the keywords AOM and *i. e. sulfate* in a year / # of papers with the keywords AOM that year)\*100). Pioneer



studies demonstrating the occurrence of each relevant process for the first time are indicated with arrows for sulfate<sup>8</sup>, nitrate<sup>11</sup>, nitrite<sup>10</sup>, metallic oxides<sup>12</sup> and humic substances<sup>14</sup>.

However, a clear linking between CH<sub>4</sub> consumption, the electron acceptor responsible for this redox process to be possible (sulfate, SO<sub>4</sub><sup>2-</sup>), and the responsible microbes was clearly demonstrated until the early 2000's<sup>8,9</sup>. The discovery of AOM was the beginning of an environmental science *hot topic*, which during the following 19 years has resulted in the elucidation of several anaerobic modalities of AOM fueled by the reduction of relevant environmental inorganic electron acceptors, such as nitrite (NO<sub>2</sub><sup>-</sup>)<sup>10</sup>, nitrate (NO<sub>3</sub><sup>-</sup>)<sup>10,11</sup>, and iron oxides<sup>12,13</sup> just to mention the most abundant ones in nature (**Fig. 6.1**)

During this period, AOM was detected, linked to electron acceptors, and adjudicated to specific types of methanotrophic archaea (ANME)<sup>15</sup> and/or bacteria (NC10)<sup>16</sup> in the marine environment<sup>8</sup>, freshwater lakes and ponds,<sup>17,18</sup> as well as subsurface aquifers<sup>19</sup>. However, wetland ecosystem, which in fact is the main contributor to global CH<sub>4</sub> emissions,<sup>20,21</sup> remained elusive regarding its mechanisms of biological CH<sub>4</sub> consumption.

Studies on the dynamics of CH<sub>4</sub> in wetlands were inconclusive when trying to link methanotrophic activities to the reduction of known inorganic electron acceptors responsible for AOM in other ecosystems<sup>22,23</sup>. These electron acceptors, often scarce in organotrophic environments like wetlands, marshes, peatlands and bogs, led to hypothesize a potential role of humic substances, the most abundant electron acceptor in these settings, to be the potential electron sink fueling AOM activities<sup>24</sup>.

Humus-fueled AOM was firstly reported in a coastal wetland in 2017 (**Chapter I** of this thesis)<sup>14</sup>. Documenting this elusive process was indeed difficult. The main challenges to link AOM to the reduction of external humic material, such as purified *Pahokee Peat* humic substances (PPHS) or quinones such as anthraquinone-2,6-disulfonate, were originated by the high content of labile NOM that the wetland sediment possessed. The high content of intrinsic NOM triggered high rates of methanogenesis, as well often unexplained methanotrophic rates, which were mostly related to the important contents of sulfate coming from sea water, in addition to NOM intrinsic to the sediments, which showed a high electron accepting capacity.

An experimental strategy including sulfate-reduction inhibition, as well as monitoring all the reducing processes going on in the wetland sediment, such as ferric iron reduction, denitrification, and intrinsic NOM reduction, allowed to estimate rates of HS-driven AOM of ~100 nmol of CH<sub>4</sub> oxidized per cubic centimeter of wetland sediment per day. By using this data, and considering the global wetland area, the contribution of HS-dependent AOM was proposed to be 1,300 Tg of CH<sub>4</sub> per year<sup>14</sup>. This approximation might be much higher considering that the electron-accepting capacity of HS could be regenerated by shuttling electrons to abiotic reactions *i.e.* with metallic oxides (not only iron but also manganese, arsenic and other electron accepting minerals). Furthermore, HS can also be regenerated by biological extracellular electron transport processes (EET),<sup>25,26</sup> such as those mediated by quinones (QUIET),<sup>27</sup> which could shuttle electrons towards other microbes to accomplish the reduction of more oxidized electron acceptors (*i.e.* N<sub>2</sub>O, **Chapter IV** of this thesis).

Of course, not every reaction triggered by HS could suppress CH<sub>4</sub> emissions. In **Chapter V** of this thesis, it was shown how strong inorganic electron donors, such as dissolved sulfide (HS<sup>-</sup>), could compete with methanotrophs for the reduction of

quinone moieties in HS. In the naturally complex composition of soils and sediments, this could be one of the factors mainly hindering HS-dependent AOM. However, this and other aspects, such as the effect of temperature<sup>28-30</sup> and pH,<sup>31</sup> in humus chemistry and availability for microbial reduction by methanotrophs, as well as the overall effect on AOM rates, should be addressed in future studies.

## **6.3 Future Challenges**

The discovery of GHG-consuming, HS-reducing/oxidizing microbes described in this thesis, opens up several knowledge gaps regarding the taxonomical identity of these microorganisms, the environmental factors determining their activity in natural environments, as well as their applicability in environmental biotechnology. These future challenges and new directions will be further discussed.

### **6.3.1 Identification of microbes responsible for HS-dependent AOM in natural organotrophic settings**

According to the results obtained in **Chapters II** and **IV** of this thesis, as well as those data obtained by very recent studies on HS-mediated CH<sub>4</sub> consumption, the potential identity of the methanotrophic microorganisms carrying out this process will be addressed.

#### **6.3.1.1 Involvement of ANME in HS-dependent AOM**

Identifying the microorganisms responsible for any of the modalities of AOM known to date has been one of the most challenging facets of this research

topic. This aspect has been tackled by using the recently emerging technological development in culture independent techniques, such as fluorescence in situ hybridization coupled with secondary ion mass spectrometry (FISH-SIMS) and metagenomics (16s high-throughput sequencing). These novel techniques are particularly useful given the remarkably slow doubling times (2 – 7 months) that *anaerobic methanotrophic archaea* (ANME) possess<sup>32,33</sup>, which impede obtaining these microbes in pure culture.

Despite the 2d subgroup of ANME has been proven to be able to use HS as TEA for AOM in a recent study<sup>34</sup>, the results obtained in **Chapter II** and **IV** of the present thesis showed almost negligible percentages of ANME phylotypes within sediment microbial communities. These findings suggest the participation of microbes outside the ANME groups in the HS-dependent AOM process<sup>14</sup>. Considering that the study by Bai and colleagues<sup>34</sup> employed an inoculum taken from a 2-year running bioreactor fed with  $\text{NO}_3^-$ ,  $\text{NO}_2^-$  and  $\text{CH}_4$ , this ex-situ source of microorganisms was already highly enriched in ANME-2d and NC10 bacteria. Thus, further information is needed about the feasibility of finding this type of ANME archaea under the natural conditions prevailing in organic rich sediments mediating HS-dependent AOM. In the case of the incubations described in **Chapter II**,  $\text{NO}_3^-$  and  $\text{NO}_2^-$  were present in very low concentrations in the pore water of Sisal wetland sediment and their consumption was not linked to AOM. This is another hint supporting the lack of involvement of ANME-2d in this specific case of HS-dependent AOM in incubations mimicking natural conditions. It is worth mentioning that ANME-2c, the methanotrophic archaeon found linking AOM coupled to artificial electron acceptors, including quinones and humic acids, by Scheller and colleagues<sup>35</sup> was also absent from the microbial communities found in the high throughput sequencing performed at this thesis (**Chapter II** and **IV**). A possible explanation for this is that ANME-2c has been almost exclusively found in

the sea floor and in an obligate syntrophic partnership with sulfate-reducers from the *Desulfosarcina* and *Desulfococcus* genera<sup>36</sup>. These bacteria were also absent in our incubations (**Chapter II**<sup>14</sup> and **IV**) agreeing with the poor development of sulfate-reducing processes also observed in **Chapter III**<sup>37</sup>.

**Table 6.1 | Known anaerobic methanotrophic archaea (ANME) and the terminal electron acceptors they can employ to carry out anaerobic oxidation of methane (AOM).**

| ANME clusters   | Sub-clusters | Terminal electron acceptor    |                              |                              |                    |                 |                 |
|---|--------------|-------------------------------|------------------------------|------------------------------|--------------------|-----------------|-----------------|
|   |              | SO <sub>4</sub> <sup>2-</sup> | NO <sub>3</sub> <sup>-</sup> | NO <sub>2</sub> <sup>-</sup> | Fe(III)            | Mn(IV)          | Q*/HS**         |
| <b>ANME-1</b><br>(related to <i>Methanosarcinales</i> and <i>Methanomicrobiales</i> ) | a            | ● <sup>8</sup>                |                              |                              |                    |                 |                 |
|   | b            | ● <sup>38</sup>               |                              |                              |                    |                 |                 |
| <b>ANME-2</b><br>(related to <i>Methanosarcinales</i> )                               | a            | ● <sup>39</sup>               |                              |                              |                    |                 |                 |
|   | b            | ● <sup>39</sup>               |                              |                              |                    |                 |                 |
|   | c            | ● <sup>40</sup>               |                              |                              |                    |                 | ● <sup>35</sup> |
|   | d            |                               | ● <sup>10</sup>              |                              | ● <sup>13,41</sup> | ● <sup>13</sup> | ● <sup>34</sup> |
| <b>ANME-3</b><br>(related to <i>Methanococoides</i> )                                 |              | ● <sup>42</sup>               |                              |                              |                    |                 |                 |

\*Quinones, \*\*Humic Substances. Grey shaded areas indicate those phylotypes in need of a sulfate reducer bacterial partner to accomplish SO<sub>4</sub><sup>2-</sup> dependent AOM.

### 6.3.1.2 Involvement of non-ANME Euryarchaeota in HS-dependent AOM

Members of the Euryarchaeota phylum different than the ANME clades have been proposed to perform HS-dependent AOM. Such is the case of the methanogenic archaeon, *Methanobacterium*, which was found to be highly enriched in experiments in which HS and quinones were employed as electron

shuttles for the reduction of ferrihydrite<sup>43</sup>. This archaeon was found to be in syntrophy with partner bacteria from the genera *Cellulomonas*, *Desulfovibrio* and *Actinotalea*. This agrees with the results obtained in the experiments testing the simultaneous consumption of CH<sub>4</sub> and N<sub>2</sub>O presented in **Chapter IV**. In this chapter, two methanogens, an uncultured phylotype from the Methanomicrobiaceae family, and a bacterium of the *Rice Cluster I* lineage of the Methanocellaceae family, were found to potentially enable microbial partnership with the bacteria *Acinetobacter* (a  $\gamma$ -proteobacteria) in an EET mediated by the quinone moieties in HS.

Methanotrophic processes involving HS are not the only case in which non-ANME archaea have been proposed to carry out the AOM process. Bar-Or and colleagues<sup>44</sup> have proposed that *Methanosarcina* species could have the capacity to mediate iron-dependent AOM based on isotopic observations in the presence of methanogenesis/methanotrophy inhibitors, in anoxic incubations inoculated with sediments from a ferruginous lake in which the presence of ANME-1 and 2 sub-clusters was remarkably low. Apart from the experimental results, they have based this hypothesis on the fact that under high CH<sub>4</sub> concentrations, AOM coupled to iron reduction might be highly thermodynamically feasible (more than methanogenesis) and thus archaea, which have been reported to be able to conduct iron reduction,<sup>45,46</sup> could shift their metabolism from methanogenesis to iron-dependent AOM<sup>44</sup>. Under the same reasoning, and considering that several species of non-ANME archaeal phylotypes (*M. acetivorans* and *M. vulcani* from the Methanosarcinales<sup>47,48</sup>, *M. voltaei* and *thermolithotrophicus* from the Methanococcales<sup>48,49</sup> and *M. hungatei* from the Methanomicrobiales<sup>50</sup>) have been reported to conduct quinone reduction instead of methanogenesis<sup>51</sup>, it is possible that under certain conditions of high CH<sub>4</sub> concentration and availability of great amounts of quinone-containing organic electron acceptors, certain methanogens

could reverse its metabolism to perform AOM. Further efforts must be done in this matter to be able to clarify the potential versatility of methanogens reversing its metabolism coupled to organic electron acceptors such as NOM and its structural analogues.

### **6.3.1.3 Involvement of archaea outside the Euryarchaeota phylum in HS-dependent AOM**

In **Chapter II** of this thesis<sup>14</sup>, we identified members of the Bathyarchaeota phylum (formerly known as the *Miscellaneous Crenarchaeotal Group*) to be consistently present in the PPHS enriched set-ups, as well as in the AQDS microbial enrichments performing AOM. These findings agree with the microbial communities previously found in sediments in which CH<sub>4</sub> consumption was suspected to be linked to humic-like materials acting as TEAs<sup>52</sup>. The role that these archaea play in ecosystems has been mostly identified as the metabolization of complex and recalcitrant organic matter in the marine environment<sup>53</sup>. However, recent studies have emerged demonstrating that Bathyarchaeota possess divergent homologues of the genes necessary to encode the methyl-*coenzyme M reductase* (MCR) complex necessary for CH<sub>4</sub> metabolism in archaea<sup>54</sup>. This is also the case for the newly discovered phylum Verstraetearchaeota<sup>55</sup>. Consequently, in the light of the recent discoveries, which challenge the long-lasting dogmas regarding the CH<sub>4</sub> cycle, further research must focus on the possible methanotrophic activity of archaeal phyla of yet unknown metabolism<sup>56</sup>.

### 6.3.2 Elucidation of environmental factors affecting HS-dependent AOM

As in any biological process, several environmental factors, such as temperature, pH, and the presence of chemical compounds with a positive or negative effect on the HS-driven AOM reaction, must be considered in future studies assessing the potential of CH<sub>4</sub> emission suppression by this novel process.

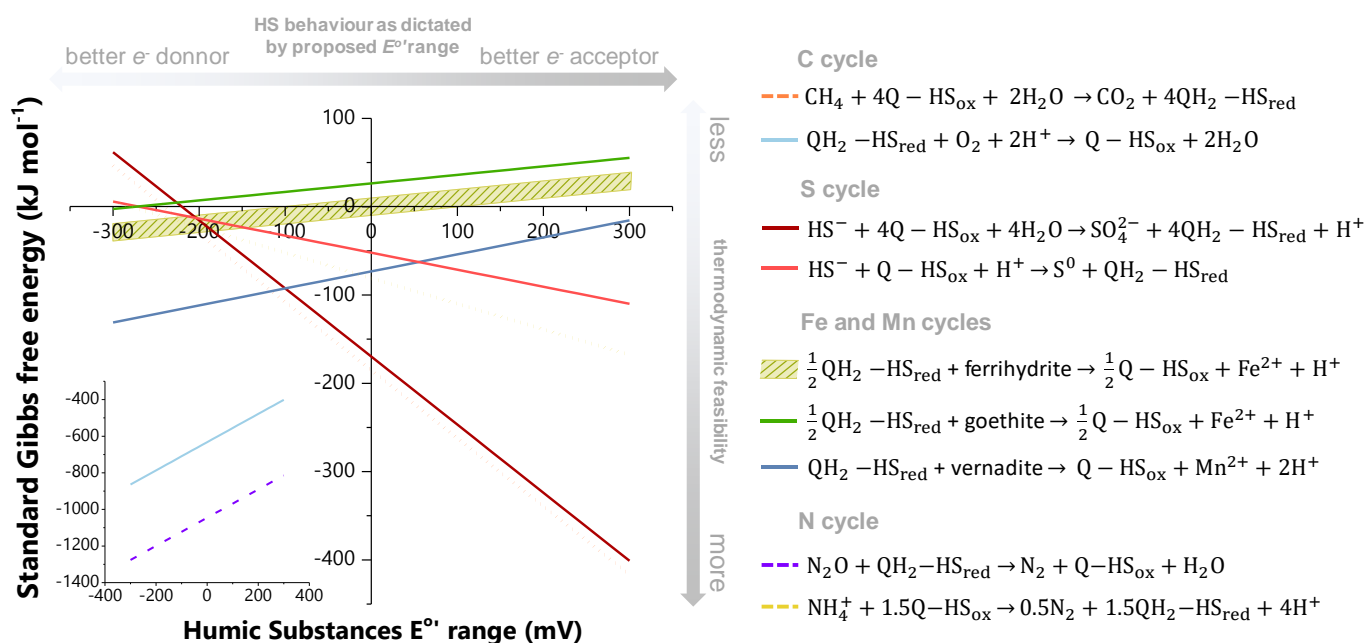


**Figure 6.2 | Compendium of thermodynamic feasibility and stoichiometry of environmentally relevant reactions driven by humic substances (HS) with a potential impact on the emission of greenhouse gases: CH<sub>4</sub>, CO<sub>2</sub> and N<sub>2</sub>O.** Biological and chemical reactions are depicted with dotted and continuous lines respectively. A description of each reaction presented in order of appearance is as follows: **C cycle:** HS-driven CH<sub>4</sub> oxidation<sup>14</sup>, HS oxidation by molecular oxygen<sup>58</sup>, **S cycle:** sulfide oxidation to sulfate by HS, sulfide oxidation to elemental sulfur by HS<sup>59</sup>, **Fe and Mn cycles:** ferrihydrite ((Fe<sup>3+</sup>)<sub>2</sub>O<sub>3</sub>•0.5H<sub>2</sub>O), goethite (α-Fe<sup>3+</sup>O(OH)) and vernadite



(amorphous  $\text{MnO}_2$ ) reduction by  $\text{HS}^{37}$ , and **N cycle**: nitrous oxide reduction driven by the oxidation of HS, anaerobic ammonium oxidation driven by HS reduction<sup>60</sup>. Calculations were made according to Nernst equation considering the whole range of standard redox potentials ( $E^{\circ}$ ) reported for HS (-300 to +300)<sup>31,57</sup>. Standard Gibbs free energy for the reduction of ferrihydrite with reduced HS as electron donor was calculated as an area due to the range of  $E^{\circ}$  reported for this iron oxide which goes from -100 to +100 mV<sup>57</sup>.

In this thesis, it has been demonstrated how HS may overlap biogeochemical cycles by linking the AOM process to dissimilatory iron reduction (goethite and ferrihydrite, **Chapter III**)<sup>37</sup> and to the consumption of a second greenhouse gas ( $\text{N}_2\text{O}$ , **Chapter IV**). These reactions could not be possible without the wide range of redox potential ( $E^{0'}$ ) that HS have, ranging from -300 to +300 mV according to electrochemical evaluation of several sources of purified humic materials<sup>31,57</sup>. This property turns HS into the most versatile electron donor and acceptor (and therefore as an electron shuttle) and allows that several biological and chemical reactions analyzed in this thesis, proceed depending on their  $E^{0'}$  value (**Figure 6.2**).

The coupling of HS-driven AOM with other processes, such as iron oxides or nitrous oxide reduction via electron shuttling or QUIET, resulted in an improved AOM activity in terms of the extent and rates of the reaction (**Chapters III and IV** of this thesis)<sup>37</sup>. Nevertheless, additional processes, which co-occur in specific environmental settings, such as those in which organic matter and sulfurous compounds (*e.g.* dissolved sulfide) prevail, were found to out-compete HS-reducers for the available oxidized moieties in HS.

### 6.3.2.1 HS-dependent AOM in recurrently anoxic environments

An important aspect of HS is that their redox active functional moieties can be quickly and fully regenerated from a reduced (electron-donating phenols) to an oxidized state (electron-accepting quinones) when exposed to dissolved molecular oxygen ( $O_2$ )<sup>61,62</sup>. This can be theoretically deduced by the high thermodynamic feasibility of this aerobic chemical reaction under standard conditions ( $\Delta G^\circ = -401$  to  $-863 \text{ kJ mol}^{-1}$ ) (**Fig. 6.2**). Previous studies have evaluated the possibility of HS acting as a fully regenerable TEA in biological processes, such as the oxidation of lactate by *Shewanella oneidensis*, a facultative bacterium<sup>58</sup>. Since many organic-rich environments in which HS are the most abundant TEA are only temporarily anoxic, this demonstration had huge implications. This is because HS may undergo numerous cycles of reduction and oxidation, which implies that the prevalence of HS as TEA for organics oxidation<sup>50,63,64</sup> might be enhanced in a temporary scale considering several cycles of HS reduction/oxidation and thus higher amounts of organic electron donors being oxidized to  $CO_2$  instead of going through the methanogenic pathway<sup>58</sup>. In a similar fashion, it is feasible that HS-dependent AOM could extend its  $CH_4$  emission mitigation potential under the scenario of a recurrently anoxic environment (**Figure 6.3**), *e.g.* in an agricultural soil temporarily anoxic due to flood irrigation (*i.e.* a rice paddy), or a coastal wetland temporarily being inundated by sea water inputs. Considering this scenario, the bottleneck for this mechanism to be an important sink of  $CH_4$ , is the capability of the methanotrophic microbial community to be resistant to  $O_2$  exposure.

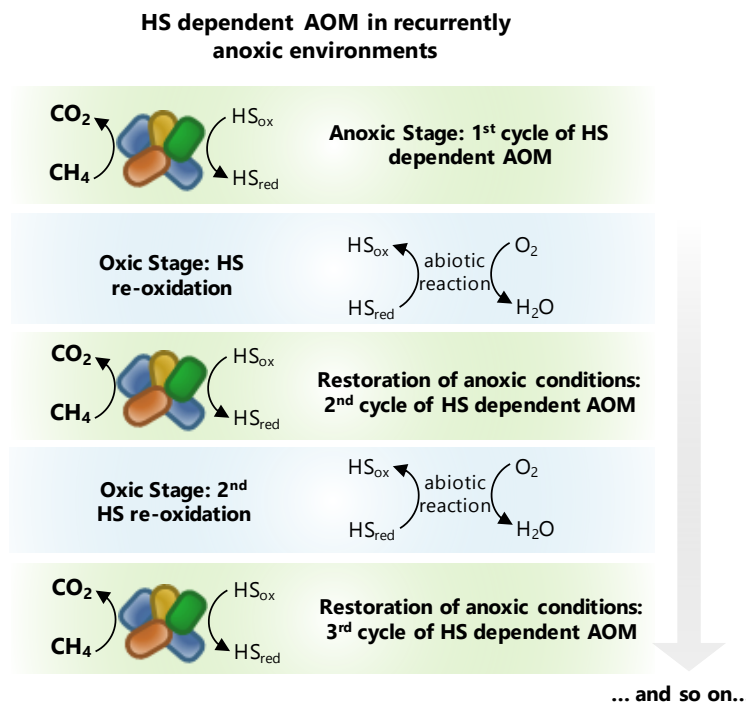


**Fig. 6.3 | Schematic representation of theoretical cycles of Humics Substances (HS) oxidation by oxygen (O<sub>2</sub>) perpetuating anaerobic oxidation of methane (AOM) during several cycles in a hypothetical recurrently anoxic environment.**

While the study by Klüpfel and colleagues (2014)<sup>58</sup> employed a facultative bacterial strain to demonstrate the feasibility of such HS cycling by oxygen, fueling several cycles of lactate oxidation, not every microbe involved in the anaerobic part of CH<sub>4</sub> oxidation might be tolerant to oxygen. Thus, in order to prove if the hypothesis previously stated could be feasible, the resistance of the anaerobic methanotrophic communities performing AOM to oxygen at recurrently anoxic environments must be tested.

## 6.4 Biotechnological Potential of CH<sub>4</sub> oxidizing/humus reducing microorganisms

Besides contributing to lessen the amount of methane naturally generated and released to the atmosphere, microorganisms involved in HS-dependent AOM could also contribute to this end by being applied in bio-engineered processes that could take advantage of the versatile metabolic characteristics of these microbes.

Some likely applications of these microorganisms in environmental biotechnologies will be further described.

### 6.4.1 CH<sub>4</sub>-oxidizing/humus-reducing microbes and their potential role in electricity production

With the discovery of the capacity of artificial electron acceptors, such as AQDS, decoupling AOM from sulfate reduction, a concept for a bio-electrochemical system for energy harvesting from CH<sub>4</sub> was proposed and patented. Scheller and colleagues (2016,2018) <sup>35,65</sup>, conceptualized a system in which ANME-2c, a marine archaeon with capacity of using AQDS as the terminal electron acceptor for AOM, constitutes the ideal biological agent fueling CH<sub>4</sub> oxidation coupled to electricity production (**Figure 6.4A**). This strategy presents several advantages as compared to previously reported methods: **i)** this system could work at ambient temperature; **ii)** CH<sub>4</sub> obtained from the biogas in anaerobic wastewater treatment systems could be used, which represents an inexpensive source of primary matter; and **iii)** implementing this kind of bio-electro technologies makes the actual wastewater scheme more integral by diminishing its own GHG emissions.

Of course several thermodynamical, electrochemical and kinetic limitations must be addressed when considering the design of a pilot system to run such a complex process<sup>65</sup>. However, in this thesis, the discovery of microorganisms able to oxidize  $\text{CH}_4$  linked to the reduction of HS in wetland sediments represents an additional option as inoculum source to employ in this kind of novel bio-electrochemical systems. One of the main reasons for this claim is that microorganisms present in the wetland sediment, employed as inoculum in  $\text{CH}_4$  consuming/HS reducing microcosms, do not need high salinity conditions, which may represent a disadvantage for ANME-2c and its implementation in engineered systems. Additionally, the potential of the wetland sediment to oxidize hydrocarbons further expand the possibility for energy harvesting from several hydrocarbons.

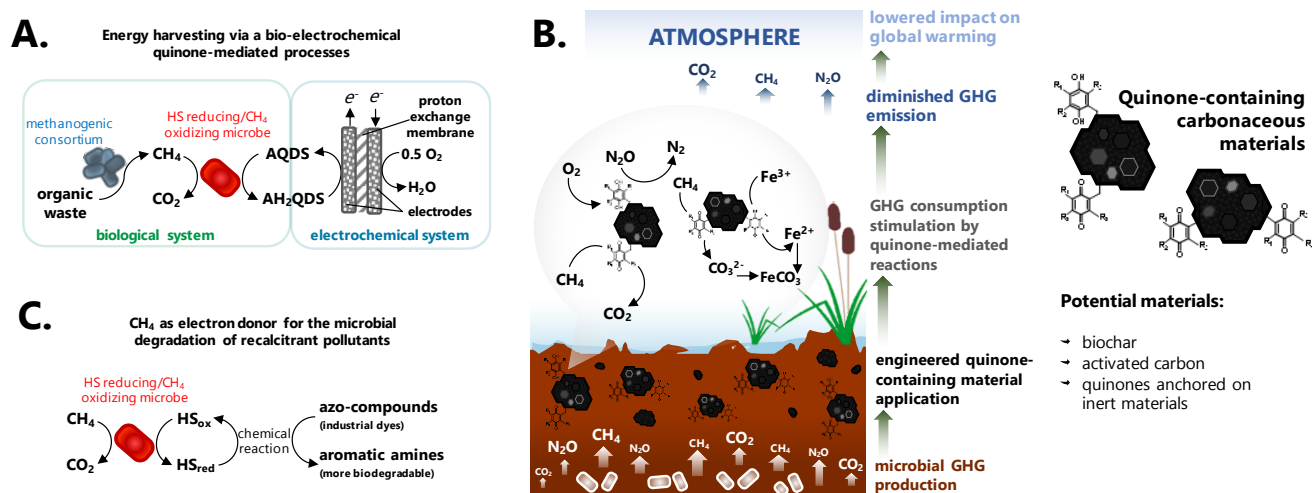


**Fig. 6.4 | Potential technologies based on the capabilities of quinone/HS-reducing,  $\text{CH}_4$ -oxidizing microorganisms.** Panel A displays an electricity harvesting method, which uses  $\text{CH}_4$ -oxidizing/quinone-reducing microorganisms based on reports by Scheller and colleagues (2016, 2018)<sup>35,65</sup>. Panel B depicts the possible amendment of soils and sediments with high  $\text{CH}_4$ ,  $\text{CO}_2$  and  $\text{N}_2\text{O}$  emissions with quinone-containing materials, such as biochar or activated carbon, which according to the results discussed

in this thesis, would trigger several reactions resulting in the lessening of the emission of these gases to the atmosphere. **Panel C** shows a model for the use of HS as an electron shuttle for the decomposition of recalcitrant azo dyes with the use of CH<sub>4</sub> as the sole electron donor and anaerobic methanotrophic microorganisms biologically driving this process.

#### **6.4.2 CH<sub>4</sub>-oxidizing/quinone-reducing microbes for engineered CH<sub>4</sub> emission suppression in natural environments by using quinone-containing materials**

The discovery of quinone-mediated processes with the potential to suppress CH<sub>4</sub> and N<sub>2</sub>O emissions could be applicable in ecosystems with excessive emissions of these gases, such as any kind of wetland or even anthropogenically intervened settings, such as rice paddies. Due to the high availability of quinone-containing materials, such as activated carbon, biochar, and similar inexpensive carbonaceous materials, it is feasible to apply them as a bio-stimulating agents in the soils and sediments to promote the biological and chemical reactions demonstrated in this thesis and, as a consequence, lessening the emission of these harmful gases (**Figure 6.4B**). Some examples of the viability of this proposal, are the very recent studies linking biochar to CH<sub>4</sub> and N<sub>2</sub>O consumption. For instance, wood derived black carbon, an specific kind of biochar, has been demonstrated to function as electron donor and acceptor for biologically mediated reactions carried out by *Geobacter metallireducens*.<sup>66</sup> Also, very recently, biochar has been demonstrated to suppress N<sub>2</sub>O emissions from a soil matrix by stimulating electron shuttling reactions directly promoted by its quinone-containing asset<sup>67</sup>. Regarding the CH<sub>4</sub> cycle, biochar has been proven as TEA for AOM,<sup>68</sup> which agrees with the study of HS-dependent AOM by Bai and colleagues (2019).<sup>34</sup> In both studies, the quinone-reduction process was found to be carried out by ANME-2d type of archaea.

### 6.4.3 CH<sub>4</sub>-oxidizing/humus-reducing microbes in wastewater treatment processes

To date, the most advanced biotechnological method employing anaerobic methanotrophic biota for wastewater treatment purposes is the AOM process coupled to denitrification (DAMO)<sup>69</sup>. The DAMO process accomplishes simultaneous removal of nitrogenous compounds, such as NO<sub>3</sub><sup>-</sup> and NO<sub>2</sub><sup>-</sup>, by using CH<sub>4</sub> as the sole electron donor<sup>70</sup>. Furthermore, the possibility of coupling DAMO to the process of anaerobic oxidation of ammonium (ANAMMOX)<sup>71</sup> has also been subject of research interest in the last years. This is due to the advantages that such coupled processes would have in lessening operational costs of the traditional nitrification/denitrification wastewater treatment strategy by taking advantage of the CH<sub>4</sub> produced in wastewater treatment plants via the anaerobic digestion process<sup>71</sup>.

However, wastewater pollutants, different than nitrogenous compounds, also demand novel strategies for their removal under low operational costs, simple operational parameters, and low potential collateral environmental impacts for which biotechnological processes are an excellent option. Despite this, anaerobic processes employing methane as the only electron donor (methanotrophic processes) have been scarcely explored. One of the few studies found in literature by Fu and colleagues (2019) has shown the possibility of employing AOM-performing cultures to treat wastewater polluted with azo dyes<sup>72</sup>. This proof of concept proved the effectiveness of a microbial consortium dominated by the archaeon *Candidatus Methanoperedens Nitroreducens* (*M. nitroreducens*, ANME-2d) and *Pseudoxanthomonas* (a  $\gamma$ -proteobacteria) to couple CH<sub>4</sub> oxidation to the breakdown of methyl orange (an azo-dye) into simpler, more biodegradable compounds via an inter-species electron transfer process<sup>72</sup>. Previously, HS, soluble

quinones, and quinone-containing carbonaceous materials have been extensively explored to treat this kind of recalcitrant pollutants. Under this treatment strategy, redox-active organic molecules or materials, have been used as electron shuttles to couple the oxidation of organic electron donors to accomplish the break-down of azo dyes, which usually remain recalcitrant in conventional biological wastewater treatment systems ( *i.e.* activated sludge)<sup>51,73,74</sup>. Therefore, it is proposed that CH<sub>4</sub>-oxidizing HS-reducing microorganisms introduced in the present work, could be applied in a microbial fuel cell for both producing electricity and degrading recalcitrant pollutants, such as azo dyes (**Fig. 6.4C**).

## 6.5 Conclusions

Microorganisms constitute the littlest living entities driving the pivotal biogeochemical cycles, which allow life on Earth to continue. Redox-active organic molecules (RAOMs), such as HS, maybe one of the most versatile and widespread electron transporting agents in nature, and thus their involvement in mediating microbial processes has a huge potential in the regulation of the emission of GHG to the atmosphere and consequently in controlling the Earth's climate.

This thesis provided the first pieces of evidence into the direct involvement of humus-reducing and -oxidizing microbes on mitigating the emission of CH<sub>4</sub>, CO<sub>2</sub> and N<sub>2</sub>O from wetland sediments via novel mechanisms of electron transport. These contributions to the body of knowledge sum up to almost 20 years of work in the understanding of the biogeochemical role of RAOMs and their importance on the environment (**Figure 6.5**).



## CHAPTER VI

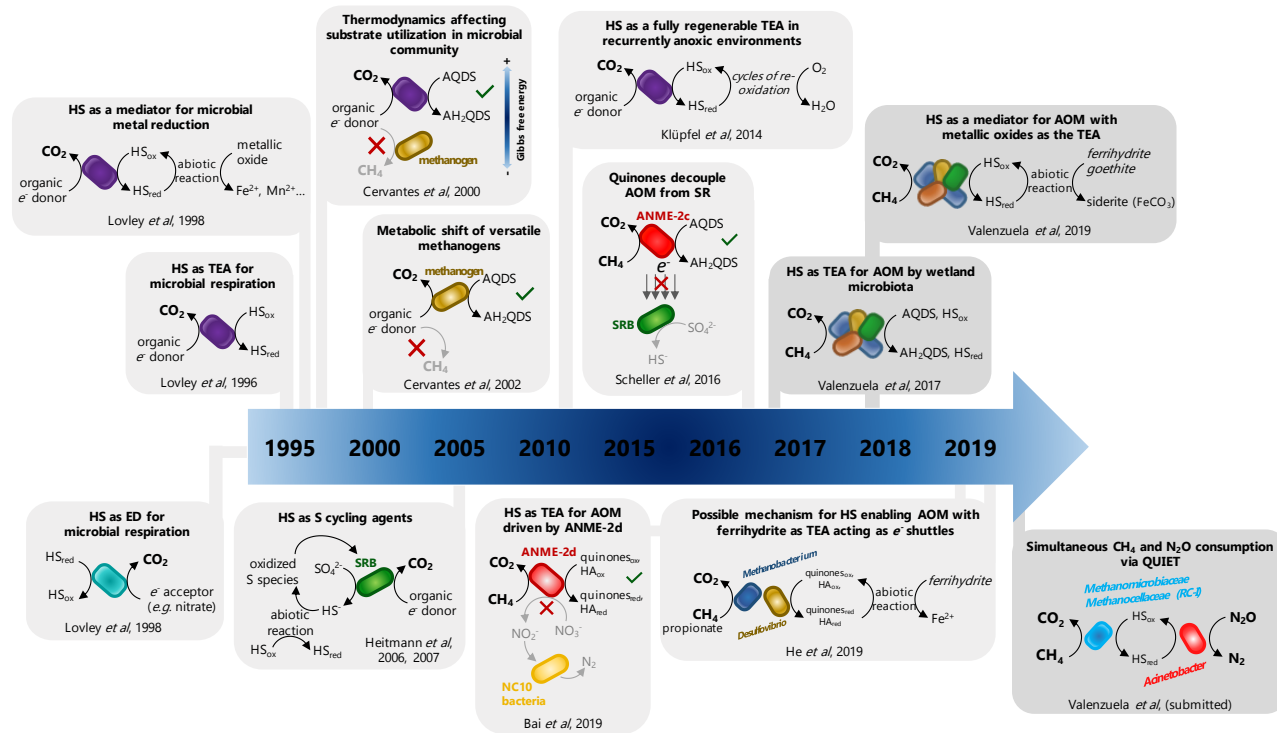


**Fig. 6.5 | Chronology of the scientific contributions made in this thesis within the 20 years of research on the role of redox-active organic compounds (RAOMs) in ecologically relevant reactions.** Studies depicted in this figure include pioneer papers on humic substances (HS) mediated reactions by: Lovley *et al.*, 1996<sup>75</sup>, 1998<sup>76</sup>, 1999<sup>77</sup>: HS as electron acceptor, shuttle and donor for microbially catalyzed reactions. Cervantes *et al.*, 2000<sup>50</sup>, 2002<sup>63</sup>: suppression of methanogenesis by HS. Heitmann *et al.*, 2006<sup>59</sup>, 2007<sup>78</sup>: HS as electron acceptors for sulfur compounds. Klöpffel *et al.*, 2014<sup>58</sup>: HS cycling in recurrently anoxic environments. Scheller *et al.*, 2016<sup>35</sup>, Valenzuela *et al.*, 2017<sup>14</sup> and 2019<sup>37</sup>, Bai *et al.*, 2019<sup>34</sup>, He *et al.*, 2019<sup>43</sup>: HS as electron acceptor and shuttle for the anaerobic oxidation of methane (AOM).

## 6.6 References

1. **Crowley, T. J.** Causes of climate change over the past 1000 years. *Science (80-. )*. **2000**, *289* (5477), 270–277.
2. **Kirschke, S.**; Bousquet, P.; Ciais, P.; Saunoy, M.; Canadell, J. G.; Dlugokencky, E. J.; Bergamaschi, P.; Bergmann, D.; Blake, D. R.; Bruhwiler, L.; et al. Three decades of global methane sources and sinks. *Nat. Geosci.* **2013**, *6* (10), 813–823.
3. **Singh, B. K.**; Bardgett, R. D.; Smith, P.; Reay, D. S. Microorganisms and climate change: Terrestrial feedbacks and mitigation options. *Nat. Rev. Microbiol.* **2010**, *8* (11), 779–790.
4. **Cavicchioli, R.**; Ripple, W. J.; Timmis, K. N.; Azam, F.; Bakken, L. R.; Baylis, M.; Behrenfeld, M. J.; Boetius, A.; Boyd, P. W.; Classen, A. T.; et al. Scientists' warning to humanity: microorganisms and climate change. *Nat. Rev. Microbiol.* **2019**.
5. **U.S. EPA.** Methane and Nitrous Oxide Emissions From Natural Sources. *United States Environmental Protection Agency*. 2010, p 194.
6. **Söhngen, N.** Über Bakterien, welche Methan ab Kohlenstoffnahrung und Energiequelle gebrauchen. *Z Bakteriologie Parasitenkd Infect.* **1906**, *15*, 513–517.
7. **Reeburgh, W. S.** Methane consumption in Cariaco Trench waters and sediments. *Earth Planet. Sci. Lett.* **1976**.
8. **Boetius, A.**; Ravenschlag, K.; Schubert, C. J.; Rickert, D.; Widdel, F.; Gieseke, A.; Amann, R.; Jørgensen, B. B.; Witte, U.; Pfannkuche, O. A marine microbial consortium apparently mediating anaerobic oxidation of methane. *Nature* **2000**, *407* (6804), 623–626.
9. **Orphan, V. J.**; House, C. H.; Hinrichs, K. U.; McKeegan, K. D.; DeLong, E. F. Methane-consuming archaea revealed by directly coupled isotopic and phylogenetic analysis. *Science (80-. )*. **2001**, *293* (5529), 484–487.
10. **Raghoebarsing, A.**; Pol, A.; van de Pas-Schoonen, K.; Smolders, A.; Ettwig, K.; Rijpstra, W.; Schouten, S.; Damste, J.; Op den Camp, H.; Jetten,

M.; et al. A microbial consortium couples anaerobic methane oxidation to denitrification. *Nature* **2006**, *440* (7086), 918–921.

**11. Islas-Lima, S.;** Thalasso, F.; Gómez-Hernandez, J. Evidence of anoxic methane oxidation coupled to denitrification. *Water Res.* **2004**, *38* (1), 13–16.

**12. Beal, E. J.;** House, C. H.; Orphan, V. J. Manganese- and iron-dependent marine methane oxidation. *Science* **2009**, *325* (5937), 184–187.

**13. Ettwig, K. F.;** Zhu, B.; Speth, D.; Keltjens, J. T.; Jetten, M. S. M.; Kartal, B. Archaea catalyze iron-dependent anaerobic oxidation of methane. *Proc. Natl. Acad. Sci.* **2016**, *113* (45), 12792–12796.

**14. Valenzuela, E. I.;** Prieto-Davó, A.; López-Lozano, N. E.; Hernández-Eligio, A.; Vega-Alvarado, L.; Juárez, K.; García-González, A. S.; López, M. G.; Cervantes, F. J. Anaerobic Methane Oxidation Driven by Microbial Reduction of Natural Organic Matter in a Tropical Wetland. *Appl. Environ. Microbiol.* **2017**, *83* (11), AEM.00645-17.

**15. Valentine, D. L.** Biogeochemistry and microbial ecology of methane

oxidation in anoxic environment: a review. *Antonie van leeuwenhoek* **2001**, 271–282.

**16. Ettwig, K. F.;** Van Alen, T.; Van De Pas-Schoonen, K. T.; Jetten, M. S. M.; Strous, M. Enrichment and molecular detection of denitrifying methanotrophic bacteria of the NC10 phylum. *Appl. Environ. Microbiol.* **2009**, *75* (11), 3656–3662.

**17. Schubert, C. J.;** Vazquez, F.; Losekann-Behrens, T.; Knittel, K.; Tonolla, M.; Boetius, A. Evidence for anaerobic oxidation of methane in sediments of a freshwater system (Lago di Cadagno). *FEMS Microbiol. Ecol.* **2011**, *76* (1), 26–38.

**18. Deutzmann, J. S.;** Schink, B. Anaerobic oxidation of methane in sediments of Lake Constance, an oligotrophic freshwater lake. *Appl. Environ. Microbiol.* **2011**, *77* (13), 4429–4436.

**19. Amos, R. T.;** Bekins, B. A.; Cozzarelli, I. M.; Voytek, M. A.; Kirshtein, J. D.; Jones, E. J. P.; Blowes, D. W. Evidence for iron-mediated anaerobic methane oxidation in a crude oil-contaminated aquifer. *Geobiology* **2012**, *10* (6), 506–517.

- 20. Segarra, K. E. A.;** Schubotz, F.; Samarkin, V.; Yoshinaga, M. Y.; Hinrichs, K.-U.; Joye, S. B. High rates of anaerobic methane oxidation in freshwater wetlands reduce potential atmospheric methane emissions. *Nat. Commun.* **2015**, *6* (May), 7477.
- 21. Segarra, K. E. A.;** Comerford, C.; Slaughter, J.; Joye, S. B. Impact of electron acceptor availability on the anaerobic oxidation of methane in coastal freshwater and brackish wetland sediments. *Geochim. Cosmochim. Acta* **2013**, *115*, 15–30.
- 22. Gupta, V.;** Smemo, K. A.; Yavitt, J. B.; Basiliako, N. Active Methanotrophs in Two Contrasting North American Peatland Ecosystems Revealed Using DNA-SIP. *Microb. Ecol.* **2012**, *63* (2), 438–445.
- 23. Gupta, V.;** Smemo, K. A.; Yavitt, J. B.; Fowle, D.; Branfireun, B.; Basiliako, N. Stable isotopes reveal widespread anaerobic methane oxidation across latitude and peatland type. *Environ. Sci. Technol.* **2013**, *47* (15), 8273–8279.
- 24. Smemo, K. A.;** Yavitt, J. B. Anaerobic oxidation of methane: An underappreciated aspect of methane cycling in peatland ecosystems? *Biogeosciences* **2011**, *8* (3), 779–793.
- 25. White, G. F.;** Edwards, M. J.; Gomez-Perez, L.; Richardson, D. J.; Butt, J. N.; Clarke, T. A. *Mechanisms of Bacterial Extracellular Electron Exchange.*, 1st ed.; Elsevier Ltd., 2016; Vol. 68.
- 26. Lovley, D. R.** Happy together: microbial communities that hook up to swap electrons. *ISME J.* **2016**, 1–10.
- 27. Smith, J. A.;** Nevin, K. P.; Lovley, D. R. Syntrophic growth via quinone-mediated interspecies electron transfer. *Front. Microbiol.* **2015**, *6* (FEB), 1–8.
- 28. Lipczynska-Kochany, E.** Effect of climate change on humic substances and associated impacts on the quality of surface water and groundwater: A review. *Sci. Total Environ.* **2018**, *640–641*, 1548–1565.
- 29. Tan, W.;** Xi, B.; Wang, G.; Jiang, J.; He, X.; Mao, X.; Gao, R.; Huang, C.; Zhang, H.; Li, D.; et al. Increased Electron-Accepting and Decreased Electron-Donating Capacities of Soil Humic Substances in Response to Increasing Temperature. *Environ. Sci. Technol.* **2017**, *51* (6), 3176–3186.
- 30. Liu, W.;** Wu, Y.; Liu, T.; Li, F.; Dong, H.; Jing, M. Influence of

incubation temperature on 9,10-anthraquinone-2-sulfonate (AQS)-mediated extracellular electron transfer. *Front. Microbiol.* **2019**, *10* (MAR).

**31. Aeschbacher, M.;** Vergari, D.; Schwarzenbach, R. P.; Sander, M. Electrochemical analysis of proton and electron transfer equilibria of the reducible moieties in humic acids. *Environ. Sci. Technol.* **2011**, *45* (19), 8385–8394.

**32. Girguis, P. R.;** Cozen, A.; DeLong, E. E. Growth and population dynamics of anaerobic methanotrophic archaea in a continuous flow bioreactor. *Appl. Environ. Microbiol.* **2005**, *71* (7), 3725–3733.

**33. Orphan, V. J.;** Turk, K. A.; Green, A. M.; House, C. H. Patterns of <sup>15</sup>N assimilation and growth of methanotrophic ANME-2 archaea and sulfate-reducing bacteria within structured syntrophic consortia revealed by FISH-SIMS. *Environ. Microbiol.* **2009**, *11* (7), 1777–1791.

**34. Bai, Y.-N.;** Wang, X.-N.; Wu, J.; Lu, Y.-Z.; Fu, L.; Zhang, F.; Lau, T.-C.; Zeng, R. J. Humic substances as electron acceptors for anaerobic oxidation of methane driven by ANME-2d. *Water Res.* **2019**, *164*, 114935.

**35. Scheller, S.;** Yu, H.; Chadwick, G. L.; McGlynn, S. E.; Orphan, V. J. Artificial electron acceptors decouple archaeal methane oxidation from sulfate reduction. *Science* (80-. ). **2016**, *351* (6274), 703–707.

**36. Cui, M.;** Ma, A.; Qi, H.; Zhuang, X.; Zhuang, G. Anaerobic oxidation of methane: An “active” microbial process. *Microbiologyopen* **2015**, *4* (1), 1–11.

**37. Valenzuela, E. I.;** Avendaño, K. A.; Balagurusamy, N.; Arriaga, S.; Nieto-Delgado, C.; Thalasso, F.; Cervantes, F. J. Electron shuttling mediated by humic substances fuels anaerobic methane oxidation and carbon burial in wetland sediments. *Sci. Total Environ.* **2019**, *650*, 2674–2684.

**38. Lloyd, K. G.;** Lapham, L.; Teske, A. An anaerobic methane-oxidizing community of ANME-1b archaea in hypersaline gulf of Mexico sediments. *Appl. Environ. Microbiol.* **2006**.

**39. Knittel, K.;** Boetius, A. Anaerobic oxidation of methane: progress with an unknown process. *Annu. Rev. Microbiol.* **2009**, *63*, 311–334.

**40. Pernthaler, A.;** Dekas, A. E.; Brown, C. T.; Goffredi, S. K.; Embaye, T.; Orphan, V. J. Diverse syntrophic

- partnerships from deep-sea methane vents revealed by direct cell capture and metagenomics. *Proc. Natl. Acad. Sci. U. S. A.* **2008**, *105* (19), 7052–7057.
- 41. Cai, C.;** Leu, A. O.; Xie, G.-J.; Guo, J.; Feng, Y.; Zhao, J.-X.; Tyson, G. W.; Yuan, Z.; Hu, S. A methanotrophic archaeon couples anaerobic oxidation of methane to Fe(III) reduction. *ISME J.* **2018**, No. lii.
- 42. Niemann, H.;** Lösekann, T.; De Beer, D.; Elvert, M.; Nadalig, T.; Knittel, K.; Amann, R.; Sauter, E. J.; Schlüter, M.; Klages, M.; et al. Novel microbial communities of the Haakon Mosby mud volcano and their role as a methane sink. *Nature* **2006**, *443* (7113), 854–858.
- 43. He, Q.;** Yu, L.; Li, J.; He, D.; Cai, X.; Zhou, S. Electron shuttles enhance anaerobic oxidation of methane coupled to iron(III) reduction. *Sci. Total Environ.* **2019**, *688*, 664–672.
- 44. Bar-Or, I.;** Elvert, M.; Eckert, W.; Kushmaro, A.; Vigderovich, H.; Zhu, Q.; Ben-Dov, E.; Sivan, O. Iron-coupled anaerobic oxidation of methane performed by a mixed bacterial-archaeal community based on poorly-reactive minerals Department of Geological and Environmental Sciences , Ben Gurion University of the Negev , Israel Oceanographic and Limnologic. *Environ. Sci. Technol.* **2017**, *51* (21), 12293–12301.
- 45. Zhang, J.;** Dong, H.; Liu, D.; Fischer, T. B.; Wang, S.; Huang, L. Microbial reduction of Fe(III) in illite-smectite minerals by methanogen *Methanosarcina mazei*. *Chem. Geol.* **2012**.
- 46. Yamada, C.;** Kato, S.; Kimura, S.; Ishii, M.; Igarashi, Y. Reduction of Fe(III) oxides by phylogenetically and physiologically diverse thermophilic methanogens. *FEMS Microbiol. Ecol.*
- 47. Holmes, D. E.;** Ueki, T.; Tang, H.; Zhou, J.; Smith, J. A.; Chaput, G.; Lovley, D. R. A Membrane-Bound Cytochrome Enables *Methanosarcina acetivorans* To Conserve Energy from Extracellular Electron Transfer. *MBio* **2019**, *10* (4), e00789-19.
- 48. Bond, D. R.;** Lovley, D. R. Reduction of Fe(III) oxide by methanogens in the presence and absence of extracellular quinones. *Environ. Microbiol.* **2002**, *4* (2), 115–124.
- 49. Lovley, D. R.;** Kashefi, K.; Vargas,

- M.; Tor, J. M.; Blunt-Harris, E. L. Reduction of humic substances and Fe(III) by hyperthermophilic microorganisms. *Chem. Geol.* **2000**, *169* (3–4), 289–298.
- 50. Cervantes, F. J.**; Velde, S.; Lettinga, G.; Field, J. a. Competition between methanogenesis and quinone respiration for ecologically important substrates in anaerobic consortia. *FEMS Microbiol. Ecol.* **2000**, *34* (2), 161–171.
- 51. Martinez, C. M.**; Alvarez, L. H.; Celis, L. B.; Cervantes, F. J. Humus-reducing microorganisms and their valuable contribution in environmental processes. *Appl. Microbiol. Biotechnol.* **2013**, *97* (24), 10293–10308.
- 52. Saxton, M. A.**; Samarkin, V. A.; Schutte, C. A.; Bowles, M. W.; Madigan, M. T.; Cadieux, S. B.; Pratt, L. M.; Joye, S. B. Biogeochemical and 16S rRNA gene sequence evidence supports a novel mode of anaerobic methanotrophy in permanently ice-covered Lake Fryxell, Antarctica. *Limnol. Oceanogr.* **2016**, *61*, S119–S130.
- 53. Biddle, J. F.**; Lipp, J. S.; Lever, M. A.; Lloyd, K. G.; Sørensen, K. B.; Anderson, R.; Fredricks, H. F.; Elvert, M.; Kelly, T. J.; Schrag, D. P.; et al. Heterotrophic Archaea dominate sedimentary subsurface ecosystems off Peru. *Proc. Natl. Acad. Sci. U. S. A.* **2006**, *103* (10), 3846–3851.
- 54. Evans, P. N.**; Parks, D. H.; Chadwick, G. L.; Robbins, S. J.; Orphan, V. J.; Golding, S. D.; Tyson, G. W. Methane metabolism in the archaeal phylum Bathyarchaeota revealed by genome-centric metagenomics. *Science* **2015**, *350* (6259), 434–438.
- 55. Vanwonterghem, I.**; Evans, P. N.; Parks, D. H.; Jensen, P. D.; Woodcroft, B. J.; Hugenholtz, P.; Tyson, G. W. Methylotrophic methanogenesis discovered in the archaeal phylum Verstraetearchaeota. *Nat. Microbiol.* **2016**, *1* (October), 1–9.
- 56. Evans, P.**; Boyd, J.; Woodcroft, B.; Leu, A.; Parks, D.; Hugenholtz, P.; Tyson, G. An evolving view of methane metabolism in the Archaea. *Nat. Rev. Microbiol.* **2018**.
- 57. Straub, K. L.**; Benz, M.; Schink, B. Iron metabolism in anoxic environments at near neutral pH. *FEMS Microbiol. Ecol.* **2000**, *34* (3), 181–186.
- 58. Klüpfel, L.**; Piepenbrock, A.; Kappler, A.; Sander, M. Humic substances as fully regenerable electron

- acceptors in recurrently anoxic environments. *Nat. Geosci.* **2014**, *7* (February), 195–200.
- 59. Heitmann, T.;** Blodau, C. Oxidation and incorporation of hydrogen sulfide by dissolved organic matter. *Chem. Geol.* **2006**, *235* (1–2), 12–20.
- 60. Rios-Del Toro, E. E.;** Valenzuela, E. I.; Ramírez, J. E.; López-Lozano, N. E.; Cervantes, F. J. Anaerobic Ammonium Oxidation Linked to Microbial Reduction of Natural Organic Matter in Marine Sediments. *Environ. Sci. Technol. Lett.* **2018**, acs.estlett.8b00330.
- 61. Ratasuk, N.;** Nanny, M. A. Characterization and quantification of reversible redox sites in humic substances. *Environ. Sci. Technol.* **2007**, *41* (22), 7844–7850.
- 62. Bauer, I.;** Kappler, A. Rates and extent of reduction of Fe(III) compounds and O<sub>2</sub> by humic substances. *Environ. Sci. Technol.* **2009**, *43* (13), 4902–4908.
- 63. Cervantes, F. J.;** De Bok, F. A. M.; Duong-Dac, T.; Stams, A. J. M.; Lettinga, G.; Field, J. A. Reduction of humic substances by halorespiring, sulphate-reducing and methanogenic microorganisms. *Environ. Microbiol.* **2002**, *4* (1), 51–57.
- 64. Keller, J. K.;** Weisenhorn, P. B.; Megonigal, J. P. Humic acids as electron acceptors in wetland decomposition. *Soil Biol. Biochem.* **2009**, *41* (7), 1518–1522.
- 65. Scheller, S.** Microbial Interconversion of Alkanes to Electricity. *Front. Energy Res.* **2018**, *6* (November), 1–6.
- 66. Saquing, J. M.;** Yu, Y. H.; Chiu, P. C. Wood-Derived Black Carbon (Biochar) as a Microbial Electron Donor and Acceptor. *Environ. Sci. Technol. Lett.* **2016**, *3* (2), 62–66.
- 67. Yuan, H.;** Zhang, Z.; Li, M.; Clough, T.; Wrage-Mönnig, N.; Qin, S.; Ge, T.; Liao, H.; Zhou, S. Biochar's role as an electron shuttle for mediating soil N<sub>2</sub>O emissions. *Soil Biol. Biochem.* **2019**, *133* (March), 94–96.
- 68. Zhang, X.;** Xia, J.; Pu, J.; Cai, C.; Tyson, G. W.; Yuan, Z.; Hu, S. Biochar-mediated Anaerobic Oxidation of Methane. *Environ. Sci. Technol.* **2019**, acs.est.9b01345.
- 69. Cai, C.;** Hu, S.; Guo, J.; Shi, Y.; Xie, G. J.; Yuan, Z. Nitrate reduction by denitrifying anaerobic methane oxidizing microorganisms can reach a practically



useful rate. *Water Res.* **2015**, *87*, 211–217.

**70. Welte, C. U.;** Rasigraf, O.; Vaksmaa, A.; Versantvoort, W.; Arshad, A.; Op den Camp, H. J. M.; Jetten, M. S. M.; Lüke, C.; Reimann, J. Nitrate- and nitrite-dependent anaerobic oxidation of methane. *Environ. Microbiol. Rep.* **2016**, *00*, 1–15.

**71. Hu, S.;** Zeng, R. J.; Haroon, M. F.; Keller, J.; Lant, P. a.; Tyson, G. W.; Yuan, Z. A laboratory investigation of interactions between denitrifying anaerobic methane oxidation (DAMO) and anammox processes in anoxic environments. *Sci. Rep.* **2015**, *5*, 8706.

**72. Fu, L.;** Bai, Y.-N.; Lu, Y.-Z.; Ding, J.; Zhou, D.; Zeng, R. J. Degradation of organic pollutants by anaerobic methane-oxidizing microorganisms using methyl orange as example. *J. Hazard. Mater.* **2019**, *364* (August 2018), 264–271.

**73. Cervantes, F. J.;** Gómez, R.; Alvarez, L. H.; Martinez, C. M.; Hernandez-Montoya, V. Efficient anaerobic treatment of synthetic textile wastewater in a UASB reactor with granular sludge enriched with humic acids supported on alumina

nanoparticles. *Biodegradation* **2015**, *26* (4), 289–298.

**74. Emilia Rios-Del Toro, E.;** Celis, L. B.; Cervantes, F. J.; Rangel-Mendez, J. R. Enhanced microbial decolorization of methyl red with oxidized carbon fiber as redox mediator. *J. Hazard. Mater.* **2013**, *260*, 967–974.

**75. Lovley, D. R.;** Coates, J. D.; Blunt-Harris, E. L.; Phillips, E. J. P.; Woodward, J. C. Humic substances as electron acceptors for microbial respiration. *Nature.* 1996, pp 445–448.

**76. Lovley, D. R.;** Fraga, J. L.; Blunt-Harris, E. L.; Hayes, L. A.; Phillips, E. J. P.; Coates, J. D. Humic substances as a mediator for microbially catalyzed metal reduction. *Acta Hydrochim. Hydrobiol.* **1998**, *26* (3), 152–157.

**77. Lovley, D. R.;** Fraga, J. L.; Coates, J. D.; Blunt-Harris, E. L. Humics as an electron donor for anaerobic respiration. *Environ. Microbiol.* **1999**, *1* (1), 89–98.

**78. Heitmann, T.;** Goldhammer, T.; Beer, J.; Blodau, C. Electron transfer of dissolved organic matter and its potential significance for anaerobic respiration in a northern bog. *Glob. Chang. Biol.* **2007**, *13* (8), 1771–178

## Curriculum Vitae

**E**dgardo I. Valenzuela was born in Durango, Mexico in 1989. After finishing his pre-university education, he moved to Victoria de Durango, Durango (2007) and completed a B. Sc. in Biochemical Engineering at the Durango Institute of Technology (ITD) with a thesis work on biofiltration systems, which he performed at the ser Institute for Scientific and Technological Research of San Luis Potosí (IPICYT at SLP, Mexico, 2012). For his M. Sc. in Environmental Sciences, he explored the capability of the microbiota of several water bodies (marine and freshwater) to employ quinones as the electron sink to anaerobically oxidize methane (2013). Afterwards, in summer 2015, he started a doctoral research aiming to elucidate novel microbial processes driving greenhouse gases ( $\text{CH}_4$  and  $\text{N}_2\text{O}$ ) consumption by the microbiota of the sediments of a tropical wetland. Both the M. Sc. and the PhD projects were supervised by Prof. Francisco J. Cervantes at IPICYT with several collaborations in and outside the institute. Within the doctoral project, he was a short-term visiting scientist, at the *Eberhard-Karls Tübingen University* in Germany where he explored S cycling aspects affecting humus-driven AOM under the co-supervision of Prof. Andreas Kappler (2018).



## Distinctions/Grants awarded derived from this thesis

**1. FEMS-ALAM Early Career Scientist Grant**, awarded to three Latin American Early career Scientists to attend the 8<sup>th</sup> edition of the congress of the *Federation of European Microbiologists* (FEMS) held in Glasgow, Scotland, July 2019.

- **Derived from this:** recipient of a FEMS Congress Poster Prize for runner up for best poster presentation by an Attendance Grantee.

**2. DAAD Short-Term Research Grant** (German Service of Academic Exchange), awarded to perform a 5 months research stay in the Geomicrobiology group of the Eberhard-Karls Tübingen Universität, Germany under the supervision of Prof. Andreas Kappler (May – November 2018).

**3. Applied and Environmental Microbiology (AEM) Spotlight recognition**, for the published version of **CHAPTER II**. This acknowledgment is given to the articles of *Significant Interest* selected by the Editors of AEM per published Issue of the journal (June 2017).

**4. Best thesis advances oral presentation given by a PhD student** at the VII and X editions of the *Thesis Advances Symposium* of the Environmental Sciences Division of IPICYT. San Luis Potosí, México (April 2017 and 2019, respectively).

**5.** Posters enlisted as number 2 and 4 in the **Conferences/symposia/seminars** relevant to this thesis were **awarded with best poster prizes** in each correspondent contest.

## Publications derived from this thesis

**1. Valenzuela, E. I.**, Prieto-Davó, A., López-Lozano, N. E., Hernández-Eligio, A., Vega-Alvarado, L., Juárez, K., et al. (2017). Anaerobic methane oxidation driven by microbial reduction of natural organic matter in a tropical wetland. *Appl. Environ. Microbiol.* 83, AEM.00645-17. doi:10.1128/AEM.00645-17.

**2. Valenzuela, E. I.**, Avendaño, K. A., Balagurusamy, N., Arriaga, S., Nieto-Delgado, C., Thalasso, F., et al. (2019). Electron shuttling mediated by humic substances fuels anaerobic methane oxidation and carbon burial in wetland sediments. *Sci. Total Environ.* 650, 2674–2684. doi:10.1016/J.SCITOTENV.2018.09.388.

**3. Valenzuela E. I.** & Cervantes F. J. Microorganismos imposibles regulando el clima del planeta. Ciencia, Academia Mexicana de Ciencias (*in press*).

**4. Valenzuela, E. I.**, Padilla-Loma, C., Gómez-Hernández, N., López-Lozano, N.E., Casas-Flores, S., Cervantes, F.J. Humic substances mediate anaerobic methane oxidation linked to nitrous oxide reduction in wetland sediments. (*submitted*).

**5. Valenzuela, E. I.**, Kappler A., Cervantes, F. J. Humic Substances Mediate Anaerobic Methane Oxidation Linked to Nitrous Oxide Reduction in Wetland Sediments. (*in preparation*).

## Other publications

**1. Valenzuela-Reyes E.**, Casas-Flores S., Isordia-Jasso I., Arriaga S. (2014) Performance and bacterial population composition of an n-hexane biofilter working under fluctuating conditions. *Applied Biochemistry and Biotechnology* 174:832–844. DOI: 10.1007/s12010-014-1079-8.

**2.** Ríos del Toro E. E., **Valenzuela E. I.**, Ramirez J. E., López-Lozano N. E., Cervantes F. J. (2018) Anaerobic ammonium oxidation linked to microbial reduction of natural organic matter in marine sediments. *Environmental Science & Technology Letters*, 5:571-577. DOI: 10.1021/acs.estlett.8b00330.

**3.** Ríos del Toro E. E., **Valenzuela E. I.**, López-Lozano N. E., Cortés-Martínez M. G., Sánchez-Rodríguez M. A., Calvario-Martínez O. C., Sánchez-Carrillo S., Cervantes F. J. (2018) Anaerobic ammonium oxidation linked to sulfate and ferric iron reduction fuels nitrogen loss in marine sediments. *Biodegradation*, 29:429-442. DOI: 10.1007/s10532-018-9839-8.

**4.** Romero R. M., **Valenzuela E. I.**, Cervantes F. J., Serrano D., Álvarez L. H. Activated carbon increases methane productivity during the digestion of liquid and raw fractions of swine effluent. (*submitted*)

**5.** García-Gigueroa C. A., **Valenzuela E. I.**, Pat-Espadas A. M. Immobilization of potentially toxic elements contained in mine waste: a biological approach for the environmental management of tailings. (*in preparation*).

## Conferences/symposia/seminars relevant to this thesis

**1. Valenzuela E. I.** & Cervantes F. J. *Anaerobic oxidation of CH<sub>4</sub> coupled to the reduction of analogues of humic substances by an anaerobic sediment from Ciénega Sisal, Yucatán.* XVI National Congress of Biotechnology and Bioengineering. **Guadalajara, Jalisco, Mexico, 2015.**

**2. Valenzuela E. I.** & Cervantes F. J. *X-ray Photoelectron Spectroscopy as a tool to support Anaerobic Methane Oxidation coupled to microbial reduction of Natural Organic Matter.* 1<sup>st</sup> XPS Anniversary from National Research Laboratory in Nanoscience and Nanotechnology (LINAN), **SLP, Mexico, 2016.**

**3. Valenzuela E. I.,** Prieto-Davó A., López-Lozano N. E., Hernández-Eligio A., Vega-Alvarado L., Juárez K., García-González A. S., López M. G., Cervantes F.J. *Natural Organic Matter Reduction Fuels Anaerobic Oxidation of Methane in Sediments From a Tropical Wetland.* 7<sup>th</sup> Congress of European Microbiologists FEMS. **Valencia, Spain, 2017.**

**4. Valenzuela E. I.,** Avendaño K. A., Balagurusamy N., Arriaga S., Nieto-Delgado C., Thalasso F., Cervantes F.J. *The iron-reduction mediated by humic substances reduces the emission of methane and promotes the carbon sequestration as carbonates of different nature.* VI Interdisciplinary postgraduate congress, IPICYT, **SLP, Mexico, 2017.**

**5. Valenzuela E. I.** & Cervantes F. J. *Exploring anaerobic methane sinks in sediments from a coastal wetland: the role of humus as electron acceptor.* VIII Thesis Advances Symposium of the Division of Environmental Sciences, IPICYT, **SLP, Mexico, 2017.**

**6. Valenzuela E. I.,** Cervantes F. J. *Microbial processes driving methane oxidation in tropical wetlands,* Mini-Symposium *The Methane Cycle: From threats to Opportunities,* IPICYT, **SLP, Mexico, 2018.**

**7. Padilla-Loma C., Valenzuela E. I.,** Cervantes F.J. *Anaerobic methane oxidation linked to nitrous oxide reduction via humus mediated interspecies electron transfer in wetland sediment,* 6<sup>th</sup> International Symposium on Environmental Biotechnology and Engineering, ITSON, **Ciudad Obregón, Sonora, Mexico, 2018.**

8. Cervantes F. J., **Valenzuela E. I.**, Ríos-Del Toro E. E. *Role of humic substances in global biogeochemical cycles*, Electromicrobiology – from electrons to ecosystems Conference, Center for Electromicrobiology, **Aarhus, Denmark, 2019.**

9. **Valenzuela E. I.** & Cervantes F. J. *Microorganismos que reducen y oxidan sustancias húmicas como reguladores de la emisión de gases de efecto invernadero: CH<sub>4</sub> y N<sub>2</sub>O*. X Thesis Advances Symposium of the Division of Environmental Sciences, IPICYT, **SLP, Mexico, 2019.**

10. **Valenzuela E. I.**, Padilla-Loma C., Casas-Flores S., Gómez-Hernández N., Cervantes F. J. *Humic substances mediate anaerobic methane oxidation linked to nitrous oxide reduction in wetland sediments*, 8<sup>th</sup> Congress of European Microbiologists FEMS. **Glasgow, Scotland, 2019.**

## **Other conferences/symposia/seminars**

1. **Valenzuela-Reyes Edgardo**, Arriaga Sonia, Saucedo-Lucero Octavio. *Microbial population analysis under fluctuating conditions in a bacterial biofilter degrading n-hexane*. 5<sup>th</sup> IWA Conference on Odors and Air Emissions. **San Francisco, USA. 2013.**